ISSN — 0132 — 1447

BULLETIN

OF THE GEORGIAN ACADEMY
OF SCIENCES

საქართველოს
მეცნიერებათა აკადემიის

მოამბე

VOLUME 159 NUMBER 1
JANUARY–FEBRUARY
1999

TBILISI
თბილისი

The Journal is founded in 1940

BULLETIN

OF THE GEORGIAN ACADEMY OF SCIENCES

is a scientific journal, issued bimonthly in
Georgian and English languages

Editorial Office:
Georgian Academy of Sciences
52, Rustaveli Avenue,
Tbilisi, 380008,
Republic of Georgia

Telephone : **+995 32 99.75.93**
Fax : **+995 32 99.88.23**
E-mail : **BULLETIN@PRESID.ACNET.GE**

CONTENTS

GEOPHYSICS

ANALYTICAL CHEMISTRY

GENERAL AND INORGANIC CHEMISTRY

ORGANIC CHEMISTRY

PHYSICAL CHEMISTRY

საქართველოს მეცნიერებათა აკადემიის მოამბე, 159, №1, 1999
BULLETIN OF THE GEORGIAN ACADEMY OF SCIENCES, 159, №1, 1999

MATHEMATICS

G. Chelidze

On the Intersection of Imbedded Sets in Normed Spaces

Presented by Corr. Member of the Academy N. Vakhania, July 23, 1998

ABSTRACT. **In this work we define the parameter $\overline{æ}(F)$ of a bounded set F that is similar to $æ(F)$, which was introduced earlier. Several statements in terms of the new parameter $\overline{æ}$ are formulated. The meaning of the critical æ for the spaces $l_p (1 \le p \le 8)$ is found as well.**

Key words: linear normed space, intersection of imbedded closed bounded sets.

For last convenience, under the sequence $\{F_n\}$ we assume the sequence of imbedded bounded closed sets F_n in a linear normed space X. Likewise, for the brevity we say "intersection of F_n" meaning the intersection of the sets F_n (n=1,2...).

In the present paper we continue to study the conditions under which the intersection of $\{F_n\}$ is non-empty. This problem is trivial if X is finite-dimensional, because in this case every bounded closed set is compact and therefore the intersection of $\{F_n\}$ is always non-empty. It is easily proved (using Riesz theorem) that the converse statement is also true. If the intersection of all sequences $\{F_n\}$ is non-empty then the space X is finite-dimensional. It is also trivial that the intersection of $\{F_n\}$ is non-empty if the diameters of F_n tend to zero (provided X is complete). For the same case of Banach space X it is shown in [1] that this intersection may be empty if the diameters do not vanish (however, if F_n are closed balls then the intersection is always non-empty).

To study the problem of the intersection for the general sets F_n, the numerical parameter $æ(F)$ of a bounded set F was introduced in [1] that characterises, in a sense, the derivation of the form of F from the spherical one. This parameter is defined as follows:

$$æ(F)=\sup_{x\in F}\frac{r_x(F)}{R_x(F)},$$

where $R_x(F)=\sup_{y\in F}\|x-y\|$, $r_x(F)=\inf_{y\in F}\|x-y\|$ and F^c denotes the complement to F (the bounded set F is supposed to contain at least two points). It was also shown in [1] that in case of Banach space the intersection of $\{F_n\}$ is non-empty if $æ := \overline{\lim} æ(F_n) > 1/2$, and it may be empty for any given $æ < 1/2$. In this sense the number $æ = 1/2$ is critical. In [2] it was proved that the intersection for the critical case $æ = 1/2$ is always non-empty for any X which is dual to some Banach space $Y, X = Y^*$. The example constructed in [3] shows that the intersection for the critical case $æ = 1/2$ may be empty if no restriction is imposed on the Banach space X.

In this paper we introduce another numerical parameter

$$\overline{æ}(F)=\frac{\sup_x(\ )}{\operatorname{int}_x(\ )}.$$

Clearly, $\overline{æ}(F) \geq æ(F)$ for any F. It is easy to show, in the same way as in [1], that the intersection of $\{F_n\}$ in Banach space X is non-empty if $\overline{æ}=\overline{\lim}\overline{æ}(F_n)>1/2$. It may be proved that the intersection is again non-empty if $\overline{æ}=1/2$ and X is a reflexive Banach space. The restriction of reflexivity cannot be removed: it follows from [3], that there exists a Banach space X and sequence $\{F_n\}$ in X, such that $\overline{\lim}\overline{æ}(F_n)=1/2$ and $\bigcap_{n=1}^{\infty}F_n=\varnothing$

The following theorem characterizes finite-dimensional spaces in terms of $\overline{æ}$.

Theorem 1. *Suppose X is a linear normed space and $æ_1$ is a given number that is less than $\frac{1}{2}$. If all sequences $\{F_n\}$ with $\overline{\lim}\overline{æ}(F) \geq æ_1$ have non-empty intersections, then the space X is finite-dimensional.*

Theorem 2 gives the meaning of critical æ for the spaces l_p, $1\leq p \leq \infty$ and shows that the previous fact is not true if we consider the parameter æ instead of $\overline{æ}$.

Theorem 2. *The intersection of $\{F_n\}$ in $X=l_p$, $1\leq p \leq \infty$ is non-empty if $æ=\overline{\lim}æF_n\geq 1(\sqrt[p]{2}+1)$. Moreover, the number $1/(\sqrt[p]{2}+1)$ is critical for l_p in the following natural sense: for any $æ_1<1/(\sqrt[p]{2}+1)$ there exists a sequence $\{F_n\}$ in l_p such that $\overline{\lim}æ\ (F_n)\geq æ_1$ and $\bigcap_{n=1}^{\infty}F_n=\varnothing$*

The following statement easily follows from the definition of $æ(F)$

Theorem 3. *Suppose X is a linear normed space and $æ_1$ is a given number less than 1/3. If all sequences $\{F_n\}$ with $\overline{\lim}æ(F_n) \geq æ_1$ have non-empty intersections then X is finite dimensional.*

Georgian Academy of Sciences
N.Muskhelishvili Institute of Computational Mathematics

REFERENCES

1. *N. Vakhania, I. Kartsivadze.* Mathematical Notes, 3,2,1968, 165-170 (Russian).
2. *G. Chelidze.* Mathematical Notes, 63, 2 1998, 310-312 (Russian).
3. *G. Chelidze.* Bull. Georg. Acad., Sci. 156, 2, 1997, 238-241.

საქართველოს მეცნიერებათა აკადემიის მოამბე, 159, №1, 1999
BULLETIN OF THE GEORGIAN ACADEMY OF SCIENCES, 159, №1, 1999

MATHEMATICS

M. Okropiridze

Radial Limits of the Partial Derivatives of the Poisson Spherical Integral

Presented by Corr. Member of the Academy V. Kokilashvili, November 7, 1998

ABSTRACT. **In the present paper we investigate the question of existence of radial limits of the partial derivatives of the Poisson spherical integral.**

Key words: Poisson spherical integral.

Throughout the rest of the paper, the function $f(\theta, \varphi)$ is assumed to be summable on the rectangle $R = \{(\theta, \varphi): 0 < \theta_0 < \pi, -\pi \le \varphi_0 \le \pi\}$ and 2π-periodic with respect to φ for all $\theta \in [0, \pi]$.

The Poisson spherical integral with density $f(\theta, \varphi)$ is

$$U_{f_x}(r,\theta,\varphi) = \frac{1}{4\pi}\int_0^{\pi}\int_{-\pi}^{\pi} f(\theta',\varphi')P_r(\theta,\varphi;\theta',\varphi')\sin\theta' d\theta' d\varphi',$$

$$P_r(\theta,\varphi;\theta',\varphi') = \frac{(1-r^2)}{G_r^{3/2}(\theta,\varphi;\theta',\varphi')},$$

where $G_r(\theta,\varphi;\theta',\varphi') = 1 - 2r[\cos\theta\cos\theta' + \sin\theta\sin\theta'\cos(\varphi' - \varphi)] + r^2, 0 \le r < 1$.

The problems on the existence of limits, angular limits and the limits with respect to the bihedral angles of the Poisson integral derivatives and $\frac{\partial}{\partial\theta}\cup f$ and $\frac{\partial}{\partial\varphi}\cup f$ are solved in [1]. In the present paper we will consider the problem on the existence of radial limits of these partial derivatives, for that we will use following definitions:

Definition 1 [2]. *A function $f(x, y)$ possesses, at the point (x_0, y_0), right (or left) partial derivative in the strong sense with respect to x, if there exists limit*

$$F_{[1]}^{+}(x_0,y_0) = \lim_{\substack{h\to 0+\\ y\to y_0}} \frac{f(x_0+h,y)-f(x_0-h,y)}{h}$$

[*correspondingly* $F_{[1]}^{-}(x_0,y_0) \equiv \lim_{\substack{h\to 0-\\ y\to y_0}} \frac{f(x_0+h,y)-f(x_0-h,y)}{h}$

This is just analogous with respect to y.

Definition 2 [3]. *A function $f(x, y)$ is said to possess at a point (x_0, y_0), symmetric*

partial derivative in the strong sense with respect to x, [with respect to y], if there exists limit

$$\lim_{(h,k)\to(0,0)} \frac{f(x_0+h, y_0+k)-f(x_0-h, y_0+k)}{2h} \equiv F^{(i)}_{[1]}(x_0, y_0)$$

[correspondingly $\lim_{(h,k)\to(0,0)} \frac{f(x_0+h, y_0+k)-f(x_0+h, y_0-k)}{2k} \equiv F^{(i)}_{[2]}(x_0, y_0)$

Proposition. *If there exist finite* $F^{+}_{[1]}(x_0, y_0)$ *and* $F^{-}_{[1]}(x_0, y_0)$, *then*

$$F^{(i)}_{[1]}(x_0, y_0) = \frac{1}{2}\left[F^{+}_{[1]}(x_0, y_0) + F^{-}_{[1]}(x_0, y_0)\right].$$

The same will be with $F^{(i)}_{[2]}$, $F^{+}_{[2]}$ and $F^{-}_{[2]}$.

Theorem 1. *If there exist finite* $f^{-}_{[1]}(\theta_0, \varphi_0)$ *and* $f^{+}_{[2]}(\theta_0, \phi_0)$, *where* $0<\theta_0<\pi$, $-\pi\le\varphi_0\le\pi$, *then*

$$\lim_{r\to 1}\left[\frac{\partial}{\partial\theta} U_f(r,\theta,\varphi)\right]_{\substack{\theta=\theta_0\\ \varphi=\varphi_0}} = \frac{1}{2}\left[f^{+}_{[1]}(\theta_0, \varphi_0) + f^{-}_{[1]}(\theta_0, \varphi_0)\right].$$

Theorem 2. *If there exists finite* $f^{(i)}_{[2]}(\theta_0, \varphi_0)$, *where* $0 < \theta_0 < \pi$, $-\pi \le \varphi_0 \le \pi$, *then*

$$\lim_{r\to 1}\left[\frac{\partial}{\partial\varphi} U_f(r,\theta,\varphi)\right]_{\substack{\theta=\theta_0\\ \varphi=\varphi_0}} = f^{(i)}_{[2]}(\theta_0, \varphi_0).$$

Remark. The $\theta_0 = 0$ and $\theta_0 = \pi$ cases see in [4].

We are planning to publish the results in detail in Proc. A. Razmadze Math. Inst.

Georgian Academy of Sciences
A. Razmadze Mathematical Institute

REFERENCES

1. *O. P. Dzagnidze*. Proc. A. Razmadze Math. Inst., **98**, 1990, 52-57.
2. *O. P. Dzagnidze*. Unilateral continuity and unilateral partial derivatives in various senses, in preparation.
3. *M. U. Okropiridze*. Bull. Georg. Acad. Sci., **158**, 2, 1998, 181-182.
4. *O. P. Dzagnidze*. Proc. A. Razmadze Math. Inst., **98**, 1990, 99-111.

საქართველოს მეცნიერებათა აკადემიის მოამბე, 159, №1, 1999
BULLETIN OF THE GEORGIAN ACADEMY OF SCIENCES, 159, №1, 1999

MATHEMATICS

I. Gabisonija

Two-weight Inequalities for Discrete Hilbert Transform

Presented by Corr. Member of the Academy V. Kokilashvili, February 9, 1998

ABSTRACT. **The optimal sufficient conditions under the pairs of decreasing weight sequences for the fulfillment of two weight strong (weak) type inequalities for discrete Hilbert transform are derived.**

Key words: Hilbert transform, two-weight inequality, weight.

In this paper the sufficient conditions for pairs of decreasing weight sequences guaranteeing validity of two-weight strong and weak type inequalities for discrete Hilbert transform are derived. The necessary conditions for corresponding inequalities are presented as well. Analogous problem for classical Hilbert transform and for general singular integrals were investigated in [1-5]. For discrete Hilbert transform this problem was investigated in [6] in case of pairs of increasing weight sequences.

For the sequence $\{\beta_k\}$ the discrete Hilbert transform is defined in the following way

$$(T\beta)_n = \sum_{k\neq n} \frac{\beta_k}{n-k} .$$

In case when this series diverges we put $(T\beta)_n = \infty$.

Definition. *Let $1 < p < \infty$. A positive sequence ρ_k belongs to $A_p(Z)$, if*

$$\sup_{m,n} \frac{1}{(n-m+1)^p} \left(\sum_{k=m}^{n} \rho_k\right)\left(\sum_{k=m}^{n} \rho_k^{1-p'}\right) < \infty ,$$

a sequence ρ_k belongs to $A_1(Z)$, if there exists a constant $C > 0$ such that the inequality

$$\frac{1}{n-m+1}\sum_{k=m}^{n} \rho_k \le C \min_{m\le k\le n} \rho_k$$

is satisfied for any m and n, $m \le n$.

One-weight problem for Hilbert transform as well as in discrete case was solved by R.A. Hunt, B. Muckenhoupt, and R. Wheeden [7].

By Z^+ we denote the set of all nonnegative integers.

Theorem 1. *Let $1 < p < \infty$, $\{\sigma_k\}$ and $\{u_k\}$ be positive decreasing sequences on Z^+. Assume that, ρ_k is defined on Z^+, $\{\rho_{|k|}\} \in A_p(Z)$. $a_k = \sigma_k\rho_k$, $b_k = u_k\rho_k$. Then if condition*

$$\sup_{n\geq 0}\left(\sum_{k=0}^{n} a_k\right)\left(\sum_{k=n+1}^{\infty}\frac{b_k^{1-p'}}{k^{p'}}\right)^{p-1} < \infty ,$$

is fulfilled, then there exists a positive constant C such that the inequality

$$\sum_{k=-\infty}^{+\infty}\left|(T\beta)_k\right|^p a_{|k|} \leq C\sum_{k=-\infty}^{+\infty}|\beta_k|^p b_{|k|} \qquad (1)$$

is valid for any $\{\beta_k\}$.

Theorem 2. *Let* $1 < p < \infty$. *If for positive sequences* $\{a_k\}$ *and* $\{b_k\}$ *on* Z^+ *inequality (1) holds then the condition*

$$\sup_{n\geq 0}\left(\sum_{k=0}^{n} a_k\right)\left(\sum_{k=n+1}^{\infty}\frac{b_k^{1-p'}}{k^{p'}}\right)^{p-1} < \infty$$

is satisfied.

Theorem 3. *Let* $\{\sigma_k\}$ *and* $\{u_k\}$ *be positive decreasing sequences on* Z^+. *Assume that,* ρ_k *defined on* Z^+, $\{\rho_{|k|}\}\in A_1(Z)$. $a_k = \sigma_k\rho_k$, $b_k = u_k\rho_k$. *Then under the following condition* $\sup_{n\geq 0}\left(\sum_{k=0}^{n} a_k\right)\sup_{k\geq n+1}\frac{1}{kb_k} < \infty$, *the inequality* $\sum_{\{k:|(T\beta)_k|>\lambda\}} a_{|k|} \leq \frac{C}{\lambda}\sum_{k=-\infty}^{+\infty}|\beta_k|b_{|k|}$ *holds.*

Theorem 4. *Let* $1 < p < \infty$, $\{\sigma_k\}$ *and* $\{u_k\}$ *be positive decreasing sequences on* Z^+ *with the condition* $\rho_{|k|}\in A_1(Z)$. *Then from inequality* $\sum_{k=-\infty}^{+\infty}\left|(T\beta)_k\right|^p\sigma_{|k|} \leq C\sum_{k=-\infty}^{+\infty}|\beta_k|^p u_{|k|}$

it follows the fulfillment of following estimate $\sum_{k=-\infty}^{+\infty}\left|(T\beta)_k\right|^p\sigma_{|k|}\rho_{|k|}^{1-p} \leq C_1\sum_{k=-\infty}^{+\infty}|\beta_k|^p u_{|k|}\rho_{|k|}^{1-p}$,

$C_1 > 0$.

Georgian Academy of Sciences
A. Razmadze Mathematical Institute

REFERENCES

1. *B. Muckenhoupt, R.L Wheeden.* Studia Math. **55,** 3, 1976, 179-194.
2. *E.G. Gusseinov.* Math. Sb. **132** (174), 1, 1977, 28-44 (Russian) .
3. *D.E. Edmunds, VM. Kokilashvili.* Canad. Math. Bull. **38,** 3, 1995, 295-303.
4. *V. Guliev.* Georgian Math. J. **1,** 4, 1994, 367-376.
5. *V. Kokilashvili, A. Meskhi.* Proc. A. Razmadze Math. Inst. Georg. Acad. Sci. **112,** 1997, 57-90.
6. *I. Gabisonija, A. Meskhi.* Proc. A. Razmadze Math. Inst. Georg. Acad. Sci. 116, 1998.
7. *R.A. Hunt, B. Muckenhoupt, R. Wheeden.* Trans. Amer. Math. Soc. **176,** 1973, 227-251.

საქართველოს მეცნიერებათა აკადემიის მოამბე, 159, №1, 1999
BULLETIN OF THE GEORGIAN ACADEMY OF SCIENCES, 159, №1, 1999

MATHEMATICS

Corr. Member of the Academy V. Kokilashvili, V. Paatashvili

Riemann – Hilbert Problem in the Domains with Piecewise Smooth Boundaries

Presented March 9, 1998

ABSTRACT. **Riemann - Hilbert problem in Smirnov class $E^p(D)$ for the domains with piecewise boundaries is investigated. The solvability conditions are derived and explicit formulas for solutions are presented.**

Key words: Riemann - Hilbert problem, Smirnov class, piecewise smooth boundary, conformal mapping, Cauchy type integral.

Let Γ be a closed Jordan piecewise smooth curve with angular points $C_1, C_2, ..., C_n$, by the size of angles $\pi\nu_k$, $0 \le \nu_k \le 2$, $k = \overline{1,n}$; D be a finite domain bounded by Γ. By $E^p(D)$ is denoted the Smirnov class of analytic functions Φ in D ([1],Ch. X).

Let $z = z(w)$ be the function conformally mapping the circle $U = \{w:|w| < 1\}$, onto D such that $z(0) = z_0$, $z_0 \in D$ and $z'(0) > 0$. The boundary of U we denote by γ. Let $w = w(z)$ be the inverse function to $z = z(w)$. It is well-known that any $\Phi \in E^p(D)$ has almost everywhere on Γ the angular boundary values belonging to $L^p(\Gamma)$. $E^p(U)$ coincides with Hardy class H^p.

Let us consider the following Riemann - Hilbert problem: define a function $\Phi \in E^p(D)$ ($p > 1$) satisfying the following boundary condition

$$\operatorname{Re}\left[(a(t)+ib(t))\Phi^+(t)\right] = f(t), \tag{1}$$

where a, b and f are real-valued measurable functions on Γ, with the conditions: $f \in L^p(\Gamma)$ and a and b are bounded.

The problem (1) has been investigated in several classes of functions (see [2-5]).

In case of Liapunov curve Γ when Φ is the function representable by Cauchy type integral with the density from $L^p(\Gamma, \rho)$ the problem (1) was considered in [3-5] (When $\rho \equiv 1$ this class coincides with $E^p(D)$ [6]). The appropriate results are similar as in the case of analytic in D and continuous in $\bar{D}$ functions Φ.

In our paper [7] we considered the problem (1) in case when Γ is piecewise Liapunov curve with angular points by the sizes of angles $\pi\nu_k (0 < \nu_k < 2)$. These investigations were based on N.Muskhelishvili's method of reduction of problem (1) to the problem of linear conjugation in passing of Warschawsky's theorem on behaviour of the derivative of conformal mapping function of U onto the domain with piecewise Liapunov boundary and two-weight estimate for singular integrals.

Thanks to the further progress in investigation of behaviour of derivative of confor-

mal mapping of unite circle on the domain with nonsmooth boundary and refined two weight inequality for singular integral now we are able to investigate the problem (1) for the domain with arbitrary piecewise smooth boundary. Moreover we succeeded some weakening of assumptions under the coefficients.

Let the coefficients $a(t)$ and $b(t)$ be the measurable functions and the function

$$G(t) = (a(t) - ib(t))(a(t) + b(t))^{-1}$$

belong to the class $\widetilde{A}(p)$, $p > 1$, i.e. 1) $\inf |G| > 0$, $\sup |G| < \infty$;

2) for all $t \in \Gamma$ except possible, a finite number of points t_k $k = 1, 2, \ldots, n$, there exists a neighbourhood on Γ in which the values of $G(t)$ are contained in a sector with vertex at the origin whose angle is less than $a(p) = 2\pi / \max(p, p')$, $p' = p(p-1)^{-1}$;

3) in the points t_k there exist limits $G(t_k \pm)$ and values of the angles δ_k between the vectors $G(t_k-)$ and $G(t_k+)$ are such that $\frac{2\pi}{p} < \delta_k \le \frac{2\pi}{p'}$ for $p > 2$ and $\frac{2\pi}{p'} \le \delta_k < \frac{2\pi}{p}$ for $1 < p < 2$ and $\delta_k \ne \pi$ for $p = 2$. For such G we define the quantity $\theta_p(t) = \arg_p G(t)$ and integer $\chi(p) = \chi(p; G) = \frac{1}{2\pi}[\theta_p]_\Gamma$ ([8]).

The points t_k will be called p-points of discontinuity of G.

The Main Theorem. *Let the problem* (1) *be considered in* $E^p(D)$, *where the domain* D *is bounded by the curve* Γ *and the origin lies in* D. *Let us assume that:*

(i) Γ *be a piecewise smooth curve with angular points* C_k $k = \overline{1,n}$ *by the values of angles* $\nu_k \pi$, $0 \le \nu_k \le 2$.

(ii) $G(t) = (a(t) - ib(t))(a(t) + ib(t))^{-1} \in \widetilde{A}(p)$, $C_k \ne t_i$, *where* t_i *are* p-*points of discontinuity of* G, G *is continuous in some small neighborhood of* C_k; $\chi(p) = \chi(p; G)$ *is an index of* G, $\theta_p = \arg G$.

$$Y(w) = \begin{cases} \exp\left(\frac{1}{2\pi}\int_\gamma \frac{\theta_p(\xi)}{\xi - w} d\xi\right), & |w| < 1, \\ w^{-\chi(p)} \exp\left(\frac{1}{2\pi}\int_\gamma \frac{\theta_p(\xi)}{\xi - w} d\xi\right), & |w| > 1, \end{cases} \tag{2}$$

$$c_k = w(C_k), h_p = \{c_k : \nu_k \ge p\}, h_0 = \{c_k : \nu_k = 0\},$$

$$h_{p,1}=\{c_k: \nu_k=p, Z(w)=Y(w)(w-c_k)^{-1/p}z_0^{1/p}(w)\notin H^p\}, z_0(w)=z'(w)\prod_{i=1}^{n}(w-c_i)^{1-\nu_i}$$

$$h_{0,1}=\{c_k: \nu_k=0, Z(w)=Y(w)(w-c_k)^{-1/p}z_0^{1/p}(w)\notin H^p\}$$

and let n_p, $n_{p,1}$, $n_{0,1}$ *be number of points of the sets* h_p, $h_{p,1}$, $h_{0,1}$, *respectively. Further, put*

$$\chi=\chi(p;G)+n_p-n_{p,1}-n_{0,1} \tag{3}$$

and

$$T(w)=Y(w)\rho(w), \tag{4}$$

where

$$\rho(w)=\begin{cases}\prod\limits_{c_k\in h_p}(w-c_k)^{-1}, & if \quad h_p\neq\varnothing,\\ 1, & if \quad h_p=\varnothing.\end{cases} \tag{5}$$

Then:

1) *All the solutions of the homogeneous problem are given by the equality*

$$\Phi_0(z)=AY(w(z))\prod_{c_k\in h_{p,1}\cup h_{0,1}}(w(z)-c_k)P_\chi(w(z)), \tag{6}$$

where $P_\chi(w)=\sum\limits_{k=0}^{\chi}a_k w^k$ *is an arbitrary polynomial with conditions*

$$a_j(-1)^\chi\prod_{c_k\in h_p}c_k\prod_{c_k\in h_{p,1}\cup h_{0,1}}c_k^{-1}=\overline{a}_{\chi-j}, \quad j=\overline{0,\chi} \tag{7}$$

when $\chi\geq 0$ *and* $P_\chi(w)=0$ *when* $\chi<0$.
The constant A *in* (6) *is defined by condition*

$$\overline{AY\left(\frac{1}{w}\right)}=w^\chi AY(w), \quad |w|\neq 1 \tag{8}$$

2) *For the nonhomogeneous problem we have the following conclusions:*
If $\chi\geq -1$ *and*

$$f(t)\ln\left|\prod_{\nu_k\in\{0,p\}}(w(t)-w(C_k))\right|\in L^p(\Gamma) \tag{9}$$

then the problem is solvable.
If $\chi<-1$ *and* (9) *is fulfilled then the problem* (1) *is solvable iff*

$$\int_{\Gamma} \frac{w^{\chi}(t) f(t) w'(t)}{T^{+}(w(t))} dt = 0, \ k = 0,1,\ldots,|\chi| - 2. \tag{10}$$

In all cases of solvability the solutions are given by the formula

$$\Phi(z) = \Phi_f(z) + \Phi_0(z),$$

where Φ_0 *is defined by* (6) *and*

$$\Phi_f(z) = \frac{T(w(z))}{2\pi i} \int_{\gamma} \frac{f(z(\xi))}{T^{+}(\xi)} \frac{\sqrt[\pi]{z'(\xi)}\, d\xi}{\xi - w(z)} + w(z) \overline{\left(\frac{T\left(\overline{\frac{1}{w(z)}} \right)}{2\pi i} \right)} \int_{\gamma} \frac{f(z(\xi))}{T^{+}(\xi)} \frac{\overline{\sqrt[\pi]{z'(\xi)}}\, d\xi}{\xi(\xi - w(z))}. \tag{11}$$

This work was supported by Grant 1.7/1998 of the Georgian Academy of Sciences.

Georgian Academy of Sciences
A. Razmadze Mathematical Institute

REFERENCES

1. *G.M.Goluzin.* The geometric theory of functions, Moscow, 1966 (Russian).
2. *N.I. Muskhelishvili.* Singular integral equations (Translated from Russian) P.Noordhoff, Groningen, 1953.
3. *B.V. Khvedelidze.* Trudy Tbiliss. math. inst. 23,1956, 3-158.
4. *B.V. Khvedelidze.* Itogi nauki i tekhniki, sovr. prob. mat. 7,1975, 5-162.
5. *I.B. Simonenko.* Izv. akad. nauk SSSR, ser. math. 28, 2, 1964, 277-306.
6. *V.A. Paatashvili.* Trudy Tbiliss. mat. inst. 42, 1972, 87-94.
7. *V. Kokilashvili, V. Paatashvili.* Georgian Math. J. 4, 3, 1997, 279-302.
8. *V.M. Kokilashvili, V.A. Paatashvili.* Trudy Tbiliss. Mat. Inst. 55, 1977, 59-92.

საქართველოს მეცნიერებათა აკადემიის მოამბე, 159, №1, 1999
BULLETIN OF THE GEORGIAN ACADEMY OF SCIENCES, 159, №1, 1999

MATHEMATICS

G.Lepsveridze

On the Spherical Divergence of Double Fourier-Haar Series

Presented by Member of the Academy L.Zhizhiashvili, July 15, 1998

ABSTRACT. **The theorem about spherical divergence of double Fourier-Haar series is stated.**

Key words: Fourier-Haar series, spherical divergence.

Let $\{\chi_k(t)\}$, $t \in [0,1]$ be Haar orthonormal system on $[0,1]$. Fourier-Haar coeficients of the function $f \in L([0,1]^n)$ are defined as follows:

$$C_{k_1\dots k_n} = \int_{[0,1]^n} f(x_1,\dots,x_n)\, \chi_{k_1}(x_1)\dots\chi_{k_n}(x_n)\,dx_1\dots dx_n .$$

By $S_{m_1\dots m_n}(f)(x)$ and $S_r(f)(x)$, $m_i \in N$, $i = 1,2,\dots n$, $r > 0$, $x \in [0,1]^n$ $(n \geq 2)$ we denote rectangular and spherical partial sums of multiple Fourier-Haar series of the function $f \in L([0,1]^n)$, respectively:

$$S_{m_1\dots m_n}(f)(x) = \sum_{k_1=1}^{m_1}\dots\sum_{k_n=1}^{m_n} C_{k_1\dots k_n}\chi_{k_1}(x_1)\dots\chi_{k_n}(x_n),$$

$$S_r(f)(x) = \sum_{k_1^2+\dots+k_n^2\leq r^2} C_{k_1\dots k_n}\chi_{k_1}(x_1)\dots\chi_{k_n}(x_n).$$

It is known [1, 2] that multiple Fourier-Haar series of the function $f \in L(\ln^+ L)^{n-1}([0,1]^n)$ converge to f a.e. on $[0,1]^n$ by rectangles as well as by sphere.

It is known [3], that in every integral class $\Phi(L)([0,1]^n)$ $(n \geq 2)$, which is wider than $L(\ln^+ L)^{n-1}([0,1]^n)$, there exists a summable function whose multiple Fourier-Haar series unboundedly diverges to $+\infty$ a.e. on $[0,1]^n$ by rectangles.

G.Kemkhadze [4] has stated, that for a given number ε, $0 < \varepsilon < 1$ there exists a function $f \in L([0,1]^2)$ whose spherical sums of Fourier-Haar double series unboundedly diverge to $+\infty$ on the set with the two-dimensional measure more than $1-\varepsilon$.

Later G.Tkebuchava [5] stated more strong result: in every integral class $\Phi(L)([0,1]^2)$, which is wider than $L(\ln^+ L)([0,1]^2)$, there exists a summable function, whose spherical sums of double Fourier-Haar series unboundedly diverge to $+\infty$ a.e. on $[0,1]^2$.

In this paper we present the following result.

Theorem. *The set of functions whose spherical sums of double Fourier-Haar series unboundedly diverge to $+\infty$ a.e. on $[0,1]^2$, forms the set of second category in $L([0,1]^2)$*

(*in the sense of Baire*).

Similar result for rectangular sums of multiple Fourier-Haar series is stated in [3].

Telavi Pedagogical State University

REFERENCES

1. *O.Dzagnidze.* Bull Georg. Acad. Sci., **34**, 2, 1964 (Russian).
2. *G.Kemkhadze.* Trudy Razmadze. Tbil. Mat. Inst. 55, 1977 (Russian).
3. *T.Zerekidze.* Trudy. Razmadze. Tbil. Mat. Inst. 76, 1985 (Russian).
4. *G.Kemkhadze.* Trudy Gruzinskogo politekhnicheskogo instituta. 3(285), 1985 (Russian).
5. *G.Tkebuchava.* Anal. Math., 3, 1994, 147-153.

საქართველოს მეცნიერებათა აკადემიის მოამბე, 159, №1, 1999
BULLETIN OF THE GEORGIAN ACADEMY OF SCIENCES, 159, №1, 1999

MATHEMATICS

A. Lashkhi, D. Chkhatarashvili

On the Fundamental Theorem of Affine Geometry Over Ring

Presented by Corr. Member of the Academy H. Inassaridze, August 31, 1998

ABSTRACT. **For free modules over the rings with invariant basis property the fundamental theorem of affine geometry is proved.**

Key words: semilinear isomorphism, unimodular element, affine space, free module.

Thorough investigation in geometric algebra over the last 30-40 years has charted the evolution of the classic setting into a stable form for general rings.

What is the fundamental theorem of geometric algebra? For different geometries it can be stated in various ways. However, in general, the problem is to represent specific geometrical maps by the linear functions, i. e. with the elements of $GK(k,X)$, where X is a k-module (see the books E. Artin (1957), R. Bear (1952), F. Buekenhout (1995), J. Dieudonne (1951), B. McDonald (1976)).

In the respective case the most significant result is M. Ojanguren and R. Sridharan's theorem [1] which generalizes the classical theorem of projective geometry to commutative rings. In [2] B. Sarath and K. Varadarajan generalized the theorem for some classes of noncommutative rings.

The problem can be considered for the affine case too. Affine geometry can be realized as the coset lattice of k-module X. Our aim is to prove the Fundamental theorem of Affine geometry for free modules over the non-commutative rings.

The classical version could be found in M. Berger (1977) and J. Lelong-Ferrand (1985). For the first generalization see the papers J. Lipman (1961), P. Scherrk (1962). For the evolution of the problem and related questions see F. D. Veldcamp, V. Benz, O. T. O'Maeda, J. Tits, C. Bartolone, U. Brehm, D. S. Carter, A. Vogt, A. Lashkhi, A. Brezuleanu, D. K. Radulescu, C. A. Faure and others.

The notion and definitions are standard. All the rings considered will be associated and processing a unit element $1\neq 0$. If k is a ring, by a subring $s \subset k$ we mean one with the property that the unit element of S is the same, as the unit element of k. All the module considered will be left modules over k.

A free module over a ring is said to be rank n, if it has a basis of cardinal n. The rank may not be unique (although it is unique whenever the module has no finite basis see [3-5]). Thus one is led to consider the following three successively stronger properties of a ring $k(\neq 0)$.

I. The rank of any free k-module is uniquely determined.

II. A free k-module of any rank n cannot be generated be less than n elements.

III. I a free k-module of rank n, any generated set of n elements is free.

The conditions I-III occur frequently among the hypotheses in theorems about rings.

In particular, I is known as the invariant basis property, or invariant basis number (IBN). Each of I-III fails to hold only for what may be regarded as pathological rings, but it is not all easy to decide whenever a given ring has any of these properties. The given examples show that the classes I-III are distinct [3].

Definition 1. *The ring k is said to be Invariant Basis Number (IBN-ring) if any two bases of k-module X have the same number of elements.*

Definition 2. *The ring k is said to be IB-ring if the property I-III holds in k. The class of all IB rings will be denoted by [IB].*

Furthermore we always suppose that $k \in$[IB] and X is free k-module. By $R(X)$ we define the complete lattice of all k-submodules; by $\langle Y\rangle$ we denote the submodule generated by the set $Y \subset X$. For each k-free module X we can construct a new object the projective space $P(X)$ corresponding to X (see [1-2, 4]). The elements of $P(X)$ are k-free direct summands of rank 1. It is clear that each element of $P(X)$ has the form ke, i.e. is a one-dimensional submodule generated by the unimodular element $e \in X$. Remember that, an element e is unimodular if there exists a linear form $\mu: X \to k$ such that $\mu(e) = 1$, i.e. the K-module X then $e = \Sigma a_i e_i$ is unimodular if and only if $\Sigma k a_i = k$.

Let X and X' be modules over rings k and k' respectively. Suppose that $\sigma: k \to k'$ is ring isomorphism. The bijection $\mu: X \to X'$ will be called σ-semilinear isomorphism or semilinear isomorphism with respect to σ if

$$\mu(x_1 + x_2) = \mu(x_1) + \mu(x_2),$$
$$\mu(\alpha x) = \sigma(\alpha)\mu(x),\ x, x_1, x_2, \in X,\ \alpha \in k.$$

Let us consider the set $CL(X)$ consisting of all coset of k-module X whith respect to all submodules and of the empty set $\varnothing$. On $CL(X)$ we can introduce the following partial order:

$$X_1 \le X_2 \Leftrightarrow X_1 \subseteq X_2$$

The coset lattices for linear algebras were studied [4].

Proposition 1. ([4] $CL(X)$ *is a complete lattice; the operations "$\cap$" and "$\cup$" are defined as follows: let* $U_\alpha = \alpha_\alpha + A_\alpha$, $A_\alpha \in R(X)$, *then*

(i) $\cap_{\alpha \in J} U_\alpha$ *is the set-theoretical intersection;*

(ii) $\cup_{\alpha \in J} U_\alpha = \alpha_\beta + \langle A_\alpha\ \alpha_\alpha - \alpha_\beta\ \alpha \in J\rangle$, *where β is some fixed index from J.*

Analogously to the projective case the affine space of a k-module X could be defined by the following way.

Definition 3. *The affine space Aff(X) which corresponds to k-module X is the set of all unimodular elements of X.*

By $AG(k,X)$ we define the sublattice of $CL(X)$ generated by the set $Aff(X)$. When X is a free k-module the lattice $AG(k, X)$ realized the affine geometry k-module X. If now on the $AG(k, X)$ we will look from the lattice-theoretical point of view, the unimodular elements of X will be atoms in this lattice. They are points of geometry. The union of two points $x \cup y = x + \langle x - y\rangle = l$ will be a line in $AG(k,X)$. Though, in case of rings, no one atom (point) will be covered by a line i. e. between the atom x and the line $l \in AG(k,X)$, $x \in l$ we can always find another line l_1 for which $x \in l_1 \subset l$.

Definition 4. *The bijection $f: X \to X'$ will be called an (affine) collineation if for each $x_1, x_2, x_3 \in X$ we have $x_1 \in x_2 \cup x_3 \Rightarrow f(x_1) \in f(x_2) \cup f(x_3)$.*

It is obvious that if $e \in X$ is unimodular then the submodule $\langle e \rangle$ is a maximal submodule of rank1.

Definition 5. *The lines* $x_1+\langle y_1 \rangle = l_1$ *and* $x_2+\langle y_2 \rangle = l_2$ *will be called parallel and denoted* $l_1 \| l_2$ *if there exists a submodule* l *of rank 1 such that*

$$\langle y_1 \rangle \subseteq l, \ \langle y_2 \rangle \subseteq l_2.$$

Example. The parallel relation is general not a transitive relation.

Proof. Suppose $a \in k$ is a zero divisor. Let $e_1, e_2 \in X$ *be basis elements. So the element* $e = \alpha e_1 + e_2$ *is unimodular. If* $q \in k$ *is such that* $q\alpha = 0$, $q \neq 0$ *and* $y = qe$ *then* $\langle y \rangle \subset \langle e \rangle \Rightarrow qe = q(\alpha e_1 + e_2)\alpha = q\alpha e_1 + qe_2 \Rightarrow \langle y \rangle \subset \langle e_2 \rangle$ *and* $\langle e \rangle$ *is parallel to* $\langle e_2 \rangle$.

Theorem 1. *Let* X *and* X' *be free modules over the ring* k *and* k' *respectively. Suppose that* k, $k' \in [IB]$ *and rank* $X = rank X' = n \geq 2$. *Let* $\varphi: X \to X'$ *be a collineation such that* $\varphi(0)=0$ *and if* $l \| l_1$ *then* $f(l) \| f(l_1)$ *for all lines,* $l\ l_1 \in AG(k,X)$. *Then there exists an isomorphism* $\varphi(0)=0$ *and if* $l \| l_1$ *then* $f(l) \| f(l_1)$ *for all lines,* $l, l_1 \in AG(k,X)$. *Then there exists an isomorphism* $\sigma : k \to k'$ *for which* φ *is a* σ- *semilinear isomorphism.*

Proposition 5. *Suppose that* $\alpha \in h$ *is invertible in* k *and every element* $x \in X$ *has the form* $x = \alpha e$ *where* e *is unimodular and* $\alpha \in k$, *then* $CL(X) = AG(k,X)$.

Remark. It is easy to check that we can replace 2 by any invertible $\alpha \in k$ for which α-1 is invertible as well.

Theorem 2. *Let* X *and* X' *be free modules of rank* $n \geq 3$ *over the rings* k *and* k' *respectively and* k, $k' \in [IB]$. *Let* $\varphi : AG(k,X) \to AG(k',X)$ *be a lattice isomorphism for which* $\varphi(0) = 0$ *and* φ *maps parallel lines in parallel lines. Then there exists an isomorphism* $\sigma : k \to k'$ *such that for any unimodular element* $e = \Sigma a_i e_i$, *where* $e_1, \ldots, e_i$ *is a basis of* X *we have* $\varphi(e) = \sigma(a_1)\varphi(e_1) + \ldots + \sigma(a_k)\varphi(e_n)$.

The theorems 1 and 2 could be considered as the fundamental theorems of affine geometry.

Georgian Technical University

REFERENCES

1. *M. Ojanguren, R. Sridharan.* Commentary Math. Helv. 44, 1965, 310-315.
2. *B. Sarath, K. Varadarajan.* Fund. theorem of proj. geom. Communications in Algebra, **12, 8**, 1984, 937-952.
3. *P. M. Cohn.* Some remarks on the invariant Basis Property. Topology, 5, 1966, 215-228.
4. *A. Lashkhi.* J. Math. Sci., 74, 3, 1995, 1044-1077.
5. *J. S. Shepherdson.* Proc. London Math. Soc. 1995.

საქართველოს მეცნიერებათა აკადემიის მოამბე, 159, №1, 1999
BULLETIN OF THE GEORGIAN ACADEMY OF SCIENCES, 159, №1, 1999

MATHEMATICS

B.Mesablishvili

Galois Theory in a Category of Modules over an Elementary Topos

Presented by Corr. Member of the Academy H. Inassaridze, February 11, 1998

ABSTRACT. **The present paper reports that in the case of module categories over an elementary topos the Galois theory of Chase and Sweedler and the Galois theory of Ligon are equivalent .**

Key words: closed symmetric monoidal category, Galois object, Morita context, locally progenerator.

Presented closed symmetric monoidal category $(\underline{C}, -\otimes -, I)$, $M(\underline{C})$ (resp.$CM(\mathbb{C})$, $CoM(\underline{C})$, $HM(\underline{C})$, $CHM(\underline{C})$) denotes the category of monoids (resp. commutative monoids, comonoids, Hopfmonoids, commutative Hopfmonoids) in $\underline{C}$, where a monoid in $\underline{C}$ is to be understood as in [1], and a Hopfmonoid in $\underline{C}$ is defined in the same way as a Hopfalgebra in K-mod is defined in [2]. A left A-object in $\underline{C}$ with to some $A \in Ob(M(\underline{C}))$ is a pair $(\underline{C}, \nabla_{\underline{C}})$ where $\nabla_{\underline{C}}$ is a left action in the sense of [1]. ${}_A\underline{C}$ (resp. ${}_A\underline{C}_B$, ${}^A\underline{C}$, $\underline{C}^A$) denotes the category of left A-objects (resp. right A-objects, A-B-biobjects, left A-coobjects, right A-coobjects). Similarly one has the notion of groups, cogroups etc.

The categories $\underline{C}$, ${}_A\underline{C}$, ${}_A\underline{C}_B$ etc are related by the following two functors, provided $\underline{C}$ has equalizers and coequalizers (cp. [3]):

Let $A, B \in Ob(M(\underline{C}))$ then any $P \in Ob(\underline{C}_A)$ defines a functor

$$P \otimes_A -: {}_A\underline{C} \to \underline{C}$$

and any $P \in Ob({}_B\underline{C})$ defines a functor

$$ {}_B[P,-]: {}_B\underline{C} \to \underline{C}$$

where ${}_B[P, P]$ again becomes a monoid .

If now $P \in {}_A\underline{C}_B$, these functors may be interpreted as functors between categories $\underline{C}_A$, ${}_B\underline{C}$, ${}_A\underline{C}_B$ etc. in various ways, such that become adjoint [3].

Using these facts, one gets for $A \in Ob(M(\underline{C}))$, $P \in Ob({}_A\underline{C})$ a morphism $g_A : {}_A[P,A] \otimes_{A[P,P]} P \to A$ corresponding to $1_{A[P,A]}$, and a morphism $f_A : P \otimes_A [P,A]_A \to {}_A[P,P]$ corresponding to $1_P \otimes g_A$.

Definition 1 [4]. *P is called*

a) finite over A, if f_A is an isomorphism;

b) faithfully projective over A, if P is finite and g_A is an isomorphism.

Let

$$A \in Ob(M(\underline{C})), H \in Ob(HM(\underline{C})), \alpha_A \in M(\underline{C})(A, A \otimes H), \quad (A, \alpha_A) \in Ob(\underline{C}^H),$$

$$\gamma_A = (\nabla_A \otimes 1_A)(1_A \otimes \alpha_A) \in M(\underline{C})(A \otimes A, A \otimes H).$$

Definition 2 [4]. *A is called H-Galois over I if A is faithfully projective over I, and γ_A is an isomorphism in $\underline{C}$.*

Let $H \in Ob(HM(\underline{C}))$ be finite over I and $(A,\alpha_A) \in Ob(\underline{C}^H)$. The fix -object A^{H^*} is defined as the equalizer of the following pair of morphisms $(\alpha_A, 1_A \otimes \eta_H)$.

In the case $A^{H^*} \approx I$ in [4] the Morita -context (D, I, A, Q, f, g) is defined, where

$$D = A\#H^*, Q = D^{H^*}, \varphi = \nabla_A(1_A \otimes \beta_A) \in \underline{C}(D \otimes A, A),$$

$$f = \nabla_D(j_A \otimes J_Q) \in_D \underline{C}_D(A \otimes Q, D),\ g = \varphi(j_Q \otimes j_A) \in \underline{C}(Q \otimes_D A, I)$$

(here the morphism $\beta_A \in C(H^* \otimes A, A)$ is obtained from $\alpha_A \in \underline{C}(A, A \otimes H^*)$ by the bijection $\underline{C}(H^* \otimes A, A) \approx \underline{C}(A, A \otimes H^*)$, and $j_A : A \to D$ and $j_Q : Q \to D$ are canonical inclusions).

Theorem 1 [4]. *If $H \in Ob(CHM(\underline{C}))$ is finite over I, $A \in Ob(CM(\underline{C}))$ and $(A,\alpha_A) \in Ob(\underline{C}^H)$, then the following statements are equivalent:*

a) A is H-Galois over I;

b) A is faithfully projective over I and the morphism $A\#H^* \to [A,A]$ induced by the left $A\#H^*$ - monoid structure on A is an isomorphism;

c) $A^{H^*} \approx I$ and the Morita context (D, I, A, Q, f, g) is strict .

Now, let $\underline{E}$ be an arbitrary category with finite products and equalizers. An object $A \in Ob(\underline{E})$ is called faithfull if the functor $A \times - : \underline{E} \to \underline{E}$ creates isomorphisms. If this functor preserves coequalizers then A will be called coflat in $\underline{E}$.

Definition 3 [5]. *Let G be a group in $\underline{E}$. A faithfull object A is called Galois G-object if there exists a morphism $\beta_A : G \times A \to A$ in $\underline{E}$ such that $(A,\beta_A) \in_G \underline{E}$ and the morphism $\gamma_A : G \times A \to A \times A$ defined by the product diagram is an isomorphism.*

Let $\underline{E}$ be an elementary topos with a natural numbers object. If R is a commutative ring object with identity in $\underline{E}$, then $(R-\mathrm{mod}, -\otimes_R -, R)$ is a symmetric monoidal closed category [6,7].

Definition 4. *$P \in Ob(R-\mathrm{mod})$ will be called R - progenerator if there are natural numbers n, m such that $P^{[n]}$ is a retract of R and $R^{[m]}$ is a retract of P in R - mod.*

Theorem 2. *An R - module P is faithfully projective over R in the monoidal category $(R-\mathrm{mod}, -\otimes_R -, R)$ if and only if P locally is R - progenerator [8].*

Corollary 1. *For arbitrary $P \in Ob(R-\mathrm{mod})$ the Morita context ([P, P], R, P, [P, R], f, g),*

where f, g are morphisms from definition 1, is strict if and only if P locally is R - progenerator.

By $CR(\underline{E})$ we denote the category of commutative R-algebras in $\underline{E}$. Then $CR(\underline{E})^{op}$ is a category with finite products and coequalizers [7].

Proposition 1. *A group in $CR(\underline{E})^{op}$ is a commutative Hopf algebra with antipode in $CR(\underline{E})$, and if it is finite over R, then it locally is R - progenerator .*

Proposition 2. *a) An object $A \in Ob\left(CR(\underline{E})^{op}\right)$ is faithfull in $CR(\underline{E})^{op}$ if and only if the following condition holds : whenever $f : M \to N$ is a homomorphism of R-modules such that $1_A \otimes_R f$ is an isomorphism, then f likewise is an isomorphism.*

b) A is a coflat object in $CR(\underline{E})^{op}$ if and only if A is a flat R-module.

Let $H \in Gr\left(CR(\underline{E})^{op}\right)$ be finite over R.

Theorem 3 [8]. *Let A be a Galois H-object in $CR(\underline{E})^{op}$. The following statements are equivalent:*

a) A is a coflat Galois H-object in $CR(\underline{E})^{op}$;

b) A locally is finitely generated projective R-module, a faithfull object in $CR(\underline{E})^{op}$ and the homomorphism $A\#H^* \to [A, A]$ is an isomorphism ;

c) $A^{H^*} \approx R$ and the Morita context (D, R, A, Q, f, g) is strict.

Proposition 3 [8]. *Let A be a Galois H-object in $CR(\underline{E})^{op}$. Then A is a coflat object in $CR(\underline{E})^{op}$.*

Combining the results , we obtain the following

Theorem 4. *In the closed symmetric monoidal category $(R-\mathrm{mod}, -\otimes_R -, R)$ the Galois theory of Ligon [4] and Galois theory of Chase and Sweedler [5] are equivalent.*

This work is supported by INTAS - 93-436 - ext .

Georgian Academy of Sciences
A. Rasmadze Mathematical Institute

REFERENCES

1. *S. MacLane.* Categories for the Working Mathematician. Springer, Berlin - Heidelberg - New York, 1971.
2. *M.E. Sweedler.* Hopf Algebras. New York, 1969.
3. *B. Pareigis.* Publ. Math. Debrecen, **24**, 1977, 189-204 and 351 - 361; **25**, 1978, 177-186.
4. *S. Ligon.* C. R. Acad. Sc. Paris, **288**, Ser. A, 1979.
5. *S.U. Chase, M.E. Sweedler.* Hopf algebras and Galois theory. Lect. Notes in Math., 97, 1969.
6. *D. Howe.* J. Pure Appl. Algebra, **21**, 1982, 161 - 166.
7. *M. Barr.* J. Pure Appl. Algebra, **25**, 1982, 227 - 247.
8. *B. Mesablishvili.* Proc. Vekua institute of appl. mathematics, **36**, 1990, 28-44.

საქართველოს მეცნიერებათა აკადემიის მოამბე, 159, №1, 1999
BULLETIN OF THE GEORGIAN ACADEMY OF SCIENCES, 159, №1, 1999

MATHEMATICS

O.Chkadua, R.Duduchava

Asymptotics of Potential-Type Functions

Presented by Member of the Academy T. Burchuladze, July 13, 1998

ABSTRACT. **A complete asymptotics of solutions represented by potentials is investigated when the density asymptotics is known. Here the potentials are taken from a general matrix elliptic differential operator with constant coefficients. Relation between the first coefficients of the asymptotic expansion of potential-type functions, and the first coefficient of the density asymptotics are established.**

Key words: potential-type functions, pseudodifferential equations, asymptotics.

Let Ω be domain in the Euclidean space R^n, $n \geq 2$, not necessarily compact, with a compact and sufficiently smooth boundary $\partial\Omega = S$. We consider a homogeneous $N \times N$ system of differential equations

$$A(D_x)u = 0 \text{ in } \Omega, \tag{1}$$

of order $2r$, $r \in N$

$$A(D_x) := \sum_{|\alpha|=2r} a_\alpha D_x^\alpha \text{ with } D_{x_l} := i\partial_{x_l} = i\frac{\partial}{\partial x_l} \tag{2}$$

with constant matrix coefficients $a_\alpha = \| a_\alpha^{jk} \|_{N\times N}$. We suppose that the homogeneous principal symbol of $A(D_x)$

$$A_{pr}(\xi) = A(\xi) := \sum_{|\alpha|=2r} a_\alpha \xi^\alpha , \tag{3}$$

which coincides with the symbol in this case, is elliptic: $\det A_{pr}(\xi) \neq 0$ for all $|\xi| = 1$. The fundamental matrix-function [1] for equation (1) can be written as follows

$$H_A(x) = F_{\xi'\to x'}^{-1}\left[\pm\frac{1}{2\pi}\int_{L\pm} \big(A(\xi',\tau)\big)^{-1} e^{-i\tau x_n} d\tau \right], \tag{4}$$

where the signs "–" and "+" refer to the cases $x_n > 0$ and $x_n < 0$, respectively; $x = (x', x_n)$, $x' = (x_1,\ldots, x_{n-1})$, $\xi' = (\xi_1,\ldots, \xi_{n-1})$; the contours $L\pm$ are situated in the complex half-planes $C^\pm := R \oplus iR^\pm$, are oriented counterclockwise and circumvent all roots of the polynomial $\det A(\xi', \tau)$ with respect to τ in the corresponding half-planes $\tau \in C^\pm$ [2].

We introduce the simple layer potential

$$Vg(x) = \int_S H_A(x-y)g(y)d_y S, \qquad x \notin S. \tag{5}$$

Let S_0 be an infinitely differentiable submanifold of $S = \partial\Omega$ of the same dimension $n-1$ and C^∞ - smooth boundary ∂S_0.

Let B_0 be a classical pseudodifferential operator of order $q \in R$ on the manifold S_0.

We will investigate asymptotics of the following potential-type function

$$u(x) = V_{\circ} B_0 \varphi_0(x), \quad \operatorname{supp}\varphi_0 \subset \overline{S}_0, \; x \in \Omega \tag{6}$$

in the neighbourhood of ∂S_0 under the assumption that the asymptotics of the density $\varphi_0 = (\varphi_{01}, \ldots, \varphi_{0N})$ is already known and given, in s.l.c.s. by formula (see[3]):

$$\varphi_0(x'', x_{n-1,+}) = K(x'') x_{n-1,+}^{\frac{\nu}{2}+\Delta(x'')} B^0_{a_{pr}}\left(-\frac{1}{2\pi i}\log x_{n-1,+}\right) K^{-1}(x'') c_0(x'') +$$

$$+ \sum_{k=1}^{M} K(x'') x_{n-1,+}^{\frac{\nu}{2}+\Delta(x'')+k} B_k(x'', \log x_{n-1,+}) + \varphi_{M+1}(x'', x_{n-1,+}) \tag{7}$$

$$\text{with } \varphi_{M+1} \in \tilde{H}{}^{(\infty, s+M+1), \infty}_{p} \qquad (R^{n-1}_{+})$$

for all sufficiently small $x_{n-1,+} > 0$, where first coefficient $c_0 \in C_0^\infty(R^{n-2})$, $K \in C_0^\infty(R^{n-2})$,

$$\Delta := (\underbrace{\delta_1, \ldots, \delta_1}_{m_1\text{-times}}, \ldots \underbrace{\delta_\ell, \ldots, \delta_\ell}_{m_\ell\text{-times}})^T, \; \operatorname{Re}[\nu/2 + \delta_i(x'')] > -1 \quad \text{for all} \quad i = 1, \ldots, \ell,$$

$$\frac{1}{p} - 1 < s - \frac{\nu}{2} - \operatorname{Re}\delta_i(x'') < \frac{1}{p}, \quad i = 1, \ldots, \ell.$$

For the definition of the matrix $B^0_{a_{pr}}(t)$ see [3]. Here $B_k(x'', t)$ is a polynomial of the order $\nu_k = k(2m_0 - 1) + m_0 - 1$, $m_0 = \max\{m_1, \ldots, m_\ell\}$ with respect to the variable t with vector coefficients depending on the variable x''.

Let $\lambda_i = -N_i + \mu_i$, $-1 < \operatorname{Re}\mu_i \le 0$, where $N_i > 0$ is an integer and the coefficient $d^{m_i(M)}_{pl}(\lambda_i)$ be defined by means of the recurrence relations

$$d^{m_i(M)}_{pl}(\lambda_i) = \sum_{q=l}^{p} d^{m_i(M-1)}_{pl}(\lambda_i) d^{m_i(1)}_{ql}(\lambda_i + M - 1),$$

$$d^{m_i(1)}_{ql}(\lambda_i + M - 1) = (-1)^{q-l} \frac{q!}{l!} \frac{1}{(\lambda_i + M)^{q-l+1}}. \tag{8}$$

$$i = 1, \ldots, \ell, \quad M = 1, 2, \ldots$$

Let us introduce the upper triangular matrix-function

$$\widetilde{B}^0_{a_{pr}}(t) = \operatorname{diag}\{\widetilde{B}^{m_1}(t), \ldots, \widetilde{B}^{m_\ell}(t)\}, \tag{9}$$

where

$$\widetilde{B}^{m_i}(t) = \begin{cases} B^{m_i}(-t) & \text{if } \lambda_i \neq -1, -2, \ldots, \\ \| h^{m_i}_{kp}(t) \|_{m_i \times m_i} & \text{if } \lambda_i = -1, -2, \ldots \end{cases}$$

$$\lambda_i := -\frac{\nu}{2} - \delta_i(x'') - 2r + q + j, \quad i = 1, \ldots, \ell$$

$$h_{kp}^{m_i}(t) := \begin{cases} \dfrac{1}{(p-k)!}\displaystyle\sum_{s=0}^{p-k+1}\left(\frac{1}{2\pi i}\right)^{p-k-s} \widetilde{c}_{p-k+1,s}^{\,m_i}(\lambda_i)t^s, & \text{if } p \geq k, \\ 0, & \text{if } p < k, \end{cases}$$

$$\widetilde{c}_{p-k+1,s}^{\,m_i}(\lambda_i) = \begin{cases} i^{\lambda_i}\displaystyle\sum_{l=1}^{p-k+1}(-1)^l(l-1)!(2\pi i)^l d_{p-k,l-1}^{m_i(N_i)}(\lambda_i)b_{0l}^{m_i}(0), \\ \qquad \text{if } s = 0, \\ i^{\lambda_i}\displaystyle\sum_{l=s}^{p-k+1}\frac{(-1)^l(l-1)!}{s!}(2\pi i)^{l-s} d_{p-k,l-1}^{m_i(N_i)}(\lambda_i)b_{sl}^{m_i}(0), \\ \qquad \text{if } s = 1,2,\ldots,p-k+1, \end{cases}$$

$$N_i = 1, 2, \ldots$$

$$b_{kp}^{m_i}(t) = \begin{cases} \left(\dfrac{1}{2\pi i}\right)^{p-k}\dfrac{(-1)^{p+k}}{(p-k)!}\dfrac{d^{p-k}}{dt^{p-k}}\left(\Gamma(t+1)e^{\frac{i\pi(t+1)}{2}}\right), & \text{if } k \leq p, \\ 0, & \text{if } k > p, \end{cases}$$

$$p = 0, \ldots, m_i - 1, \; i = 1, \ldots, \ell,$$

the coefficients $d_{pl}^{m_i(0)}(-1) = \delta_{pl}$ $l = 0, \ldots, p$ (δ_{pl} is the Kroneker symbol) and the coefficients $d_{pl}^{m_i(N_i)}(\lambda_i)$ ($N_i = 1,2,\ldots$) are defined in (8).

Theorem 1. *Let $\varphi_0(x'', x_{n-1,+})$ be as in (7). We suppose $q \in R$, $M \in N_0$ and*

$$M > \max\left\{\frac{n-1}{p} - s,\ 2r - 3 - [q],\ \frac{n-1}{p} - \min\{[s-q], 0\},\ r-1\right\}.$$

Then the potential-type function $u(x)$ in (6) has the following asymptotic expansion:

$$u(x'', x_{n-1}, x_n) = \sum_{s=1}^{\ell(N)}\left\{\sum_{j=0}^{n_s-1} x_n^j\left[d_{sj}(x'', +1)z_{s,+1}^{\frac{\nu}{2}+\Delta(x'')+2r-1-q-j}\widetilde{B}_{a_{sp}}^0\left(\frac{1}{2\pi i}\log z_{s,+1}\right)\right.\right.$$

$$\left.\left. - d_{sj}(x'', -1)z_{s,-1}^{\frac{\nu}{2}+\Delta(x'')+2r-1-q-j}\widetilde{B}_{a_{sp}}^0\left(\frac{1}{2\pi i}\log z_{s,-1}\right)\right]c^{(j)}(x'')\right.$$

$$+\sum_{\vartheta=\pm1}^{M+3-2r+[q]}\sum_{l,k=0}^{M+2-l}\sum_{j+p=2r-[q]-1}^{} x_{n-1}^{l}x_n^{j}d_{sljp}(x'',\vartheta)$$

$$l+k+j+p\neq 2r-[q]-1$$

$$\times z_{s,\vartheta}^{\frac{\nu}{2}+\Delta(x'')+p+k-[q]}B_{skjp}(x'',\log z_{s,\vartheta}) \Bigg\} \tag{10}$$

$$+\ u_{M+1}(x'',x_{n-1},x_n)\quad for\quad x_n>0$$

with the coefficients $d_{sj}(\cdot,\pm1)$, $c^{(j)}$, $d_{sljp}(\cdot,\pm1)\in C_0^{\infty}(R^{n-2})$ *and the remaineder* $u_{M+1}\in C^{M+1}(\overline{R}_+^n)$; *here*

$$z_{s,+1}=-x_{n-1}-x_n\tau_{s,+1},\quad z_{s,-1}=x_{n-1}-x_n\tau_{s,-1},\quad \tau_{s,\pm1}\in C_0^{\infty}(R^{n-2})$$

and $\{\tau_{s,\pm1}\}_{s=1}^{\ell(N)}$ *are all different roots of the polynomial* $\det A(J_{\varkappa}^{T}(x'',0)\cdot(0,\pm1,\tau))$ *of multiplicity* n_s, $s=1,\dots,\ell(N)$, *in the complex lower half plane* ($J_{\varkappa}$ *is the Jacoby matrix of the diffeomorphism* $\varkappa$); $[q]\in Z$ *is the integer part of the number* q *and* $\{q\}\in[0,1)$ *is the fractional part of the number* $q=[q]+\{q\}$.

$B_{skjp}(x'',t)$ *is a polynomial of the order* $\nu_{kjp}=\nu_k+p+j-(2r-1-[q])$ *if* $\lambda_{m_0}\neq-1,-2,\dots$ ($\nu_k=k(2m_0-1)+m_0-1$, $m_0=max\{m_1,\dots,m_d\}$), *with respect to the variable* t *with vector coefficients depending on the variable* x'' *and* $B_{skjp}(x'',t)$ *is a polynomial of the order* $\nu_{kjp}+1$ *if* $\lambda_{m_0}=-1,-2,\dots(\lambda_{m_0}=-\nu/2-\delta_{m_0}(x'')-2r+q+j)$.

Note that the matrix $\widetilde{B}^0_{a_{pr}}(t)$ for $\lambda_l=-\nu/2-\delta_l(x'')-2r+q+j=-1,-2,\dots$ depends on j(see(9)).

Theorem 2. *For the leading (first) coefficients* $c_0(x'')$ *and* $d_{sj}(x'',\pm1)$, $c^{(j)}(x'')$ *of asymptotic expansions* (7) *and* (10) *respectively, we have the following relations*

$$d_{sj}(x'',-1)=\frac{1}{2\pi}\mathcal{G}_{\varkappa}(x'',0)V^{(s)}_{1-2r,j}(x'',0,0,-1)B^0_q(x'',0,0,-1)K(x'')\,e^{i\pi\lambda_0},$$

$$d_{sj}(x'',+1)=\frac{1}{2\pi}\mathcal{G}_{\varkappa}(x'',0)V^{(s)}_{1-2r,j}(x'',0,0,+1)B^0_q(x'',0,0,+1)K(x''),$$

$$\lambda_0=-\frac{\nu}{2}-\Delta(x''),\qquad s=1,\dots,\ell(N),$$

where $\mathcal{G}_{\varkappa}(x'',0)$ *is the square root the Gramm determinant,* B^0_q *denotes the principal symbol of a pseudodifferential operator* $\boldsymbol{B}_q$ *and*

$$V^{(s)}_{1-2r,j}(x'',0,0,\pm1)$$

$$=-\frac{i^{j+1}}{j!(n_s-1-j)!}\frac{d^{n_s-1-j}}{d\tau^{n_s-1-j}}(\tau-\tau_{s,\pm1})^{n_s}\left(A(J_{\varkappa}^{T}(x'',0)\cdot(0,\pm1,\tau))\right)^{-1}\Big|_{\tau=\tau_{s,\pm1}}.$$

The coefficient $c^{(j)}(x'')$ *in* (10) *is defined as follows*

$$c^{(j)}(x'') = a_j(x'')b_0(x'')K^{-1}(x'')c_0(x''),$$

where $b_0(x'')$ *and* $a_j(x'')$ *are upper triangular:*

$$b_0(x''): = \operatorname{diag}\{b^{m_1}(\frac{\nu}{2} + \delta_1(x'')), \ldots, b^{m_\ell}(\frac{\nu}{2} + \delta_\ell(x''))\},$$

$$b^{m_i}(t) = \|b_{kp}^{m_i}(t)\|_{m_i \times m_i}$$

and for $b_{kp}^{m_i}(t)$ *see*(9); *further*

$$a_j(x'') = \operatorname{diag}\{a^{m_1}(\lambda_1), \ldots, a^{m_\ell}(\lambda_\ell)\}, \quad a^{m_i}(\lambda_i) = \|a_{kp}^{m_i}(\lambda_i)\|_{n\, m_i \times m_i}, \tag{11}$$

$$\lambda_i = -\frac{\nu}{2} - \delta_i(x'') - 2r + q + j, \quad i = 1, \ldots, \ell,$$

where

$$a_{kp}^{m_i}(\lambda_i) = \begin{cases} (-1)^{p+k} b_{kp}^{m_i}(\lambda_i) & \text{if } Re\ \lambda_i > -1,\ k \le p, \\ (-1)^k \left(\dfrac{1}{2\pi i}\right)^{p-k} \dfrac{k!}{p!} c_{pk}^{m_i}(\lambda_i) & \text{if } Re\ \lambda_i < -1,\ \lambda_i \notin Z,\ k \le p, \\ \delta_{pk} & \text{if } \lambda_i = -1, -2, \ldots,\ k \le p, \\ 0 & \text{if } k > p \end{cases}$$

with the Kroneker symbol δ_{pk}; *if* $\lambda_i = -N_i + \mu_i$, $-1 < Re\ \mu_i \le 0$, $\lambda_i \notin Z$, $N_i > 0$ *is an integer, then*

$$c_{pk}^{m_i}(\lambda_i) = i^{\lambda_i - \mu_i} \sum_{l=k}^{p} (-1)^l (2\pi i)^{l-k} \frac{l!}{k!} d_{pl}^{m_i(N_i)}(\lambda_i) b_{kl}^{m_i}(\mu_i)$$

and coefficients $d_{pl}^{m_i(N_i)}$ *are defined in* (8)

Note that we know only one investigation [4] devoted to the asymptotics of functions represented by potentials for the canonical half-case and particular potentials.

Georgian Academy of Sciences
A.Razmadze Mathematical Institute

REFERENCES

1. *L. Hörmander.* The Analysis of Linear Partial Differential Operators, I-IV. Springer - Verlag, Heidelberg 1983.
2. *O. Chkadua.* Candidate Thesis, Tbilisi, 1984 (Russian).
3. *O. Chkadua, R. Duduchava.* Bull. Georg. Acad. Sci. **158**, 2, 1998, 207-210.
4. *G. Eskin.* Boundary Value Problems Pseudo-Differential Equations, vol. 52 of Translations of Mathematical Monographs. AMS, Providence, Rhode Island 1981.

საქართველოს მეცნიერებათა აკადემიის მოამბე, 159, №1, 1999
BULLETIN OF THE GEORGIAN ACADEMY OF SCIENCES, 159, №1, 1999

MATHEMATICS

A.Danelia

On the Approximation Property of Cesaro Transformations of Multiple Conjugate Trigonometric Series

Presented by Member of the Academy L.Zhizhiashvili, May 25, 1998

ABSTRACT. **In the theory of functions of real variables there are many works, related to the approximation properties of Cesaro transformations of $\sigma[f]$ and its conjugate series for one as well as multi variables. Approximation state of Cesaro transformations of positive degrees of conjugate trigonometric series of a function of the class $H(\omega, \mathbb{C}(T^m))$ is considered.**

Key words: conjugate functions, multi variables, L^p- modulus of continuity, Cesaro m-th transformation.

1. Let $R^m(m=1,2,...,R^1\equiv R)$ be m-dimensional Euclidean space. Let us consider the set $M=\{1....,m\}$ and assume that B is a nonempty subset of M. We denote the number of elements of a set B by the symbol $|B|$ and by x_B a point in the space $\mathbf{R}^m$ for which all the coordinates with the indices $M\setminus B$ are zeros.

If $T^m=[-\pi,\pi]^m(T^1\equiv T)$ then $C(T^m)$ is the set of continuous functions defined on T^m, with period 2π in each variable and with the norm

$$\|f\|_{C(T^m)} = \max_{x\in T^m}|f(x)|,$$

and $L^p(T^m)$ $(1\le p<\infty)$ is the set of Lebesgue integrable in p-th power functions, defined on T^m, with period 2π in each variable and with the norm

$$\|f\|^p_{L^p(T^m)} = (2\pi)^{-m}\int_{T^m}|f(x)|^p\,dx.$$

It implies that $L^\infty(T^m)\equiv C(T^m)$.

Let $f:R^m\to R$, $m \ge 2$. Let's consider the differences

$$\Delta_i(h)f(x)=f(x+h\,\ell_i)-f(x), \quad \Delta(h_1,...,h_m)f(x) = f(x_1+h_1,...,x_m+h_m) - f(x_1,...,x_m),$$

where $x\in\mathbf{R}^m$, $h\in\mathbf{R}$ and ℓ_i $(i=1,..., m)$ is the axial vector of i-coordinate.

For a function $L^p(T^m)$ $(1\le p\le\infty, m\ge2)$ let us use its structural characteristics:

1. L^p-modulus of continuity with respect to each variable

$$\omega_i(f;\delta)_{L^p(T^m)} = \sup_{|h|\le\delta}\|\Delta_i(h)f\|_{L^p(T^m)}$$

$$(0<\delta\le\pi,\ \ i=1,...,m);$$

2. L^p-modulus of continuity with respect to a set of varibles which form the set B

$$\omega_B(f;\delta)_{L^p(T^m)} = \sup_{\substack{|h_i|\le\delta_i \\ i\in B}} \left\| \Delta(h_B) f \right\|_{L^p(T^m)}$$

$$(0 < \delta_i \le \pi, \ \ i\in B);$$

3. L^p-modulus of complete continuity

$$\omega(f;\delta)_{L^p(T^m)} = \sup_{|h_i|\le\delta_i} \left\| \Delta(h_1, \ldots, h_m) f \right\|_{L^p(T^m)}$$

$$(0 < \delta_i \le \pi, \ \ i=1,\ldots,m);$$

Let f and g be nonnegative functions on a set $E\subset R$. If there exists a positive constant D such that $f(x) \le Dg(x)$ for every $x\in E$, then we write

$$f(x)<<g(x), \ x\in E.$$

Let $H(\omega; C(T^m))$, where ω is a modulus of continuity [1], be a set of the functions such that

$$\omega(f;\delta)_{C(T^m)} << \sum_{i=1}^{m} \omega(\delta_i)$$

$$(0<\delta_i\le\pi, \ \ i=1,\ldots,m),$$

and the symbols $\sigma_m^{\alpha}(x,f)$ and $t_m^{\alpha}(x,f,B)$ be Cesaro m-th trasformations [2,p.185] of $\sigma_m[f]$ and $\overline{\sigma}_m[f,B]$, respectively.

If $f\in L(T^m)$, then [2, p. 182] the expression

$$\widetilde{f}_B(x) = \lim_{\varepsilon_B\to 0} \widetilde{f}_B(x,\varepsilon_B) = \left(-\frac{1}{2\pi}\right)^{|B|} \lim_{\varepsilon_B\to 0} \int_{\prod_{j\in B}\{T\setminus[-\varepsilon_j,\varepsilon_j]\}} f(x+S_B) \prod_{i\in B} \operatorname{ctg}\frac{S_i}{2} dS_B$$

$$(\varepsilon_j>0, \ j\in B)$$

is called the conjugate function of f with respect to the variables, the indices of which form the set B $\left(\widetilde{f}_B \equiv \widetilde{f}, \text{ when } m=1\right)$.

Definition. We say that a modulus of continuity ω satisfies Zygmund's condition if

$$\int_0^{\delta} \frac{\omega(u)}{u} du + \delta \int_{\delta}^{\pi} \frac{\omega(u)}{u^2} du << \omega(\delta), \ \ (\delta\to 0+).$$

2. In the theory of functions of real variables there are many works related to the approximation properties of Cesaro transformations of $\sigma[f]$ and its conjugate series for one variable as well as for multi variables.

In 1912 S.Bernstein [3] proved the following statement: if $f\in H(\delta^{\alpha}; C(T^m))$ $(0<\alpha\le 1)$, then

$$\left\| \sigma_n^1(f) - f \right\|_{C(T)} \le \begin{cases} A(f)n^{-\alpha}, & 0<\alpha<1, \\ A(f)n^{-\alpha}\ln(n+2), & \alpha=1, \end{cases} \quad n\in N,$$

It must be noted that these estimates are exact.

On the basis of the works of S.Bernstein [3] and I.Privalov [4] we can assert that if $f\in H(\delta^{\alpha};\ C(T))$ $(0<\alpha<1)$ then

$$\left\|t_n^1(f)-\widetilde{f}\right\|_{C(T)}\le A(f)n^{-\alpha},\ n\in N.$$

The case $\alpha=1$ was considered by G.Alexits [5] in 1941. He proved that if $f\in H(\delta;\ C(T))$, then

$$\left\|t_n^1(f)-\widetilde{f}\right\|_{C(T)}\le A(f)n^{-1},\ n\in N.$$

By this G.Alexits showed that the function $\widetilde{f}$ may not possess these properties which a function f has (integrable, continuity and others) but in some cases it may have better approximation properties.

In the case of many variables the following statement is valid.

Theorem ([2]). *Let $f\in L^p(T^m)$ $(1\le p\le+\infty)$. Then for every $B\subset M$*

$$\left\|t_n^{\alpha}(\cdot,f,B)-\widetilde{f}_B\left(\cdot,\frac{\pi}{n}\right)\right\|_{L^p(T^m)}\le A(p,m,\alpha)\left\{\sum_{B_1\subset M}\prod_{i\in B_1}\lambda(n_i,\alpha_i)\omega_{B_1}\left(\frac{1}{n},f\right)_{L^p(T^m)}+\right.$$

$$+\sum_{B_1\subset B}\sum_{B_2\subset M\setminus B_1}\prod_{i\in B_2}\lambda(n_i,\alpha_i)\omega_{B_2}\left(\frac{1}{n},\widetilde{f}_{B_1}\left(\cdot,\frac{\pi}{n}\right)\right)_{L^p(T^m)}+$$

$$\left.+\sum_{i\in M\setminus B}n_i^{-1}\int_{1/n_i}^{\pi}S_i^{-2}\omega_i\left(S_i,\widetilde{f}_B\left(\cdot,\frac{\pi}{n}\right)\right)_{L^p(T^m)}dS_i+\sum_{i=1}^{m}n_i^{-1}\int_{1/n_i}^{\pi}S_i^{-2}\omega_i\left(S_i,f\right)_{L^p(T^m)}dS_i\right\},$$

where

$$\lambda(n_i,\alpha_i)=\begin{cases}n_i^{\alpha_i}, & \alpha_i\in(-1,0)\\ \ln(n_i+2), & \alpha_i=0\end{cases}\qquad \alpha_i\in(0,+\infty),\ n_i\in N\ \ (i=1,\dots,m).$$

In the given work we present the following

Theorem. *Let $f\in H(\omega;\ C(T^m))$ $(m\ge2)$ and ω the modulus of continuity satisfy Zygmund's condition, then*

$$\text{a)}\ \left\|t_n^{\alpha}(\cdot,f,B)-\widetilde{f}_B\left(\cdot,\frac{\pi}{n}\right)\right\|_{C(T^m)}<<\left\{\sum_{B_1\subset B}\left(\sum_{B_2\subset M\setminus B_1}\left[\sum_{i\in B_2}\omega\left(\frac{1}{n_i}\right)\right]\cdot\prod_{j\in B_1}\ln n_j\right)+\right.$$

$$+\sum_{i\in M\setminus B}\omega\left(\frac{1}{n_i}\right)\prod_{j\in B}\ln n_j+\sum_{i=1}^{m}\omega\left(\frac{1}{n_i}\right)\Bigg\},$$

where $0<\alpha<+\infty$ and $n=(n_1,\ldots,n_m)$;

b) there exists a function $F\in H(\omega;\ C(T^m))$ such that

$$\left\|t_n^{\alpha}(\cdot,F,B)-\widetilde{F}_B\left(\cdot,\frac{\pi}{n}\right)\right\|_{C(T^m)}>>\omega\left(\frac{1}{n'}\right)\ln n'^{|B|},\quad B\neq M,$$

$$\left\|t_n^{\alpha}(\cdot,F,B)-\widetilde{F}_B\left(\cdot,\frac{\pi}{n}\right)\right\|_{C(T^m)}>>\omega\left(\frac{1}{n'}\right)\ln n'^{|B|-1},\quad B=M,\ n=(n',\ldots,n'),\ n'\in N.$$

Tbilisi I. Javakhishvili State University

REFERENCES

1. *S.M.Nikolskii.* Dokl. Akad.Nauk SSSR, 52, 3, 1946, 191-194 (Russian).
2. *L.V.Zhizhiashvili.* Some Problems of the Theory of Trigonometric Fourier Series and their Conjugates. Tbilisi, 1993 (Russian).
3. *S.Bernstein.* Mem.Acad.Roy. Belgique, 2-me serie, 4, 1912, 1-104.
4. *Privalov.I.* Bull. Soc. Math. France, 44, 1916, 100-103.
5. *G.Alexits.* Math.Fiz.Lapak., 48, 3-4, 1941, 410-422.

საქართველოს მეცნიერებათა აკადემიის მოამბე, 159, №1, 1999
BULLETIN OF THE GEORGIAN ACADEMY OF SCIENCES, 159, №1, 1999

Member of the Academy T. Burchuladze, R. Rukhadze, Yu. Bezhuashvili

On the Matrix of Fundamental Solutions of the System of Equations for Oscillation of Hemitropic Micropolar Medium

Presented February 12, 1998

ABSTRACT. **The matrix of fundamental (singular) solutions of a homogeneous system of equations for oscillation of hemitropic micropolar medium in three-dimensional Euclidean R_3 is effectively constructed.**

Key words: hemitropic, micropolar, oscillation, fundamental matrix.

A system of homogeneous differential equations of stationary oscillation for hemitropic micropolar medium has the form [1,2].

$$\begin{cases} (\mu+\alpha)\Delta u + (\lambda+\mu-\alpha)\ \text{grad div}\, u + (\upsilon+\eta)\Delta\omega + \\ +(\delta+\upsilon-\eta)\ \text{grad div}\,\omega + 2\alpha\ \text{rot}\,\omega + \rho\sigma^2 u = 0, \\ (\nu+\beta)\Delta\omega + (\varepsilon+\nu-\beta)\ \text{grad div}\,\omega + (\upsilon+\eta)\Delta u + \\ +(\delta+\upsilon-\eta)\ \text{grad div}\, u + 2\alpha\ \text{rot}\, u + 4\eta\ \text{rot}\,\omega + (I\sigma^2 - 4\alpha)\omega = 0, \end{cases} \tag{1}$$

where Δ is a three-dimensional Laplace operator, $u(x) = u(u_1, u_2, u_3)$ a displacement vector, $\omega(x) = (\omega_1, \omega_2, \omega_3)$ rotation vector, $x = (x_1, x_2, x_3)$ a point in R^3, ρ the density medium, I inertia momentum, σ oscillation frequency; λ, μ, α, ε, ν, β, υ, η, δ are elasticity constants.

We introduce the differential operators

$$M^{(1)}(\partial x) = (\mu+\alpha)(\Delta + \lambda_1^2) + (\lambda+\mu-\alpha)\ \text{grad div},$$
$$M^{(2)}(\partial x) = M^{(3)}(\partial x) = (\upsilon+\eta)\Delta + (\delta+\upsilon-\eta)\ \text{grad div} + 2\alpha\ \text{rot},$$
$$M^{(4)}(\partial x) = (\nu+\beta)(\Delta + \lambda_2^2) + (\varepsilon+\nu-\beta)\ \text{grad div} + 4\eta\ \text{rot},$$

where $\lambda_1^2 = \dfrac{\rho\sigma^2}{\mu+\alpha}$, $\lambda_2^2 = \dfrac{I\sigma^2 - 4\alpha}{\nu+\beta}$. Then system (1) can be rewritten in the form

$$\begin{cases} M^{(1)}(\partial x)u(x) + M^{(2)}(\partial x)\omega(x) = 0, \\ M^{(3)}(\partial x)u(x) + M^{(4)}(\partial x)\omega(x) = 0. \end{cases} \tag{2}$$

The solution of system (2) will be sought in the form

$$\begin{cases} u(x) = M^{(4)}(\partial x)\widetilde{X}(x) - M^{(2)}(\partial x)\widetilde{Y}(x) \\ \omega(x) = -M^{(2)}(\partial x)\widetilde{X}(x) + M^{(1)}(\partial x)\widetilde{Y}(x) \end{cases} \tag{3}$$

where $\widetilde{X}$ and $\widetilde{Y}$ are unknown three-dimensional vector-functions. Substituting (3) in (2) to determine $\widetilde{X}$ and $\widetilde{Y}$, we obtain

$$D(\partial x)\widetilde{X}(x) = 0, \quad D(\partial x)\widetilde{Y}(x) = 0,$$

where $D(\partial x) = M^{(1)}(\partial x)\, M^{(4)}(\partial x) - M^{(2)}(\partial x)\, M^{(2)}(\partial x)$.

Calculations give us

$D(\partial x) = d_1(\Delta + \lambda_3^2)(\Delta + \lambda_4^2) + d_1 d_2(\Delta + \lambda_5^2)$ rot + $(d_0 - d_1)(\Delta + \lambda_6^2)$ grad div,

where

$$d_0 = (\lambda + 2\mu)(\varepsilon + 2\nu) - (\delta + 2\upsilon)^2 > 0,\ d_1 = (\mu + \alpha)(\nu + \beta) - (\upsilon + \eta)^2 > 0,$$

$$d_2 = \frac{4(\mu\eta - \alpha\upsilon)}{d_1},\ \lambda_3^2 + \lambda_4^2 = \frac{(\mu + \alpha)I\sigma^2 - 4\alpha\mu + \rho\sigma^2(\nu + \beta)}{d_1},$$

$$\lambda_3^2\lambda_4^2 = \frac{\rho\sigma^2(I\sigma^2 - 4\alpha)}{d_1},\ \lambda_5^2 = \frac{\rho\sigma^2\eta}{\mu\eta - \alpha\upsilon},$$

$$\lambda_6^2 = \frac{(I\sigma^2 - 4\alpha)(\lambda + \mu) - I\sigma^2\alpha + \rho\sigma^2(\varepsilon + \nu - \beta)}{d_0 - d_1}.$$

Let $D(\partial x)Z(x) \equiv \Phi(x)$

where $Z(x)$ is an arbitrary vector-function.

According to (4), we have div $D(\partial x)Z(x)$ = div $\Phi(x)$

Transformations yield $d_0(\Delta + k_1^2)(\Delta + k_2^2)$ div $Z(x)$ = div Φ, (5)

where $k_1^2 + k_2^2 = \dfrac{(\lambda + 2\mu)(I\sigma^2 - 4\alpha) + \rho\sigma^2(\varepsilon + 2\nu)}{d_0},\ k_1^2 k_2^2 = \dfrac{\rho\sigma^2(I\sigma^2 - 4\alpha)}{d_0}.$

Analogously, from (4) we get

$$[d_1(\Delta + \lambda_3^2)(\Delta + \lambda_4^2)\text{rot} + d_1 d_2(\Delta + \lambda_5^2)(\text{grad div} - \Delta)]Z = \text{rot}\,\Phi. \quad (6)$$

Now acting by an operator $(\Delta + \lambda_3^2)(\Delta + \lambda_4^2)(\Delta + k_1^2)(\Delta + k_2^2)$ on equality (4) and taking into account the relations (5) and (6), we get

$$\prod_{i=1}^{6}(\Delta + k_i^2)Z = \frac{1}{d_1}(\Delta + k_1^2)(\Delta + k_2^2)(\Delta + \lambda_3^2)(\Delta + \lambda_4^2)\Phi - \frac{d_2}{d_1}(\Delta + k_1^2)(\Delta + k_2^2) \times$$

$$\times(\Delta + \lambda_5^2)\,\text{rot}\,\Phi + \left[\frac{d_2^2}{d_0}(\Delta + \lambda_5^2)^2 - \frac{d_0 - d_1}{d_0 d_1}(\Delta + \lambda_3^2)(\Delta + \lambda_4^2)(\Delta + \lambda_6^2)\right]\text{grad div}\,\Phi,$$

where $k_i^2\ (i = \overline{3,6})$ satisfy the conditions

$$k_3^2 + k_4^2 + k_5^2 + k_6^2 = 2(\lambda_3^2 + \lambda_4^2) + d_2^2,\ k_3^2 k_4^2 k_5^2 k_6^2 = \lambda_3^4\lambda_4^4,$$

$$k_3^2 k_4^2 + k_5^2 k_6^2 + (k_3^2 + k_4^2)(k_5^2 + k_6^2) = (\lambda_3^2 + \lambda_4^2)^2 + 2\lambda_3^2\lambda_4^2 + 2d_2^2\lambda_5^2,$$

$$(k_3^2+k_4^2)k_5^2k_6^2+(k_5^2+k_6^2)k_3^2k_4^2=2(\lambda_3^2+\lambda_4^2)\lambda_3^2\lambda_4^2+d_2^2\lambda_5^4.$$

Introduce the differential operator

$$A(\partial x)=\frac{1}{d_1}(\Delta+k_1^2)(\Delta+k_2^2)(\Delta+\lambda_3^2)(\Delta+\lambda_4^2)-\frac{d_2}{d_1}(\Delta+k_1^2)(\Delta+k_2^2)(\Delta+\lambda_5^2)\,\mathrm{rot}+$$

$$+\frac{d_2^2}{d_0}(\Delta+\lambda_5^2)^2\,\mathrm{grad}\,\mathrm{div}-\frac{d_0-d_1}{d_0d_1}(\Delta+\lambda_3^2)(\Delta+\lambda_4^2)(\Delta+\lambda_6^2)\mathrm{grad}\,\mathrm{div}. \tag{7}$$

If now we assume that $\widetilde{X}=AX$ and $\widetilde{Y}=AY$ in (2), then we get

$$\begin{cases} u(x)=M^{(4)}(\partial x)A(\partial x)X(x)-M^{(2)}(\partial x)A(\partial x)Y(x) \\ \omega(x)=-M^{(2)}(\partial x)A(\partial x)X(x)+M^{(1)}(\partial x)A(\partial x)Y(x) \end{cases} \tag{8}$$

To determine X and Y, we have

$$\prod_{i=1}^{6}(\Delta+k_i^2)X(x)=0,\quad \prod_{i=1}^{6}(\Delta+k_i^2)Y(x)=0.$$

Consider the equality

$$\prod_{i=1}^{6}(\Delta+k_i^2)X_0(x)=0, \tag{9}$$

where $X_0(x)$ is an unknown scalar function. It follows from (8) that we must construct such a solution of equation (9) whose partial tenth order derivatives have the singularity of the kind $|x|^{-1}$. It is easily seen that the desired solution will be

$$X_0(x)=\frac{1}{4\pi}\sum_{l=1}^{6}\prod_{j=1}^{5}\frac{1}{k_{l+j}^2-k_l^2}\cdot\frac{e^{ik_l|x|}}{|x|},\quad k_{6+j}^2=k_j^2,\ j=\overline{1,5},$$

$$\sum_{l=1}^{6}\prod_{j=1}^{5}\frac{k_l^{2m}}{k_{l+j}^2-k_l^2}=\delta_{2m,10},\quad m=\overline{0,5}, \tag{10}$$

where δ_{kj} is the Kronecker symbol.

Introduce a six-component vector $\upsilon=(u,\omega)=(u_1,u_2,u_3,\omega_1,\omega_2,\omega_3)=(\upsilon_1,\upsilon_2,\upsilon_3,\upsilon_4,\upsilon_5,\upsilon_6)$. Let $\delta_k=(\delta_{k1},\delta_{k2},\delta_{k3})$, $k=\overline{1,3}$. If in (8) we take $X\equiv X_k=X_0\delta^k$, $k=\overline{1,3}$, $Y=(0,0,0)$ and then $Y\equiv Y^k=X_0\delta^k$, $k=\overline{1,3}$; $X=(0,0,0)$, then we get six solutions of system (2), which we denote by $\upsilon^k=(u^k,\omega^k)$, $k=\overline{1,6}$.

Consider a quadratic matrix of dimension 6×6: $\Gamma(x,\sigma)=\|\Gamma_{mn}(x,\sigma)\|_{6\times6}$, where $\Gamma_{mn}=\upsilon_n^m$, $m,n=\overline{1,6}$. By definition, each column of the matrix $\Gamma(x,\sigma)$, taken as a vector, is the solution of system (2) at all points of the space R^3, except at the beginning of the

coordinates. Taking into consideration the expressions for the operators $M^{(1)}A$, $M^{(2)}A$, $M^{(4)}A$, we can introduce the matrix $\Gamma(x,\sigma)$ in the following form

$$\Gamma(x,\sigma)=\left\|\begin{matrix}\Gamma^{(1)}(x,\sigma) & \Gamma^{(2)}(x,\sigma)\\ \Gamma^{(3)}(x,\sigma) & \Gamma^{(4)}(x,\sigma)\end{matrix}\right\|, \tag{11}$$

where $\Gamma^{(p)}(x,\sigma)=\|\Gamma^{(p)}_{mn}(x,\sigma)\|_{3\times 3}$, $p=\overline{1,4}$;

$$4\pi\Gamma^{(1)}_{mn}=\sum_{l=3}^{6}\prod_{j=1}^{5}\frac{(k_1^2-k_l^2)(k_2^2-k_l^2)}{k_{l+j}^2-k_l^2}\left[\frac{\nu+\beta}{d_1}(\lambda_2^2-k_l^2)(\lambda_3^2-k_l^2)(\lambda_4^2-k_l^2)+\right.$$

$$\left.+\frac{4\eta d_2}{d_1}(\lambda_5^2-k_l^2)(-k_l^2)\right]\frac{e^{ik_l|x|}}{|x|}\delta_{mn}+\sum_{l=3}^{6}\prod_{j=1}^{5}\frac{(k_1^2-k_l^2)(k_2^2-k_l^2)}{k_{l+j}^2-k_l^2}\times$$

$$\times\left[\frac{4\eta}{d_1}(\lambda_3^2-k_l^2)(\lambda_4^2-k_l^2)-\frac{(\nu+\beta)d_2}{d_1}(\lambda_2^2-k_l^2)(\lambda_5^2-k_l^2)\right]\sum_{q=1}^{3}\varepsilon_{mnq}\frac{\partial}{\partial x_q}\frac{e^{ik_l|x|}}{|x|}+$$

$$+\frac{\varepsilon+2\nu}{d_0}\sum_{l=1}^{6}\prod_{j=1}^{5}\frac{(\lambda_3^2-k_l^2)}{k_{l+j}^2-k_l^2}\left[d_2^2(\lambda_5^2-k_l^2)^2-\frac{d_0-d_1}{d_1}(\lambda_3^2-k_l^2)(\lambda_4^2-k_l^2)(\lambda_6^2-k_l^2)\right]\times$$

$$\times\frac{\partial^2}{\partial x_m\partial x_n}\cdot\frac{e^{ik_l|x|}}{|x|}+\sum_{l=3}^{6}\prod_{j=1}^{5}\frac{(k_1^2-k_l^2)(k_2^2-k_l^2)}{k_{l+j}^2-k_l^2}\left[\frac{\varepsilon+\nu-\beta}{d_1}(\lambda_3^2-k_l^2)(\lambda_4^2-k_l^2)-\right.$$

$$\left.-\frac{4\eta d_2}{d_1}(\lambda_5^2-k_l^2)\right]\frac{\partial^2}{\partial x_m\partial x_n}\cdot\frac{e^{ik_l|x|}}{|x|},$$

$$-4\pi\Gamma^{(2)}_{mn}=-4\pi\Gamma^{(3)}_{mn}=\sum_{l=3}^{6}\prod_{j=1}^{5}\frac{(-k_l^2)(k_1^2-k_l^2)(k_2^2-k_l^2)}{k_{l+j}^2-k_l^2}\left[\frac{\upsilon+\eta}{d_1}(\lambda_3^2-k_l^2)(\lambda_4^2-k_l^2)+\right.$$

$$\left.+\frac{2\alpha d_2}{d_1}(\lambda_5^2-k_l^2)\right]\frac{e^{ik_l|x|}}{|x|}\delta_{mn}+\sum_{l=3}^{6}\prod_{j=1}^{5}\frac{(k_1^2-k_l^2)(k_2^2-k_l^2)}{k_{l+j}^2-k_l^2}\left[\frac{2\alpha}{d_1}(\lambda_3^2-k_l^2)(\lambda_4^2-k_l^2)-\right.$$

$$\left.-\frac{(\upsilon+\eta)d_2}{d_1}(-k_l^2)(\lambda_5^2-k_l^2)\right]\sum_{q=1}^{3}\varepsilon_{mnq}\frac{\partial}{\partial x_q}\frac{e^{ik_l|x|}}{|x|}+\sum_{l=3}^{6}\prod_{j=1}^{5}\frac{(k_1^2-k_l^2)(k_2^2-k_l^2)}{k_{l+j}^2-k_l^2}\times$$

$$\times\left[\frac{\delta+\upsilon-\eta}{d_1}(\lambda_3^2-k_l^2)(\lambda_4^2-k_l^2)-\frac{2\alpha d_2}{d_1}(\lambda_5^2-k_l^2)\right]\frac{\partial^2}{\partial x_m\partial x_n}\cdot\frac{e^{ik_l|x|}}{|x|}+$$

$$+\frac{\delta+2\upsilon}{d_0}\sum_{l=1}^{6}\prod_{j=1}^{5}\frac{(-k_l^2)}{k_{l+j}^2-k_l^2}\left[d_2^2(\lambda_5^2-k_l^2)^2-\frac{d_0-d_1}{d_1}(\lambda_3^2-k_l^2)(\lambda_4^2-k_l^2)(\lambda_6^2-k_l^2)\right]\times$$

$$\times\frac{\partial^2}{\partial x_m\partial x_n}\cdot\frac{e^{ik_l|x|}}{|x|},$$

$$4\pi\Gamma_{mn}^{(4)}=\frac{\mu+\alpha}{d_1}\sum_{l=3}^{6}\prod_{j=1}^{5}\frac{(k_1^2-k_l^2)(k_2^2-k_l^2)(\lambda_1^2-k_l^2)(\lambda_3^2-k_l^2)(\lambda_4^2-k_l^2)}{k_{l+j}^2-k_l^2}\cdot\frac{e^{ik_l|x|}}{|x|}\delta_{mn}-$$

$$-\frac{(\mu+\alpha)d_2}{d_1}\sum_{l=3}^{6}\prod_{j=1}^{5}\frac{(k_1^2-k_l^2)(k_2^2-k_l^2)(\lambda_1^2-k_l^2)(\lambda_5^2-k_l^2)}{k_{l+j}^2-k_l^2}\sum_{q=1}^{3}\varepsilon_{mnq}\frac{\partial}{\partial x_q}\frac{e^{ik_l|x|}}{|x|}+$$

$$+\frac{\lambda+\mu-\alpha}{d_1}\sum_{l=3}^{6}\prod_{j=1}^{5}\frac{(k_1^2-k_l^2)(k_2^2-k_l^2)(\lambda_3^2-k_l^2)(\lambda_4^2-k_l^2)}{k_{l+j}^2-k_l^2}\cdot\frac{\partial^2}{\partial x_m\partial x_n}\cdot\frac{e^{ik_l|x|}}{|x|}+$$

$$+\frac{\lambda+2\mu}{d_0}\sum_{l=1}^{6}\prod_{j=1}^{5}\frac{\lambda_7^2-k_l^2}{k_{l+j}^2-k_l^2}\left[d_2^2(\lambda_5^2-k_l^2)^2-\frac{d_0-d_1}{d_1}(\lambda_3^2-k_l^2)(\lambda_4^2-k_l^2)(\lambda_6^2-k_l^2)\right]\times$$

$$\times\frac{\partial^2}{\partial x_m\partial x_n}\cdot\frac{e^{ik_l|x|}}{|x|},$$

where ε_{mnq} is Levi-Civita's symbol.

Therefore, (11) is the matrix of fundamental solutions of system (1). If in (11) we assume $\sigma = 0$, then we get the known matrix of fundamental solutions of statics [3].

Georgian Academy of Sciences
A. Razmadze Mathematical Institute

REFERENCES

1. *E. V. Kuvshinskii, E. L. Aero*. FTT., **5**, 5, 1963, 2592-2598 (Russian).
2. *P. Nowacki, W. Nowacki*. Bull. Acad. Polon. Sci., Ser., Techn., **25**, 151[297], 1997, 1-14.
3. *L. Giorgashvili*. Trudy Inst. Prikl. Mat. I. Vekua. 16, 1985, 56-79 (Russian).

საქართველოს მეცნიერებათა აკადემიის მოამბე, 159, №1, 1999
BULLETIN OF THE GEORGIAN ACADEMY OF SCIENCES, 159, №1, 1999

CYBERNETICS

G. Kashmadze

Entropy of Function Linear Approximation

Presented by Member of the Academy V.Chavchanidze, June 15, 1998

ABSTRACT. **The graph of function is represented as a fuzzy set. The measure of proximity of broken line to the graph of function is considered.**

Key words: linear approximation, fuzzy set, membership function, entropy.

During linear approximation of function on the interval $[a, b]$ sometimes it is desirable to have a broken line with comparatively few corner points [1]. In such cases arrangement of abscissas of corner points on number line acquires essential value, since even partition of interval $[a, b]$ may be no more advisable. It doesn't always give the best approach of broken line to the graph of function $f(x)$. Problem of comparison of two broken lines from the point of view of proximity to graph of function $f(x)$ in case fixed parameter n arises naturally.

We represent graph of function f as a fuzzy set. Any point $(x, g_n(x))$ of broken line g_n belongs to this set with degree $\mu_{g_n}(x)$.

$$\mu_{g_n}(x) = 1 - \frac{2}{\pi} Arctg \left| \frac{f(x) - g_n(x)}{f(x)} \right|, \quad x \in [a, b] \tag{1}$$

Let us take

$$H(g_n) = -\int_a^b (\mu_{g_n}(x) \ln \mu_{g_n}(x) + (1 - \mu_{g_n}(x)) \ln(1 - \mu_{g_n}(x)))dx \tag{2}$$

as a measure of proximity of g_n to f and call this expression entropy of approximation of function f with g_n.

Assume that it is possible to change abscissas of corner points of broken line with step h. Then a quantity of possible values of abscissas will be $m = \frac{b-a}{h} - 1$; and a quantity of approximating broken lines with n intervals will be $N = C_m^{n-1}$. Choose a step $h' < h$ and calculate entropy $H(g_n^j)$ for every broken line g_n^j $(j = 1..., N)$ according to the expression

$$H(g_n^j) = -\sum_{i=1}^{l} [\mu(a + ih') \ln \mu(a + ih') + (1 - \mu(a + ih')) \ln(1 - \mu(a + ih'))] \tag{3}$$

$$l = \frac{b-a}{h'} \quad \text{and} \quad \mu \equiv \mu_{g_n^j}$$

instead of expression (2).

Let us take, for example, density function of normal distribution

$$f(x)=\frac{1}{\sqrt{2\pi}\sigma}e^{-\frac{(x-x_0)^2}{2\sigma^2}},\quad x_0=0,\quad \sigma=1,\quad x\in[-3,3].$$

The broken line with abscissas -2,6; -2,2; -1,7; -0,4; 0; 0,4; 1,7; 2,2; 2,6 of corner points has minimal entropy among broken lines having ten intervals.

In the case of density function of Coachy distribution

$$f(x)=\frac{1}{\pi}\cdot\frac{t}{t^2+(x-x_0)^2},\quad \text{when}\quad t=1,\quad x_0=0,\quad x\in[-3,3],$$

abscissas get values: -2,5; -2,0; -1,6; -1,2; 0; 1,2; 1,6; 2,0; 2,5.

In the case of the density function of Maxwell distribution

$$f(x)=\frac{x^2}{\sigma_c^3}\sqrt{\frac{2}{\pi}}e^{-\frac{x^2}{2\sigma_c^2}},\quad \text{when}\quad \sigma_c=1,$$

on [0;3] the broken line with abscissas 0,4; 1,7; 2,2; 2,6 of corner points has minimal entropy among broken lines having five intervals. In the considered examples $h=0{,}1$.

Other expression may be applied as the entropic measure of fuzziness too [3].

Tbilisi I.Javakhishvili State University.

REFERENCES

1. *A. N. Tikhonov, D.P. Kostomarov.* Vvodnye lektsii po prikladnoi matematike. Moscow, 1984 (Russian).
2. *De Luka, S. Termini.* Inf. and Control. **20**, 1972, 301-302.
3. *T. Gachechiladze, G. Kashmadze.* Bull. Georg. Acad. Sci. **149**, 1, 1994, 38-40 (Russian).

საქართველოს მეცნიერებათა აკადემიის მოამბე, 159, №1, 1999
BULLETIN OF THE GEORGIAN ACADEMY OF SCIENCES, 159, №1, 1999

CYBERNETICS

N.Archvadze, M.Pkhovelishvili

Questions of Representing the Syntax of the Programming Languages through Semantic Networks

Presented by Member of the Academy V.Chavchanidze,February 24,1998

ABSTRACT. **The syntax of the programming languages has been represented through semantic networks of a certain type. These constructions permit to establish correctness of the program or a part of it made by the students.**

Key words: programming, concept of knowledge, training systems, programming languages.

The basic characteristic property of systems of artificial intelligence, by which they differ from traditional systems of the information processing, is that their work is based on the use of a new type of the information which is called the knowledge.

Japanese scientist Osucha defines the knowledge as follows: "The Knowledge is accepted to be the name of information stored (in the computer) and formalized according to certain structural rules. The computer can use it independently for solving the problems in such algorithms as logic conclusions " [1]. Formalism of such description of knowledge is determined as representation of knowledge. The component, using the knowledge of the experts to solve a problem in the preliminarily chosen form, represents the mechanism of application.

The intelligent training system, implying opportunity of the use of Georgian language, also provides automatic check of knowledge of the student. For example, let the system require the student to make the program or its fragment for any certain problem in a particular programming language. At checking its correctness the so-called question of conformity arises, i.e. how it corresponds to the correct program. It naturally means, that the student can use various sequences of the operators to get correct results.

The question of representation of algorithmic designs in any form of knowledge representation arises to solve the problem of similarity, to prove the syntax correctness. We have chosen a special class of semantic nets, the so-called nets with connected tops, which are described by I. P. Kuznetsov [2]. This choice predetermined the fact, that we could represent the syntax of Becus-Naur language and its expansion by these semantic nets. For the beginning we shall describe the semantic language or apparatus offered by I. P. Kuznetsov.

1.Semantic language. To imagine the situations consisting of a set of objects and relations a set of elementary fragments is applied which is called a net. The net can be written as follows: $\Phi_1 o \Phi_2 o \Phi_3 o ... \Phi_N$, where Φ_i, i=1..N is an elementary fragment and o is a special separating mark. The elementary fragment, which corresponds to an elementary situation or complex object, is represented as a set of directly connected tops.

The elementary fragment is set as a train: < d_1, d_2, d_3, d_4,..., d_k >, where d_1 is the name if the fragment is considered as uniform complex object or situation. Otherwise a special symbol "-" is used to mark an empty place. The second component d_2 corresponds to a logic top the value of which is *t* if the fact is true, and it is *f* if the fact is false. On the third place of a train there is the top of connections d_3, which represent the relation. The tops of a train from d_4 up to d_k correspond to considered or not considered objects.

2 .Representation of the Becus-Naur form and its expansion through semantic nets. Most often for the correct description of syntactic designs of algorithmic languages the Becus-Naur form (BNF) or extended Becus - Naur form (EBNF) is applied [3,4]. Our purpose is to represent a metalanguage used in the above-said forms with the help of semantic language. Thus, we will be able to represent the syntax of those algorithmic languages, which are described with the help of BNF or EBNF, as sets of circuits. It will give us an opportunity to solve the problem of similarity in training systems between the net of a correct answer and the net given by the student.

To the left part of metasymbol "=" of EBNF we shall put in conformity the name of an object, that is the first element of a train - d_1. If in the right part of EBNF there is only one component, then we use the relation '=dF' (according to definition). To it we put in conformity an element of an elementary fragment d_3. In case if the right part of EBNF contains several components, then to it we put in conformity a net < d_1, t, '=dF', γ> o <γ_i, t, "PACK", D_4, D_5 >, where γ is the top of situations and "PACK" is a blank free relation.

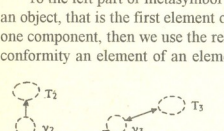

Fig. 1. The net appropriate to the relation "or".

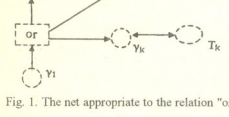

Fig. 2. Example with the use of relation "or"

For metasymbol "||" we shall introduce the relation "or" through the following net. [Fig. 1.]. γ_i is a complex object and it is either complex object γ_2 (situation T_2) or comlex object γ_3, (situation T_3) or ... or complex object γ_k, (situation T_k. The net is represented as a train: <γ_1, t, 'or', γ_2, γ_3,... γ_k>.

Let us consider an example: the identifier B1 accepts values a_1 or a_2. It is represented as a net <-, t, "or", "B_1",> 0 <, t, "or", "a_1", "a_2"> [Fig. 2.]

In semantic language to the EBNF metasymbol corresponds a symbol ', and the metasymbol "." appears to be unnecessary as the beginning and the end of a net are limited by the brackets < >.

In semantic language a symbol ^ is introduced which corresponds to metasymbol " { } " from BNF. The symbol ^ is written above the

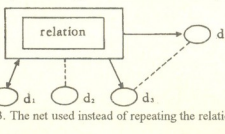

Fig.3. The net used instead of repeating the relation.

relation and means recurrence of this relation 0 or N times: < -, t, "relation", F, N>.

To the EBNF metasymbol "[]" we shall put in conformity a net < -, t, "or", A, l>, where l designates the empty, non-existent member.

Instead of metasymbol " () " the mark "o" is used in nets.

3.Representation of algorithmic language Pascal through semantic nets. Let us consider the representation of syntax of an algorithmic language PASCAL represented by the Becus-Naur form and its extended form, through semantic nets[3,5].

< " base-type ", t, " = dF ", " serial-type " >.

-< "Block", t, "=dF", γ_1> o < γ_1, t, "PACK", γ_2, γ_3, γ_4, γ_5, γ_6, " section of the operators " > o <γ_2, t, "or", " -section-of-the description-of-labels ", l > o < γ_3, t, "or", " section - of definition-of-constants ", λ > o < γ_4, t, "or", " section - of definition - of- types ", λ> o < γ_5, t, "or", " section-of-description-of-variables ", λ> o < γ_6, t, "or", " section - of description of procedures and - functions ", λ >.

< " the block - of-program ", t, "=dF", "block" >.

< " the block - of-procedure ", t, "=dF", "block" >.

< " the block - of-function ", t, "=dF", "block" >.

< "Letter", t, "=dF", l> o < 1, t, "or", "A", "B", "C", "D", " E, " F "," G ", " H "," I "," J "," K ", " L "," M "," N "," O "," P "," Q "," R "," S', "T", "U", "V", "W", "X", "Y", "Z", "a", "b", "c", "d", "e", "f", "g", "h", " i", "j", "k", "l", "m", "n", "o", "p", "q", "r", "s", "t" "," u "," v "," w ", " x ", " y"," z " >.

< " buffer - file -variable ", t, "=dF", γ_1> o < γ_1, t, "PACK", " file - variable ", " ^" >.

< " alternative - part ", t, "=dF", γ_1> o < γ_1, t, "PACK", "CASE", " an-indicator-of - variant ", "OF", "variant", γ_2> o < γ_2, t, "PACK", ":", "variant" >.

< " unsigned - real ", t, "=dF", γ_1> o < γ_1, t, "PACK", " unsigned - integer ", "fractional - part ", γ_2> o < γ_2, t, "or", "E", "order", λ>.

< " signed - real ", t, "=dF", γ_1> o < γ_1, t, "PACK", γ_2, " unsigned - real " > o < γ_2, t, "or", 'sign', λ>.

In the end we shall note, that in training systems the representation of syntax of the programming language in such form gives us an opportunity to check only the syntax of the programs or their fragments made by students. In future it will become possible to check the semantic correctness of the programs at the expense of more advanced designs of semantic nets.

This work is supported by the Grant №1.19 of the Georgian Academy of Sciences.

Georgian Academy of Sciences
N.Muskhelishvili Institute of Computational Mathematics

REFERENCES

1. *S. Osucha.* Processing of knowledge, M., 1989, 292 (Russian).
2. *I.P. Kuznetsov.* Semantic representations. M., 1986,.295 (Russian).
3. *O.N. Perminov.* Programming in language Pascal. M., 1988, 222 (Russian).
4. *N. Wurth.* Compilerbau. Eine Einfuhrung. Stuttgart, B.C. Teubner, 1977, 93.
5. *K.Iensen, N.Virt.* Pascal. Users manual and the description of the language. M., 1982, .152 (Russian).

საქართველოს მეცნიერებათა აკადემიის მოამბე, 159, №1, 1999
BULLETIN OF THE GEORGIAN ACADEMY OF SCIENCES, 159, №1, 1999

CYBERNETICS

N.Tkemaladze

Automatized System of Pattern Recognition with Learning

Presented by Member of the Academy V.Chavchanidze, February 5, 1998

ABSTRACT. **The automatized system of pattern recognition with learning - PRL functioning of which does not depend on the physical essence of investigating objects and a number of their initial parameters is suggested.**

Key words: pattern recognition, learning model, knowledge, data base, formal parameter, BIB, PBIB(2)-design, geometrical configuration.

The process of pattern recognition with learning consists of two stages. The first stage corresponds to learning process and the second one to recognition. The automatized system of pattern recognition with learning - PRL, which is suggested in this article, consists of two subsystems: the first subsystem is a learning model - LM, the second one is a model of recognition - MR.

The purpose of the first subsystem - LM is to determine the knowledge base and the data base on the basis of which the second subsystem recognizes a new object from the given list of classes.

For constructing the knowledge base and the data base LM must solve the following problems: 1. Determination of initial parameters on the basis of initial information. Sequences of parameter values (features) make up learning descriptions, i.e. such descriptions of objects, for which the classes of these objects belong to, are known beforehand; 2. Choice of different variants of learning and recognizable descriptions from the initial learning descriptions using random numbers and slipping control procedure.In these variants every initial learning description is considered as recognizable description or as learning description; 3. Separation of informative parameters by means of balanced incomplete block-designs (BIB-designs) [1] and correlation matrices, corresponding to the blocks of the indicated designs; 4. Determination of artificial (formal) parameters - implicit relations among the initial parameters by means of geometrical configurations and BIB-designs [2,3]; 5. Determination of intervals of parameter values and their coding; 6.Choice of optimal parameters on the basis of coded learning descriptions; 7. Determination of characteristics of classes and their measures of informativity by means of the balanced or partially balanced incomplete block-design (BIB- or PBIB(2)-design), i.e. the configuration of (v, b, k, r, λ) or $(v, b, k, r, n_p, \lambda_i, P^i)$, $i = 1,2$ type, where $v, b, k, r, n_p, \lambda_i$ are the parameters of the first kind and P^i is the parameter of the second kind for it is given as a matrix $P^i = (P^i_{vu})$ [4]; 8. Calculation of threshold measures; 9. Determination of well-grounded learning sampling, i.e.the necessary number of parameters, learning descriptions and optimal BIB- or PBIB(2)-design used for determination of characteristics of classes; 10. Construction of the knowledge base and the data

base on the basis of the results of solving the aforementioned problems 3÷9. When the initial information is given in the form of the learning descriptions, the problem 1 is omitted.

The second subsystem - MR must: 1) on the basis of the knowledge base transform the recognizable initial descriptions and code them; 2) determine the criteria and recognize to which class belong the objects separated for recognition after solving the problem 2 of the learning model; 3) on the basis of different variants of recognizable and learning descriptions determine the matrices of the results for solution of the problem 9 of the learning model; 4) correct the knowledge base and the data base on the basis of the information obtained after the recognition; 5) after correction of knowledge base and data base recognize new objects - make the decision: the objects belong to one concrete class authentically,or to one or more then one class with some degree of accuracy or the objects are not recognized.

Our approach to the solution of the problems of pattern recognition with learning significantly differs from all the works that we know. We consider not only the values of initial parameters (i.e. features), not their simple combinations to be the characteristics of pattern (class), but: 1) their combinations, determined by means of BIB- or PBIB(2)-design without a complete exhaustive search and 2) specific groups of features characterizing and not characterizing the patterns [5] composing of which is impossible by other well-known methods. The advantage of our approach is also determination of formal parameters by means of BIB-designs and geometrical configurations. For determination of formal parameters by means of the initial parameters the configuration of (v, b, k, r, λ) type is constructed, where $k = 3$ or 4 or 5. After this on the basis of numbered blocks of the used configuration one of the above mentioned configurations is constructed. This configuration consists of extended blocks, elements of which are blocks of the previously used configuration (BIB-design). After twofold application of BIB-designs, the learning descriptions are transformed into geometrical configuration, coordinates of tops of which are the elements of the extended blocks. By means of such geometrical configurations the artificial (formal) parameters are determined, which may be trigonometrical functions, angular coefficients of straight lines passing through the tops of the geometrical configurations etc.The formal parameters make it possible: 1) to determine the implicit relations which exist among the initial parameters (they have great importance in determination of characteristics of classes); 2) to draw together the descriptions of the same pattern (class) and move apart from each other the descriptions of different patterns; 3) to expand the space of the parameters when there are few initial parameters and otherwise to narrow it down.

These advantages make it possible to determine the characteristics of patterns (classes) for recognition even in cases when the following difficulties arise: 1.The initial information includes a small (M=2 or 3) or too large (M>40) number of only less informative values of initial parameters; 2. The descriptions of the same pattern differ from each other more than descriptions of different patterns; 3. Just the same parameter takes values from 0 to 10^6 and over.Our approach to creation of the system of pattern recognition with learning (PRL) is unique, the methods and algorithms,which are used in this system,with the help of geometrical configurations, BIB- and PBIB(2)-designs and vector-optimizing

mechanism of choosing [6] remove the above mentioned difficulties [4].

The suggested system does not depend on the physical essence of investigating object and number of initial parameters. In this system for the first time were used geometrical configurations and BIB-designs to define artificial (formal) parameters and BIB- and PBIB(2)-designs to define characteristics of classes.

The automatized system PRL is realized on PC Pentium-133 by the collaborators of the Department of Classification of Complex System of the Institute of Cybernetics. It was often used for recognition and classification of different objects.

The system PRL can be used for prediction of natural calamities as well, if we have suitable initial information for learning and prediction. The system PRL on the basis of minimum initial information will be able to solve complicated problems of pattern recognition.

This work is supported by the grant from the Georgian Academy of Sciences.

Georgian Academy of Sciences
Institute of Cybernetics

REFERENCES

1. *Marshall Hall.* Combinatorial Theory. M., 1970.
2. *N.T. Tkemaladze.* Theoretical Cybernetics-3, Tbilisi, 1980.
3. *N. Tkemaladze.* Collected Articles. Some Problems of Pattern Recognition with Learning and Expert Systems, Tbilisi, 1998.
4. *N.T. Tkemaladze.* Recognition, Classification, Estimation, Tbilisi, 1990.
5. *V.V. Chavchanidze.* Works of IV IUC about Artificial Intelligence, Tbilisi, 1975.
6. *M.A. Aizerman, A.B. Malishevsky.* Automatics and Telemechanics, N 2, 1981.

საქართველოს მეცნიერებათა აკადემიის მოამბე, 159, №1, 1999
BULLETIN OF THE GEORGIAN ACADEMY OF SCIENCES, 159, №1, 1999

PHYSICS

N.Kekelidze, V.Gogiashvili, L.Kvinikadze, Z.Davitaya, L.Milovanova, G.Chikhradze, Z.Chubinishvili

The Analysis of the Electron Mobility and the Determination of the Impurity Concentration in n-type Gallium Arsenide

Presented by Corr. Member of the Academy T. Sanadze, January 29, 1998

ABSTRACT. **In the present work the method of determination of electrically active impurity concentration in n-type gallium arsenide is given. The method is based on the analysis of the experimentally measured free carrier mobility taking into account all major scattering mechanisms. The corresponding practical recommendations are worked out on the basis of the obtained results.**

Key words: semiconductor, mobility, concentration, compensation ratio.

It is known that the analysis of the theoretical and experimental values of the electron mobility allows to estimate the number of impurity ions in the crystal. Of course, low temperature measurements would eliminate a number of complications in the theoretical calculations, making it possible to investigate directly the ionized impurity scattering. But in this case, some other complications of technical nature will arise. That is why we considered it reasonable to determine the impurity concentration at room temperature, that is supported by our studies, described below.

We have used the Matthiessen's rule for calculations of theoretical values of mobility. According to this rule the reciprocal values of mobilities, corresponding to all major scattering mechanisms are added that reflects the probability addition law. However, we have considered necessary to compare our results with the data of [1]. A number of experiments have been carried out to study electrical properties on GaAs samples with electron concentration $n\sim(10^{16}\text{-}10^{18})cm^{-3}$ at room and liquid nitrogen temperatures in the magnetic field of 7 kG.

The analysis of the results has been performed with allowance for all major scattering mechanisms [2 – 6] . The theoretical values of mobility have been calculated on the computer and represented in the form of corresponding tables and graphics (Tables 1, 2). On their basis the compensation ratio θ in the investigated samples has been determined, which is connected with impurity concentration N_i by a simple expression

$$N_i = n\frac{1+\theta}{1-\theta}$$

Table 1

The theoretical values of electron mobility in gallium arsenide at room temperature

n \ θ	0.0	0.1	0.2	0.3	0.4	0.5	0.6	0.7	0.8	0.9
$1x10^{16}$	6962	6901	6827	6633	6612	6450	6222	5874	5885	4062
1.5	6960	6878	6777	6652	6492	6281	5988	5557	4858	3526
2	6984	6886	6766	6618	6431	6185	5851	5367	4605	3230
3	6882	6745	6581	6382	6134	5818	5401	4824	3975	2601
4	6611	6412	6180	5905	5574	5169	4960	4004	3124	1883
5	6636	6424	6178	5888	5541	5119	4594	3923	3037	1810
6	6665	6450	6199	5904	5552	5125	4594	3917	3026	1799
7	6508	6263	5982	5655	5271	4814	4259	3574	2703	1562
8	6436	6174	5876	5532	5131	4659	4094	3406	2549	1452
9	6401	6128	5818	5463	5052	4570	3998	3308	2459	1390
$1x10^{17}$	6500	6198	5858	5472	5030	4915	3921	3213	2361	1314
1.5	6129	5768	5372	4936	4454	3919	3320	2646	1882	1009
2	5973	5561	5119	4645	4134	3584	2986	2337	1629	853
3	5374	5320	4843	4343	3818	3265	2682	2067	1417	729
4	5876	5358	4826	4279	3718	3141	2548	1938	1311	665
5	4760	4226	3707	3202	2709	2229	1761	1304	859	424
6	5051	4501	3962	3434	2915	2406	1907	1417	936	464
7	4801	4245	3707	3189	2687	2202	1733	1279	839	413
8	4702	4137	3597	3080	2584	2109	1654	1216	795	390
9	4694	4117	3569	3048	2551	2077	1624	1191	777	380
$1x10^{18}$	4566	3987	3442	2927	2440	1979	1543	1128	733	358
1.5	4180	3582	3038	2542	2087	1670	1284	927	596	288
2	3886	3305	2785	2316	1892	1505	1152	828	530	255
3	3763	3178	2661	2201	1789	1417	1080	774	494	237
4	3224	2690	2228	1826	1471	1157	876	624	396	189
5	3050	2535	2092	1709	1374	1077	814	579	366	175

The results of the investigations are given in Table 3. It follows from Table 3, that the compensation ratio for GaAs can be calculated with high precision at room temperature.

Therefore, on the basis of our study a simple practical method of determination of impurity concentration in gallium arsenide crystals has been developed.

Moreover, it has been confirmed, that:

1.The investigations may be carried out in the magnetic field of 7 – 8 kG, instead of 100 – 150 kG, which was used in [1]. It is noticed, that production of such fields is

Table 2

The theoretical values of electron mobility in gallium arsenide at liquid nitrogen temperature

n \ θ	0.0	0.1	0.2	0.3	0.4	0.5	0.6	0.7	0.8	0.9
$1x10^{16}$	38350	32030	26550	21770	17550	13810	10460	7449	4728	2256
1.5	30450	25310	20890	17070	13720	10760	8131	5778	3660	1743
2	24280	20110	16550	13490	10820	8469	6389	4533	2867	1364
3	21270	17580	14450	11760	9418	7366	5552	3936	2488	1183
4	18200	15020	12330	10020	8019	6266	4719	3343	2112	1003
5	17700	14600	11980	9735	7788	6085	4581	3245	2050	974
6	9621	7906	6466	5239	4181	3259	2449	1732	1092	518
7	11150	9171	7505	6083	4856	3788	2847	2014	1270	603
8	11320	9309	7617	6174	4929	3844	2890	2044	1289	612
9	10360	8511	6961	5640	4501	3509	2637	1865	1176	558
$1x10^{17}$	9955	8179	6688	5418	4323	3370	2532	1791	1129	536
1.5	9119	7487	6118	4954	3951	3079	2313	1635	1031	489
2	6754	5540	4523	3660	2917	2272	1706	1205	760	360
3	6756	5540	4523	3659	2916	2271	1705	1205	759	360
4	6574	5390	4400	3558	2835	2208	1657	1171	738	350
5	5082	4164	3397	2747	2188	1703	1278	903	569	270
6	5500	4507	3677	2973	2369	1844	1384	977	616	292
7	4517	3700	3018	2440	1943	1512	1135	802	505	239
8	4768	3906	3186	2575	2051	1597	1198	846	533	253
9	4877	3995	3259	2635	2099	1633	1226	866	545	258
$1x10^{18}$	4310	3530	2879	2327	1854	1442	1082	764	482	228
1.5	3923	3212	2620	2117	1686	1312	985	695	438	207
2	3545	2903	2367	1913	1523	1185	889	628	395	187
3	3399	2783	2269	1834	1460	1136	853	602	379	180
4	3230	2645	2156	1742	1388	1080	810	572	360	171
5	2863	2344	1911	1544	1229	957	718	507	319	151

Table 3

№№	300K n, cm^{-3}	300K u_{exp}, $cm^2/V\,s$	300K θ_b	77K n,cm^{-3}	77K u_{exp}, $cm^2/V\,s$	77K θ_b	material
1	$1,85x10^{17}$	$3,80x10^3$	0,45	$1,35x10^{17}$	$4,28x10^3$	0,40	GaAs
2	$8,70x10^{17}$	$2,75x10^3$	0,35	$8,10x10^{17}$	$2,57x10^3$	0,30	"-"
3	$1,00x10^{18}$	$2,60x10^3$	0,35	$9,60x10^{17}$	$2,80x10^3$	0,35	"-"
4	$1,20x10^{18}$	$3,20x10^3$	0,20	$1,10x10^{18}$	$3,30x10^3$	0,15	"-"

connected with great technical complications; it requires an application of superconductive solenoids and expensive liquid helium or it is necessary to use high-power cooling and feed systems.

2. We have showed that the compensation ratio established at liquid nitrogen temperature is in perfect agreement with that defined at room temperature; it is not shown in [1].

3. [1] for the analysis of experimental values of electron mobilities the complicated mobility calculations, based on a variational procedure were used. It is shown, that the values determined by us using Matthiessen's rule do not almost differ from the values, presented in [1], which does not exert essential influence on the determination of electrical parameters of the studied crystals.

The investigation has been carried out in the framework of the state target programs of Department of Science and Technology of Georgia.

Tbilisi I. Javakhishvili State University

REFERENCES

1. *W.Walukiewicz, L.Lagowski, L.Jastrzebski et al.* J.Appl.Phys., 50, 2, 1979, 899.
2. *J.Bardeen, W.Shockley.* Phys.Rev., 80, 1950, 72.
3. *H.Ehrenreich.* J..Phys. Chem. Solids, 2, 1957, 131.
4. *H.Ehrenreich.* J. Phys. Chem. Solids, 8, 1959, 130.
5. *H.Ehrenreich.* J. Phys. Chem. Solids, 9, 1959, 129.
6. *H.Mansfield.* Proc. Phys. Soc., 69B, 1956, 76.

საქართველოს მეცნიერებათა აკადემიის მოამბე, 159, №1, 1999
BULLETIN OF THE GEORGIAN ACADEMY OF SCIENCES, 159, №1, 1999

PHYSICS

G. Devidze, L. Slepchenko

Neutrino Masses in the MSSM

Presented by Member of the Academy N. Amaglobeli, December 12, 1997.

ABSTRACT. **On the basis of direct experimental, cosmological and astrophysical bounds the neutrino one-photon radiative decays are studied. The possible values of neutrinos masses are considered.**

Key words: neutrino, supersymmetry, mass, photon

Massive neutrinos contribute to the energy density of the Universe. Requiring that this contribution doesn't exceed the observed upper limit on the density of the Universe, we can obtain constraints on the masses of the stable neutrinos and conditions on the masses and lifetimes of unstable neutrinos. A stable neutrino is lighter than 65 eV or heavier than 8 GeV [1-4]. An unstable neutrino can have a mass in the forbidden range (from 65 eV to 8 GeV) if its lifetime satisfies the conditions[1-4]:

$$\begin{aligned} m^2(\nu)\tau(\nu)/t_0 &\le 4\cdot 10^3\ \text{eV}^2, \quad \text{for } m(\nu) \le 0\ \text{(MeV)},\\ m^4(\nu)\tau(\nu)/t_0 &\le 4\cdot 10^{-39}\ \text{eV}^2, \quad \text{for } m(\nu) \ge 0\ \text{(MeV)}, \end{aligned} \tag{1}$$

where t_0 is the age of the Universe ($t_0 = 1.3\cdot 10^{10}$ yr), if among the neutrino decay products there are charged particles, there are additional constraints following from the fact that the black-body background radiation should not be destorted, primordial nuclear synthesis should not be changed, the γ-ray flux in $e^{\pm}$ annihilation should not exceed the observed flux and deuterium should not be broken up by photodisintegration. Each of these effects allows the neutrino lifetime to be found in a particular range. Combining these, we obtain[5, 6]:

$$\tau(\nu) \le 5\cdot 10^3 \text{sec} \tag{2}$$

In the extended version of the standard model (SM) a massive neutrino is unstable and therefore the study of possible ranges of neutrino mass becomes expedient from the viewpoint of cosmological and astrophysical bounds. Let us proceed to considering radiative neutrino decay in the minimal supersymmetric standard model (MSSM) [7]. One-photon neutrino decay takes place at one loop level. The diagrams describing one-photon neutrino decay are presented in Fig.1.

The on-shell decay amplitude $A(\nu \to \nu_b\gamma)$ has the form:

$$A(\nu_a \to \nu_b\gamma) = \epsilon^{\mu}\bar{\nu}_b(p_2)\sigma_{\mu\nu}(p_1 - p_2)^{\nu}(F_V + \gamma_b F_A)\nu_a(p_1) \tag{3}$$

Calculation of the width of the decay $\nu_a \to \nu_b\gamma$ gives:

$$\Gamma(\nu_a \to \nu_b\gamma) = \frac{F_V^2 + F_A^2}{8\pi}\left(\frac{m^2(\nu_a) + m^2(\nu_b)}{m(\nu_a)}\right)^3 \tag{4}$$

Let us present the contributions of the diagrams of Fig.1 to the decay $\nu_a \to \nu_b\gamma$:

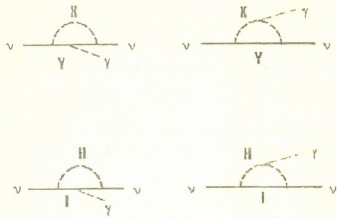

Fig. 1. Neutrinos one-photon radiative decay in the MSSM (X = charged scalar leptons, Y = charged gauge fermions, H = charged higgs particles, l = charged leptons.)

$$F_V^L = \frac{1}{(4\pi)^2} eg^2 \sum_{i,j} \lambda_i \left\{ \frac{m(\widetilde{\chi}_j^+)}{\sqrt{2} m_W \cos\beta m^2(\widetilde{\chi}_j^+)} \frac{1}{} (m(\nu_a) U_{j1} V_{j2} + m(\nu_b) U_{j1}^* V_{j2}^*) f_1(x_{ij}^L) + \right.$$

$$\left. + (U_{j1}^2 + \frac{m(\nu_a) m(\nu_b) V_{j2}^2}{2 m_W^2 \cos^2\beta}) \frac{m(\nu_a) + m(\nu_b)}{m^2(\widetilde{\chi}_j^+)} f_2(x_{ij}^L) \right\} \tag{5}$$

$$F_V^R = \frac{1}{(4\pi)^2} eg^2 \sum_{i,j} \lambda_i U_{j2}^2 \frac{m(\nu_a) + m(\nu_b)}{m_W^2 \cos^2\beta} x_{ij}^R f_2(x_{ij}^R) \tag{6}$$

$$F_V^H = \frac{1}{(4\pi)^2} eg^2 \sum_{i,j} \lambda_i \left\{ \frac{m(\nu_a) + m(\nu_b)}{m_W^2} y_i f_3(y_i) - \frac{1}{2} f_2(y_i) (y_i \tan^2\beta + \right.$$

$$\left. \frac{m(\nu_a) m(\nu_b)}{m_H^2} \cot^2\beta) \frac{m(\nu_a) + m(\nu_b)}{m_W^2} \right\}, \tag{7}$$

where $\lambda_i = U_{ai} U^*_{bi}$, U_{ij} are supersymmetric particles mixing matrix elements[8] and we have introduced the following notation:

$$f_1(x) = \frac{1 - x + x\ln x}{2(1-x)^2}, \quad f_2(x) = \frac{x^2 - 1 - 2x\ln x}{8(1-x)^3}, \quad f_3(x) = \frac{x - 1 - \ln x}{4(1-x)^2},$$

$$x_{ij}^{L} = \frac{m^2(\tilde{l}_{Li})}{m^2(\tilde{\chi}_j^+)}, \quad x_{ij}^{R} = \frac{m^2(\tilde{l}_{Ri})}{m^2(\tilde{\chi}_j^+)}, \quad y_i = \frac{m^2(l)}{m_E^2} \tag{8}$$

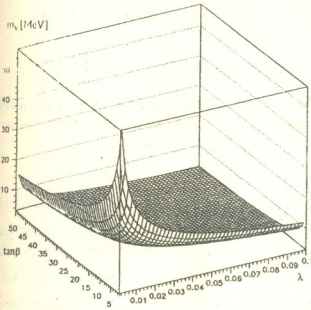

Fig. 2. Upper bound on the neutrinos masses.

Formfactors F_A satisfied the following condition:

$F_A(m(\nu_a), m(\nu_b))=F_V(m(\nu_a)-m(\nu_b))$

Applying limitations (1),(2) to expressions (3)-(9) we obtain lower bound on the neutrino mass (Fig.2). The combined analysis in the light of cosmological and astrophysical constraints imposed on neutrino decays in the frame of supersymmetric extended standard model version leads to the following results: muon and electron neutrinos should be light ($m(\nu_e)<9$ eV [9], $m(\nu_\mu)<65$ eV) and τ- neutrino may be relatively heavy $5\text{MeV}<m(\nu_\tau)< 23$ MeV.

The authors express their deep gratitude to N.Amaglobeli, T.Kopaleishvili, A. Tavkhelidze, M.Kopadze, N.Lomidze, T. M.Sakhelashvili for fruitful discussions and support.

Tbilisi I.Javakhishvili State University
High Energy Physics Institute

REFERENCES

1. *H. Harari, Y.Nir.* Nucl. Phys. V. B 292, 1985, 251.
2. *E. W. Kolb.* In: Proceeding of the 1986 Santa Crus JASJ (World Scientific,Singapore 1987).
3. *B. W. Lee, S. Weinberg.* Phys. Rev. Lett. 39, 1977, 165.
4. *J.Berstein et al.* Phys. Rev. **D 32**, 1985, 3261.
5. *M. Kawasaki et al.* Phys. Lett. **B 178**, 1986, 71.
6. *S. Sarker, A. M. Cooper.* Phys. Lett. **B 148**, 1984, 347.
7. *G. Degrasi, A. Masiero.* Phys.lett. **B 202**, 1988, 117.
8. *H. E. Haber, G.L.Kane.* Phys. Rep. **117**, 1985, 75.
9. Review of Particle Properties.Phys. Rev., **D 54**, 1996.

საქართველოს მეცნიერებათა აკადემიის მოამბე, 159, №1, 1999
BULLETIN OF THE GEORGIAN ACADEMY OF SCIENCES, 159, №1, 1999

PHYSICS

A.Lomidze, Sh.Tsiklauri

Modified Hyperspherical Function Method for Inverse Square Potential

Presented by Corr. Member of the Academy A.Kheiashvili, January 16, 1998

ABSTRACT. **The method of modified hyperspherical function has been applied for nonmodel representation of the solution of three particles problem for the potential r^{-2}. Finite quantity of ground-state energy has been obtained.**

Key words: few body system, hyperspherical function, singular potential.

Many physical phenomena may be described by singular potentials [1]. Potentials of the type g/r^2 are of special interest, especially in polymers [2], and in the interaction between Rydberg atom and polar molecules [3]. One dimensional integrating models with interaction of the type g/r^2 should be of significance for fractional quantum Hall effect. The problem of three particles for paired interaction of g/r^2 type in one dimensional space in a field harmonic oscillator has been analytically solved by F.Calogero [4]. Properties of a ground state of three boson system are universal and defined by effective interaction of $\sim 1/r^2$ type , therefore microscopic theory of three particles for paired interaction of a type g/r^2 is of high priority. Use of the hyperspherical function method (HFM) is convenient, as by this method the equation of radial wave function has a form of the equation of radial wave function for two bodies and the methods used for the solution of the latter can be successfully used for the solution of three bodies problem.

Schrodinger equation in a system of centre of masses for three nonidentical, nonrelativistic particles in hyperspherical coordinates is defined in [5]. On solving the problem for hyperradial functions we obtain a system of the coupled differential equations. Let's consider one equation from this system, when $K=K'$ (K is the hypermoment of the particles). This gives the equation:

$$\left(\frac{\partial^2}{\partial\rho^2}-\left[\kappa^2+\frac{(K+2)^2-.25}{\rho^2}\right]\right)\varphi_K(\rho)=\frac{2\mu}{\rho^2}J_K\varphi_K(\rho), \tag{1}$$

where

$$J_K=\int\Phi^*_K(\Omega)\Phi_K(\Omega)(\cos\alpha)^{-2}d\Omega \tag{2}$$

and $\kappa^2=-2\mu E$; $\Phi(\Omega)$ is eigenfunctions of the generalized angular-momentum operator whose analytical form is known [5], $\Omega\equiv(\alpha,\vec{x},\vec{y})$-five angles, ρ and α are

defined by the expressions: $\rho^2 = x^2 + y^2$; $\vec{x}$ and $\vec{y}$ are the Jacoby coordinates; $|\vec{x}| = \rho\cos\alpha$; $|\vec{y}| = \rho\sin\alpha$; $(0 < \rho < \infty;\ 0 < \alpha < \pi/2)$. $E < 0$ is a binding energy for three particles; μ is a reduced mass. The integral (2) can be calculated analytically [6] and it equals

$$J_K = \frac{\Gamma(K/2+1)\Gamma(K/2+2)(K+2)}{\Gamma(K/2+3/2)\Gamma(K/2+3/2)} \times$$

$$\times \sum_{k}^{K/2} \left[\binom{K/2+0,5}{k} \binom{K+0,5}{K/2-k} \right]^2 \mathrm{B}(K-2k+0,5;\ 2k+1,5) \qquad (3)$$

Usual analysis shows that under these conditions the ground state energy has infinitely large negative value, thereby rendering the solution to be physically meaningless. To avoid this situation we use two methods:

1. We should define the cut off parameter ρ_0. ρ_0 depends on the interaction constants between the particles g_{ij}, then the function $\varphi_K(\rho)$ is defined within the interval $[\rho_0, \infty]$ and satisfies the condition $\varphi_K(\rho_0) = 0$. The solution of the equation (1) is in [7] and equals $\varphi(\rho) = (\kappa\rho)^{1/2} \mathrm{h}_{i\lambda}(\kappa\rho)$, where $\mathrm{h}_{i\lambda}(\kappa\rho)$ is the modified Bessel function of the third order: $\lambda^2 = K^2 + 4K + 3{,}5 + 2\mu J_K$;

For small values of $\kappa\rho$ the zeroes of this function are given by the equation:

$$(\kappa\rho)_N = 2\exp(-N\pi/\lambda - \gamma), \qquad (4)$$

where γ is the Euller's constant, and $N = 1,2,3\ldots$;

From the expression (4) for binding energy we have:

$$E_N = -\exp(-2N\pi\lambda^{-1})(2\rho_0^{-1}\exp(-\gamma))^2/(2\mu). \qquad (5)$$

For fixed λ, when $\rho_0 \to 0$, then energy levels tend to negative infinity. Renormalization should be made according to the method offered in [7]. To receive a physical solution we assume, that constant λ is such function of the cut off parameter ρ_0, for which the ground state energy $E_1 - (N = 1)$ is independent of ρ_0. This fact can be written as $dE_1/d\rho_0 = 0$. Taking this fact into consideration the ground state energy (also any level of energy) has finite value.

2. Method of modified hyperspherical function (MMHF), worked out in [8-10].

The main idea of the MMHF consists in that the wave function Ψ represents the product of two functions, where the first function is the ordinary hyperspherical function and the second is the correlation function $\zeta = \exp(f)$, which defines singularity and clustering properties of the wave function and is equal to [9]

$$f = -\sum_{i=1}^{3} \gamma_i r_i, \qquad (7)$$

where r_i is a distance between the particles and γ_i is determined according to physical considerations. Using the relation between three different sets of Jacobi coordinates [5] the expression (7) can be presented as follows:

$$\sum_{i=1}^{3}\gamma_i z_i = \rho(G_1\cos\alpha + G_2\sin\alpha),$$

where $G_1 = \gamma_1 + \gamma_2\cos(\phi_{23}+\phi_{31}) - \gamma_3\cos\phi_{31}$; $G_2 = \gamma_2\sin(\phi_{23}+\phi_{31}) - \gamma_3\sin\phi_{31}$.

Employment of MMHF [9] shows, that paired correlation in effective potential introduces a correction producing finite quantity of ground state energy.

Substituting expressions (7) into (1), and carrying out some transformations, we can finally derive hyperradial differential equation. Let us consider one equation when K=0:

$$\left(\frac{\partial^2}{\partial\rho^2} + \left(\frac{5}{\rho} - W_2'\right)\frac{\partial}{\partial\rho} + \frac{W_4' + W_3'}{\rho} + \left(\kappa^2 + W_6'\right) - \frac{2\mu J_0}{\rho^2}\right)\psi(\rho) = 0 \qquad (8)$$

where:

$$W_2' = (G_1 - G_2)*\frac{4}{15}; \quad W_4' = 3W_2'; \quad W_6' = G_1^2 + G_2^2; \quad W_3' = G_1\left(\frac{4}{15} - \frac{3\pi}{8}\right) - \frac{42}{105}G_2;$$

Taking into account the asymptotic behaviour of the equation (8), let us seek a solution as follows:

$$\psi(\rho) = \exp(-\delta\rho)\rho^{\sigma}\varphi(\rho) \qquad (9)$$

where $\sigma = -2 + \left[4 + 2mJ_0\right]^{1/2}$; $\delta = \left(\left[W_2'^2 - 4\left(\kappa^2 + W_6'\right)\right]^{1/2} - W_2'\right)/4$.

Substituting expression (9) in the equation (8), for $\varphi(\rho)$ we obtain a hypergeometrical equation :

$$\left(r\frac{\partial^2}{\partial r^2} + (-r+\sigma+5)\frac{\partial}{\partial r} + \frac{(W_4' + W_3' - 2\delta\sigma - 5\delta - \sigma W_2')}{2\delta + W_2'}\right)\varphi(r) = 0 \qquad (10)$$

where: $r = (2\delta + W_2')\rho$.

Taking into account a three body system being binded solution of the equation (10) represents a hypergeometrical function of the following type:

$$\varphi(\rho) = C_1 F(a,b,r) \qquad (11)$$

where $b = \sigma + 5$; $a = \dfrac{(W_4' + W_3' - 2\delta\sigma - 5\delta - \sigma W_2')}{2\delta + W_2'} = -N$, $\quad N = 1,2....$

For binding energy we receive:

$$E_N = -\frac{1}{2\mu}\left\{\frac{1}{4}\left[\left(\frac{4W_4' + 4W_3' - W_2'(2\sigma + 5 - 3N)}{2\sigma + 5 - N}\right)^2 - W_2'^2\right] + W_6'\right\} \qquad (12)$$

It is clear, that expression in curly brackets should be more than zero. It permits us

to establish relationship between three independent correlation parameters. Using formula (12), for the ground state energy ($N=1$) correlation parameters may be chosen in such way that the magnitude of the energy determined by (5) would be equal to that of obtained by means of renormalization method.

Hyperspherical function method permits us to advance comparatively simple and nonmodel representation of the solution three particles problem for the potential of a type $1/r^2$ in case of paired interaction. In a first approximation the problem is decided analytically, which allows us to carry out nonperturbation renormalization and determine a ground-state energy.

The correlation function can be used, which is due to the appearance of singularity of a type $\sim\rho^{-1}$ simultaneously with that of a type $\sim\rho^{-2}$ in effective potential, that leads us to the ground-state energy of finite quantity.

This work was supported by International Science Foundation (G.Sorros Fund) Grant No. KZ 8200.

I. Javakhishvili Tbilisi State University

REFERENCES

1. *WM.Frank, D.Land, R.M.Spector.* Rev. Mod.Phys. 43, 1971, 36.
2. *E.Marinari, G.Parisi.* Europhys. Lett. **15**, 1991, 721.
3. *C.Desfranqois, H. Abdoul-Carime, N.Khelifa, J.P.Schermann.* Phys. Rev. Lett. **73**, 1994, 2436.
4. *FCalogero.* J.Math.Phys. **10**, 1969, 2191.
5. *R.I.Jibuty, N.B.Krupennikova.* The Hyperspherical Functions Method in Few - Body Quantum Mechanics. Tbilisi, 1984 (Russian).
6. *R.I.Jibuty, A.M.Lomidze, Sh.M.Tsiklauri.* Journal of the Georgian Physical Society **A2**, 1994, 198.
7. *K.G.Gupta, S.G.Rajeev.* Phys. Rev. **D48**, 1993, 5940.
8. *A.M.Gorbatov, A.V.Bursak, Yu.N.Krilov, B.V.Rudak.* Yad. Fiz. **40**, 1984, 233.
9. *M.I.Haftel, V.B.Mandelzweig.* Phys. Lett. **A120**, 1987, 232, Ann. Phys. (N.Y.) **189**, 1989, 29.
10. *Fabre de la Ripelle.* Ann. Phys. (NY), 147, 1982, 281.

საქართველოს მეცნიერებათა აკადემიის მოამბე, 159, №1, 1999
BULLETIN OF THE GEORGIAN ACADEMY OF SCIENCES, 159, №1, 1999

PHYSICS

I. Loria, V. Kevanishvili, F. Bogdanov

Diffraction of Flat Electromagnetic Wave on the Lattice Formed of Cylinders Located in Semi-Infinite Medium

Presented by Corr. Member of the Academy A. Khelashvili, February 10, 1998

ABSTRACT. **A problem discussed in the paper describes a situation when E-polarized flat electromagnetic wave is incidented from free space on a flat semi-infinite dielectric, while inside the dielectric there is located a lattice formed of infinitely long compietely admitting circular cylinders, a distance from the inner surface of the dielectric being the specific one.**

There have been determined diffraction and multipolar spectra of the scattered field. Numerical results were obtained and appropriate physical interpretations were made.

Key words: electromagnetic wave, diffraction, scattered field, diffraction spectra, multipolar spectra.

One of the most significant problems of radiophysics is a study of the phenomenon of electromagnetic diffraction. Classes of scattering diffraction are represented by diffraction lattices. Their using is based on the properties of interfractional summation of scattered field of separate elements. In the present paper there is discussed a task of diffraction of a flat electromagnetic wave on the lattice formed of cylinders located in semi-infinite medium.

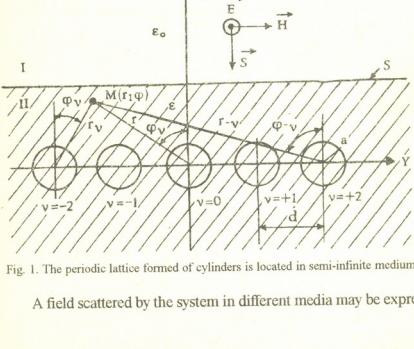

Fig. 1. The periodic lattice formed of cylinders is located in semi-infinite medium.

A cross-section of the above mentioned subject in $Z=0$ plane is shown in Fig. 1.

Primary E-polarized flat wave $E_{z0} = e^{ikx}$ is incident on an intermedium surface S. Our goal is to determine electromagnetic field structure in the (I) and (II) media and a wave reflection factor in the (I) medium.

A field scattered by the system in different media may be expressed by the following way

$$E_{z1} = E_{z0} + \sum_{p=-\infty}^{\infty} R_p e^{ig_p y - ih_p x} \qquad x \geq l \tag{1}$$

$$E_{z2} = E^*_{z2} + \sum_{p=-\infty}^{\infty} C_p e^{ig_p y + ih'_p x} \qquad x < l \tag{2}$$

$$E^*_{z2} = \sum_{m=-\infty}^{\infty} \sum_{\nu=-\infty}^{\infty} X_m H_m^{(2)}(k_2 \nu_\nu) e^{im\varphi_\nu} \qquad x < l \tag{3}$$

E^*_{z2} is a field scattered immediately from the lattice.

It can be expanded into the Furier Series (so called diffraction spectrum)

$$E^*_{z2} = \begin{cases} \sum_{p=-\infty}^{\infty} A_p^{(-)} e^{ig_p y - ih'_p x} & a \leq x \leq l \\ \sum_{p=-\infty}^{\infty} A_p^{(+)} e^{ig_p y + ih'_p x} & -\infty < x < -a \end{cases} \tag{4}$$

$$E_{z3} = \sum_{p=-\infty}^{\infty} B_p e^{ig_p y + ih'_p x} \quad -\infty < x < -a, \tag{5}$$

where R_p, C_p, B_p are any unknown quantities;

X_m are multipolar coefficients, $A_p^{(-)}$ and $A_p^{(+)}$ are the unknown amplitudes of diffraction spectrum.

$$g_p = \frac{2\pi p}{d}, \quad h_p = \sqrt{k^2 - g_p^2}, \quad h'_p = \sqrt{k^2 \varepsilon_r - g_p^2}$$

In case of using the limiting conditions one can establish a relationship between the diffraction factors of the field.

Let us establish relationship between the coefficients of multipolar spectrum X_m and the $A_m^{(-)}$, $A_m^{(+)}$ coefficients of the diffraction spectrum. Using the Green formula [1] we can write:

$$A_p^{(\pm)} = \begin{cases} \dfrac{1}{\pi\sqrt{D^2 - p^2}} \sum_{m=-\infty}^{\infty} i^{\mp m} X_m e^{\pm im\varphi_p} & |p| < D' \\ \dfrac{1}{\pi\sqrt{p^2 - D'^2}} \sum_{m=-\infty}^{\infty} X_m e^{\mp m\varphi'_p} & p > D' \\ \dfrac{1}{\pi\sqrt{p^2 - D'^2}} \sum_{m=-\infty}^{\infty} (-1)^m X_m e^{\pm m\varphi'_p} & p < -D' \end{cases} \tag{6}$$

where $\varphi_p = arctg\dfrac{p}{\sqrt{D'^2 - p^2}}$; $\varphi'_p = arctg\dfrac{\sqrt{p^2 - D'^2}}{|p|}$

$$D' = D\sqrt{\varepsilon_r}\ ;\ D = d/\lambda \tag{7}$$

Using the limiting conditions, summarizing theoreme [2] and the expressions (6), (7) one can write functional equation.

Solution of this equation is possible if a method of projection is used. Let us assume $e^{im\varphi}$ to be basic functions, then we can write:

$$x_s = -\xi_s \bar{\varpi}_s - \sum_{m \neq s}^{\infty} x_s \overline{Q}_{sm} \tag{8}$$

where

$$\xi_s = \left(2i^s / l + \sqrt{\varepsilon_r}\right) e^{i(k-k_2)l} \tag{9}$$

$$\bar{\varpi}_s = \frac{1}{H_s^{(2)}(\alpha) + I_s(\alpha)\left\{z_0(\beta) + \Delta_{ss} + (1+\delta_{s0})(-1)^s\left[z_{2s}(\beta) + \Delta_{-ss}\right]\right\}} \tag{10}$$

$$\overline{Q}_{sm} = \bar{\varpi}_s \left\{z_{m-s}(\beta) + \Delta_{ms} + (-1)^m(1-\delta_{m0})\left[z_{m+s}(\beta) + \Delta_{-ms}\right] \times I_m(\alpha)\right\} \tag{11}$$

$$\Delta_{ms} = \sum_{p=0}^{[D']} \left(2 - \delta_{p0}\right) \frac{b_p i^{s+m} \cos(s+m)\overline{\varphi}_p}{\pi d_p \sqrt{D'^2 - p^2}} +$$

$$+ \sum_{p=1+[\sum p']}^{\infty} i \frac{b_p}{\pi d_p \sqrt{p^2 - D'^2}} \left[e^{i(m+s)\varphi'_p} + (-1)^{m+s} e^{-(m+s)\varphi'_p}\right] \tag{12}$$

Free members of the system (8) $\xi_s \bar{\varpi}_s$ and the matrix elements Q_{sm} are satisfying the conditions of quadratic elasticity (by modulus).

The system (8) is changeable by the finite system and solved on a computer by the reduction method. If one sees that an approximate solution is not changing practically beginning from $N \geq N_0$, then, $x_m^{(N)}$ $(N \geq N_0)$ must be considered as a reliable solution [3].

The system (8) will be solved on the (IBM-PCAT-286) computer for the various values of parameters, such as $D = d/\lambda$, $s = 2a/d$, e/d, ε_r; the results can be used for the building of various curves which express a dependence of the reflection factor modulus $|R_0|$ on the lattice relative period d/λ. Calculations are made for the various numerical quantities of the rest of parameters shown in Fig. 2.

The given medium almost completely reflects the incident E-polarized flat wave within the range of long waves ($d/\lambda << 1$). With the increase of d/λ, the reflection constant

decreases monotonously. Its velocity is high as much as ε_v is a large and the lattice filling constant is small $s = 2a/d$. Futher increase of d/λ promotes the formation of acute resonances of reflection constants which, in fact, are the Wood anomalies. These anomalies appear when d/λ is not integer quantity pointing to the fact that a wave-length in dielectric is not equal to that in the void. The increase of ε_1 promotes formation of additional resonance. This phenomenon is not related to the Wood anomalies. Bending points can be observed on the $\varepsilon_r = 1,2$ curves built for the definite d/λ. These resonanes are characteristic for the area of long-(one-harmonic) as well as $d/\lambda > 1$ short-waves. Hence, they are not connected to the phenomenon of energy redistribution in the diffraction spectrum. A character of complex relationship of the reflection constant with d/λ can be explained basing on the following consideration: area between the dielectric surface and lattice represents a resonator with transparent (open) walls. It has intrinsic wave length representing determinant roots of the system of homogenous algebraic equations.

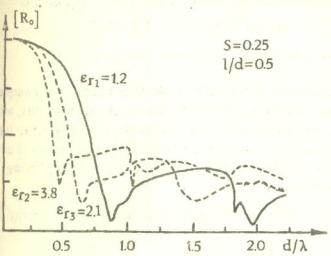

Fig. 2. The dependence graphic of the reflection factor modulus $|R_0|$ on the lattice relative period d/λ when $s = 0.25$, $\lambda/d = 0.5$.

$$x_s + \sum x_s \overline{Q}_{sm} = 0 \tag{13}$$

If external (primary) wave length coincides with intrinsic frequency of the resonator, the latter may become home for gathering of large electromagnetic energy promoting a low value of the reflection constant.

Georgian Technical University

REFERENCES

1. *F. G. Bogdanow, G. Sh. Kevanishvili.* Difraktsia voln na reshetkakh i wolnowodnykh neodnorodnostyakh. Tbilisi, 1994 (Russian).
2. *J. A. Stratton.* Teoriya electomagnetizma. Moscow, 1948, (Russian).
3. *A. V. Kontorovich, B. V. Abimov.* Funcktsionalnyi analiz. Moscow, 1984 (Russian).

საქართველოს მეცნიერებათა აკადემიის მოამბე, 159, №1, 1999
BULLETIN OF THE GEORGIAN ACADEMY OF SCIENCES, 159, №1, 1999

PHYSICS

T. Nadareishvili

Relations Between Relativistic and Non Relativistic Equations Eigenvalues by Using Comparison Theorem

Presented by Corr. Member of the Academy A. Khelashvili, February, 23, 1998

ABSTRACT. **In the paper quasipotential model relativistic equation is compared with Schrödinger equation using comparison theorem. We received theorems, which show that for potentials having only negative relativistic levels, level's spacing (splitting) increase in the relativistic case compared with Schrödinger equation. For the potentials, which have only positive relativistic levels, level's spacing (splitting) decrease in the relativistic case is expected.**

Key words: comparison theorem Schrödinger and relativistic equations, energy level spacing (splitting)

In quantum mechanics comparison theorem [1-3] is well known, particularly, if in Schrödinger equation for V_1 and V_2 potentials the condition $V_1<V_2$ is fulfilled, then for corresponding eigenvalues we have $E_1<E_2$. In [4-6] is given generalization of this theorem for that case, when potentials cross each other (i.e., $V_1<V_2$ condition is not always fulfilled). By using the comparison theorem and known solutions of Schrödinger equation we can determine low and upper threshold for the potentials, which we can't solve analytically. For example, consider three potentials

$$V_1 = -\frac{\alpha}{r}; \qquad V_2 = -\frac{\alpha}{r} + \alpha r; \qquad V_3 = gr^2. \tag{1}$$

It is obvious, that $V_1<V_2<V_3$. (2)

Therefore $E_1<E_2<E_3$. (3)

But for V_1 and V_3 eigenvalues are known, but for V_2 it is not known. Therefore by using (3) we get

$$-\frac{m\alpha_2}{2(n_r+l+1)^2} < E_2^{n,l} < \sqrt{\frac{g}{2m}}\{4n_r+2l+3\}. \tag{4}$$

More interesting relations may be received comparing Schrödinger equation and various relativistic equations. Let's compare in detail π-A trajectory relativistic equation (equal masses case) received in [7, 8] with Schrödinger equation

$$-U''+\left\{mV+\frac{J(J+1)}{r^2}\right\}U = mE^{Shr}U\,, \tag{5}$$

$$-U''+\left\{mV+\frac{J(J+1)}{r^2}+\frac{V^2}{4}\right\}U = \left\{\frac{M_{Rel}^2}{4}-m^2\right\}U\,. \tag{6}$$

It is obvious, that (6) equation may be considered as Schrödinger equation with effective potential $V_2 = mV + \frac{J(J+1)}{r^2} + \frac{V^2}{4}$ and $\lambda = \frac{M_{Rel}^2}{4} - m^2$ "energetic" parameter. It is also obvious, that always $V_1 < V_2$, where $V_1 = mV + \frac{J(J+1)}{r^2}$. Therefore from (5) and (6) by using comparison theorem we receive

$$mE_n^{Shr} < \frac{M_{n,Rel}^2}{4} - m^2 \tag{7}$$

$$M_n^{Shr} < \frac{M_{n,Rel}^2}{4m} + m \tag{8}$$

$$E_n^{Shr} < E_n^{Rel} + \frac{E_{n,Rel}^2}{4m}. \tag{9}$$

As we see from (8), if it is known for some potential Schrödinger equation exact spectrum, for the same potential (6) equation spectrum is restricted from below $M_{n,Rel} > 2\sqrt{mM_n^{Shr} - 4m^2}$.

(8) and (9) give possibility to compare masses energies spacing in relativistic and non relativistic cases. Indeed if we write (8) and (9) twice for $M_{n+1}(E_{n+1})$ and $M_n(E_n)$ levels, we can prove that

$$M_{n+1}^{Shr} - M_n^{Shr} < \frac{1}{4m}[M_{n+1,Rel}^2 - M_{n,Rel}^2] \tag{10}$$

In the [7] the (6) equation is solved for V=kr potential, when J=0, and in the [9] the same equation is solved for $V = -\frac{\alpha}{r}$ potential. It's easy to verify, that (10)relation is true for eigenvalues of the mentioned papers. In [7] it is mentioned, that for V=kr potential, when J=0, levels spacing (splitting) decrease compared to Schrödinger equation i.e., inequality $M_{n+1,Rel} - M_{n,Rel} < M_{n+1}^{Shr} - M_n^{Shr}$ takes place.

(10) inequality gives possibility to study this question deeper and show generally, what happens to levels spacing (splitting) in relativistic case. For this let's write (10) so

$$M_{n+1}^{Shr} - M_n^{Shr} < (M_{n+1,Rel} - M_{n,Rel})\frac{1}{4m}(M_{n+1,Rel} + M_{n,Rel}) \tag{11}$$

or

$$E_{n+1}^{Shr} - E_n^{Shr} < (E_{n+1,Rel} - E_{n,Rel})(1 + \frac{E_{n+1,Rel} + E_{n,Rel}}{4m}). \tag{12}$$

Based on (11) and (12) we can formulate such theorems:

Theorem 1. *For those potentials which have only negative relativistic levels, level's spacing (splitting) increase in the relativistic case compared to Schrödinger equation*

$$\Delta M^{Shr} < \Delta M^{Rel};\ \Delta E^{Shr} < \Delta E^{Rel}. \tag{13}$$

Proof. Let's make designation in (11) inequality

$$\varepsilon_0 = \frac{1}{4m}(M^{Rel}_{n+1} + M^{Rel}_n) = (1 - \frac{E^{Rel}_{n+1} + E^{Rel}_n}{4m}) < 1, \tag{14}$$

because according to condition we have only negative relativistic levels. Therefore it is seen from (11), that $\frac{\Delta M^{Shr}}{\Delta M^{Rel}} < \varepsilon_0 < 1$. We receive (13), the correctness of which is verified obviously on example of Coulomb potential, if we use formulas for levels received in [9].

Theorem 2. *For those potentials, which have only positive relativistic levels it's expected level's spacing (splitting) decrease in the relativistic case compared with Schrödinger equation*

$$\Delta M^{Shr} > \Delta M^{Rel}; \ \Delta E^{Shr} > \Delta E^{Rel}. \tag{15}$$

Proof. Indeed, in this case

$$\varepsilon_0 = 1 + \frac{E^{Rel}_{n+1} + E^{Rel}_n}{4m} > 1. \tag{16}$$

Therefore ε_0 may be so "great", that (15) is carried out (so it was for V=kr potential, when J=0 [7]). As it is seen from (16) if E^{Rel}_n depends upon mass so, that $E^{Rel}_n \sim m^{1+\beta}(\beta > 0)$, then $\varepsilon_0 >> 1$, when $m \to \infty$, and in this case for heavy quark families we can expect that (15) takes place. On the contrary, when $E^{Rel}_n \sim m^{1+\beta}(\beta < 0)$, then $\varepsilon_0 >> 1$, when $m \to 0$ and in this case for light quark families we can expect that (15) takes place.

Equation (6) also may be solved for infinitive square well potential

$$M_{nj} = 2m\sqrt{1 + \frac{t^2_{nj}}{(mr_0)^2}}, \tag{17}$$

where t_{nj} are Bessel's function zeroes, and r_0 is width of the well. From (17) it may be seen that in (8) we have equality instead of inequality. This fact is physically clear and is in accordance with comparison theorem, because in $0 < r < r_0$ area V=0 and both (5) and (6) equations are just the same. From (17) also it may be proved, that (15) takes place, because in this case we have positive levels.

Now let's investigate (11) inequality dependence upon masses. From (11) and (15) we have

$$\frac{\Delta M^{Shr}}{\Delta M^{Rel}} < \varepsilon_0 < 1. \tag{18}$$

In this case we consider such potentials, which have only negative relativistic levels and suppose, that M dependence upon masses is such

$$M = m^\beta f, \tag{19}$$

where in f enters the potential characteristic values and various quantum numbers. Then from (6) and (19) we have

$$\varepsilon_0 = m^{\beta - 1} f. \tag{20}$$

Let's study (20) a) $\beta = 1$, then $\varepsilon_0 = f$ and ε_0 does not depend upon m and in this case for various quark families (13) relation is just the same. Indeed, it is so, as it is shown in [9], where for $V = -\frac{\alpha}{r}$ $M = mf(\alpha, n, j)$: b) $\beta < 1$, then ε_0 decreases with m increasing and therefore without fail $\frac{\Delta M^{Shr}}{\Delta M^{Rel}}$ decreases, .i.e. in heavy quarks families it should be less levels distance in relativistic case; c) $\beta > 1$, then ε_0 increases with m increasing and it is possible, that $\frac{\Delta M^{Shr}}{\Delta M^{Rel}}$ increases. It should be also noticed using (8) and (10) we can show, that for potentials which have negative relativistic levels such relation inquality is fulfilled

$$M^2_{Shr,n+1} - M^2_{Shr,n} < M^2_{Rel,n+1} - M^2_{Rel,n}. \qquad (21)$$

As we have noticed above Schrodinger equation and various relativistic equations can be also compared. Particularly comparing Schrodinger and Dirac equation with $\frac{1+\beta}{2}V$ potential [10-13]. We receive: a) For potentials which have only negative relativistic levels it can be that $\Delta M^{Shr} < \Delta M^{Rel}$ (but it is not necessary), i. e., in this case first theorem looses its "strictness" in comparison with (6) equation. The same situation is if we compare in this case Schrodinger and Klein - Gordon equations. Solutions for $\frac{1+\beta}{2}V$ Dirac and Klein-Gordon equations for Coulomb potential are known and (13) is verified; b) In Dirac equation for potentials which have only positive relativistic levels situation is the same which was in the second theorem and this is verified in the $V = kr^2$ potential case.

Tbilisi I.Javakhishvili State University
High Energy Physics Institute

REFERENCES

1. *M. Read, B. Simon.* Methods of Modern Math. Physics IV: New York. 1981, 76.
2. *W. Thirring.* A Course in Mathematical Physics 3; Berlin. 1981, 152.
3. *B. Epstein.* Linear Functional Analysis. Philadelphia. 1970.
4. *R. L. Hall.* J. Phys. A: Math. Gen. 25, 1992, 4459.
5. *R. L. Hall.* Phys. Rev. A 39, 1989, 5500.
6. *R. L. Hall.* Phys. Rev. A 32, 1985, 14.
7. *Z. K. Silagadze, A.A. Khelashvili.* TMP 61; 1984, 431. (Russian).
8. *T. P. Nadareishvili, A.A. Khelashvili.* Proceedings of Tbilisi University Physics. **286**, 1989, 27, (Russian).
9. *T. P. Nadareishvili, A.A. Khelashvili.* Proceedings of Tbilisi University Physics. **265**, 1986, 22. (Russian).
10. *L. D. Landau, E. M. Lifshitz.* Quantum Mechanics Science. 1974 (Russian).
11. *E. Marguary.* Phys. Lett; 95B; 2, 1980, 295-298.
12. *C. Long, D. Robson.* Phys. Rev. D27, 3, 1983, 644-650.
13. *N. Barik, S. Jena.* Phys. Rev. D26, 9, 1982, 2420-2429.

საქართველოს მეცნიერებათა აკადემიის მოამბე, 159, №1, 1999
BULLETIN OF THE GEORGIAN ACADEMY OF SCIENCES, 159, №1, 1999

ASTRONOMY

T. Toroshelidze, S. Chilingarashvili, M. Chichikoshvili

The 11-year Variation of the Solar Radiation in 130-175 nm Spectral Region on the Basis of 630 nm Emission Observation in Twilight

Presented by Member of the Academy E. Kharadze, February 2, 1998

ABSTRACT. **Regular observations in the thermosphere emission 630 nm of the atomic oxygen in twilight in 1962-1992 at the Abastumani Observatory ($41^0.48N,42^0.48E$) enabled to determine the 11-year variation cycle with the average max/min ratio of 2.85. From the observed emission photodissociation mechanism the hard UV emission variation in the 130-175 nm spectral region is estimated. Mean annual data on the 630 nm emission are compared with the characteristic values of the solar radioemission and other indices of activity. It is discovered that on the growing phase of the solar 11-year cycle the radioemission increase exceeds that of 630 nm radiation, while at the fall phase the UV prevails. All these may perhaps denote on the different heights of the formation of UV and radioemission in the solar atmosphere. The numerical relation between absolute intensity of 630 nm emission and the photons flux in 130-175 spectral region is established.**

Key words: thermosphere of the Earth, 630 nm emission of atomic oxygen, solar hard UV radiation, 11-year cycle.

The solar UV radiation (λ<200nm) is fully absorbed in the upper atmosphere and for the measurement of the radiation flux rockets and orbiting satellites are used. In spite of this, there is a huge difference in the estimation of the energy flux in the region, especially in the measurements, conducted in different periods of the solar activity [1,2]. The estimation of the solar radiation in the Shumann-Runge continuum region (130-175 nm) is possible by the indirect method. It is well known that the region of solar radiation is absorbed by oxygen molecules [3]. The cross-section of the absorbtion is maximum near 140 nm and reaches 2.10^{-17} cm^2 [3]. The rate of photodissociation of O_2 is defined by the following relation:

$$\frac{dn(O_2)}{dt} = -I(O_2)\cdot n(O_2),$$

where $I(O_2)$ is the probability of the photodissociation ($2\cdot10^{-5}$ s^{-1}), and $n(O_2)$ is the maximum of the oxygen molecules concentration ($2\cdot10^9$ cm^{-3}). From these data the rate of O_2 dissociation reaches $4\cdot10^4$ cm^{-3} s^{-1} [3].

As a result of the photodissociation of O_2 (the quantum release is 1) the oxygen atom finds itself at the excited O('D) level and radiates 630 nm emission while it returns to the basic level. I_{630} - the absolute intensity reaches the value of several dozens of *kR* (1*R* is equal to 10^6 photon/cm^2 s) in the daytime, while in the twilight it is of the order of 1*kR*

[4]. The dayglow radiation of the atmosphere is practically lost in the strong scattered background. As for the twilight period, when the lower dense layers of the atmosphere are in shadow, I_{630} is easely registered and its intensity is linearly connected with the radiation in 130-175 nm spectral region, which permits to estimate this radiation.

In Abastumani Observatory the I_{630} observations in twilight have been regularly conducted by electrophotometric and spectrographic methods since 1962. The device description and observation methodology is presented in [5]. The relative error of the measurement does not exceed 5%. The emission intensity in twilight reaches the maximum at the solar zenith angles of 98-99^0 and the shadow height near the terminator reaches 150-160 km taking into account the screen height [5], while the whole I_{630} emission layer is illuminated by the sun rays.

The morphological behavior of I_{630} emission is given in [5,6]. According to T. G. Megrelishvili [6] the 11-years emission amplitude exceeds almost by 20 times the amplitude of 22 and 5.5 years. Let us consider the I_{630} seasonal variation average in 1965-1975 morning and evening periods (Fig.1). As it is seen from Fig.1 the evening intensity 1.3-1.5 times exceeds the morning intensity throughout the year. This fact is explained by the accumulation of O('D) atoms in the daytime as the result of the photodissociation. In winter this accumulation is lower compared with other seasons, what is shown in Fig. 1. In the seasonal behavior of I_{630} the object of special attention is the fact that the spring and autumn intensities exceed that of summer. This fact could be named as the so-called summer anomaly because it contradicts with the linear theory, according to which the I_{630} is proportional to the photodissociation rate and the solar radiation flux. The latter must increase in the summer with the increase altitude as well as with the decline of the air optical mass. One of the possible explanations of this anomaly is the fact that in summer the upper atmosphere layers at the middle latitudes are hotter than in the other periods, which causes the increase of O('D) desactivation. For instance, the following reaction becomes very effective at the heights more than 100 km.

$$O(^1D)+O(^3P)+M \rightarrow O_2(a'\Delta^3)+M,$$

whose rate depends on the temperature $\alpha=3.8\times10^{-30}\exp(-170/T)$. The increase of the temperature by 200 degrees causes the increase of efficiency by a factor of 1.3, which is in good accordance with the decline of I_{630} in summer compared to the equinox period (Fig.1).

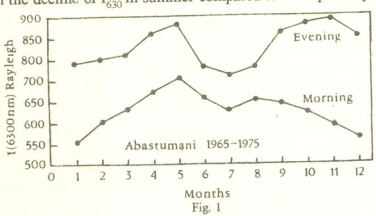

Fig. 1

Average annual data of I_{630} in the combined morning and evening observations obtained in Abastumani in 1962-1992 are given in Fig. 2. In the same picture one can see the

average annual values for solar radioemission $F_{10.7}$, Wolf numbers W, annual number of the flares (SF), calcium floccula (CPA) and the data on the solar hard UV flux in 1979-1992, obtained from the "Pioneer Venus" (in nanoampers are the current units) [7,8].

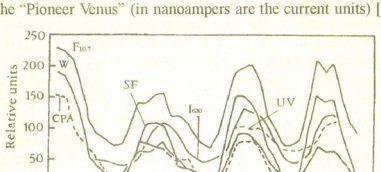

Fig. 2

All the presented data describe the variation of the energy in the 11-year cycle. As it is seen from the Fig.2 the tiny amplitude deviations characterise the $F_{10.7}$, W and I_{630} data. According to [1] the flares are characterised by the strong increase of UV and X-radiation, but their duration does not exceed the matter of minutes, rarely a few hours. The influence of the flares on the I_{630} twilight annual data is less noticeable. The chromosphere torches are formed a few hours or one day earlier than the sunspots and are still observed 200-300 days later after their disappearance. That is why the time between the minima of the solar cycles are much more important than that between the maxima.

For the maxima of the 630 nm emission solar activity the fluctuations after 2-3 years are typical, which might be connected with the UV radiation from the torches.

In the table there are presented the values of the max/min ratio for I_{630} and other characteristics for the 19-22 cycles of solar activity.

Max/Min ratios of the 11-year cycles

Index of Solar Activity	19th cycle	20th cycle	21th cycle	22th cycle	Average
$F_{10.7}$	3.2	2.17	3.12	2.90	2.82
W	14.0	8.15	11.16	8.55	10.47
SF	-	5.11	5.8	5.0	5.3
CPA	12.5	6.02	6.04	-	8.5
EUV	-	-	1.82	2.02	1.92
I_{630}	-	2.70	3.0	2.90	2.86

The Table shows us that these values greatly vary for the different indexes of the solar activity, only those for I_{630}, $F_{10.7}$ and EUV indexes are close to each other.

The I_{630} max/min ratio varies between 2.7-3.0 within 20-22 cycles, which is in a good accordance with the theoretical calculations [9,10], according to which the hard solar UV flux variation in the 12-300 nm spectral region is possible to change between 2.5 and 4.3 times.

For the detailed comparison the radioemission indices $F_{10.7}$ and I_{630} separately for the

growth phase and the fall phase for the 20-22nd 11-year cycles are chosen. This dependence is presented in Fig. 3, from which it is seen, that on the growth phase of solar activity $F_{10.7}$ index undergoes much greater increase than that of I_{630}, while on the fall phase the ratio $F_{10.7}/I_{630}$ is declining. This fact justifies the idea that during the evolution time of the active solar regions the radioemission and UV are produced at the different heights and undergo considerable time variation [10].

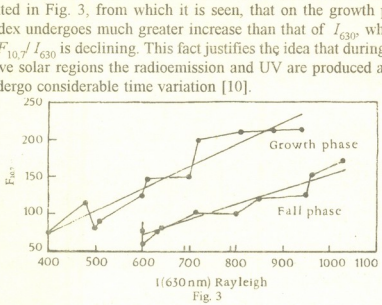

Fig. 3

The measurments of 630 nm emisssion intensity in the absolute units enable to estimate numerically the proton flux of solar emission in 130-175 nm spectral region. If we use the rocket data according to which in 1979-1983 this flux varied between 1.5×10^{12} ph/cm^{2}s (maximal activity) and 0.76×10^{12} ph/cm^{2}s (middle of cycle) [11,12], then corresponding relation is expressed by the following equation:

$$I_{130\text{-}175} = 5.4 \cdot 10^{11} + 0.0095(I_{630} - 400) \text{ph/cm}^2\text{s},$$

where I_{630} is measured in rayleighs.

Thus, on the basis of long term observation of the twilight emission 630 nm by ground base method the control of the hard UV irradiations of the Sun has been proposed and approbated.

This work was supported by the Georgian Academy of Sciences foundation, under grant 97-2.32.

Georgian Academy of Sciences
Abastumani Astrophysical Observatory

REFERENCES

1. *P. White.* The flux energy of the Sun and its variation. 1980, 350.
2. *P. C. Simon.* Solar Phys., **74**, 1982, 273-287.
3. Atmosphera. Spravochnic., 1991, 503 (Russian).
4. *R. Link, L. Gogger.* J. Geophys. Res., **93**, 1988, 9883-9893.
5. *T. I. Toroshelidze.* Analiz problem aeronomii po izlucheniyu verknei atmosphery. 1991, 216 (Russian).
6. *T. G. Megrelishvili.* Bull. Abastum. astrophiz. obs., **70**, 1992, 169- 220(Russian).
7. Solar-Geophysical Data. Part 2, 1992-1995.
8. *W. R. Hoegy.* Solar-Geophysical Data. Part 2, **615**, 1995, 39-55.
9. *E. A. Burevich, A. A. Nusinov.* Geomagnetizm i aeronomiya, **24**, 4, 1984, 581-585 (Russian) .
10. *J. L. Lean, O. P. White, Livengston et al.* J. Geophys. res., **87**,1982, 1037-1052.
11. *G. H. Mount, G. I. Rothman.* J. Geophys. Res. **90**, 1985, 13031-13036.
12. *G. Rothman, C. Rarth, R. Thomas et al.* Geophys. Res. Letters, **9**, 1982, 587-593.

საქართველოს მეცნიერებათა აკადემიის მოამბე, 159, №1, 1999
BULLETIN OF THE GEORGIAN ACADEMY OF SCIENCES, 159, №1, 1999

GEOPHYSICS

E. Elizbarashvili, T. Aladashvili

On Circulation Factors of Climate Centennial Fluctuation (Tbilisi Case)

Presented by Member of the Academy G. Svanidze, February 19, 1998

ABSTRACT. **Investigation of atmospheric circulation influence on climate fluctuation is based on the observation of meteorological elements in Tbilisi for 150 years and 100 years data on frequency of the main types of atmospheric circulation in the North hemisphere. The correlation coefficients between climatic annual elements and frequency of the main types of atmospheric circulation have been found. Regression equations, which make possible to predict development of climate in the nearest future in Tbilisi are obtained.**

Key words: fluctuation, atmospheric circulation, climate.

The global Earth climate warming that began last century and is going on today attracts the attention of the world scientists. The present warming can be explained mainly by antropogenic factors [1] . But, as it was shown in paleogeographic [2] and climatological [3,4] investigations, climate had been changing in the geological past as well. Therefore, to perform fundamental study of climate centennial and recent fluctuation, the natural factors of climate creation must be taken into account.

In the present paper we consider the role of main natural factor of climate change and fluctuation - atmospheric circulation in Tbilisi climate change.

Table 1 represents correlation coefficients between frequency of the main types of atmospheric circulation in the North hemisphere and Tbilisi climate main elements, as well as estimated values of their statistical importance for 100 years period (1890 - 1990).

Table 1

Correlation coefficients between frequency of the main types of atmospheric circulation in the North hemisphere and Tbilisi climate main elements, and their statistical importance (1890 - 1990)

Circulation type	Parameter	Air annual temperature	Annual sum of precipitation
Western (W)	Correlation coefficient Importance	-0.255 99	0.040 insignificant
Eastern (E)	Correlation coefficient Importance	0.167 95	0.039 insignificant
Meridional (C)	Correlation coefficient Importance	-0.052 insignificant	-0.068 insignificant

According to Table 1, only correlation between the western and eastern circulation and air temperature is important. Correlation with precipitation is insignificant for any circulation type.

The regression equations for the important correlations giving a possibility to calculate the air average temperature according to frequency of the western and eastern circulation types were obtained. They have the following form:

$$T_w = -0.004\ P_w + 13.3 \quad (1)$$

$$T_E = 0.002\ P_E + 12.5 \quad (2)$$

where P_w and P_E are frequencies of the western and eastern circulation types, T_w and T_E are the corresponding temperatures.

A comparison of actual temperatures and calculated temperatures based on the obtained regression equations showed satisfactory results for both: 11-year moving averages and average annual temperatures (Table 2).

Table 2

Actual annual (T), 11-year moving average and calculated temperatures' values for various years (Tbilisi)

Year	T	T_{11}	T_W	T_E
1900	12.30	12.46	13.00	12.81
1910	13.00	12.55	12.70	12.83
1920	11.70	12.95	12.83	12.90
1930	13.00	12.69	12.84	12.87
1940	13.60	13.08	12.92	12.80
1950	12.80	12.96	12.88	12.83
1960	13.20	13.24	13.02	12.77
1970	13.40	12.95	13.06	12.80
1980	13.00	12.92	12.97	12.82
1990	14.00	13.28	13.40	13.34

Based on integral-differential curves presented in Figs. 1, 2 we can discuss fluctuation of Tbilisi air temperature and precipitation in epoch periods of atmospheric circulation.

As it can be seen in Figs. 1, 2 there is no clear correspondence between fluctuations of the main types of atmospheric circulation and climate fluctuations, although some general tendencies are observed.

Decrease of average annual air temperature and increase of annual precipitation corresponds to active phase of the western circulation type (1890 - 1930), while the increase of annual temperature and decrease of annual precipitation correspond to passive phase of that circulation (1950 - 1990).

Decrease of annual temperature and increase of annual precipitation correspond to passive phase of the eastern circulation type (1890 - 1930), while increase of annual temperature and decrease of annual precipitation values correspond to active phase of this circulation in 1950 - 1970 and 1982 - 1990.

The increase of annual temperature corresponds to the active phase of meridian

circulation type (1940 - 1970). Temperature is also increasing during the period of circulation's decrease 1970 - 1990. Annual precipitations of 1940 - 1952 are near the standard value and then they decrease (1952 - 1970). Precipitation fluctuations are not evident in 1970 - 1990.

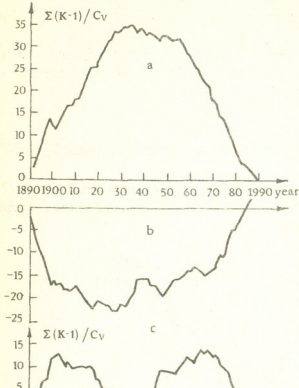

Fig. 1. Integral - differential curves: a) frequency of the western circulation; b) frequency of the eastern circulation; c) frequency of meridian circulation.

The connection between difference of the western and eastern circulation frequency and anomalies of temperature and precipitation is found. In particular, it was determined, that low level of annual temperatures and high level of annual precipitation correspond to positive difference. On the contrary, high level of temperature and low level of precipitation correspond to negative difference. Such correlation is presented by linear regression equations:

$$T = 12.9 - 0.005\,\Delta P, \quad (3)$$

$$Q = 515 + 0.2\,\Delta P, \quad (4)$$

where T is an average annual temperature, Q is annual sum of precipitation, $\Delta P = P_W - P_E$ is the difference of the western and eastern circulation frequencies.

Equations (3) and (4) give good results for 11-years moving averages. With regards to annual values, clear correspondence between values of actual and calculated temperatures and precipitation is not found.

Based on equations (3) and (4) we can predict climate conditions in the nearest future in Tbilisi, if we assume, that the main tendencies of the western and eastern circulation types do not change during this period (Fig. 1 (a) - (b)). In the Table 3 we represent expected scenario for Tbilisi climate in the nearest future.

Table 3

Expected values of annual air temperature (T) and annual precipitation (Q) (Tbilisi)

Scenario	Year	Δ P	T ^{0}C	Q_{mm}
I	2010	-35	13.07	508
II	2025	-70	13.25	501
III	2050	-105	13.42	494

Therefore, some reaction of the main climate elements centennial movement towards an atmospheric circulation variation is observed. It is obvious, that connection is not evident as in addition to the atmospheric circulation, other main natural factors participate in the climate creation.

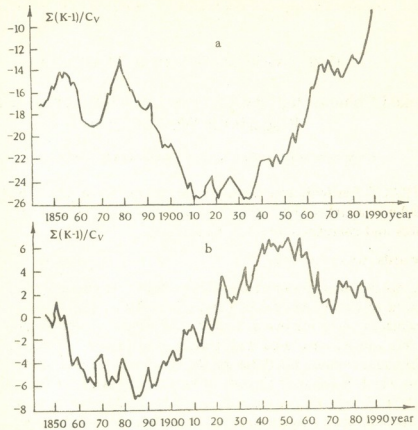

Fig. 2. Integral - differential curves: a) air average annual temperature; b) precipitation annual sums.

Georgian Academy of Sciences
Institute of Hydrometeorology

REFERENCES

1. Climate Change 1995. The Science of Climate Change, Contribution of Working Group I to the Second Assessment Report of the Intergovernmental Panel on Climate Change. Cambridge Univ. Press-IPCC, 1996.
2. *L. I. Maruashvili.* Tselesoobraznost peresmotra suschestvuyushikh predstavlenii o paleogeograficheskikh usloviyah lednikovogo perioda na Kavkaze, Tbilisi, 1956 (Russian).
3. *E. Elizbarashvili, T. Aladashvili.* Bull. Georg. Acad. Sci., **155**, 3, 1997, 368-371.
4. *E. Elizbarashvili, T. Aladashvili.* Inform. Bull. of Climate Research National Center, 6, 1997 (Georgian).

საქართველოს მეცნიერებათა აკადემიის მოამბე, 159, №1, 1999
BULLETIN OF THE GEORGIAN ACADEMY OF SCIENCES, 159, №1, 1999

N.Chkhartishvili, Sh.Shatirishvili, F.Machavariani

Packed Column High Performance Chromatography Analysis of Pesticides in Wine Materials

Presented by Member of the Academy T. Andronikashvili, March 9, 1998

ABSTRACT. **Pesticide content has been studied by means of high performance packed and micropacked columns in "Gorouli Mtsvane", "Chinouri" and "Tavkveri" grape juices and corresponding new wines.**

Key words: wine, pesticide.

It is known that after crushing the pesticides move from grapes into juice and its content changes in the process of fermentation and aging. The purpose of our work was to study pesticide content in juice original as well as after a short post-fermentation seasoning.

With this aim we have used high performance packed and micropacked columns. High performance columns are those specific efficiency (the number of theoretical plates 1 meter) of which is equal or exceeds 2000. Researches on micropacked columns are given in [1-2]. Besides, it is expedient to use high performance packed columns with immobilized polar phases on the basis of a super class carrier [3], especially while using such columns for solving such specific goal as determining of pesticide content in wines. Today such sorbents with bonded mono-molecular layers called "ultra-columns", (analogous to the American "ultra-bond") are made of several types. "Tsvetochrom-c" obtained by special technology is always used as a solid support. Polarity of sorbents is to a smaller extent connected with the polarity of the output stationary phase but at the same time it heavily depends on their molecular masses.

Thermal stability of this sorbent after thermal treatment of the suspended phase (in the process of the following extraction of the bonded residue) constitutes 220^0C [3]. These particular features make it possible actually to use them for the analysis of microcontent of such components and primarily for such compounds as pesticides. The minimum registered concentration for the compounds containing polar chlorphosporus is determined mainly by the utilized selective detector sensitivity. In our case the sensitivity of ionization detector on "Mega" chromatograph in case of 2 mkl sample, when sorbent ultra-column - PEG was used, was the following: in relation to tributhylphosphate $1x10^{-5}$ mg/ml, in relation to lindan - $1x10^{-6}$ mg/ml. Effectiveness of exploited sorbent is quite high and practically does not depend on the speed of carrier gas (at least within the reasonable range of consumption about 100ml/min), which is naturally determined by the easing of mass transmission on a stationary bonded phase of a very thin about 20A layer. The main feature of the sorbents of this type is a sharp decline of retention (5-10 times) compared to a traditional sorbent which makes it possible to carry out analysis at a low temperature ($40-70^0$C below average). Besides, pesticides can be determined by the amount of trace

10^{-4}-10^{-5} mg/ml, as the carrier has a lowered adsorbtive capacity and at the same time gives the probability of using high performance columns.

We studied pesticide content in "Gorouli Mtsvane", "Chinouri" and "Tavkveri" grape juices as well as on the post initial fermentation stage. The sample vineyards were treated with such pesticides as phazelone and carbophos. Extraction of pesticides from samples was made with pentane (5ml on 50 cm^3 sample).

The analysis was carried out without further concentration as well as with vacuum distillation with 20-fold concentration on a specially worked out equipment for this purpose. In the first case (in the juice output) the concentration was not necessary. In the second one only the trace of pesticides or their metabolities were found after concentration (Table, Fig. 1).

Grape Sort	Amount of Pesticides	
	in juice output	after 2 months fermentation
Gorouli Mtsvane	$5x10^{-4}$mg/ml	$8x10^{-7}$mg/ml
Chinouri	$2x5x10^{-4}$mg/ml	$2x10^{-7}$mg/ml
Tavkveri	$3x3x10^{-4}$mg/ml	$2.5x10^{-7}$mg/ml

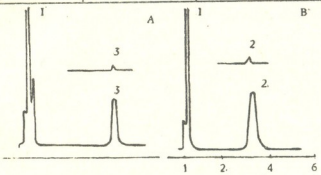

Fig.1. Chromatogram of a mixture fractioning on high performance packed column.
A- Chromatogram of determining carbophos in "Gorouli Mtsvane" in newly made juice and after 2 months aging.
B- B - Chromatogram of determining phozanol in "Tavkveri" newly made juice and after 2 months aging.
1-vehicle, 2- phozanol, 3- carbophos.

Table

Chromatographic analysis was carried out on Chromatograph "Tsvet-530". The column length was 1m, temperature 190^0 and 160^0C. Ultratsvet polyethylene glycol was used as a sorbent. The speed of a gas carrier was 25cm^3/min.

Thus it was shown that the trace of pesticides practically vanishes after short fermentation. There was found no trace of pesticides at all after long fermentation and aging.

Georgian State Agrarian University

REFERENCES

1. *G. Reflero, T. Hezzaiz, M. Herrait, MD. Cabezuclo.* J. Chromatographia **22**, 8, 1986, 358-362.
2. *V. G. Berezkin, D. Gavrichev, A. Malik.* J. Liq. Chromat **10**, 8-9, 1987, 1707-1716.
3. *A. D. Aripovskii et al.*In: Itogi nauki i techniki. 6, 1986, 61-107 (Russian).

საქართველოს მეცნიერებათა აკადემიის მოამბე, 159, №1, 1999
BULLETIN OF THE GEORGIAN ACADEMY OF SCIENCES, 159, №1, 1999

GENERAL AND INORGANIC CHEMISTRY

M.Samkharadze, R.I.Gigauri, M.Ugulava, R.D.Gigauri

Synthesis and Study of Tetrathioantimonates of Argentum (I), Cadmium and Mercury (II)

Presented by Member of the Academy T.Andronikashvili, July 16, 1998

ABSTRACT. **Tetrathioantimonates Ag_3SbS_4 and $M_3(SbS_4)_2\cdot 2H_2O$ with M=Cd and M=Hg were first synthesized under hydrochemical conditions. Their composition, structure, dehydration and thermal resistance within the 20-100°C temperature range have been studied by the method of IR-spectroscopy, and roentgenophase, chemical and thermal analyses.**

Key words: tetrathioantimonate, argentum, cadmium, mercury.

Tetrathioantimonates of alkaline metals are well studied [1-3]. As to the tetrathioantimonates of transitional metals, there are no literary data about them or if there are any, they are mutually exclusive. The goal of our investigation was to obtain tetrathioantimonate of some d^{10} metals and study them by physico-chemical methods.

On the basis of numerous experiments it has been established that the target products can be easily obtained by exchange reactions:

a) $3AgNO_3+Na_3SbS_4\rightarrow Ag_3SbS_4\downarrow+3NaNO_3$

b) $2Na_3SbS_4+3MX_2+2H_2O\rightarrow M_3(SbS_4)_2\cdot 2H_2O\downarrow+6NaX$,

where M=Cd, X=Cl; or M=Hg, X=NO_3.

Reactions were carried out in aqueous solutions. On mixing the reacting substances fine crystalline compounds of different colours were precipitated immediately, which were held in the mother solution for a day to complete the crystalline form. After that the precipitant was filtered, washed with water and spirit and dried to the constant mass in P_2O_5 containing exicator. It must be noted, that the change of the sequence of adding the reacting substances and the mixing intensity causes the change of the precipitant composition. It is especially evident, when natriumtetrathioantimonate solution is added (slowly, in small doses) by the aqueous solution of d^{10}-metal salt. As it appeared, apart from the complete tetrathioantimonate the mixed salt was produced as well:

$$Na_3SbS_4+MX_2+nH_2O\rightarrow NaMSbS_4\cdot nH_2O+2NaX$$

In order to exclude this process the soluble salt of d^{10} metal was taken 5% more than the theoretical one and the reaction was carried out with the addition of natriumtetrathioantimonate solution to it.

Synthesized compounds are solid substances of different colours, insoluble in water, spirit and nonpolar organic solvents. At high temperature they decompose.

The structure and composition of the substances of study were established by means of elementary analysis and physico-chemical methods. Namely, on the basis of IR spectroscopy data it has been established that synthesized compounds with the exception of

silver salt are crystalhydrates. The maxima of absorption band waves (cm^{-1}) are given below:

Ag_3SbS_4: 450, 600, 720, 850, 890, 1130.

$Cd_3(SbS_4)_2 \cdot 2H_2O$: 450, 600, 720, 850, 890, 1130, 1630, 3300.

$Hg_3(SbS_4)_2 \cdot 2H_2O$: 450, 600, 720, 820, 1130, 1620, 3300.

Analysis of absorption IR spectra shows that absorption bands are observed in all thiocompounds (except silver) at 1630 and 3300 cm^{-1} regions indicating the existence of crystallized water [5].

According to the roentgenophase investigations the fine crystalline monophase compounds do not contain yielding materials. Calculations show that synthesized compounds are crystallized in a rhombic syngony. Roentgenograms of different kinds of distribution of interplanar separation show a certain degree of structure regularity of the mentioned compounds.

Chemical behavior of argentum (I) cadmium (II), mercury (II) tetrathioantimonates heated at 1000°C has been studied. Mercury (II) thiosalt mass decreases at 165°C. At 165-280°C the sample loses 5.88% of its mass corresponding to splitting off 1 mole of sulfur (theoretically 5.58%). Within the 490°-625°C temperature range with the minimam at 610°C the sample mass is reduced by 3.84% caused by splitting off one more mole of sulfur. Two exoeffects are noted within the same temperature range with the maximum at 600-620°C. The mentioned exoeffects must have been caused by intramolecular postdethionization regrouping.

From the chemical point of view the sample transformation at the temperature over 650°C is of interest. At this stage TG curve shows the mass increase by 3.70%. The residue appears to be oxidized in air. If we take into account the above said, argentum (I) tetrathioantimonate thermolysis can be presented as follows:

$$2Ag_3SbS_4 \xrightarrow[-S]{165\text{-}300^oC} Ag_6Sb_2S_7 \xrightarrow[-S]{490\text{-}625^oC} 2Ag_3SbS_3 + 2"O" \longrightarrow 2Ag_3SbS_3O$$

Cadmium (II) tetrathioantimonate thermolysis occurs analogously with the difference that decomposition starts with splitting off 2 mole of water. Sulfur is split off at 215°C and TG curve shows mass increase at 600°C caused by oxygen adjoining.

Mercury (II) tetrathioantimonate decomposition proceeds in a different way. Sample dehydration starts at 60°C which is shown by endothermic effect on the DTA curve within the 60°-160°C temperature range with the minimum at 130°C. The sample mass is reduced by 3.66% corresponding to splitting off 2 mole of water (theoretically 3.16%). Further decrease of the sample mass occurs within the 200-300°C temperature range (with the minimum at 230°C). The sample mass decreases by 5.28% corresponding to splitting off 2 moles of sulfur (theoretically 5.81%). Within the 335-450°C the sample mass decreases by 38.25%, which must have been caused by separation of 2 mole of mercury (theoretically 38.75%). Complete decomposition of the sample without any residue occurs at the temperature over 450°C. Proceeding from the above said the scheme of mercury (II) tetrathioantimonate thermic decomposition is as follows:

$$Hg_3(SbS_4)_2 \cdot 2H_2O \xrightarrow[-2H_2O]{60\text{-}160\ ^oC} Hg_3(SbS_4)_2 \xrightarrow[-2S]{200\text{-}300\ ^oC} Hg_3(SbS_3)_2 \longrightarrow$$

$$\xrightarrow[-2Hg]{335\text{-}450\ ^oC} Hg(SbS_3)_2 \xrightarrow{>450\ ^oC} \text{Sublimation}$$

Synthesis of cadmium tetrathioantimonate. 3.74 g aqueous solution of $CdCl_2 \cdot 2H_2O$ was added by 4.50 g of $Na_3SbS_4 \cdot 9H_2O$ dissolved in 20 ml of water with constant stirring at room temperature. Yellowish-orange substance was precipitated at once. It was held in the mother solution and next day was filtered, then washed well, first with water then by spirit, and dried in P_2O_5 vacuum exicator until the constant mass was obtained. 3.82 g of $Cd_3(SbS_4)_2 \cdot 2H_2O$ (93.7% of theoretically expected) was obtained (Tables 1-2).

Table 1

Charge of starting materials and yield of synthesized product

N	Charge of starting materials						Yield of Ag_3SbS_4 and $M_3(SbS_4)_2 \cdot 2H_2O$		
	$MX_2 \cdot nH_2O$				$Na_3SbS_4 \cdot 9H_2O$				
			g	mole	g	mole	g	mole	%
1	$AgNO_3$	x.r.	4.24	0.0249	4.0	0.0083	4.69	0.0082	98.45
2	$Cd(CH_3COO)_2 \cdot 2H_2O$	x.r.	3.74	0.0140	4.5	0.0094	3.82	0.0044	93.67
3	$Hg(NO_3)_2 \cdot H_2O$	x.r.	4.49	0.0131	4.2	0.0087	4.62	0.0041	94.34

Table 2

Results of chemical analysis

Found, %				Compound	Calculated, %			
M	Sb	S	H_2O		M	Sb	S	H_2O
56.02	21.04	22.13	-	Ag_3SbS_4	56.42	21.24	22.33	-
38.14	27.71	29.03	3.92	$Cd_3(SbS_4)_2 \cdot 2H_2O$	38.63	27.90	29.33	4.12
52.71	21.21	22.01	3.01	$Hg_3(SbS_4)_2 \cdot 2H_2O$	52.91	21.41	22.51	3.17

Similarly were synthesized argentum (I) and mercury (II) tetrathioantimonates (V).

IR spectral investigation of the sample was carried out at 4000-400 cm^{-1} region by means of SPECORD 75 IR. Roentgenophase analysis was made by means of roentgen difractometer DPOH-3M (CuKr-radiation, quarts monochromator), roentgen tube worked under the regime: tension – 25v, power 15 mA; recording speed – 2 grad/min.

Thermal analysis was carried out on the derivatograph of Paulic-Paulic-Erdei system Q-1500D. 0.1 mg of sample was placed in the platine crucible: heating 10 grad/min, DIG sensitivity 250, DTA 500 mKv.

Thus, the thiosalts Ag_3SbS_4, $Cd_3(SbS_4)_2 \cdot 2H_2O$, $Hg_3(SbS_4)_2 \cdot 2H_2O$ were first synthesized under hydrochemical conditions.

Tbilisi I.Javakhishvili State University

REFERENCES

1. Rukovodstvo po neorganicheskomu sintezu. Pod.red.G.M.Brauera, 2, 1985, 640 (Russian).
2. *F.Kirchhof.* Z.Anorg. Allgem. Chem., 112, 67, 1920.
3. *G.Iander, E.Blasius.* Einführung in das anorg. Chem. Prakticum, Hirzel, Stuttgart, 1970, 425.
4. *F.Umland, K.Adam.* Übungsbeispiele aus der anorg. Experimental Chemie, Hirzel, Stuttgart, 1968, 198.
5. *K.Nakamoto.* Infrakrasnye spektry neorganicheskikh i koordinatsionnykh coedinenii. M., 1966, 411 (Russian).

საქართველოს მეცნიერებათა აკადემიის მოამბე, 159, №1, 1999
BULLETIN OF THE GEORGIAN ACADEMY OF SCIENCES, 159, №1, 1999

ORGANIC CHEMISTRY

L. Tevzadze, M. Sikharulidze, L. Kurkovskaya, T. Khoshtariya

Some Electrophilic Substitution Reactions of 1H-Pyrrolo-[3,2-b]- and 3H-Pyrrolo-[2,3-c]-phenoxathiines

Presented by Member of the Academy K. Japaridze, February 17, 1998

ABSTRACT. **The reactivity of 1H-pyrrolo-[3,2-b]- and 3H-pyrrolo-[2,3-c]-phenoxathiines characteristic of indole electrophilic substitution reactions (Mannich reaction, acylation, azocoupling) was investigated. It is shown that in case of Mannich and azocoupling reactions electrophilic substitution occurs according to the β-position of pyrrolic nucleus of pyrrolo-phenoxathiines. However, the reaction of acetylation by acetic anhydride leads to an N-acetylderivative. The structure of all the synthesized substances was verified by UV, IR and PMR spectral methods.**

Key words: indole, mannich reaction, acylation, azocoupling.

The present work deals with investigation of reactivity of the tetracyclic pyrrol-containing condenced systems 1H-pyrrolo-[3,2-b]-(I)

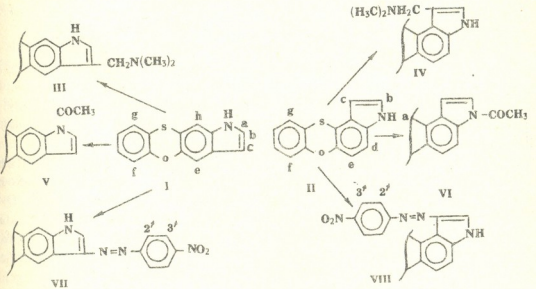

The places of protons are defined by letters in the PMR spectra.

and 3H-pyrrolo-[3,2-c]-phenoxathiines (II), which were earlier synthesized at our laboratory [1]. Because of resemblance of these cycles (I,II) with indole, their reactivity was studied in the electrophilic substitution reactions, characteristic of indole (Mannich, acylation, azocoupling) [2-5].

Compounds I and II, analogously with indole [2], readily entered in-to the Mannich-reaction. The amyno-ethylation was performed in a water solution of formalin and dim-

ethyl amine and, as a result, 3-(N,N-\dimethylaminmethyl)-1H-pyrrolo-[3,2-b]- (III) and 3-(N,N-dimethyl-\aminmethyl)-3H-pyrrolo-[2,3-c]-phenoxathiines (IV) were obtained in a tangible quantities. The structure of the obtained compounds (III, IV) was verified by PMR-, IR- and UV-spectroscopies. According to the PMR-spectra of compounds III and IV it could be concluded that substitution of the dimethyl-amino-methylic groups goes at the third carbon atom of the pyrrolic cycle (see the Table). In the spectrum of compound III no NH group sygnal was detected because of the fast NH→ND exchange, while in the IV spectrum the NH group proton sygnal lays in 10.0 p.p.m.. In the given spectra no C_3 proton sygnals were detected as well. At the same time sygnals of 3.5; 2.3 p.p.m. were detected for compound III and 3.7; 2.2 p.p.m. for compound IV, which belong to CH_2 and $(CH_2)_3$-functional groups, respectively.

The PMR spectra of the obtained compounds

Substrates	The chemical mobility								δ, p.p.m.		J, Hz
	a	*b*	*c*	*d*	*e*	*f*	*g*	*h*	CH_2	CH_3	
III*	***	7,4	-	-	7,4	7,3	7,1	7,3	3,5	2,3	$J_{eh} = 0,9$
IV*	10,0	7,5	-	7,4	7,0	7,3	7,2	-	3,7	2,2	$J_{de} = 8,8$
V*	-	8,1	7,5	-	8,1	7,3	7,4	8,3	-	2,5	$J_{eh} = 0,9$
VI*	-	8,5	7,7	7,9	7,8	7,6	7,5	-	- 2'	2,6 3'	$J_{de} = 9,0$
VII*	10,3	7,4	-	-	7,4	7,3	7,1	7,3	7,2	8,3	$J_{eh} = 0,9$
VIII*	10,5	7,4	-	7,4	6,9	7,3	7,4	-	8,1	8,4	$J_{de} = 9,0$

*-The spectra of compounds III,IV,VII and VIII, recorded in ACETONE-d_6

** -Compouds V and VI, in DMSO-d_6, at 60^0C.

*** - NH→ND

The IR spectrum of above compounds (III, IV) in 3420, 3390 cm^{-1} region correspond to the NH group of pyrrol cycle, while, at the same time, it is characteristic for C-N(functional group absorption spectrum in the region of 1460, 1420 cm^{-1}.

During acetylation of compounds I and II in the anhydrous acetyc acid, 1-acetyl-1H-pyrrolo-[2,3-b]-(V) and 3-acetyl-3H-pyrrolo-[2,3-c]-phenoxathiines (VI) were obtained, respectively. In the analogous conditions indole yields the mixture of mono- and diacetyl-derivatives [3]. Unlike the indole case, in our experiments an unequivocal N-acetylation is evidenced. In compounds V and VI no proton sygnals of NH group were detected, which testifies that acetylation in the mentioned heterocycles goes with the nitrogen atom.

In the IR spectra of the heterocycles V and VI, the valency oscillations due to the C=O functional group, were detected in 1700, 1690 cm^{-1} regions, respectively.

Because of certain resemblance of the compounds I and II with indole, the azocoupling was performed in the conditions analogous for indole – in the dioxan-water mixture (pH=5-6). With an aim to study the azocoupling reaction, the p-nitrophenyl-diazonium chloride was chosen. The azocoupling ocurrs with the C_3 carbon atom and 3-(4-nitrophenylazo)-1H-pyrrolo-[3,2-b]-(VII) and 1-(nitrophenylazo)-3H-pyrrolo-[2,3-c]-phenoxathiines (VIII) are obtained. The PMR-, IR- and UV-spectra verify the structure

of the obtained compounds.

Thus, we can conclude that the reactions of pyrrolo-phenoxathiines (I,II) with the weak electrophils go in the same way as in indole – according to the β-position of pyrrolic nucleus, while acetylation is determined by the nitrogen atom of the pyrrolo-phenoxathiine molecule.

The control over reaction course and compound purity was performed by thin-layer chromatography with Silufol UV-254. The UV spectra were recorded on the spectrophotometer Spekord, in ethanol; The IR spectra - on the spectrometer Acculab-8 (Beckmann), in white petrolatum; The PMR spectra (in-TMS standard) were recorded on the AM-400 spectrometer (Brucker) and CFT-20 Varian (80 mHz), with precision of 0.01 p.p.m.

3-(N,N-dimethyl-amino-methyl)-1H-pyrrolo-[3,2-b]-phenoxathiine (III). 1.6 ml (2.40 mmol) of 33%-dimethyl-amine water solution, cooled to 0^0C, is slowly supplemented with 1.6 ml ice acetic acid, then with 1 ml (2.71 mmol) 40%-formalin and 0.2 g (0.8 mmol) of compound I. The reaction mass is stirred at 30^0C, for 1 h. Then the water is added, mixture is filtered and filtrate alkalized by 10%-NaOH water solution, up to pH 9. Extracted sediment is filtered, washed down by water, and dried in the vacuum-desiccator on KOH; yield: 0.19 g (78%); m.p.=52-54^{0}C; IR spectra: ν=1460 (C-N( ), 3420 cm^{-1} (NH); UV spectra, λ_{max}(lgε):212(4,41), 243(4,58), 268(4,31), 321(4,28), 340 nm (3,78); found: C 68,87; H 5,36; N 9,33; S 10,69%. $C_{17}H_{16}N_2OS$ (296). calc.:C 68.92; H 5,41; N 9,46; S 10,81%.

1-(N,N-dimethylaminmethyl)-3H-pyrrolo-[2,3-c]-phenoxathiine (IV). This compound is obtained from 3H-pyrrolo-[3,2-c]-phenoxathiine (II) in conditions described for the III; yield: 0.15 g (60%); m.p.=128-130 ^{0}C; IR spectra: ν = 3390 (NH), 1420 cm^{-1} (C-N( ); UV spectra, λ_{max}(lgε):211(4,28), 236(4,45), 263(4,39), 336 nm (4,17); found: C 68,92; H 5,33; N 9,35; S 10, 70%. $C_{17}H_{16}N_2OS$ (296). calc.:C 68,92; H 5,41; N 9,46; S 10,81%.

1-acetyl-1H-pyrrolo-[3,2-b]-phenoxathiine (V). Mixture of 0.2g (0.8 mmol) I and 10 ml (6 mmol) of freshly distilled acetic anhydride, following 15 h boiling, is cooled and poured into water and prolapsed precipitate is filtered. Then the product is washed by water and dried, purified by the column chromatography (Silica gel 100/250 μ), eluent ether-hexane 1:1; yield: 0.06 g (28%); m.p.=204-206^{0}C; IR spectra: ν=1700 cm^{-1} (C=O); UV spectra, λ_{max}(lgε):213(4,10), 248(4,17), 267(4,28), 290(3,82), 312(3,97), 347 nm (3,36); found:C 68,21; H 3,80; N 4,85; S 11,26%. $C_{16}H_{11}SNO_2$ (281). calc:C 68,33; H 3,91; N 4,98; S 11,39%.

3-acetyl-3H-pyrrolo-[2,3-c]-phenoxathiine (VI). Obtaining from the II, in conditions analogous to the V; yield: 0.05 g (22%); m.p.=187—189^{0}C; IR spectra: ν =1690 cm^{-1} (C=O); UV spectra, λ_{max}(lgε):208(4,14), 233(4,29), 281(3,83), 335 nm (3,67); found: C 68,23; H 3,83; N 4,88; S 11, 25%. $C_{16}H_{11}SNO$ (281). calc: C 68,33; H 3,91; N 4,98; S 11,39%.

3-(4-nitrophenyl-azo)-1H-pyrrolo-[3,2-b]-phenoxathiine (VII). Into 0.2 g(0.8 mmol) I, diluted in a mixture of 10 ml dioxan and 10 ml water, at 0^0C, 0.8 mmol of p-nitrophenyl-diazonium chloride is added. The pH of mixture is maintained in 5-6 range by means of sodium acetate. The reaction mass is stirred for 2 hours, the azocoupling product is isolated with ether. The ether solution is washed by 10% NaOH solution

and then by water until the neutral reaction is reached, dried on Na_2SO_4 and obtained compound (VII) is purified by the column chromatography (Silica gel, 100/250 μ) Eluent: ether-hexane 1:1; yield: 0.12 g (38%); m.p.=140-142^{0}C; IR spectra: ν =1475 (-N=N-), 3320 cm^{-1} (NH); UV spectra, λ_{max}(lgε): 217(4,29), 265(4.24), 353 (4,24), 426 nm (4,17); found:C 61,73; H 3,0; N 14,35; S 8,16 %. $C_{20}H_{12}N_4O_3S$ (388). calc: C 61,86; H 3,09; N 14, 43; S 8,25%.

1-(4-nitrophenyl-azo)-3H-pyrrolo-[2,3-c]-phenoxathiine (VIII). This compound is obtained from II in conditions analogous for VII; yield: 0.09 g (30%); m.p.=171-172^{0}C; IR spectra: ν =1470 (-N=N-), 3325 cm^{-1} (NH); UV spectra, λ_{max}(lgε):216(4,33), 254(4,42), 347(4,29), 428 nm (4,21); found:C 61,70; H 3,02; N 14,33; S 8,14%. $C_{20}H_{12}N_4O_3S$ (388); calc: C 61,86; H 3,09; N 14, 43; S 8,25%.

Georgian Technical University

REFERENCES

1. *A.Speicher, T.Eicher, L.M.Tevzadze, T.E. Khoshtariya.* J. Prakt. Chem. 339, 1997, 669-671.
2. *H.Kuhn, D.Stein.* Ber., Bd. 70, 1937, 567.
3. *J.Joul, G.Smit.* Osnovy khimii geterocyclicheskikh soedinenii. M., 1975, 290 (Russian).
4. *G.I.Jungietu, V.A.Budilin, A.H.Kost.* Preparativnaya khimiya indola. Kishiniev, 1975, 91 (Russian).
5. *V.G.Avramenko, V.D.Nazina, N.N.Suvorov.* Chem. Heterocycl. Comp. 81, 1970, 1071 (Russian).

საქართველოს მეცნიერებათა აკადემიის მოამბე, 159, №1, 1999
BULLETIN OF THE GEORGIAN ACADEMY OF SCIENCES, 159, №1, 1999

ORGANIC CHEMISTRY

L. Asatiani, M. Gverdtsiteli

Algebraic-Chemical Study of Some Ferrocene- and Germanium-Containing Acetylenic Compounds and the Reaction of their Synthesis

Presented by Corr. Member of the Academy D. Ugrekhelidze, February 16, 1998

ABSTRACT. **Algebraic-chemical investigation of some ferrocene- and germanium-containing acetylenic compounds and the reaction of their synthesis were carried out within the limits of quasi -ANB-matrices method.**

Key words: ferrocene, germanium, acetylenic, quasi-ANB-matrices.

Two main trends of algebraic chemistry are: investigation of the correlation "structure- properties" and formal-logical characterization of chemical reactions [1-3].

The reaction of synthesis of ferrocene - and germanium-containing acetylenic compounds was elaborated [4]:

$$Fc\text{-}C{\equiv}CLi \xrightarrow[-\ LiCl]{+\ RR'R''GeCl} Fc\text{-}C{\equiv}C\text{-}GeRR'R'', \qquad (1)$$

where Fc designates $C_5H_5FeC_5H_4$ fragment.

Algebraic characterization of this process was carried out within the limits of quasi-ANB -matrices method [5]. ANB-matrices are modificated contiguity matrices of molecular graphs. The diagonal elements of ANB-matrices represent the atomic number of chemical elements; nondiagonal ones - multiplicities of chemical bonds.

It must be admitted that for large molecules calculations on the basis of ANB-matrices are very labour-consuming (the most important component of this method is calculation of the determinant of ANB-matrix). We used simple model, where the fragments of molecules, which unchangeably transfers from initial to final state, are considered as "quasi-atoms". Corresponding modernized ANB-matrix is called quasi-ANB -matrices ($\widetilde{ANB}$).

The simplest model for (1) process is:

$$A\text{-}Li + B\text{-}Cl \rightarrow A\text{-}B + LiCl$$

where A designates Fc-C≡C fragment, B - GeRR'R'' fragment.

The register of (2) process in $\widetilde{ANB}$-matrices form is brought below:

$$\begin{Vmatrix} Z_A & 1 & 0 & 0 \\ 1 & 3 & 0 & 0 \\ 0 & 0 & Z_B & 1 \\ 0 & 0 & 1 & 17 \end{Vmatrix} \rightarrow \begin{Vmatrix} Z_A & 1 & 0 & 0 \\ 1 & Z_B & 0 & 0 \\ 0 & 0 & 3 & 1 \\ 0 & 0 & 1 & 17 \end{Vmatrix}, \qquad (3)$$

where Z_A and Z_B are the sums of the atomic numbers of chemical elements, which A and B fragments contain:

$$Z_A = \Sigma Z_a, \quad (4)$$
$$Z_B = \Sigma Z_b, \quad (5)$$

3 and 17 are atomic numbers of Li and Cl.

Let's consider the expression:

$$\Delta_r = \Delta_f - \Delta_I, \quad (6)$$

where Δ_I is the value of determinant of $\widetilde{ANB}$-matrix for initial system; Δ_f is the value of determinant of $\widetilde{ANB}$-matrix for final system; Δ_r is the change of value of determinant. calculations show that the value of Δ_r for (2) process is negative. Thus, the algebraic criterion of this process (in terms of this approach) is decreasing of the value of determinant of $\widetilde{ANB}$-matrix.

Three concrete A-B compounds and their $T_{melt.}$ are brought below:

$$Fc\text{-}C{\equiv}C\text{-}Ge(CH_3)_3 \qquad T_{melt.}=49\text{-}50^0,$$
$$Fc\text{-}C{\equiv}C\text{-}Ge(C_2H_5)_3 \qquad T_{melt.}=162\text{-}164^0C, \quad (7)$$
$$Fc\text{-}C{\equiv}C\text{-}Ge(C_6H_5)_3 \qquad T_{melt.}=179\text{-}181^0C.$$

The correlation equation $T_{melt.} \sim \lg(\Delta_{\widetilde{ANB}})$ was constructed on computer and it has a form:

$$T_{melt.} = 327.5 \lg(\Delta_{\widetilde{ANB}}) - 1195.5 \quad (8)$$

Correlation coefficient r is equal to r = 0.956, so correlation is "satisfactory" (according to Jaffe's criterion).

Tbilisi I. Javakhishvili State University

REFERENCES

1. *G. Gamziani.* Mathematikuri kimiis rcheuli tavebi. Tbilisi, 1990 (Georgian).
2. *G. Gamziani, M. Gverdtsiteli.* Izomeriis movlena matematikuri kimiis tvaltaxedvit. Tbilisi, 1992 (Georgian).
3. *P. R. Rouvray.* Chemical Application of Topology and Graph Theory. Ed. A. T. Balaban. Amsterdam, 1983.
4. *I. Gverdtsiteli, A. Asatiani, D. Zurabashvili.* Bull. Acad. Sci. GSSR, **79**, 2 , 1975 (Russian).
5. *N. B. Kobakhidze, M. G. Gverdsiteli, D. S. Tugushi, M. I. Gverdtsiteli.* Correlation "Structure - Properties" in Algebraic Chemistry. Tbilisi, 1997.

საქართველოს მეცნიერებათა აკადემიის მოამბე, 159, №1, 1998
BULLETIN OF THE GEORGIAN ACADEMY OF SCIENCES, 159, №1, 1998

PHYSICAL CHEMISTRY

V.Tsitsishvili, N.Dolaberidze, M.Alelishvili, G.Tsintskaladze, G.Sturua, N.Khazaradze, D.Gogoladze

Zeolitic Rocks from Newly Investigated Plots of Georgia

Presented by Member of the Academy T. Andronikashvili, February 12, 1998

ABSTRACT. **Several physical and chemical properties of zeolite-containing rocks from newly investigated plots of Georgian zeolite deposits (Tedzami, Dzegvi, Guria region and Gelati) have been studied by X-ray, IR-spectroscopy and adsorption methods.**

Key words: zeolite-containing rocks, clinoptilolite, heilandite, phillipsite, analcime.

Zeolite-containing rocks of different geological age and type are wide by spread in Georgia [1,2]. It must be mentioned that zeolite-containing rocks sampled from the same deposit but from different plots may be different both by mineralogical and chemical composition; consequently, such samples may have different physical and chemical properties and perspectives of their application [3].

The target of our research was to study composition, structure and several physical and chemical properties of zeolitic rocks from newly investigated plots of Georgian zeolite deposits in the aim of further modification of prospective samples for obtaining adsorbents and ion-exchangers.

The samples were collected at the following plots: Rkoni (R), Chachubeti (CH) and Kaprashiani (K) at Tedzami deposit; Saskhor-Dzegvi (SD) at Dzegvi deposit; Upper Shukhuti (SU) and Lower Shukhuti (SL) in Guria region; and at Gelati (G).

The qualitative identification of zeolite structure type and quantitative analysis of the content of zeolite phase in rocks was conducted by X-ray diffraction [4] and IR-spectroscopy methods.

X-ray powder diffraction patterns were acquired on "DRON-2" diffractometer using Cu-K_α radiation and scanning at 1° per minute. The intensity of peaks and d-spacings for studied natural zeolites is compared in Table 1 with the data for reference samples [5].

The results obtained on the base of X-ray data are collected in Table 2 and include information about zeolite type, content of zeolite phase in rocks, and main impurities. IR data (Table 3) are in accordance with the results of X-ray analysis.

The adsorption properties of natural zeolites is the main testimonial of their target application [6]. Water adsorption capacity was studied at usual conditions (P/P_S=0.4; 20°C). The adsorption of polar water molecules takes place due to ion-dipolar interaction in the crystal framework [7], so the different water adsorption capacity exhibits the differences in the volume of micro pores and the quantity of exchangeable cations for investigated samples.

Water adsorption capacity of dehydrated samples given in Table 4 is compared with

Table 1

Intensity of X-ray diffraction peaks (I) and d-spacings (d, Å) for zeolite-containing rocks

Clinoptilolite						Heilandite					
CtR		CtSD		Reference (a)		HK		HCH		Reference (b)	
I	d	I	d	I	d	I	d	I	d	I	d
50	10.48	75	9.82			60	10.05	37	9.82		
75	8.84	76	8.84	100	8.92			20	9.53		
25	7.83			3	7.97	100	8.84	100	8.84	80	8.845
36	6.56	48	6.56	2	6.78			10	7.76	70	7.796
10	5.83	29	5.22	2	5.61	25	6.83	24	6.62	60	6.631
25	5.22	27	5.07	7	5.15					10	5.945
40	5.06					12	5.22			50	5.277
42	4.67	52	4.56	14	4.65					70	5.096
		37	4.33	2	4.35			15	4.6	60	4.646
100	3.95	100	3.95	55	3.964			20	4.44	20	4.364
				57	3.897	40	4.23	30	4.23		
25	3.70	37	3.71	7	3.74	60	3.95	50	3.95	100	3.917
40	3.40	12	3.55	6	3.55					20	3.722
22	3.302	25	3.40	3	3.48					20	3.562
				16	2.419	80	3.34	20	3.43	70	3.420
				4	3.324			210	3.34	10	3.320
56	3.132	63	3.19	14	3.168	40	3.08			50	3.186
75	3.03			15	3.119	43	3.03			40	3.132
				8	3.07					90	2.959
80	2.98	50	2.97	80	2.974						
		51	2.80	15	2.793						
				33	2.728						

Phillipsite						Analcime					
PSU		PSL		Reference (c)		AG		ACH		Reference (d)	
I	d	I	d	I	d	I	d	I	d	I	d
5	10.4	7	11.7			7	9.79	6	9.82		
5	9.01	5	9.16	5	8.19	19	7.06	19	7.07	<10	6.87
30	7.12	27	7.21	10	7.19	37	5.54	36	5.53	80	5.61
20	6.21	18	6.09	12	6.41	6	4.91	6	4.93	40	4.86
7	5.30	7	5.46	10	5.37	10	4.71	9	4.76		
				25	5.06	15	4.16	15	4.15		
15	4.90	13	4.907	17	4.98	7	3.50	5	4.53		
				3	4.69					20	3.67
9	4.24	8	4.25	10	4.31		3.39		3.40	100	3.43
		25	4.11	40	4.13	35	3.31	34	3.30		
30	4.05			13	4.07	18	3.19	19	3.19		
				6	3.96	51	2.86	53	2.87	80	2.925
				3	3.70					20	2.801
				6	3.54	17	2.70	15	2.70	50	2.693
				6	3.47					50	2.505
				30	3.26	20	2.41	16	2.40	30	2.426
100	3.17	100	3.201	85	3.19					40	2.226
				34	3.14	References:					
24	2.91	25	2.921	14	2.93	a – natural clinoptilolite from					
				6	2.893	Vioming, USA;					
				4	2.857	b – natural heilandite from New					
18	2.73	18	2.75	21	2.754	Zeeland;					
23	2.67	24	2.67	34	2.698	c – natural phillipsite from Nevada,					
				9	2.667	USA;					
				6	2.577	d – natural analcime from					
10	2.51	12	2.54	8	2.542	California, USA [5].					

Table 2

Zeolite type and phase content in rocks, main impurities

Sampling plot	Zeolite phase		Impurities	Sample label
	type	content, %		
R	clinoptilolite	90	microfaunal	CtR
SD	clinoptilolite	70	clay minerals	CtSD
K	heulandite	60	quartz, clay minerals	HK
CH	heulandite	55	quartz, clay minerals	HCH
SHU	phillipsite	80	heulandite	PSU
SHL	phillipsite	60	heulandite	PSL
G	analcime	75	chlorite, montmorrilonite	AG
CH	analcime	70	chlorite, montmorrilonite	ACH

Table 3

IR absorption bands (cm^{-1}) for studied samples of natural zeolites

Sample	Deformational T-O	Intertetrahedral deformational	Intratetrahedral valent	Intertetrahedral valent symmetrical	Intratetrahedral valent antisymmetrical	Intertetrahedral valent antisymmetrical
Clinoptilo-lite	430, 465	527, 610, 668	730	787	1062	1210
Heulandite	435,454	522, 596, 664	725	780	1044	1200
Phillipsite	440	615	730	770	1043	-
Analcime	447	630	739	772	1042	-

Table 4

Water adsorption capacity of studied natural zeolites

Sample	Adsorption		Crystal framework density [8]
	mmol/g	cm^3/cm^3	
PSU	7.25	0.28	15.8
PSL	5.21	0.20	
CtR	4.72	0.18	17.0
CtSD	3.52	0.14	
HCH	2.51	0.10	
HK	2.03	0.08	
AG	0.30	0.012	18.6
ACH	0.15	0.006	

the density of corresponding crystal framework [8]. In spite of different zeolite type there is a significant correlation between adsorption capacity and free volume in the crystal framework.

At the same time differences in total volume of micro pores causes a strong correla-

tion between water adsorption capacity and zeolite phase content (see Tables 2 and 4) for samples of the same zeolite type but different geological genesis.

Low water adsorption capacity of analcime-containing samples (AG, ACH) is usual for zeolites of such type and is due to the small sizes of channels, inner cages and windows (approx. 2.6 Å) and corresponding strong interaction between crystal framework and charge-compensating cations that decreases the number of accessible adsorption centers.

From the results obtained it may be concluded that the natural zeolites from newly investigated plots of Georgian deposits are characterized by developed and regular system of micro pores, high zeolite phase content, and acceptable adsorption capacity, so they will have a wide application as adsorbents and other type micro porous materials.

Georgian Academy of Sciences
Institute of Physical and Organic Chemistry,

REFERENCES

1. *G.V.Gvakharia.* Zeolites of Georgia. Tbilisi, 1952, 236.
2. *N.I.Skhirtladze.* Sedimentary Zeolites of Georgia. Tbilisi, 1991, 144.
3. *G.V.Tsitsishvili.* In: Natural Zeolites, Tbilisi, 1979, 37-49.
4. *V.I.Mikheev.* X-ray Identification of Minerals. Moscow, 1957, 666.
5. *D.Breck.* Zeolite Molecular Sieves; Structure, Chemistry, and Use. N.-Y., 1974, 771.
6. *G.V.Tsitsishvili, T.G.Andronikashvili, et al.* Natural Zeolites. London, 1992, 224.
7. *G.V.Tsitsishvili.* Adsorptive, Chromatographic and Spectral Properties of Molecular Sieves. Tbilisi, 1979, 45.
8. *W.M.Meier, P.H.Olson, Ch.Baerlocher.* Atlas of Zeolite Structure Types. London, 1996, 229.

საქართველოს მეცნიერებათა აკადემიის მოამბე, 159, №1, 1999
BULLETIN OF THE GEORGIAN ACADEMY OF SCIENCES, 159, №1, 1999

PHYSICAL CHEMISTRY

R.Revia, G.Makharadze, G.Supatashvili

Investigation of River Water Fulvic Acid by HPLC

Presented by Corr. Member of the Academy D.Ugrekhelidze, April 27, 1998

ABSTRACT. **The ion-pair reversed phase HPLC has been used for the investigation of fulvic acid isolated from river water. The influence of mobile phase pH on the chromatographic separation of fulvic acid ingredients has been established. The existence of equilibrium between separated components of fulvic acid sample was also elucidated by means of their preparative collection and reinjection. It was supposed, that the separated ingredients represent the aggregates of different mass which probably are their existence form in aqueous solutions. The variation of system pH presumably results in the redistribution of molecular masses of these aggregates.**

Key words: ion-pair chromatography, microcolumn RP-HPLC, fulvic acid, association of fulvic acid.

Fulvic acid (FA) makes up the fundamental part of dissolved organic matter of natural waters [1]. The great interest regarding FA is induced by their ability to form complexes both with heavy metals [2] and organic compounds [3]. So, FA affect on chemical, physical and biological processes occuring in the natural waters. Nevertheless chemical structure of FA up to now is not established. Spectrometric methods employed for such investigation [4,5] give abundant information about functional groups included in FA structure. However creation of FA molecular model on the basis of these data is complicated by heterogeneous nature of its molecule. Therefore it would be more useful first to separate it into ingredients [6,7].

FA was isolated from water of the river Mtkvari (Georgia) by adsorption-chromatographic method [8]. Chromatographic investigation of FA sample was realized on microcolumn liquid chromatograph "Milichrom-1" (Russia) with UV detector. Detection was achieved at 230 nm. The separation of FA was performed on stainless steel column (100 x 2 mm i.d.) which was packed with Separon-C_{18} (Lachema, Brno, Czech Republic). Particle diameter was 5 μm. The eluent was a mixture of 2-propanol, 1-butanol and 20 mM tetrabutilammonium hydroxide in 0.05 M Na_2HPO_4 (12:4:84). Mobile phase flow-rate was 50 μl/min. The acidity of the mobile phase was adjusted with phosphoric acid.

The results obtained show (Fig.1) that the separation of FA into the components depends on the acidity of the mobile phase. In particular the increase of the mobile phase pH increased the relative heights of the peaks 1 (retention time - t_R- 5 min 15 sec) and 5 (t_R 13 min 40 sec) and correspondingly decreased the relative height of the peaks 2 (t_R 6 min 30 sec), 3 (t_R 7 min 10 sec) and 4 (t_R 8 min 50 sec). The number of the peaks is also varied with the alteration of the mobile phase acidity, namely, the increase of the mobile phase pH causes the decrease of the number of separated components (Fig. 1). It

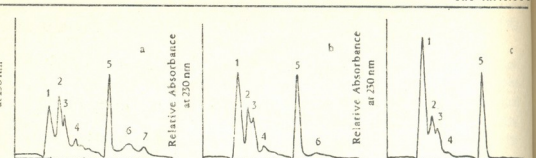

Fig. 1. Effect of variation of the mobile phase acidity on the chromatographic separation of FA : pH 3.0 (a), pH 5.0 (b), pH 7.0 (c).
Eluent: mixture of 2-propanol, 1-butanol and 20 mM tetrabutylammonium hydroxide in 0.05 M Na_2HPO_4 (12:4:84).

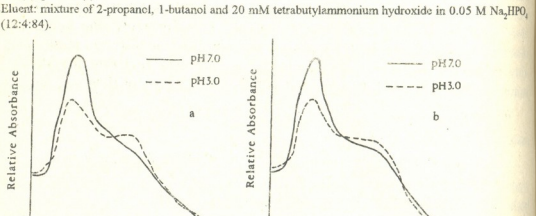

Fig. 2. Dependence of the UV-spectra of peak 1(a) and peak 5(b) as a function of the mobile phase pH.

should be noted, that the UV-spectra of the separated components altered respectively (Fig.2).

The alteration of the relative heights and the number of the peaks might be the result of the formation of associates by FA components. About the tendency of FA to the formation of a highmolecular associated compounds was mentioned in literature earlier [9]. The masses of the formed associates depend on the pH value of the solution.

To prove this idea the FA ingredients corresponding to the peak (1) and peak (5) were preparatively collected and purified from ingredients of mobile phase. 2-propanol and 1-butanol were removed by evaporation under vacuum. The dry residue was dissolved in bidistillate water and the solution was passed through the cation-exchanger (KU-2) in order to remove the tetrabutilammonium ions. After purification both preparatively collected ingredients of FA were reinjected. As it is seen in Fig.3, each of them was undergone to further separation. The results obtained show, that the peaks in Fig.1 belong to the associates which are able of further separation. Besides, this associates are in the state of equilibrium between themselves.

The experimental data obtained make possible to suggest, that FA exists in the aque-

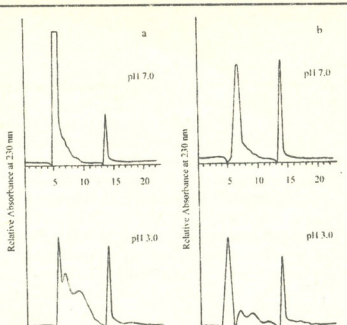

Fig. 3. Chromatographic separation of the preparatively collected fractions of peaks 1(a) and 5(b) reinjected at the different pH values of mobile phase.

ous solutions as a dynamic system of associates of different masses, which are in the state of equilibrium between themselves. At the high pH value the associates of high molecular masses predominant in the system and at the low pH value the lower molecular mass forms predominant in solution. The removal of any part of the system causes the molecular-mass redistribution and the system tries to shift to the new equilibration.

Tbilisi I. Javakhishvili State University

REFERENCES

1. *J.A.Leenheer*. Advances in Chemistry Series N237, 1994, American Chemical Society 196.
2. *N.S.Goliadze*. Candidate thesis. 1997, Tbilisi.
3. *I.Scheunert, M.Mansour.* Intern.J.Environ.Anal.Chem., **46**, 1992, 189.
4. *C.Maqueda, E.Morillo, J.L. Perez Rodriguez.* Soil Science, **148**, 1989, 336.
5. *R.C.Averett, J.A.Leenheer, D.M.McKnight and K.A.Thorn (edt.).* Humic substances in the Suwannee River, Georgia: interactions, properties, and proposed structures, U.S.Geological Survey, open-File Report 87-557, Denver, Colorado, 1989.
6. *B.Smith, P.Warwick.* J.Chromatogr., **547**, 1991, 203.
7. *A.Hirose, D.Ishii.* J.High Resol.Chromatogr.& Chromatogr. Communications, **9**, 1986, 533.
8. *G.M.Varshal, T.K.Veljukhanova, I.S.Sirotkina, R.D.Jartseva.* Gidrokhimicheskie materialy, **59**, 1973, 143 (Russian).
9. *G.M.Varshal, L.N.Intskirveli, et al.* Geokhimiya, 10, 1975, 1581 (Russian).

საქართველოს მეცნიერებათა აკადემიის მოამბე, 159, №1, 1999
BULLETIN OF THE GEORGIAN ACADEMY OF SCIENCES, 159, №1, 1999

PHYSICAL CHEMISTRY

Member of the Academy K.Japaridze, Z.Elashvili, L.Devadze, N.Sepashvili, M.Metonidze

Liquid Crystal Phase with High Coefficient of Bragg Reflection

Presented July 2, 1998

ABSTRACT. **While studying smectogenic cholesteric liquid crystal mixtures a new phase St, which is characterized by effective Bragg reflection of any polarized light, has been found. On the basis of experimental data a proposition is made that in the formation of St phase geometrical characteristics of molecules of liquid crystal system components have a decisive role.**

Key words: liquid crystal, Bragg reflection.

While studying the liquid crystal (LC) systems one of the most significant problems is to establish connection between molecular structure and mezophases properties. The influence of molecular and electron structures on the characteristics of different phases of LC mixtures is well known. The present paper aims at studying the effect of additions containing volume and bent molecules on the formation of different LC phases and properties.

The object of study was smectogenic cholesteric LC mixtures: e.g. cholesteriloleate (bent molecules) + cholesterilpelargonate (or cholesterilcaprilate, cholesterilenantoate, cholesterilundecylate, cholesterilcaprinate, cholesterilmiristate and so on) and dopants having volume molecules (terpenes and other compounds).

In such LC mixtures in cooling regime, at a definite temperature in visible region of spectrum the change of temperature dependence of selectively reflected wavelength is observed. This phenomenon [1,2] which is called "reverse" takes place when the amount of dopants is several per cents of the whole mass. Along with the increase of concentration of dopant volume molecules, the maximum of reflection corresponding to the start of reverse is hypsochromically shifted. When the temperature of reverse T_r is reached along with the change of $d\lambda/dT$ sign, gradual increase of reflection coefficient is observed. Any kind of polarization light is reflected. This strange state of LC is denoted as St (Strange) phase. The St phase exists until smectic state transition temperature T_s. The interval $T_r - T_s$ is 1^0-$1{,}5^0$C. For well oriented layers of 100 mkm thickness the selective reflection coefficient on T_{max} reaches 100% of value, temperature sensitivity is ~300mm/grad. T_r depends on matrix composition, additive nature and concentration and it changes in wide range.

Experimental Part. Cholesterilpelargonate and cholesteriloleate mixtures were prepared with 1:1-1:2 ratio. L-menthol, borneol, adamantane and other derivatives were used as additives with volume molecules. Additives concentration made 0.5-5% of mass. Melted mixture was inserted in between rubbed plane-parallel glasses.

Teflon bedding located between glasses determines the thickness of the layer (10-100mkm). The cell was placed in thermostate, temperature regulation preciseness of which is 0.01^0. The spectra have been fixed in reflection, optic density and transmission regimes. T_r, T_{max}, T_s and transition temperature T_i from isotropic into LC state depend on matrix composition, nature of additive and concentration. Along with the increase of additive concetration T_i-T_r temperature interval narrows, and the band of corresponding reflection is hypsochromically shifted. Light beam was directed on the cell with different angles. The most longwave reflection band (l_{max}) is observed while perpendicular incidence, i.e. for angles different from perpendicular incidence the maximum of selective reflection band will be replaced hypsochromically. The intensity of light reflection exponentially depends on thickness of layer [1].

Results and Discussion. The property of effective reflection of any polarization light distinguishes St phase from the known phases: TGB, reentrant and inclined chiral smectics [3,4]. In a certain interval of different from perpendicular incidence angle, there exists theoretical possibility of light complete reflection by cholesteric structures [5]. It was possible to admit that in the researched objects during temperature change, the axis of cholesteric structure in respect to glass surface inclines and theoretical proposition is realized. The obtained experimental data: after revers well-defined increase of reflection band intensity, hypsochromic shift while temperature decrease and nonperpendicular incidence of beam make us propose that we deal with the formation of a new phase. Microcalorimetric measurements also testify to phase transitions. It is known that selective reflection in optic range is connected with LC spiral structure. The formation of such structures (chiral nematics and smectics) is conditioned by chiral molecules. In chiral LC molecules of different layers make the angle and arrange in a spiral in space. In C* smectics also molecules arrange in respect to each other at an angle so that the thickness of smectic layer is preserved. On such systems while

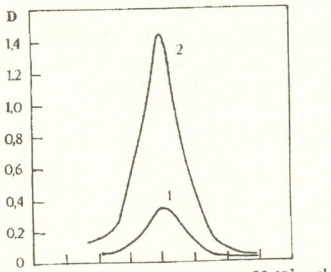

Fig. Cholesteriloleate, cholesterilpelargonate and paraetoxy-L-mentilcynnamat mixture 1:1:0.06 (mass)
1. Cholesteric phase ($t=29.3^0$ C)
2. S_t phase ($t=28.2^0$C)

perpendicular incidence of nonpolarized light about 50% of light is reflected.

As it was mentioned above LC system in St phase completely reflects any polarizatio light, and it makes possible to suppose that the structure of St phase is not helical bu bedded, where the layers thickness is variable. The section of bedded structure can be o S or ε form. The formation of such structure is possible if molecules make a certain angl with each other. But unlike C* smectics they will be arranged in one and the same plan The maximum thickness of the layer can be equal to molecule length and minimum - t width. In such corrugated systems index of refrection will be also modulated and it ca complectely reflect any polarization light of a certain wave length.

The elastic properties of the system (Frank constants: K_1-splay, K_2-twist and K_3 bend) are significant while formation of LC phase. In cholesteric systems K_1 and $K_2>K_3$ The formation of cholesteric phase is the result of K_2 smaliness. Along with temperatur decrease the increase of K_2 in cholesteric - smectogen LC systems causes the increas of spiral step while transition from cholesteric into smectic phase K_2 and $K_2>K_3$

In the studied smectogenic LC systems the existence of chiral bent and volum molecules near T_s causes the increase of K_2. The bedded (quasi-bedded) structures forma tion with variable thickness is the result of smallness of bend constant K_3. The last on conditions Bragg reflection of any polarization light.

Thus in the formation of St phase geometrical charactaristics of molecules of LC system components have a decisive role.

This work was supported by the Georgian Academy of Sciences under Grant N2.6

Georgian Academy of Sciences
Institute of Cybernetics

REFERENCES

1. *E.Vashakidze, K.Japaridze, Ts.Zurabishvili, et al.* Izvestia AN Gruzii, Chemical Series, 15,3, 1989, 225.
2. *K. Japaridze, E.Vashakidze, et al.* Ibid, 22, 1996.
3. *N.Andal, G.S.Ranganath,* 15th Intern. Liquid Crystal Conference. 1, 1994, Budapest, 263.
4. *G.Chilaia, C.Destrade, Z.Elashvili, et al.* J.Phys. Lett. 46, 1985.
5. *V.Dmitrienko, V.Beliakov.* J.E.Th. Phys. 73, 1977.

საქართველოს მეცნიერებათა აკადემიის მოამბე, 159, №1, 1999
BULLETIN OF THE GEORGIAN ACADEMY OF SCIENCES, 159, №1, 1999

PHYSICAL CHEMISTRY

P.Janjgava, V.Bakhtadze, V.Mosidze

Porous Structure and Phase Composition of Alumocalcium Carriers of CoMn Catalyst of Methane Conversion

Presented by Corr.Member of the Academy L.Japaridze, July 6, 1998

ABSTRACT. **The action of porous structure and phase composition of alumocalcium carriers on CoMn catalyst activity in the conversion process of methane with water steam is regarded in the present paper. The interrelation between the content of calcium oxide, heat treatment temperature and activity in the carrier, is established.**

Key words: methane, conversion.

For conversion process of methane with water steam a catalyst containing cobalt and manganese oxides covered alumocalcium carrier [1], which is characterized by high activity, thermal and chemical stability is elaborated. The content of Mn oxides increases CoMn catalyst mechanical steadiness during carbonization. At the same time as compared to nickel catalyst it is more stable in respect to poisoning by sulphur compounds [2,3].

Current processes during carrier formation influence on catalyst activity of methane conversion with water steam during which optimal phase composition and surface-structural parameters are formed. The influence of the mentioned factors on Co-Mn catalyst activity has been studied on the samples of the following composition:

Chemical composition of samples	Heat treatment temperature (°C) and duration (h)
I-Al_2O_3-12.0 mass.% Ca	1000, 5
II-Al_2O_3-12.0 mass.% Ca	1150, 5
III-Al_2O_3-12.0 mass.% Ca	1300, 5
IV-Al_2O_3-6.0 mass.% Ca	1300, 5
V-Al_2O_3-15.0 mass.% Ca	1300, 5

The samples were prepared by initial Al oxide (A-1 type) granules swelling with a certain concentration of calcium nitrate solution followed by drying and heat treatment. Roentgenophase analysis of alumocalcium carriers was performed on "DRON-1" apparatus with CuK_α radiation.

According to roentgenophase analysis (Table 1) unlike samples (I and II) processed at 1000 and 1150°C. Al oxide metastable modifications completely transform into stable α-modification - corundum (samples III, IV, V) after treatment at 1300°C.

Table 1

The results of roentgen phase analysis of alumocalcium carriers

Sample N	Samples composition and heat treatment temperature	Phases					
I	Al_2O_3-12.0 mass.% Ca-1000°C	α-Al_2O_3	K-Al_2O_3	δ-Al_2O_3	θ-Al_2O_3	3C·5A	C2A
II	Al_2O_3-12.0 mass.% Ca-1150°C	α-Al_2O_3	-	-	θ-Al_2O_3	3C·5A	C2A
III	Al_2O_3-12.0 mass.% Ca-1300°C	α-Al_2O_3	-	-	-	3C·5A	C2A
IV	Al_2O_3-6.0 mass.% Ca-1300°C	α-Al_2O_3	-	-	-	3C·5A	C2A
V	Al_2O_3-15.0 mass.% Ca-1300°C	α-Al_2O_3	-	-	-	3C·5A	C2A

Using mercuric phorometric method [4] of low and high pressures a total volume of four pore samples (II, III, IV, V) and radii of alumocalcium carriers are determined (Table 2). The values of samples specific surfaces obtained by chromatographic method of azote heat desorption [5] are also given.

The data given in Table 2 demonstrate that the sample IV - Al_2O_3-6.0 mass.% Ca after heat treatment at 1300°C preserves macroporous structure by insignificant portion of pores of small and average size radii. Total volume of pores makes 0.415 cm^3/g. The specific surface as compared to aluminum oxide of A-1 type sharphy decreases from 250-280 m^2/g up to 28.0 m^2/g, which is conditioned by disappearance of small size pores due to the filling of their great part with calcium oxide. In sample III after heat treatment at 1300°C polydisperce porous structure is formed. Unlike sample IV pores portion with 50-120 Å radius is significantly increased basically on account of pores with big radius.

Table 2

Porous structure characteristics of alumocalcium carriers samples

Sample N	Pore volume (ΔV), radius (r) and their share in %									phores total volume cm^3/g	Specific surface m^2/g
	to -100 Å			From –100 to 1000 Å			From –1000 to 50000 Å				
	r, Å	cm^3/g	%	r, Å	cm^3/g	%	r, Å	cm^3/g	%		
II	40.0	0.01	3.0	300	0.03	9.0	3000	0.016	5.0	0.324	40.0
	80.0	0.006	2.0	400	0.032	10.0	6000	0.018	5.5		
	100.0	0.006	2.0								
III	50.0	0.024	7.1	500	0.006	2.0	1200	0.024	7.1	0.338	15.0
	100.0	0.014	4.1				6000	0.025	8.0		
	120.0	0.016	5.0								
IV	50.0	0.014	3.4	400	0.04	2.6	1200	0.048	11.5	0.415	28.0
							6000	0.038	8.7		
							50000	0.028	6.7		
V	40.0	0.012	5.2	200	0.006	3.0	1200	0.012	5.2	0.23	20.0
	60.0	0.01	4.4	800	0.008	4.0	4000	0.01	4.4		
	100.0	0.006	3.0				6000	0.024	10.5		

The following increase of calcium oxide in carrier (sample V) causes pores redistribution: pores of average size with radius 200-800 Å are formed on account of small size pores. Total volume of pores decreases up to 0.23 cm^3/g, but specific surface equals 20 m^2/g.

Prepared on the sample of alumocalcium carriers catalysts activity was determined in the process of methane conversion with water steam on laboratory flow-type equipment [6]

in the following conditions: gas volume velocity W=2000 h^{-1} temperature 750°C, ratio CH_4:H_2O (steam)=1:2. The amount of active components in catalyst – mass.%: Co - 9.0 and Mn - 3.0.

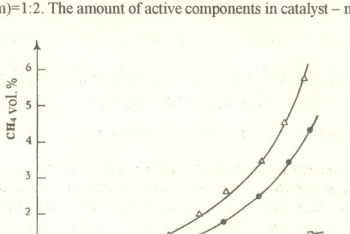

Fig. CoMn catalysts activity prepared on alumocalcium carriers (samples I-V) in conversion process of methane with water steam.

From the data illustrated in the Figure it is seen that Co-Mn catalyst prepared on sample III carrier has the highest activity in conversion reaction of methane with water steam. While testing for a long time (10h) in converted gas the residual amount of methane doesn't excess 0.5 % of volume. The decrease of Co-Mn catalysts activity prepared on samples I,II (Table 1) can be explained by the fact that the carrier formation by optimal phase composition and porous structure doesn't take place at 1000-1150°C (sample III) because the process of formation of calcium aluminate is not completed. Aluminium oxide metastable modifications K,δ,θ phases are still preserved. The decrease of calcium oxide content up to 6.0% causes the decay of activity, but the increase up to 15.0% practically doesn't affect catalyst activity.

Georgian Academy of Sciences
P.Agladze Institute of Inorganic
Chemistry and Electrochemistry

REFERENCES

1. Avtorskoe Svidetelstvo N67 1835.
2. *V.Sh.Bakhtadze, R.V.Janjgava et al.* Kataliticheskaya konversiya uglevodorodov. Kiev, 6, 1981, 33.
3. *R.V.Janjgava et al.* Bull. Georg. Acad. Sci., **145**, 3, 1992, 561.
4. *T.G.Plachenov.* Rtutnaya porometricheskaya ustanovka P-3M. 1961.
5. *M.E.Buyanova, A.P.Karakhanov.* Opredelenie udelnoi poverkhnosti tverdykh tel khromotograficheskim metodom teplovoi desorbtsii argona. Novosibirsk, 1965.
6. *V.Sh.Bakhtadze et al.* Kataliticheskaya konversiya uglevodorodov, 3, 1978, 17.

საქართველოს მეცნიერებათა აკადემიის მოამბე, 159, №1, 1999
BULLETIN OF THE GEORGIAN ACADEMY OF SCIENCES, 159, №1, 1999

PHYSICAL CHEMISTRY

I.Sarukhanishvili, N.Kurshubadze, V.Makhviladze, A.Sarukhanishvili

Physical and Chemical Processes Conducted in Trachyte Containing Quarternal System

Presented by Member of the Academy G. Tsintsadze, May 25, 1998

ABSTRACT. **We present experimental results which confirm the possibility of predicting some physical and chemical processes proceeding in the mixtures based on feldspar containing raw materials. The processes in the mentioned mixtures proceed more rapidly and are completed at lower temperature than it is known from literature data.**

Key words: trachyte, complex raw materials.

The system considered in this work is of great importance for glass containers production and optimal utilization of raw materials base for glass industry in Georgia.

The system is quarternal, consisting of trachyte, quartsfeldspar sand from Badjide later called sand, limestone from Dedoplistskaro and soda ash hereinafter known as soda.

The system is conditionally quarternal because trachyte contains as a minimum two components, such as sanidine (natrium sanidine) and plagioclasses; sand contents of quartz and alkali feldspars [1]. Thus the system (by regarding limestone and soda and regardless intermixture minerals), consists of five components: sanidine (San), plagioclasses (Pl), alkali feldspars (Fsp), calcite (Cc) and soda (S).

Trachyte and sand are complex raw materials. Their influence on the processes of glass batches differs from that of traditionally utilized materials [2]. The nature of complex raw materials causes this fact.

The studied system contains trachyte from 5 to 35%, sand from 7 to 50%, limestone between 15 and 25% and soda between 12 and 20%.

Considerable action of trachyte on the processes conducted in the batches of the mentioned system begins with 10% of trachyte. When the content of trachyte in the system is less than 10%, the processes characterised for the batches containing Badjide sand with quartz described in [1] are left without considerable changes. The further increase in trachyte content results in activization of physical and chemical processes, which could be explained by the example of the mixture containing 32.5% of trachyte, 50% of sand, 13% of soda and 17.5% of limestone.

By heat treatment at 500^{0}C the above-mentioned mixtures undergo rather intensive processes resulting in the formation of Na and Ca binary carbonates, integration of feldspars and separation of CO_2. These processes are proved by mineralogical, derivatographical and roentgenophase analyses and thermochemical and thermodynamic calculations. The Figure on dyphractogram shows the existence of binary carbonates of Na and Ca. The feldspars are so integrated, that their identification is impossible, while in non-processed

mixture they can easily be separated.

By means of heat treatment at 800°C the reflexes of Fsp reduce, as well as those of carbonates. The reduction of the d α/n lines intensity characteristic for quartz takes place as well. Liquid phase is observed in the mixture, which amount reaches 20-30% of the whole weight. It was determined that this is the result of processes taking place simultaneously, out of which the following should be mentioned: solid phase reactions among carbonates and feldspars; interaction between carbonates and quartz (Q); formation of low-temperature eutectics by participation of the products and system components obtained as a result of solid phase reactions; melting of easy-melting compounds.

There are almost no feldspars at 950°C. Besides quartz tridymite (Tr) can be found within the system, that is approved by taking into consideration the data given in [3]: Transformation of quartz into tridymite is possible by coexistence of alkali oxides. There is only silica in the system at 1100°C, which is completely dissolved in melt at 1250°C. It is worthwhile to mention that incongruent melting of sanidine within the system and forming of leucite (1150°C) characteristic of trachyte was not observed, which increases the temperature of transformation system in amorphous phase in binary and ternary component trachyte containing systems.

The processes conducted in the system can be expressed by the scheme as follows:

400-500°C $CaCO_3+Na_2CO_3 \rightarrow Na_2Ca(CO_3)_2$

$2(K, Na)AlSi_2O_8+Na_2CO_3 \rightarrow 2(Na,K)AlSi_2O_8+K_2O+CO_2$

$2(K,Na)AlSi_2O_8+CaCO_3 \rightarrow CaAl_2Si_2O_8+(K,Na)_2O+4SiO_2$

There is no liquid phase

500-800°C $CaNa_2(CO_3)_2+2SiO_2 \rightarrow CaSiO_3+Na_2SiO_3+2CO_2$

$K_2O+4SiO_2 \rightarrow K_2Si_4O_9$

$Na_2O+4SiO_2 \rightarrow Na_2Si_4O_9$

At 400-500°C the intensification of the processes start, eutectic is formed:

$K_2SiO_3+KAlSi_2O_8$+liquid (726°C)

melting of $K_2Si_4O_9$(770°C)

eutectic $Na_2Si_2O_5+NaAlSi_2O_8$+liquid (767°C)

eutectic $KAlSi_2O_8+SiO_2+K_2Si_4O_9$+liquid (715°C)

eutectic Q+$K_2Si_4O_9+K_2Si_2O_5$+liquid (695°C)

melting of $Na_2Si_2O_5$ (874°C)

$Na_2Si_2O_5$+Ab+SiO_2+liquid (740°C)

liquid phase-30%

800-950°C Continuation of the above-mentioned processes. Excess amount of An and its beginning of dissolution in melt

α-quartz →α-tridymite transformation.

liquid phase -60%

950-1100°C Ab melting. Complete dissolving of An and SiO_2 in melt. Amorphous mass%-100%

By reducing the content of trachyte with the help of sand increase the temperature

intervals of the present processes shift to higher temperature when the content of soda and limestone are constant. As a result of interchange of soda with limestone, when trachyte (no less than 20-25 wt.%) and sand are constant, the temperature intervals change insignificantly. When the content of trachyte is less, the increase of limestone at the expense of decreasing of soda amount makes physical and chemical processes complicated.

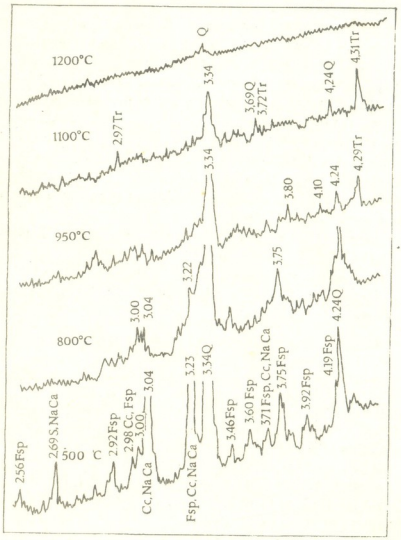

Fig. Diphractograms of "trachyte-sand-limestone-soda" system

Georgian Technical University

REFERENCES

1. *A. B.Sarukhanishvili, H. H. Khurshbadze.* Georgian Engineering News. **1**, T., 1996, 35-38 (Russian).
2. *V. Eitel.* Fisicheskaya khimiya silikatov. M., 1962, 392 (Russian).
3. *A. N. Vinchel, G. Vinchel.* Opticheskie svoistva iskusstvennykh mineralov. M., 1967, 86(Russian).

საქართველოს მეცნიერებათა აკადემიის მოამბე, 159, №1, 1999
BULLETIN OF THE GEORGIAN ACADEMY OF SCIENCES, 159, №1, 1999

PHYSICAL CHEMISTRY

S. Gedevanishvili, Z. A. Munir, Member of the Academy I. Baratashvili

Formation of Titanium Based Composites through Electric Field Activated Combustion

Presented September 21, 1998

ABSTRACT. **The synthesis of TiB_2-$TiAl_3$ composites with $TiB_2/TiAl_3 = x$ molar ratios from $x = 1.0$ to $x = 5.0$ were investigated by electric field-activated combustion using elemental powders as reactants. Using amorphous boron powders, composites with $x \leq 2.0$ can be synthesized in the absence of a field. Those with $3.0 \leq x \leq 5.0$ can only be formed in the presence of a field. For all cases, the product contained the desired phases with minor amounts of Ti_5Al_{11}. Higher values of x, resulted in relatively higher amounts of this phase. The effect of the use of crystalline boron and the influence of its particle size were also investigated. In the absence of a field, no self-sustaining combustion wave could be initiated even when the smallest particles (<20 μm) were used. Under the influence of 18Vcm^{-1} field, combustion waves were initiated and the products were virtually identical to those obtained with the amorphous boron powders.**

Key words: combustion synthesis, composites , electric field.

The direct synthesis of composites from elemental powders is one of the attractive features of the self-propagating high-temperature synthesis (SHS) method. The use of this method to synthesize numerous ceramic-ceramic and ceramic-metal composites has been reported [1-6]. In all cases, however, the compositional limits of the composites that can be synthesized are dictated by the enthalpies of formation of the two phases in their given stoichiometry. According to the thermodynamic calculations it is expected that composites with $TiAl_3$/TiB_2 molar ratios of > 3 (T_a<2000K) cannot be synthesized by SHS. Recent investigations, however, have shown that compositional limits can be extended through electric field activation [1]. The application of a field simultaneously with an ignition source initiates self-propagating combustion waves in less energetic systems, i. e. to those systems with T_a<2000K [7,8]. In this paper we report the field-activated combustion synthesis of $TiAl_3$-TiB_2 composites from elemental powders according to the reaction:

$$(1 + x)Ti + 2B + 3xAl = x\ TiAl_3 + TiB_2,$$

where x (the molar ratio $TiAl_3/TiB_2$) being 0.5, 1.0, 2.0, 3.0, 4.0 and 5.0.

The titanium and aluminum powders utilized in this work were 99% and 99.5% pure, respectively, and had a sieve classification of -325 mesh. Three types of boron powders were used: two types of amorphous powders, 99.99% and 92% pure and a crystalline powder being 99% pure and had a-325 mesh sieve classification. The crystalline powder was further sieved to give powders with particle sizes in the ranges of <20, 20-30, and 30-

44 μm.

The powders were dry-mixed in the desired stoichiometry and cold-pressed to give rhombohedrally-shaped samples with dimensions of 2.15 x 0.75 x 1.1 cm. The pressed samples were placed between graphite electrodes inside a combustion chamber. A tungsten coil (placed near one face of the sample) effects ignition while a voltage is applied across the graphite electrodes. Combustion wave temperatures were measured by a two-color optical pyrometer with a response time of 0.01s. Wave velocities were determined from video camera recordings with the aid of a time-code generator. All experiments were conducted under a one-atmosphere pressure of argon gas. Phase analysis of the products was made by X-ray diffraction (XRD).

Using the 92% pure amorphous boron powder samples with x = 0.5, 1.0 and 2.0 can be ignited without the application of a field. A wave propagated at a velocity whose magnitude decreased roughly linearly with increasing x, as shown in Fig. 1. A similar, but less dramatic decrease in the combustion temperature was observed as x increased from 0.5 to 2.0, as also shown in Fig. 1. However, using the same powder with x = 3.0, no SHS wave can be initiated even after prolonged exposure of the samples to the tungsten igniter

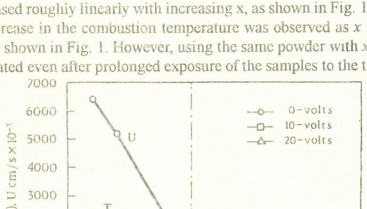

Fig. 1. The dependence of the measured combustion wave temperatures and velocities on the $TiAl_3/TiB_2$ molar ratio: results with amorphous boron.

(>3 min). Similar results were obtained when the high purity (99.99%) amorphous boron powders were used.

To synthesize composites with ratios x = 3.0 using amorphous boron, it was necessary to apply an electric field across the samples before activating the ignition source. Self-sustaining waves could be initiated for x = 3.0, 4.0, and 5.0 when fields of 9 and 18 Vcm^{-1} were applied. The velocity of such waves and the associated combustion temperature decreased only slightly with increasing x, as shown in the right-hand side of Fig. 1. For these compositions, the wave propagated in pulsating (non-steady state) mode. It is likely that the observed, relatively minor influence of the field on wave velocity and temperature is a consequence of this non-steady state propagation.

X-ray diffraction analyses of products synthesized without and with field show the presence of TiB_2, $TiAl_3$, and minor amounts of Ti_5Al_{11}. However, the amount of Ti_5Al_{11}

became larger as the $TiAl_3/TiB_2$ ratio increased.

The effect of boron particle size was investigated using the classified crystalline powders and a fixed molar ratio of $x = 1$. As seen above, for this stoichiometry the powders react without a field in a self-sustaining mode when the boron powder is amorphous. However, when crystalline boron powders were used in the absence of a field, no self-sustaining reaction was possible for any of the powder particle size fractions used (i. e. <20, 20-30, 30-44 μm) or for the as-received (-325 mesh) powder. But when a field of 18 $V \cdot cm^{-1}$ was imposed, self-propagating waves were initiated in all cases. The waves propagated in a steady-state mode for reactants containing <20 and 20-30 μm powders but advanced in a non-steady state (pulsating) mode for reactants with the 30-44 μm sized boron particles. The corresponding wave velocities and combustion temperatures for these powders are shown in Fig. 2. The data of a sample made with amorphous boron (with $x = 1$) is also included in Fig. 2 for comparison. The velocity in the samples containing crystalline boron decreased by about a factor of ten as the particle size increased, as seen in Figure. The combustion temperature of the <20 and 20-30 μm powders obtained with a field of 18 Vcm^{-1} is approximately the same as that for the amorphous powders reacted without a field. However, the combustion temperature of the 30-44 μm powders is markedly lower as also shown in this Figure. It should be recalled that wave propagation for this powder size fraction is in the non-steady state mode, in contrast to the state-steady modes for the other (smaller) powder size fractions. X-ray analysis of products made using crystalline boron with a field of 18 Vcm^{-1} showed the presence of TiB_2 and $TiAl_3$ with minor amounts of Ti_5Al_{11}. Thus the product of field-free combustion using amorphous boron is the same as that of the field-activated combustion using fine crystalline boron powders, (<20 and 20-30 μm), Field-activated combustion with larger crystalline boron powders (30-44 μm) contained higher amounts of the minor phase, Ti_5Al_{11}. With the use of amorphous boron, higher amounts of this phase were detected in systems with higher x ratios (e. g. $x = 5$). In all cases investigated, the appearance of Ti_5Al_{11} in signifi-

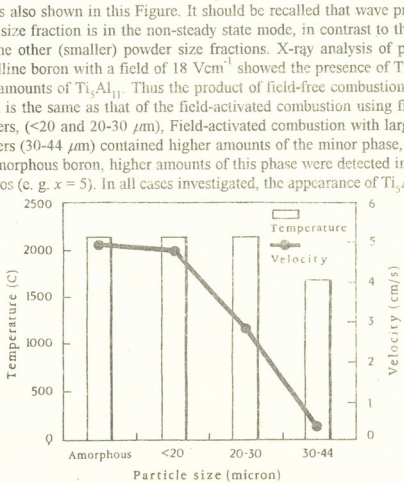

Fig. 2. The dependence of combustion temperature and wave velocity on the particle size range of the crystalline boron.

cant amounts in the product of combustion occurred in systems in which the wave propagated in a pulsating mode. As can be seen from Figures 1 and 2, cases in which non steady wave propagation occurred were associated with significantly lower combustion temperatures. These observations are consistent with recent work on the synthesis of Ti-Al intermetallics. It was shown that an increase in combustion temperature, as a result of field-activation, suppresses the formation of secondary phases for any given starting stoichiometry.

Georgian Academy of Sciences
F. Tavadze Institute of Metallurgy

University of California, Davis, USA

REFERENCES

1. *H. Xue, Z. A. Munir.* Met. Mater. Trans., **27**, 1995, 475.
2. *S. V. Gedevanishvili, Z. A. Munir.* Scripta Met. et Mater., **31**, 1994, 741.
3. *S. Gedevanishvili, Z. A. Munir.* J. Mater. Res., **10**, 1995, 2642.
4. *H. C. Yi, A. Varma, A. S. Rogachev, P. J. McGinn.* Indust. Eng. Chem. Res., **35**, 1996, 2982.
5. *D. A. Hoke, D. K. Kim, J. C. LaSalvia, M. A. Meyers.* J. Amer. Ceram. Soc., **79**, 1996, 177.
6. *W. Y. Yang, H. C. Yi, A. Petric.* Met. Mater. Trans., **26**, 1995, 3037.
7. *A. Feng, Z. A. Munir.* Metall. Mater. Trans., **26B**, 1995, 587.
8. *A. Feng, Z. A. Munir.* J. Appl. Phys., **76**, 1994, 1927.

საქართველოს მეცნიერებათა აკადემიის მოამბე, 159, №1, 1999
BULLETIN OF THE GEORGIAN ACADEMY OF SCIENCES, 159, №1, 1999

ELECTROCHEMISTRY

G.Agladze, V.Kveselava, L.Gotiashvili

Electrosynthesis of Lithium Permanganate and Study of its Physico-Chemical Properties

Presented by Corr. Member of the Academy J. Japaridze, February 3, 1998

ABSTRACT. **By anodic oxidation of metallic manganese and ferromanganese in saturated solution of lithium hydroxide the suspension has been produced. After filtration and drying it was treated by acetone for dissolution of lithium permanganate and its further separation.**

Key words: lithium permanganate, electrosynthesis, lithium hydroxide, lithium carbonate, treatment by aceton, X-ray investigation, thermogram.

By means of the various methods of analysis the 99.8% content of target product is identified. The X-ray parameters of lithium permanganate are established. By chemical and X-ray analysis it is determined, that an insoluble deposit obtained by electrolysis mainly consists of $MnO(OH)_2$ phase. The pyrolytic decomposition of $LiMnO_4 \cdot 3H_2O$ and $MnO(OH)_2$ has been studied at 1000^0C.

Nowadays the manganese-lithium compounds as a cathode material have become very perspective in rechargable cells. Therefore we have paid special attention to producing of lithium permanganate of high purity, to its identification by various physico-chemical methods, to the establishment of X-ray parameters and to the study of thermogravimetric pyrolysis.

Lithium permanganate can be obtained by electrochemical and chemical methods [1]. In the chemical method the interaction of lithium salts with the permanganates of other metals is used. But this method is of theoretical importance only, because producing of initial reagents ($AgMnO_4$, $Ba(MnO_4)$, $KMnO_4$) is a more difficult process requiring great energy consumption than that of the main product.

The electrochemical method of the lithium permanganate producing consists in the anodic dissolution of the manganese metal or ferromangenese in the saturated solution of the lithium hydroxide.

The electrolysis has been proceeded in the electrolyzer of 250 ml volume which was placed into water thermostat to maintain the constant temperature of the solution. The glass stirrer was used. The copper wire was used as a cathode. The optimal conditions of the electrolysis are: anodic current density of 5000-7000 $A \cdot m^{-2}$, cathodic current density of 125000$A \cdot m^{-2}$, the temperature of 40-55^{0}C, the current effeciency of manganese metal dissolution of 22.3%, and that of ferromanganese dissolution of 29%.

The suspension formed after electrolysis was filtered. In order to dissolve the crystals of lithium permanganate the deposit was treated by aceton and the received mass filtered again by the vacuum. Both filtrates were evaporated in the vacuum and then dissolved in

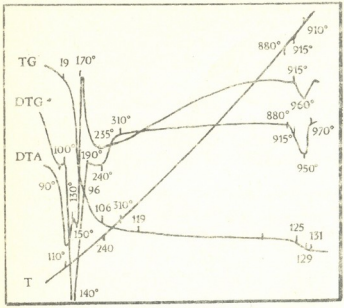

Fig.1. Thermogram of the lithium permanganate sample

the aceton again, then separated to liquid and solid phases. Solid components as $LiOH$ and partly Li_2CO_3 were dissolved in water and returned to the new cycle of electrolysis. Dark brown precipitate obtained after electrolysis was investigated to determine its composition. The aceton solution of lithium permanganate was evaporated in vacuum and dried at a temperatures of 90-100°C.

On the basis of chemical and atomic-adsorptional analysis of the sample it has been established that it consists of 99.8% of $LiMnO_4.3H_2O$.

The X-ray investigation using 'DRON-3M' diffractometer by CuK_α-irradiation in monochromatic conditions has been carried out. The set of diffraction maxima and their intensity distribution show lithium permanganate to be isostructural of $LiClO_4.3H_2O$. The interplanar distances in lithium permanganate and its comparison with corresponding data of $LiClO_4.3H_2O$ are presented in Table 1.

Table 1.

Interplanar distances of $LiMnO_4.3H_2O$ and $LiClO_4.3H_2O$

line	$LiMnO_4.3H_2O$			$LiClO_4.3H_2O$(2)*		
N	I/I_0	hkl	d Å	I/I_0	hkl	d Å
1	28	101	4.195	100	101	4.23
2	100	110	3.867	74	110	3.86
3	8	200	3.353	6	200	3.344
4	40	201	2.852	89	201	2.85
5	10	0.02	2.728	27	002	2.726
6	25	210.102	2.534	32	210.102	2.528
7	-	-	-	17	211	2.29
8	8	300.112	2.241	1	300.112	2.228
9	-	-	-	3	202	2.113
10	-	-	-	1	301	2.062
11	8	220	1.938	6	220	1.930
12	8	310.212	1.850	10	310.212	1.854
13	7	103.311	1.759	-	-	-
14	-	-	-	1	302	1.725
15	10	400	1.662	3	400	1.672
16	5	401.203	1.603	-	-	-
17	10	311.213	1.473	-	-	-

*) American Society for Testing Materials.

By means of homology method one can assume, that $LiMnO_4.3H_2O$ crystal system is hexagonal and the parameters of the elementary cell are: a = b = 7.746Å and c = 5.455Å.

In Fig 1. the thermogram of $LiMnO_4.3H_2O$ is shown. The first endothermic effect at the temperature range 25-130^{0}C corresponds to removing of adsorptional water. The second endopeak obtained at 150^{0}C is due to the loss of three molecules of crystal water. Upon this effect the exothermic effect is superposed, which probably is caused by intracrystal processes. The endothermic effect caused by decomposition of the lithium permanganate is observed at 170^{0}C. The further heating up to 915^{0}C does not influence on the mass of sample.

Lithium permanganate thermal decomposition can be expressed by following possible reactions:

$$4LiMnO_4 \rightarrow 2Li_2MnO_3 + 2MnO_2 + 3O_2 \quad (1)$$

$$4LiMnO_2 \rightarrow 2Li_2MnO_3 + 2Mn_2O_3 + 3,5O_2 \quad (2)$$

$$6LiMnO_2 \rightarrow 3Li_2MnO_3 + Mn_3O_4 + 5,5O_2 \quad (3)$$

On the basis of thermogravimetric calculations one can conclude, that the process proceeds according to the reaction 2, as in the case of reaction 1 in the range of 560-600^{0}C the Mn_2O_3 phase was to be formed, whereas in the case of reaction 3 at 950^{0}C the endopeak corresponded to $Mn_2O_3 \rightarrow Mn_3O_4$ transition would not take place

Table 2

Interplanar distances of the deposits produced by electrolysis

Deposits washed by water		Deposits washed and heated at 260^{0}C	
I/I_0	d, A	I/I_0	d, A
-	-	4	6.81
2	0.56	5	6.49
-	-	5	5.70
-	-	5	5.60
-	-	2	5.21
-	-	3	5.06
3	4.86	3	4.80
3	4.55	3	4.56
3	4.30	2	4.25
-	-	3	4.14
2	3.87	2	3.87
3	3.71	2	3.75
2	2.93	2	3.07
-	-	2	2.86
-	-	1	2.80
2	2.62	-	-
2	2.42	-	-
-	-	2	2.28
3	2.18	1	2.19
-	-	1	2.15
-	-	2	2.10

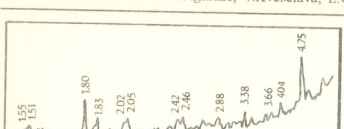

Fig. 2. The diffractogram of $LiMnO_4.3H_2O$ heated at 1000°C.

Fig. 2 represents the diffractogram of $LiMnO_4$ heated at 1000°C during 15 min. The comparison of diffraction peaks of the heated sample and their intensities distribution to theoretical data A3 shows, that the X-ray pattern corresponds to badly crystallized form of Li_2MnO_3.

X-ray investigation data of the deposits produced by electrolysis are given in Table 2.

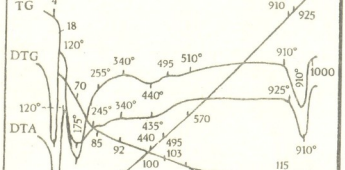

Fig. 3. Thermogram of the deposit formed after electrolysis of $LiMnO_4.3H_2O$

The Debye power patterns of the both samples are not clearly expressed, but on the basis of chemical analysis they can be reffered to $MnO(OH)_2$.

The results of pyrolysis for deposit washed and then dried on air are given in Fig.3. The first endothermic effect at 25-120°C is undoubtedly due to water desorption. The second endoeffect must be caused by the loss of water firmly bonded to the crystal lattice. According to the DGT curve the loss of weight in the temperature range of 120-495°C is equal to 17.6%. This value is near the expected total water removal and to the $MnO(OH)_2$ conversion into MnO_2 (the theoretical diminish of weight equals 17.1%).

Georgian Academy of Sciences
R. Agladze Institute of Inorganic
Chemistry and Electrochemistry

REFERENCES

1. *G. Agladze, I. Berikashvili.* Bull. Acad. of Sci. of Georgia, **16**, N9, 1953, 533; **23**, N1, 1959, 41-48.

საქართველოს მეცნიერებათა აკადემიის მოამბე, 159, №1, 1999
BULLETIN OF THE GEORGIAN ACADEMY OF SCIENCES, 159, №1, 1999

CHEMICAL TECHNOLOGY

V. Gaprindashvili, L. Bagaturia, R. Chagelishvili, L. Gogichadze

Joint Chemical Processing of Pyrite and Manganese Oxidized Concentrates

Presented by Corr. Member of the Academy L. Japaridze, February 2, 1998.

ABSTRACT. **In this paper it is suggested to use the process of the mixture mechano-chemical activation for receiving the main components (Mn, Fe) from pyrite and manganese concentrates. The process excludes the usage of high temperatures and concentrated acids and ensures the possibility of obtaining the manganese and iron sulphates with high rates (Fe – 80% and Mn – 90%) from the initial raw material.**

Key words: mechano-chemical activation, pyrite and manganese oxidized concentrates.

For enriching of manganese oxidized ores and consequent getting of manganese purposeful compounds some methods of chemical enrichment are suggested in technical literature [1]. In this direction in recent years the attention is sharpened on the problem of manganese oxidized ores and pyrites joint processing [2]. The proposed processes are mainly fulfilled at relatively high temperatures (400-600°C) and by usage of concentrated acids in the presence of a reducer the high index of manganese extraction is achieved. As regards the main constituent of pyrite the iron - its extraction is not realized and it remains in the processing wastes. This kind of processing considerably complicates the possibility of extraction of those noble metals from pyrite by traditional methods. In the present work the results of the investigation of oxidized manganese and pyrite concentrate joint mixture hydrometallurgic processing are presented.

The proposed process excludes the necessity for the usage of high temperatures and concentrated acids and guarantees the possibility of extraction of the main components (Mn, Fe) from initial raw material in the form of sulphates. The latter is attained by mechanochemical activation of the mixture (pyrite and manganese oxidized concentrate) on the first stage of its processing. In investigations the pyrite concentrate: Fe - 38.3% and S - 41.7% and manganese oxidized concentrate: Mn_{gen} – 32.5%, MnO_2 - 29.8% were examined: the rest of the manganese was presented by manganese carbonate. The mechanochemical activation of the initial raw material was made by vibrogrinding down to 0.052 mm.

In the proposed process in order to detect the influence of the mechanochemical activation the experimental investigation was performed on nonactivated and activated samples. The samples were treated with water as well as with sulphuric acid 5-10% solution.

In the process of the mechanochemical activation the increase of the examined mixture's specific area takes place, which leads to the activity of the substances in the

process of the subsequent processing.

It looks like that during the mechanochemical activation the sharp, impulsive increase of the temperature happens (up to 1000°C and more) in the touching points of the mixture components. The temperature does not spread through the entire mass of the mixture, because the spontaneous drop of the temperature takes place [3]. In such conditions the demolition of the substance crystal lattice is expected and the free energy increases, which is realized by phase and topochemical reactions.

Taking into account aforesaid, in the process of the mixture mechanochemical activation, dissociation of the pyrite into the free sulphur and pyrotine is expected [4]:

$$FeS_2 \rightarrow FeS + S,$$

which is proved by the results of performed experimental study. In particular, in the remainings of the activated mixture sulphuric acid leaching elementary sulphur in the amount of 5-6% is presented.

At high local temperature conditions it is reasonable to expect onset of the reaction between the sulphur and manganese dioxide:

$$MnO_2 + S + O_2 \rightarrow MnSO_4. \quad (2)$$

As soon as the process (2) takes place in micropoints, where high temperature is localized, the outcome of the reaction is low and according to the rate of the mixture grinding the production of sulphates does not exceed 1.2-6.2%.

The role of mechano-chemical activation for the examined complex mixture processing conditions is clearly represented by the results presented in the Figure.

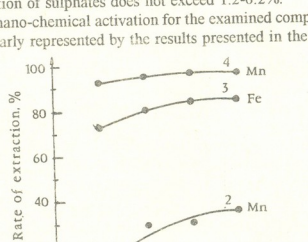

Fig. The dependence of the rate of Fe and Mn outcome on the concentration of the acid: curves 1 and 2: without vibrogrinding; curves 3 and 4: with vibrogrindig.

When the mixture is not activated by mechanochemical methods, during its leaching by sulphuric acid, iron does not pass to the solution (curve 1), while the rate of the manganese passing is relatively low (curve 2) and corresponds to the amount of the manganese, presented in the mixture. As it was expected, pyrite and manganese dioxide from nonactivated mixture do not dissolve in the sulphuric acid. The rate of the iron and

manganese outcome from mechanochemically activated mixture is high (curves 3 and 4) and exceeds 90% and 80%, respectively.

Above presented reaction (1) indicates that in the process of sulphuric acid leaching pyrotine and manganese dioxide participate. The process may be described by the following reaction equation:

$$FeS + MnO_2 + 2H_2SO_4 \rightarrow FeSO_4 + MnSO_4 + S + 2H_2O \quad (3)$$

The analogous idea is argued by the American scientists for the examination of the stein's processing [5].

The solutions obtained in result of the leaching are suitable for obtaining of the iron and manganese compounds.

Georgian Academy of Sciences
R.Agladze Institute of Inorganic
Chemistry and Electrochemistry

REFERENCES

1. *Ya. Klimenko, A. Kvasko.* Khimicheskoye obogashcheniye margantsevich rud. M., 1943 (Russian).
2. *A. V. Tsereteli, V. N. Goprindashvili, I. G. Berikashvili, I. G. Zedgenidze.* Manganese, **1**, 18, 1969 (Russian).
3. *E. E. Avvakumov, V. V. Boldirev.* Uspekhi Khimii, **40**, 10, 1971, 18-35 (Russian).
4. *E. E. Avvakumov, O. L. Samarin, V. G. Kulebakin.* Isv. SO AN SSSR, ser. khim 7, 1981, 29-35 (Russian).
5. *Richard G. Sandberg, Terry L. Heble, Danton L. Paulson.* Rep. Invest. Bur. Mines U.S. Dep. Inter. 8371, 1979, 11.

საქართველოს მეცნიერებათა აკადემიის მოამბე, 159, №1, 1999
BULLETIN OF THE GEORGIAN ACADEMY OF SCIENCES, 159, №1, 1999

CHEMICAL TECHNOLOGY

E.Buadze

Study of Bentonites Application Possibility in Boiling of Fabrics from Natural Silk

Presented by Corr. Member of the Academy L.Khananashvili, November 9, 1998

ABSTRACT. **The action of bentonite application in boiling process is studied. The dependence of sericin transition into solution on the concentration of boiling solution temperature, pH, and duration of treatment was researched.**

Key words: bentonite, sericine, boiling, fabric.

The techniques of silk degumming used at present are based on sericin ability to solve in water, acid solutions and alkali. As it is known from literature data [1,2], alkaline reaction at pH=9.0 and acid reaction at pH=2.5 are considered to be optimal for the rapid removal of sericin from the fiber. Reactive concentration and time of boiling process affect silk degumming.

In the present work, we have studied the dependence of fabric weight loss on the above mentioned indices. To study the action of bentonite concentration in boiling solution on fabric weight loss i.e. on the amount of removed sericine we took concentrations of 2% and more (Fig.1). The fabric was treated for 30 min at 100°C and bath modulus was 1:40. The results of investigation testify that along with the increase of bentonite concentration (curve 2) from 2% to 5-6% the loss of weight makes correspondingly 9% and 13-13.2%. The same Fig. illustrates the curves of dependence of mass loss on the boiling time. The curve 3 shows the maximum amount of sericine (18%) which transmits into solution under 60 min boiling, 100°C, bath modulus (M) 40 and concentration 5%. As it is seen, by changing of curve 2 trajectory over 6% concentration of bentonite the transition of sericine into solution delay and fabric weight starts to increase. It is explained by the fact, that boiling solution becomes more dense, viscous. It doesn't promote washing off the fabric, on the contrary, bentonite itself starts to precipitate on the fabric increasing its weight. On the one hand, this process is positive before definite limit because along with the increasing in weight, the sorption properties of the fabric increase, which gets heavy and takes beautiful and soft grif [3,4]. But the boiling process in thickened solution becomes difficult. Therefore the limit of bentonite concentration appears to be 5-6%.

Sericine is known to possess amphoteric properties with prevalence of acidic properties. Therefore, while boiling in alkaline solution of insufficient buffer capacity the binding of alkali with sericine at the beginning of the process can rapidly decrease pH in the bath causing the delay of degumming. The bath is to be frequently replenished which causes productivity decrease and the process becomes labour- consuming.

The bentonite, we have used, is alkaline variety the exchange ions of which reenter in reaction with acidic groups of sericine very actively which causes the decrease of pH

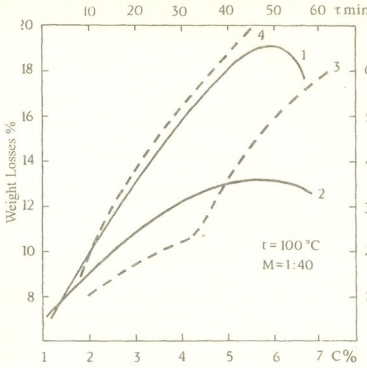

Fig.1. Dependence of weight loss on bentonite concentration and boiling time
(1) bentonite and 1% of sodium — Dependence curves
(2) pure bentonite — on concentration
(3)pure bentonite — Dependence curves
(4)bentonite and 1% of sodium — on duration

in the bath. Therefore, the question about buffering of solution was put forward. For this hicarbonate-carbonate mixture (further sodium carbonate) of 1% concentration was used. This allows to reduce bentonite expense a little and as it is shown in Fig. 1. (curve 1), sericine amount going into solution suddenly increases. Curve 4 illustrates weight loss depending on duration of treatment.

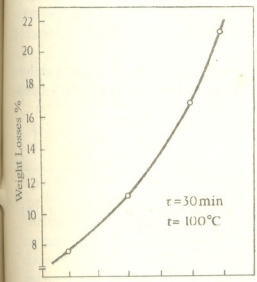

Fig.2. The action of pH solution on sericine removing rate.

On changing pH in boiling solution (8-10.5) it was established that increasing the pH of medium the weight loss increases correspondingly from 6% to 22% (Fig.2).

The temperature also greatly affects silk degumming (Fig.3). The treatment was conducted during 60 min at M=40. Within the temperature range up 75°C at 60 min treatment by soap solutions (pH=12) and sodium bisulfite solution (pH=11) the curves 1 and 3, the small portion of sericine is removed. While treating by bentonite-sodium solution (curve 2) the removed portion of sericine is more

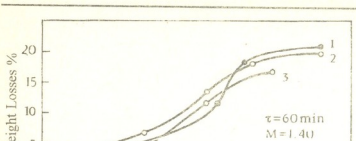

Fig.3. Curves dependence of sericine solubility on temperature
(1) soap solution (pH=12);
(2) bentonite-sodium solution (pH=11);
(3) sodium-bisulfite solution (pH=11).

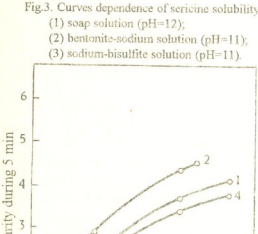

Fig.4. Curves of boiling efficiency
(1) soapy solution;
(2) bentonite-sodium solution;
(3) sodium bisulfite solution;
(4) pure bentonite solution.

than that of the first two cases. At temperature increasing over 75°C the loss of the silk weight increases and at 92-93°C while treating in soap and bentonite-sodium solutions (curve 1 and 2) the silk is completely degumming.

We determine the efficiency of silk fabric boiling according to capillarity (Fig.4). This index was determined by curves of capillarity dependence on duration of boiling at M=40, t=100°C, C=5%.

As it is seen from the Figure the fabric capillarity boiling in soap solution (curve 1) for 27 min equalled 4.2 cm, the fabric boiled in pure bentonite solution (curve 4) 3.7 cm, the fabric treated in sodium-bisulfite solution (curve 3) has 2.5 cm, and in solution of bentonite-sodium (curve 2) the capillarity reached 4.5 cm.

We conclude that natural bentonites characterized by soapy properties giving to the fabrics required whiteness and increased sorption activity can be used for boiling the silk fabrics.

Kutaisi N. Muskhelisvili
Technical University

REFERENCES

1. *G.E.Krichevski, M.V.Korchagin, A.V.Senikhov.* Khimicheskaya tekhnologiya tekstilnykh materialov. M., 1985.
2. *G.E.Kricherski et al.* Metody issledovaniya v tekstilnoi khimii. M., 1993 (Russian).
3. *E.Buadze.* Candidate thesis. M., 1983.
4. *E.Buadze.* Avtorskoe svidetelstvo SSSR, N1348392, 1987.

საქართველოს მეცნიერებათა აკადემიის მოამბე, 159, №1, 1999
BULLETIN OF THE GEORGIAN ACADEMY OF SCIENCES, 159, №1, 1999

GEOLOGY

T.Shengelia

To the Petrology of Volcanogenic Formations of North-Eastern Slope of Akhaltsikhe-Imereti (Meskheti) Ridge

Presented by Member of the Academy N.Skhirtladze, July 22, 1998

ABSTRACT. **Middle Eocene volcanic slopes of north-east part of Akhaltsikhe-Imereti ridge are researched. Mineralogic paragenesises of rocks and petrochemical peculiarities indicate that as a result of magma differentiation the formation of two formative series occurred: dominating (olivian basalt trachybasalt-trachyte) and subordinate (basalt-andesite-dellenite).**

Key words: volcanosedimentary formations.

The studied part of northern slope of Akhaltsikhe-Imereti ridge is situated on the left bank of the river Chkherimela (Tsablaristskali-Zvarula interfluve (Fig.1)). Petrographic and volcanogenic data about this territory as well as its neighboring region are given in [1-4]. The territory under investigation is mainly constructed from Middle Eocene volcanogenic formations, whose petrologic study is based on detailed petrographic research of rocks, analysis of mineralogical and petrochemical and normative compositions.

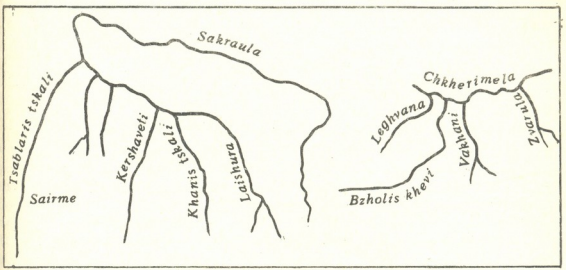

Fig. 1. Variational diagram of the Middle Eocene formations of Na_2O+K_2O/SiO_2 Akhaltsikhe - Imereti (Meskheti) Ridge

Within the researched territory the Middle Eocene volcanosedimentary formations are mainly constructed of basaltoids among which there are found olivian kalibasalts, olivian and nonolivian trachybasalts, as well as dellenites, trachytes, andesi-basalts and andesites. It should be noted that trachybasalts and dellenites are spread in western part

of the region (Tsablaraistskali-Sakraula interfluve), but andesi-basalts and andesites are mainly found in eastern part of the researched territory (Leghvana-Zvare interfluve).

From the viewpoint of chemism the studied rocks represent contrastly differentiated row of rocks in which the representatives with high alkalinity dominate (90%) although the small part (10%) comes on rocks with normal alkalinity (Fig.1). Rocks with normal alkalinity belong to alkali-lime series (Fig.2). In the western part of the studied area they are of $Na(K_2O/Na_2O - 0.08\text{-}0.24)$ order, although kalium $K(K_2O/Na_2O - 1.00\text{-}2.00)$ varieties are also found with rare exceptions. In the eastern part of the region the great majority of volcanic rocks are of K-Na $(K_2O/Na_2O - 0.03\text{-}0.95)$ order. Along with the change of alkaline ratio (K_2O/Na_2O) the content of K_2O in the rocks increases in the same direction which sometimes is in correlation with the tendency of increasing TiO_2 content. Basaltoid and subvolcanic bodies of sienite composition are connected spatially with the studied series which as a rule belong to $Na(K_2O/Na_2O - 0.10\text{-}0.23)$ order of normal alkalinity rocks.

As to the rocks with high alkalinity, both subalkaline and alkaline varieties are identified. At the same time unlike the rocks of alkali-calcic $(K_2O/Na_2O - 0.25\text{-}1.73)$ association in the western part of the studied area $K(K_2O/Na_2O - 0.99\text{-}5.78)$ vivid prevalence of antimony rocks over K-Na is distinctly observed, whereas in the eastern part rocks with K-Na series dominate. Together with the latter ones besides K, very seldom $Na(K_2O/Na_2O - 0.12\text{-}0.22)$ varieties are marked.

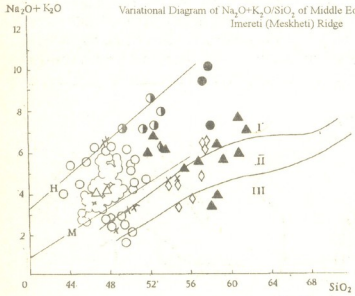

Fig. 2.

It is not excepted that here the role of K series rocks was far greater, but under the action of postvolcanic processes intensive evacuation of K_2O from the rocks took place, which is proved by vermiculite transplantation of this mineral in biotite rocks. As to trachytes they are of K order as a rule, but dellenites are of K-Na order. The mentioned petrochemical peculiarities and mineralogic paragenesises of rocks indicate that as a result of magma differentiation the formation of two formative series occurred; dominating – olivian basalt, trachybasalt – trachyte and subordinate – basalt–andesite–dellenite.

Norm composition of the studied slopes (calculations were done for dry system – CIPW) shows that they are constructed of both inert and rather mobile (K_2O and Na_2O) virtual components. Excess and separated components are found near them. Mineral paragenesises are represented by: Q; C; Or; Ab; An; Ne; Di; Hy; Ol; Hm; Il; Ap. In rocks of alkali series the origin of Q cause both Di, and Hy formation. When along with the increase of SiO_2 amount, the Al_2O_3 amount increases and correspondingly there appears C then Di disappears from norm constituent and only Hy is left. In case, when Q≤O, Ol appears, sometimes in K and K-Na series rocks there additionally appears Ne.

As to the alkali-calcic series of rocks, the quantitative increase of SiO_2 (when together with Q appears C) also cause Hy formation, but when its amount decreases and in norm composition we have only Q, then Di and Hy appear. The rocks of this series are not characterized by the lack of SiO_2 (Q>O).

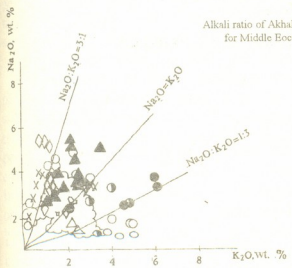

1. Gabbro-monzonite, quartz gabbro-monzonite, monzonite (intrusives) r. Tsablaristskali, Sakraula;
2. Busalts r. Tsablaristskali, -Zvarula;
3. Trachybasalts, Mt. Najikhura;
4. Trachytes r. Tsablaristskali;
5. Dellenites, r. Tsablaristsnali, Khanistskali;
6. Limburhites r. Tsablaristskali;
7. Trachyandesibasalts, r. Tsablaristskali;
8. Andesites, r.r. Kershaveti, Sakraula, Bjolis khevi, Zvarula.

Fig.3.

If we base on earlier works [4,5] about pyroxene crystallization in fused basalts and account thermodynamic conditions of pyroxenes formation [6] on the studied area and bring them into correlation with our norm composition we can suppose that the fused basalt whose differentiation occurred in the direction of traily basalts, trachytes, etc., is characterized by Ol; Cpx; Plag; Opx norm composition. We can suppose that magmatic centre was on the depth of ≈40-50 km, and during the motion of fusion to the surface on the depth of ≈20 km a part of fused basalt started fractionation and in its average composition normative quarts appeared.

As a result of this favourable conditions of T and P portion of fusion and further fractional melting varieties of alkali-calcic composition are formed.

Thus both alkali and alkali-calcic series of rocks must represent the result of melting crystallization of one basaltic composition.

So Middle Eocene volcanic rocks of north-east part of Akhaltsikhe-Imereti ridge mainly belong to the type of high and normal alkaline formation which is divided into representatives of alkali and alkali-calcic series. These last ones consist of K, Na and K-Na series of rocks and create: olivian basalt – trachybasalt–trachyte and basalt–andesite–dellenite associates. Norm

composition of rocks is represented by the following paragenesises: Q, C, Or, Ab, An, Ne, Di, Hy, Ol, Hm, Il, Ap which is characteristic of the initial basalt fusion which further was subjected to fractionation and in case of corresponding T-P conditions gave alkali-calcic series of rocks. Therefore the initial magma whose differentiation occured both in magmatic chamber and along the effluent channels gave diversity of rocks spread on the studied territory.

Caucasian Institute of Mineral Resources

REFERENCES

1. *G.Dzotsenidze*. Collective Works of Geological Institute. N1, 1948 (Russian).
2. *P.Lordkipanidze, G.Nadareishvili*. In: Voprosy geologii Gruzii. Tbilisi, 1964.
3. *G.Nadareishvili*. Candidate Thesis, Tbilisi, 1968 (Russian).
4. Problemy geologii Adjara-Trialeti. Tbilisi, 1974 (Russian).
5. *D.Kh.Grin, A.E.Ringwud et al*. Petrologiya verkhnei mantii. Moscow, 1968 (Russian).
6. *A.A.Makushev*. Petrologia, 1988 (Russian).
7. *T.Shengelia*. Bull. Georg. Acad. Sci. 158, 2, 1998.

საქართველოს მეცნიერებათა აკადემიის მოამბე, 159, №1, 1999
BULLETIN OF THE GEORGIAN ACADEMY OF SCIENCES, 159, №1, 1999

GEOLOGY

Member of the Academy I.Gamkrelidze, D.Shengelia

Petrogenetic Model of the Dzirula Crystalline Massif Magmatites in the Light of Tectonic Layering of the Earth's Crust

Presented October 13, 1998

ABSTRACT. **It is shown that the Earth's crust of the Dzirula crystalline massif is tectonically layered. The presence of such horizontal layering allows to consider genesis of Dzirula massif magmatites in the new light. In particular, it is supposed that the character of various magmatic rocks is stipulated by its formation in diverse conditions in different layers of the Earth's crust.**

Key words: tectonic layering of the earth's crust,genesis of magmatites.

At present one can hardly doubt that in SE part of Dzirula massif we have fragments of vertical-accretionary complex consisting of conglomeration of various terranes and subterranes, which were formed in absolutely different geodynamic conditions[1]. Such a tectonic layering comprise seemingly more deep horizons of Earth's crust. It is supposed[2,3] that in the depth the sialic basement, from which apparently the late Hercynian eutectic granitic magma is generated, is overlain by thick tectonic nappe of femic rocks. In our opinion the following data indicate in favour of such assumption: 1) wide development in Dzirula massif of intensive tectonized relics of metabasites which are analogues by composition to metabasites of ophiolites (fragments of the third and second layers of oceanic crust) [1] and to paleooceanic crust of mid-oceanic ridge type[4]) included in Chorchana-Utslevi accretionary allochthonous complex; 2) close spatial connection of pregranitic femic basement with Chorchana-Utslevi allochthonous complex (we suppose that the latter is overthrust along with pregranitic femic crystalline basement) 3) geophysical data, in particular materials of deep seismic sounding through the profile Gali-Rustavi [5]. Velocity profiles are constructed to the depth about 120 km. In upper part there is observed layer of 8-11 km thickness with velocity 4.9-5.2 km/sec that apparently corresponds to the rocks of sialic complex. Lower there is situated the second layer with considerably heightened velocity of P waves - 7.2-7.5 km/sec, the thickness of which changes from 0 in the east and in the west to 8 km in central part (width of spread of the layer makes about 40-50 km). It apparently consists mainly of basic rocks and, as mentioned above, is overthrust. Lower follows "inversion layer" with 12-14 km in thickness and with lower velocity - 5.4-5.6 km/sec presented seemingly by sialic rocks. The fourth layer is characterized by velocity - 7.3-7.6 km/sec and again corresponds to mafic rocks. The fifth layer with thickness 6-8 km and lowered velocity (6.6-6.9 km/sec) is situated directly above Moho discontinuity and apparently represent the so-called "crustal asthenolayer" (asthenolens).

It is noteworthy that this crustal asthenosphere, which also was named as "inversion layer," has been established in the Caucasus for the first time by the method of magnetotelluric sounding[6]. It is observed almost all over the Transcaucasus and has the

greatest thickness (15-20 km) within the Greater and Lesser Caucasus and Caspian sea. Along the surface of this layer most likely there is another plane of tectonic displacement (detachment fault).

Thus on the basis of the above mentioned data we consider that Earth's crust of the Dzirula massif is tectonically layered.

The presence of such layering allows us to consider the formation mechanism of magmatic rocks of the Dzirula massif in a new fashion.

At present in Dzirula crystalline massif one can distinguish granitoids of three groups: Precambrian quartz-dioritic gneisses , Early Hercynian massive quartz-diorites and Late Hercynian K-feldspathic granites[7].

Quartz-dioritic gneisses and massive quartz diorites we consider as formations strictly separated in time[7].

As a result of pre-Hercynian (Early Ordovician) regional metamorphism, initial rocks of quartz-dioritic gneisses and metabasites of second generation, apart from foliation, experienced neomineralization and metamorphic differentiation.

We think that the rocks of pre-granitic crystalline basement of the Dzirula massif present oceanic formations of gabbro-diorite-quartz-dioritic complex with the fragments of regionally metamorphosed sedimentary and volcanogenic-sedimentary rocks, whereas Late Hercynian magmatic homogeneous granites of eutectic composition and also porphyraceous granitoids of Rkvia intrusion are typical products of sialic crust's selective fusion.

Resulting from the genetic studies of old granitoids of the Dzirula crystallyne massif and the petrochemical data[2,3] indicate that quartz-dioritic gneisses belong to I type granitoids and anatectic microcline granites - to S type. K.Chikhelidze[8]also distinguished genetically independent gabbro-quartz-dioritic and Late Hercynian granitic series. She has shown that on petrogenic elements and distribution character of rare-earth elements the rocks of the first series are identical with the rocks of mantle genesis and the granitic series – with the rocks of continental crust. Besides, K.Chikhelidze has stated peculiar associations and quantitative ratio of accessori minerals in the rocks of above mentioned magmatic series. It should be noted that many rocks samples of gabbro-diorite-quartz-dioritic series contain chemically highly stable xenogenous mineral – moissanite occuring mainly in the rocks of mantle origin.

Precambrian quartz-dioritic gneisses can be considered as generated in ensimatic immature island arc during the process of subduction in intraoceanic conditions without participation of continental material.

Massive quartz diorites represent the products of secondary fusion of mafic oceanic crust rocks (metabasites,amphibolites)and also partially of quartz-dioritic gneisses. They correspond to the granitoids of I type or to the mantle-crustal Subduction type after V.Khain[9].

Accepted before, especially in the works of last decade the idea about the Earth's crust structure in the Dzirula crystalline massive area doesn't allow to prove petrologically the genesis of magmatic eutectic granites rich in potassium which have saturated huge masses of non-sialic rocks.According to the up to now accepted scheme of geological structure of Dzirula crystalline massif it should be supposed that these eutectic and porphyraceous K-

feldspathic granites were formed by means of selective fusion of potassium-free rocks of gabbro-quartz-dioritic series or more deep-seated basic and ultrabasic rocks of the oceanic crust what is hardly probable. Vague remained the question of genesis of potassium felspatic gabbro as well.

Late Hercynian microcline granites of Dzirula massif in terms of geodynamic conditions of granitoid formation concern to the island arc group and of magma source after V.Khain[9] – to the crustal-anatectic. We suppose that microcline granites of Dzirula massive can be formed without participation of mantle heat and material. Source of heat is transition to the heat energy of mechanical energy of tectonic deformations. The fact is that tectonic layering of Earth's crust accompanied by the increase of heat flow, anatexis and metamorphism of rocks participating in its structure. Certain part in introduction of heat can play a radioactivity of continental crust.

Pregranitic allochtone of femic rocks, reaching in thickness several kilometres, established high PT gradient in sialic basement. Thickening of the Earh's crust(its tectonic doubling) stimulated a process of selected fusion of constituting rocks(Fig.1).

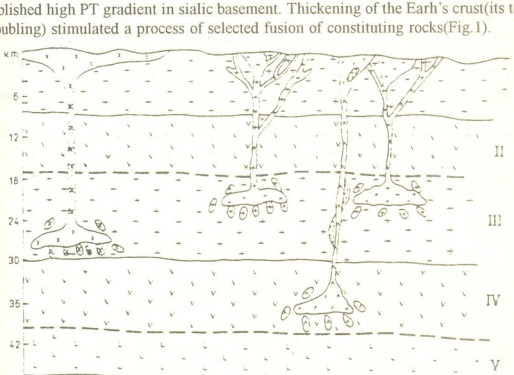

Fig. The structure of the Earth's crust after deep seismic sounding data and principle scheme of formation of Dzirula massif magmatic rocks.
1-sialic layers, 2-mafic layers, 3-" crustal asthenosphere ", 4-upper mantle, 5-Rkvia intrusion, 6-microcline granites, 7- K-feldspathic gabbros ("ricotites"), 8-quartz-feldspathic anatexite, 9-planes of tectonic displacement (detachment faults).

Some ivestigators consider the Rkvia intrusion granites to be of hypabyssal or mesoabyssal origin. R.Manvelidze's data[10] show a great depth of formation of the Rkvia intrusion magma. It seems to us that in sialic basement (in the third" inversion layer") at

different depth initial magmas of Late Hercynian equigranular eutectic and porphyraceous (Rkvia type) K-feldspathic granites were generated. Latters were of more high-temperature than the equigranular granites and formed in most deep parts of "inversion layer" (Fig. 1) separately from the area of generation of eutectic granitic magma. Formation of microcline granites took place after overthrusting of mafic layer[1].

In the new light the problem of formation of potassium feldspathic gabbros("ricotites") should be considered as well.

It has been supposed that initial magma of K-feldspathic gabbro was basic magma, crystallization products of which are presented by pyroxene gabbro. This magma was generated at the depth more than 30 km, according to our scheme in fourth mafic layer of deep section of Dzirula massif Earth' crust (see Fig.1). Newly formed high-temperature and superheated dry magma,with phenocrystalls of basic plagioclase and clinopyroxene, penetrates in the third "inversion" - sialic layer. From this new medium it adopts volatile components, promoting selective fusion of leucocratic material of quartz-feldspathic composition and simultaneously in basic magma - intensive development of hornblende by pyroxene. Basic magma mixed with newly formed acidic magma or remained partially unmixed. Granitic and partially crystallized basic magma intruded from the first into allochthonous basic (second) layer without undergoing considerable alterations and then - into the first (sialic) layer, where hardened at the depth about 7-10 km. Newly formed in "inversion" sialic layer leucocratic granitic magma belongs to S type but its mixing with initial basic magma allows to include products of its crystallization in special hybrid type of granites - H, proposed by Spanish scientists [11]. On the final stage of magmatic process basic rocks (gabbros)became saturated with feldspathic material and form anorthoclase or high orthoclase.

REFERENCES

1. *I.Gamkrelidze,G.Dumbadze, et al.* Geotectonica,5,198123-33 (Russian).
2. *A.V.Okrostsvaridze,D.M.Shengelia.* Bull. Georg. Acad. Sci., **154**, 1, 1996, 93-95 (Russian).
3. *D.M.Shengelia,A.V.Okrostsvaridze.* Dokl.RAN,1998.
4. *G.S.Zakariadze,SH.A.Adamia,K.K.Kolchèva et al.* Petrologia,1,1993,50-87(Russian).
5. *M.S.Ioseliani,V.K.Chichinadze,Sh.Diasamidze et al.* Structure of lithosphere of the territory of Georgia according to seismic data, Tbilisi,1989,150 (Russian).
6. *G.E.Gugunava.* Doctor thesis. Baku,1988,47 (Russian).
7. *I.Gamkrelidze, D.Shengelia.* Bull. Georg. Acad. Sci., 158, 1, 1998.
8. *K.S.Chikhelidze.* Candidate thesis. Tbilisi,1997,25 (Russian).
9. *V.E.Khain.* Main problems of modern geology (geology on the threshold of XX1 century. Moscow, 1995, 188 (Russian).
10. *R.M.Manvelidze.* Geologic-petrographical significance of K-feldspars of Georgian granitoids. Tbilisi, 1983, 124 (Russian).
11. *A.Castro, J.Moreno-Ventas, T.D.De La Ros.* Earth Scienc., Rev. .31, 1991,237-253.

საქართველოს მეცნიერებათა აკადემიის მოამბე, 159, №1, 1999
BULLETIN OF THE GEORGIAN ACADEMY OF SCIENCES, 159, №1, 1999

V. Mdzinarishvili

The New System of the Orthonormal Functions

Presented by Member of the Academy V.Chichinadze, March 4, 1998

ABSTRACT. **The new system of the orthonormal functions is received. The illustrative example is given. Stochastical nature of the received system is noted**

Key Words: Orthonormal, orthogonal, stochastic.

Let's consider a sequence of functions $f_1(t)$, $f_2(t)$, $f_3(t)$ and $f_4(t)$ shown in Figs 1-4. Laplace transform of this functions is:

$$F_1(s)=\frac{1-e^{-\tau s}}{\tau s},\ F_2(s)=\frac{(1-e^{-\tau s})^2}{\tau^2 s},\ F_3(s)=\frac{(1-e^{-\tau s})^3}{\tau^3 s}\ \text{and}\ F_4(s)=\frac{(1-e^{-\tau s})^4}{\tau^4 s};$$

where $s=\sigma+j\omega$, and $j=\sqrt{-1}$.

For function $f_n(t)$ Laplace transform is: $F_2(s)=\dfrac{(1-e^{-\tau s})^n}{\tau^n s}$.

Orthogonal conditions for functions $f_1(t)$, $f_2(t)$, ..., $f_n(t)$ are:

$$\int_0^\infty f_n(t)f_m(t)d\mu=\delta_{nm}=\begin{cases}1 & n=m\\ 0 & n\neq m\end{cases}, \tag{1}$$

where $d\mu$-Lebesgue measure.

Using Parseval's theorem to estimate expression (1):

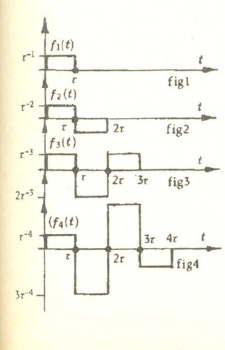

$$\int_0^\infty f_n(t)f_m(t)d\mu=\frac{1}{2\pi j}\int_{c-j\infty}^{c+j\infty}F_n(-s)F_m(s)ds \tag{2}$$

Consider behavior of integral (2) for

$$I_{nm}=\frac{2^{2n}}{2\pi j\tau^{2n}}\int_{c-j\infty}^{c+j\infty}\frac{sh^{2n}\left(\frac{\tau s}{2}\right)}{-s^2}ds, \tag{3}$$

where $n=\{2^k\}$, $k=0, 1, 2, 3, \ldots$

With change of $s=jw$ for the functional (3) we transform into frequency area. Bromvich integrated area is transformed into infinite interval:

$$I_{nn}=\frac{2^{2n}}{2\pi\tau^{2n}}\int_{-\infty}^{\infty}\frac{\sin^{2n}\left(\frac{\tau s}{2}\right)}{\omega^2}d\omega. \tag{4}$$

In (1) functions f_{2k} (k = 0, 1, 2, 3, ...) possess orthonormal property. With even underintegral expressions (4) we determine the meaning of the integral for n = 1:

$$I_{11} = \frac{2^2}{2\pi\tau^2} \cdot 2 \frac{\tau}{2} \frac{\pi}{2} = \frac{1}{\tau}.$$

For n orthonormal function, we have:

$$I_{nn} = \frac{2^{2n}}{2\pi\tau^{2n}} \cdot 2 \frac{1\cdot 3\cdot 5(2n-3)}{2\cdot 4\cdot 6(2n-2)} \cdot \frac{\tau}{2} \cdot \frac{\pi}{2}; \quad I^*_{nn} = \frac{1}{n} I_{nn} = \frac{1\cdot 3\cdot 5\ldots(2n-3)}{2\cdot 4\cdot 6\ldots(2n-2)} \cdot \frac{2^{2(n-1)}}{n\tau^{2n-1}}, \qquad n=2,4,8,\ldots$$

Functions $f_i(t)$ $\{i = 2^k\}(k = 0, 1, 2, 3, ...)$ are orthogonal, but are not orthonormals. Normalized multiplier a_n for n orthonormal system is determined from these relations $a_n^2 I^*_{nn} = 1$.

The system of n orthonormal functions is: (t = 1)

$$M_1(t) = 1(t) \qquad t \in [0,1]$$

$$M_2(t) = \begin{cases} 1 & t \in [0,1/2] \\ -1 & t \in (0,1/2] \end{cases}$$

$$M_4(t) = \sqrt{2} \begin{cases} 3^{-\frac{1}{2}} & t \in [0,1/4) \\ -1 & t \in (1/4,1/2) \\ 1 & t \in (1/2,3/4) \\ -(3)^{-\frac{1}{2}} & t \in (3/4,1] \end{cases}$$

$$M_n(t) = \left(\frac{n}{2}\right)^{\frac{1}{2}} \begin{cases} (n-1)^{-\frac{1}{2}} & t \in [0,1/n) \\ -(n-3)^{-\frac{1}{2}} & t \in (1/n,2/n) \\ \cdots & \cdots \\ -1 & t \in (1/2-1/n,1/2) \\ 1 & t \in (1/2,1/2+1/n) \\ \cdots & \cdots \\ (n-3)^{-\frac{1}{2}} & t \in ((n-2)/n,(n-1)/n) \\ -(n-1)^{-\frac{1}{2}} & t \in ((n-1)/n,1) \end{cases} \qquad (5)$$

n=2, 4, 8, ...

Orthonormal system (5) is full in L^2, that is if function $\varphi(\tau) \in L^2$, then:

$$\lim_{n\to\infty} \int_0^1 \left[\varphi(t) - \sum_{i=1}^{n} (\varphi, M_i) M_i(t) \right]^2 d\mu \to 0$$

and, consequently, possess this property, that with probability one by Lebesgue measure

has the following relation: $\lim_{n\to\infty} \sum_{i=1}^{n} (\varphi, M_i) M_i(t) \to \varphi(t)$,

where $(\bullet,\bullet)$ - symbol of scaler multiplier.

Example. *The function* $\varphi(t) = t$, $t \in [0, 1]$ *is given.*

It is necessary to represent it with the orthonormal system (5).

The function $\varphi(t)$ is decomposition by the series:

$$\varphi(t) = (C_i M_i) = C_1 M_1 + C_2 M_2 + \ldots + C^T{}_n M_n + \ldots \qquad (6)$$

where $C_n = \int M_n(t)\varphi(t)dt$.

Let's calculate coefficient C_i and find multipliers

$$C_1 = \int_0^1 M_1(t)tdt = \int_0^1 tdt = \frac{1}{2}; \quad \varphi_1 = C_1 M_1 = \frac{1}{2}\cdot 1 = \frac{1}{2}.$$

Now let's draw our attention to colculation of coefficient C_2.

$$C_2 = C_{21} + C_{22}; \quad C_{21} = \int_0^{\frac{1}{2}} M_{21}(t)tdt = \int_0^{\frac{1}{2}} tdt = \frac{1}{2}t^2\Big|_0^{\frac{1}{2}} = \frac{1}{8}, \quad t \in \left[0, \frac{1}{2}\right);$$

$$C_{22} = \int_{\frac{1}{2}}^1 M_{22}(t)tdt = \int_{\frac{1}{2}}^1 (-1)tdt = -\frac{1}{2}t^2\Big|_{\frac{1}{2}}^1 = -\frac{3}{8}, \quad t \in \left(\frac{1}{2}, 1\right]; \quad C_2 = \frac{1}{8} - \frac{3}{8} = -\frac{1}{4}.$$

By this function $\varphi_2(t)$ is: $\varphi_2 = C_2 M_2 = -\frac{1}{4}\begin{cases}1\\-1\end{cases} = \begin{cases} -\frac{1}{4} & t \in \left[0, \frac{1}{2}\right) \\ \frac{1}{4} & t \in \left(\frac{1}{2}, 1\right] \end{cases}$

with (6) we find two first members of polynoms:

$$\varphi_1 + \varphi_2 = \frac{1}{2}[0,1] + \begin{cases} -\frac{1}{4} & t \in \left[0, \frac{1}{2}\right) \\ \frac{1}{4} & t \in \left(\frac{1}{2}, 1\right] \end{cases} = \begin{cases} \frac{1}{4} & t \in \left[0, \frac{1}{2}\right) \\ \frac{3}{4} & t \in \left(\frac{1}{2}, 1\right] \end{cases}$$

We find the value of coefficient C_4. Corresponding vector-line is $C_4 = |C_{4134}\ C_{1223}|$, where: $C_{4134} = C_{41} + C_{34}$, $C_{1223} = C_{12} + C_{23}$.

$$C_{41} = \int_0^{\frac{1}{4}} M_{41}(t)tdt = \frac{\sqrt{2}}{\sqrt{3}} \int_0^{\frac{1}{4}} tdt = \frac{\sqrt{2}}{2\sqrt{3}} t^2 \Big|_0^{\frac{1}{4}} = \frac{\sqrt{2}}{32\sqrt{3}}, \quad t \in \left[0, \frac{1}{4}\right),$$

$$C_{34} = \int_{\frac{3}{4}}^{1} M_{34}(t)tdt = -\frac{\sqrt{2}}{\sqrt{3}} \int_{\frac{3}{4}}^{1} tdt = -\frac{\sqrt{2}}{2\sqrt{3}} t^2 \Big|_{\frac{3}{4}}^{1} = -\frac{7\sqrt{2}}{32\sqrt{3}}, \quad t \in \left(\frac{3}{4}, 1\right],$$

$$C_{12} = \int_{\frac{1}{4}}^{\frac{1}{2}} M_{12}(t)tdt = \sqrt{2} \int_{\frac{1}{4}}^{\frac{1}{2}} tdt = \frac{\sqrt{2}}{2} t^2 \Big|_{\frac{1}{4}}^{\frac{1}{2}} = \frac{3\sqrt{2}}{32}, \quad t \in \left(\frac{1}{4}, \frac{1}{2}\right),$$

$$C_{23} = \int_{\frac{1}{2}}^{\frac{3}{4}} M_{23}(t)tdt = -\sqrt{2} \int_{\frac{1}{2}}^{\frac{3}{4}} tdt = -\frac{\sqrt{2}}{2} t^2 \Big|_{\frac{1}{2}}^{\frac{3}{4}} = -\frac{5\sqrt{2}}{32}, \quad t \in \left(\frac{1}{2}, \frac{3}{4}\right),$$

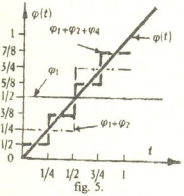

fig. 5.

$$C_{4134} = \frac{\sqrt{2}}{32\sqrt{3}} - \frac{7\sqrt{2}}{32\sqrt{3}} = -\frac{3\sqrt{2}}{16\sqrt{3}},$$

$$C_{1223} = \frac{3\sqrt{2}}{32} - \frac{5\sqrt{2}}{32} = -\frac{\sqrt{2}}{16}.$$

Now the value of function φ_4 may be determined:

$$\varphi'_4 = C_{4134} \cdot M_{41342} = \left(-\frac{3\sqrt{2}}{16\sqrt{3}}\right) \cdot \frac{\sqrt{2}}{\sqrt{3}} \begin{cases} 1 \\ -1 \end{cases} = \begin{cases} -\frac{1}{8} & t \in \left[0, \frac{1}{4}\right) \\ \frac{1}{8} & t \in \left(\frac{3}{4}, 1\right] \end{cases};$$

$$\varphi''_4 = C_{1223} \cdot M_{1223} = \left(-\frac{\sqrt{2}}{16}\right) \cdot \sqrt{2} \begin{cases} -1 \\ 1 \end{cases} = \begin{cases} \frac{1}{8} & t \in \left[\frac{1}{4}, \frac{1}{2}\right) \\ -\frac{1}{8} & t \in \left(\frac{1}{2}, \frac{3}{4}\right] \end{cases};$$

$$\varphi_4 = \varphi'_4 + \varphi''_4.$$

At last we can find the first three members of the polynom (6):

$$\varphi_1+\varphi_2+\varphi_4=\varphi_1+\varphi_2+C_4^T M_4=\begin{Bmatrix}\frac{1}{4}\left[0,\frac{1}{2}\right)\\ \frac{3}{4}\left(\frac{1}{2},1\right]\end{Bmatrix}+\begin{Bmatrix}-\frac{1}{8}\left[0,\frac{1}{4}\right)\\ \frac{1}{8}\left(\frac{1}{4},\frac{1}{2}\right)\\ -\frac{1}{8}\left(\frac{1}{2},\frac{3}{4}\right)\\ \frac{1}{8}\left(\frac{3}{4},1\right]\end{Bmatrix}=\begin{Bmatrix}\frac{1}{8}\left[0,\frac{1}{4}\right)\\ \frac{3}{8}\left(\frac{1}{4},\frac{1}{2}\right)\\ \frac{5}{8}\left(\frac{1}{2},\frac{3}{4}\right)\\ \frac{7}{8}\left(\frac{3}{4},1\right]\end{Bmatrix}.$$

The initial function $\varphi(t) = t$ and this approximation with orthonormal functions M_i (i=1,2,4) is shown in Fig. 5. Fig. 5 shows that convergence is uniform. The received system is stochastic and is unlike Haar's orthonormal system.

For the received system of the orthonormal function the following limited relation may be written down:

$\lim\limits_{n\to\infty}\alpha_n^2 C_n^{\frac{n}{2}}=\lim\limits_{n\to\infty}\frac{D_n}{d_n}\to 0$, where $D_n=C_n^{\frac{n}{2}}\Big/2^n$ is the maximal probability in Bernuli

symmetrical scheme with n tests, and $d_n=\frac{1\cdot3\cdot5\ldots(2n-3)}{2\cdot4\cdot6\ldots(2n-2)}\cdot\frac{2^{n-2}}{n}$.

The approximation with the received orthonormal system may be considered as the approximation with deterministic chaos.

Gori State Economical-Humanitarian Institute

საქართველოს მეცნიერებათა აკადემიის მოამბე, 159, №1, 1999
BULLETIN OF THE GEORGIAN ACADEMY OF SCIENCES, 159, №1, 1999

N. Jibladze

On One Method of Solving the Optimal Control Problems

Presented by Member of the Academy V.Chichinadze, May, 4, 1998

ABSTRACT. **The possibility of solving, to an acceptable accuracy and with insignificant computer time consumption, the optimal control problems through ψ-transformation is shown on the example of fuel consumption minimization problem.**

Key words: control, optimal, infinite dimensionality, approximation, finite dimensionality, transformation, algorithm.

Control problems in engineering, economics and other fields of practical importance are directly connected with optimal control problems and working out of practical algorithms for their solution. Let us consider a general problem of optimal control of lumped-parameter continuous dynamic system:

$$\min \{J[u(t)] = \int_{t_0}^{t_k} F[y(t), u(t), t]\, dt + \Phi[y(t)] \,/\, \dot{y} = f(y, u, t);\ y(t_0) = y_0,\ y(t_k) = y_k;$$

$$y(t) \in Y;\ u(t) \in U\ \}. \qquad (1)$$

The notation J[u(t)] (and not J[y(t), u(t)]) in problem (1) accentuates the circumstance that u(t) is an independent variable, while y(t) is considered to be a solution of the given differential equation.

According to the way how the optimization functional J[u(t)] is presented, several special cases of optimal control problem may be encountered in practice. Thus, for example, if $F \equiv 1$ and $\Phi \equiv 0$, then $J[u(t)] = \int_{t_0}^{t_k} dt$ and we shall have a time-control problem; if $F \equiv 0$, then $J[u(t)] = \Phi[y(t_k)]$ and such problem is called a terminal control problem; if $\Phi \equiv 0$ and $F(y, u, t) = F(y, t)$, then such problem is a trajectory optimization problem; if $\Phi \equiv 0$ and $F(y, u, t) = F(u, t)$, then we have the problem of control power minimization. An important special case of problem (1) is a linear problem where differential equation is presented as:

$$\dot{y} = A\, y(t) + B\, u(t), \qquad y(t_0) = y_0, \qquad (2)$$

where A and B are constant-coefficient matrices. In spite of the mentioned variety, any problem of optimal control, in general case, implies minimization of functional J[u(t)] determined on some U set of Banach space E, or, in other words, determination of such control function $u^*(t) \in E$ when the following conditions are satisfied

$$J[u^*(t)] \le J[u(t)], \qquad \forall u(t) \in U \subset E. \qquad (3)$$

Thus, from mathematical point of view, optimal control problem is an infinite-dimensional problem of mathematical programming in infinite-dimensional space and is solved

after the functional extremum is found. Among calculation methods of the problems of the mentioned class, the so-called direct methods [1] are of importance, as they found application in different spheres of mathematical physics and engineering practice. The idea, according to which the infinite-dimensional problem of optimization is reduced to finite-dimensional type, is realized in these methods, so as afterwards the well known methods of nonlinear programming be used.

The reduction of problem (1) to finite-dimensional type can be realized by approximation of the given infinite-dimensional functional space by finite-dimensional subspace, on the basis of which instead of variable function u(t) a certain linear variety with definite structure can be considered to some accuracy:

$$u_n(t) = \sum_{i=1}^{n} \lambda_i \varphi_i , \quad (n = 1, 2, ...), \tag{4}$$

where λ_i are determinable coefficients, while φ_i are the known analytical functions (step, polynomial, exponential, trigonometrical) making a full system of functions in the given space.

Taking into consideration (4), optimization function at fixed n in transformed into common function of variable n: $J[u_n(t)] = J(\lambda_1, \lambda_2, ..., \lambda_n)$, while the initial problem of optimal control is reduced to finite-dimensional problem of mathematical programming:

$$\min \{J(\lambda) = \int_{t_0}^{t_k} F[y, u_n, t] dt + \Phi[y(t_k)] \;/\; \dot{y} = f(y, u_n, t);\ y(t_0) = y_0;\ y(t_k) = y_k;$$
$$y(t) \in Y;\ u_n(t) \in U_n;\ \lambda = (\lambda_1, \lambda_2, ..., \lambda_n) \in Q_\lambda \subset R^n \} \tag{5}$$

It is evident that in case of concrete structure of control function $u_n(t)$, if λ_i values be chosen so that the condition min $J(\lambda_1, \lambda_2, ..., \lambda_n) = J(\lambda_1^*, \lambda_2^*, ..., \lambda_n^*)$ is held, then function $u_n^*(t) = \sum_{i=1}^{n} \lambda_i^* \varphi_i$ determined on optimal parameters λ_i^* can be to a certain approximation considered as the solution of problem (1).

In order to state the optimal values of parameters λ_i, i = 1, 2, ..., n we think advisable to use ψ-transformation method [2], as it allows: 1) to solve, to an acceptable accuracy, multidimensional problems of mathematical programming (including non-convex non-linear programming); 2) to solve, with consideration of limitations by "penalty functions" and using random search elements, the problems connected with solution of two-point boundary problems.

On the basis of ψ-transformation an algorithm is worked out which can be used for solution of optimal problems of type (5). This is realized in "quick BASIC" algorithmic language. In order to solve differential equations system the Runge-Kutt algorithm is used which provides considerable high accuracy of computation process.

As an illustration of the worked out algorithm, consider an optimal control problem which in technical literature is known as fuel consumption minimization problem [3]. Suppose, the variation of dynamic system state is described with differential equations:

$$\dot{y}_1 = y_2 , \quad \dot{y}_2 = u. \tag{6}$$

The initial and final states of the system are determined:

$$y(0) = \begin{pmatrix} 1 \\ 0 \end{pmatrix} \text{ and } y(3) = \begin{pmatrix} 0 \\ 0 \end{pmatrix}, \tag{7}$$

and quality functional is:

$$J = \int_0^3 |u(t)|\, dt. \tag{8}$$

There is a limitation provided for control function:

$$|u(t)| \le 1. \tag{9}$$

Such u(t) should be found which provides minimization of optimization functional (8) in case of limitations of (6), (7) and (9).

Suppose, we search for optimal solution of the class of the given structure control step functions and its modelling is done on the basis of the following formula:

$$u(t) = \begin{cases} -1, & t < \lambda_1, \\ 0, & \lambda_1 \le t < \lambda_2, \\ +1, & t \ge \lambda_2. \end{cases} \tag{10}$$

As by fixing parameters λ_1 and λ_2, the control function u(t) is uniquely defined, therefore in this case we have two-variable problems of optimization. Having "penalty function" in mind, for optimization functional we'll have

$$J(\lambda_1, \lambda_2) = \int_0^3 |u(t)|\, dt + 20\{[y_1(3)]^2 + [y_2(3)]^2\}. \tag{11}$$

According to the algorithm, for realization of ψ-transformation procedure we make S=10 of preliminary and N=100 of basic statistical tests. Their total results in case of integration step h = 0.2 is given in Table 1.

After parabolic approximation of empiric points of functions $\psi(h)$ and $\lambda_1(h)$ we have:

$$\psi(\eta) = 0.01002\eta^2 - 0.21649\eta + 1.19382; \tag{12}$$

$$\lambda_1(\eta) = -0.00107\eta^2 - 0.01557\eta + 0.63730; \tag{13}$$

$$\lambda_2(\eta) = 0.00488\eta^2 - 0.00248\eta + 2.06733. \tag{14}$$

After solution of quadratic equation $\psi(\eta)=0$ its smallest positive root $\eta^* = 10.8030$ is chosen and on its insertion into expressions (13) and (14) the assumable extremum point coordinates $\lambda_1^* = 0.34381$ and $\lambda_2^* = 2.60982$ are calculated.

As a result of local search made in the vicinity of extremum, the optimum point is specified: $\lambda_1^* = 0.31041$, $\lambda_2^* = 2.69991$; $J^* = 3.0$. On the basis of optimal values of parameters λ_1, the desired optimal control function is defined:

$$u^*(t) = \begin{cases} -1, & t < 0.31041, \\ 0, & 0.31041 \le t < 2.69991, \\ +1, & t \ge 2.69991, \end{cases} \tag{15}$$

Table

η	ζ	ψ	λ_1	λ_2
1	35.1258	1.0000	0.6350	2.0582
2	31.6673	0.7918	0.5904	2.0623
3	28.2089	0.6482	0.5718	2.1069
4	24.7505	0.4618	0.5533	2.1718
5	21.2921	0.3364	0.5287	2.2264
6	17.8337	0.2675	0.5135	2.2189
7	14.3752	0.2008	0.4914	2.2800
8	10.9168	0.0999	0.4522	2.2974
9	7.4584	0.0703	0.3876	2.4005
10	4.0000	0.0121	0.3795	2.5924

and with the help of the latter, the system's optimal trajectory is found, its final point coordinates being: $y_1^*(3) = 0.03333$, $y_2^*(3) = 0$.

It is remarkable that computer time required for the solution of optimal control problems by the worked out algorithm mainly depends on time functions of the given differential equation system solution by Runge-Kutt algorithm. Therefore, the total computer time of algorithm operation can be approximately defined by formula $T \approx (S+N)\tau$, where S is the number of preliminary statistic tests, N is the number of basic statistic tests and τ is unitary time of differential equations system solution.

The given algorithm helps to solve a number of linear as well as nonlinear problems of lumped-parameter continuous dynamic system optimal control. Optimal control discrete problems can be solved in the same way. On the basis of the obtained results we conclude that the worked out method provides the solution, to an acceptable accuracy and with insignificant computer time consumption, of a wide class of optimal control problems which is so important in engineering practice.

Georgian Technical University

REFERENCES

1. *N.N. Moiseev*. Chislennye metody v teorii optimalnykh sistem. M., 1971 (Russian).
2. *V.K. Chichinadze*. Reshenie nevipuklykh nelineinykh zadach optimizatsii. M., 1983 (Russian).
3. *D. Tabak, B.C. Kuo*. Optimal control by mathematical programming, New Jersey,1971.

საქართველოს მეცნიერებათა აკადემიის მოამბე, 159, №1, 1999
BULLETIN OF THE GEORGIAN ACADEMY OF SCIENCES, 159, №1, 1999

BOTANY

M. Akhalkatsi, G. Gvaladze

The Ultrastructure of Ovule Sterile Tissues of *Peperomia caperata* (*Piperaceae*)

Presented by Corr. Member of the Academy G. Nakhutsrishvili, February 19, 1998

ABSTRACT. **The submicroscopic peculiarities of cells of nucellus integument of *Peperomia caperata* Yunker was revealed.**

Key words: ovule, integument, nucellus, fertilization, tissues.

The structure of ovule sterile tissues was studied in several species of *Peperomia* [1-3] and in some other genera of *Piperaceae* [4-7]. The ultrastructural study was carried out on reproductive tissue of ovule in one species - *P. blanda* [8]. In the present paper the ultrastructure of ovule sterile tissues of *Peperomia caperata* Yunker is investigated for the first time. The study is needed for comparative embryological investigation of the genus *Peperomia*.

The material was collected from plants growing in the greenhouse of the Tbilisi Botanical Gardens in 1988-1989 years. For light microscopy bits of inflorescences were fixed in Karnua's fluid, dehydrated in alcohol, embedded in paraffin and sectioned at 12-20 mkm thickness. Sections were stained separately with acid hemalaun. The material was examined with "Polyvar" microscope (firm Reichert, Austria). For electron microscopy material was pre-fixed in 3% glutaraldehyde at room temperature for 2 h in 0.1 M phosphate buffer at pH 7.2. After bufferwash the samples were post-fixed in 2% osmium tetroxide overnight. The fixed materials were then dehydrated through acetone series and embedded in epon. Ultrathin sections were cut with glass knives on LKB-V ultramicrome and stained with lead citrate. Sections were examined with a Tesla BS-500 transmission electron microscope.

The ovule (Fig.1a) is orthotrpous, unitegmic and crassinucellate. The integument is 3-4-layered and forms a narrow long micropyle. Before fertilization the integument consists of highly vacuolated cells. The nucleus is located on the periphery (Fig. 1b). It has irregular outlines and contains one large nucleolus. The cytoplasm forms thin layer along the cell wall. A few free ribosomes and small lipid bodies occur. Plastids are numerous and show simple interior organization. Starch grains are absent. Mitochondria and dictyosomes are not abundant. ER is scarce. The central vacuole contains tannins. The plasma membrane borders thin polysaccharide cell walls which are penetrated by plasmodesmata.

The nucellus has more or less spherical outlines and consists of 13-16 cell layers on the median section. The outermost cell layer forms the epidermis. The inner nucellar cells don't differ in structure depending on their position in the ovule. Before fertilization they contain small vacuoles and are rich in cytoplasm (Fig. 1c). The nucleus is located in the

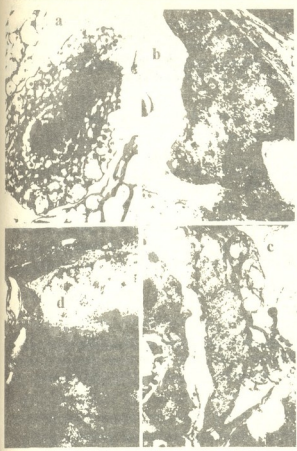

Fig. 1. a-The view of ovule of *Peperomia caperata*. x 230.
b-A part of integumentary cell showing peripherially located nucleus. x8000.
c-A part of nucellar cell. x8000.
d-Epidermal cell of nucellus. x6000.
in - integument, nc - nucellus, p - plastid.

center. It is spherical with one nucleolus. Free ribosomes are numerous. Lipid bodies are absent. Plastids are abundant. They have dense stroma and well developed interior membrane system (Fig. 1c). Mitochondria are also numerous with regular distributed cristae. Dictyosomes show moderate activity. ER is represented by a few cisternae of rough ER. Microbodies occur. Small vacuoles contain electron dense material. Polysaccharide cell walls possess plasmodesmata. The nucellar epidermis cells are more highly vacuolated (Fig.1d). Plastids containing starch are found in these cells.

After fertilization the ovule tissues undergo some transformations. The number and activity of organelles continue to decrease in the integumentary cells. Some large starch grains appear in the plastids (Fig. 2a). The amount of the tanninous substances increases in the vacuoles. Afterwards the cytoplasm gradually degenerates and cell lumen is filled in tannins. In the mature seed integument forms the seed coat. After fertilization the amount of storage substances increases considerably in the nucellar cells. Large starch grains appear in the plastids (Fig.2b). Vacuole becomes more prominent and electron dense material is accumulated in it. Gradually, the cytoplasm becomes reduced and the cells are occupied with storage starch. The nucellus is transformed into perisperm.

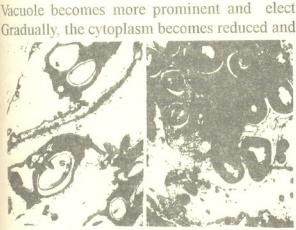

Fig. 2. a- A part of integumentary cell after fertilization. x10000.
b- A part of nucellar cell after fertilization. x10000.

The results of this study have shown that the ovule of *P. caperata* reveals low level of differentiation and characteristics to be considered as primitive for the ovules of angiosperms [1,3]. The ovule is covered with only integument which forms a seed coat. The inner nucellar cells have uniform structure in spite of their position. In a lot of angiosperm species [1,3,9] the crassinucellate ovules possess highly specialized cell layers of nucellar cells de-

pending on their position in ovule. These differences in structure are often associated with a function of substance transport in ovules [9]. In *P.caperata* no signs of specialization of nucellar cells were observed. It should be assumed that the nutritive substances are transported from funiculus to the embryo sac through nucellar cells uniformly without formation of special paths through the nucellus.

Georgian Academy of Sciences
N. Ketskhoveli Institute of Botany

REFERENCES

1. *Z. Nikiticheva.* Sravnitelnaya embbryologiya tsvetkovykh rastenii-*Winteraceae - Juglandaceae.* Leningrad, 1981, 84-90.
2. *B. Johri et al.* Comparative Embryology of Angiosperms. Berlin, 1992, 309-312.
3. *C. Sh. Tucker.* Amer. J. Bot. **67**, 5, 1980, 686-702.
4. *A. C. Joshi.* Proc. Nat. Inst. Sci. .India, 10, 1944, 105-112.
5. *Y. S. Murty.* Proc. Indian Acad. Sci. **49**, 11, 1959, 52-65.
6. *K. Kanta.* Phytomorphology, **12**, 3, 1962, 207-221.
7. *E. J. H. Corner.* The seeds of dicotyledons. Gambridge, London, 1976.
8. *T. Playushch.* Submikroskopicheskaya kharakteristika reproduktivnykh structur semyazachatka *Peperomia blanda.* Ph. Dr. Thesis. Leningrad, 1983.
9. *M. Chyamporova, M. Akhalkatsi, G. Gvaladze.* Bot. J. (Leningrad), **73**, 12, 1988, 1722-1730 (Russian).

საქართველოს მეცნიერებათა აკადემიის მოამბე, 159, №1, 1999
BULLETIN OF THE GEORGIAN ACADEMY OF SCIENCES, 159, №1, 1999

A. Shatirishvili, N. Baratashvili, Kh. Gogaladze

Induction of Mitotic Recombinations by Pesticides (Zinebi and Acartan)

Presented by Corr. Member of the Academy D. Jokhadze, February 23, 1998

ABSTRACT. **Genetic activity of pesticides -Zinebi and Acartan applied in viticulture has been studied in different yeast test systems. Intergene mitotic segregation induced by these preparations is more frequent than intragene. Zinebi are found to be genetically more active than Acartan.**

Key words: yeast, pesticide, mitotic recombination, genetic activity.

Mutagenesis, recombination and repair processes have many common stages with DNA replication. Substances affecting this process are genetically active factors. The study of genetic activity of pesticides applied in agriculture is very significant [1]. Georgia is a wine-making country and pesticides are widely applied. The study of genetic activity of Zinebi and Acartan as the most dangerous environmental pollutants (along with the other pesticides) has a great importance.

Two different test-systems, worked out in yeast *Saccharomyces*, were used to study a recombinogenic activity of pesticides. Using these test-systems we've registered intragene and intergene mitotic segregation processes. T51 (Genotype aαADE2ade2HIS8his8) and T423 (Genotype aαADE2ade2HIS8his8sp12sp12) [2] genetic lines constructed from *S. cerevisiae* var. vini were applied to analyze intergene mitotic segregation, using the system ade2-his8. Genes ade2 and his8 are located in XV chromosome and are in trans position. Gene sp12 controls mitosis, meiosis and recombination processes. At high temperature (35^0C) mitosis and meiosis are blocked, while recombination frequency increases. As for intragene recombination it was registered in T1 (Genotype aαADE2-192ade2-G45RADRAD) and T2 (Genotype aαADE2-192ade2-G45rad2rad2) lines, which are constructed by prof. Zakharov using *S.cerevisiase's* Petergoff stocks [3]. The strains, mentioned above, have been grown on the complete media supplied with the preparations 0.1% solution. This concentration is close to the doze usually used.

Diploid vegetative cell survival dependence upon the duration of exposure to the pesticides is the main criterion for the lethal effect of the chemicals studied. As it turned out the substances mentioned above exhibited different lethal effects (Tables 1,2; Figures 1, 2). 50% lethal effect (LE50%) is used to compare lethal effect of various factors. These data were: 63 sec. for T51; 18 sec. for T423; 99 sec. for T1; 87 seconds for T2, when cells were exposed to Acartan. In case of Zinebi the same data looked as follows: 112 sec., 108 sec., 72 sec. and 66 sec. respectively. According to this evidence Acartan revealed high toxic effect on T51 and T423, while T1 and T2 strains were more sensitive to Zinebi.

Table 1

Mitotic segregation in T51 and T423 strains induced by Acartan and Zinebi

Substance	Strain	Exposure time (min)	Survival %	Total Number of colonies	Mitotic segregation Number of segregants	%
Acartan	T423	Control	100	12402	0	0
		30	39.2	4862	11	0.23±0.04
		60	29.6	3670	9	0.24±0.05
		90	25.4	3145	8	0.25±0.04
		120	19.2	2386	6	0.25±0.01
	T51	Control	100	6723	1	0.01±0.01
		30	78.1	5250	5	0.09±0.02
		60	56.7	3811	6	0.15±0.01
		90	31.1	2093	4	0.19±0.03
		120	25.00	1680	3	0.17±0.02
Zinebi	T51	Control	100	4183	1	0.02±0.03
		30	85.00	3550	9	0.25±0.04
		60	63.00	2630	8	0.30±0.07
		90	53.8	2650	9	0.40±0.06
		120	43.2	1807	10	0.55±0.05
	T423	Control	100	3684	2	0.05±0.03
		30	97.3	3585	8	0.22±0.07
		60	74.00	2721	14	0.51±0.13
		90	73.00	2691	18	0.67±0.15
		120	39.1	1442	13	0.90±0.19

Table 2

Mitotic segregation in T1 and T2 strains induced by Acartan and Zinebi

Substance	Strain	Exposure time (min)	Survival %	Total Number of colonies	Mitotic segregation Number of segregants	%	Number of cross-overs	%
Acartan	T1	Control	100	8300	0	0	0	0
		30	92.3	19152	4	0.02±0.01	0	0
		60	72.4	30253	9	0.03±0.01	0	0
		90	54.5	45240	18	0.04±0.01	0	0
		120	42.6	176750	53	0.03±0.01	0	0
	T2	Control	100	8848	0	0	0	0
		30	88.2	19510	5	0.03±0.01	1	0.005±0.002
		60	62.4	27610	10	0.04±0.01	0	0
		90	49.5	43770	17	0.04±0.01	0	0
		120	43.4	191800	48	0.03±0.004	0	0
Zinebi	T1	Control	100	4200	1	0.02±0.02	0	0
		30	67.2	7430	8	0.11±0.04	0	0
		60	56.2	11802	15	0.18±0.04	0	0
		90	39.3	16506	26	0.16±0.04	0	0
		120	16.2	34000	78	0.28±0.03	0	0
	T2	Control	100	3501	2	0.06±0.04	0	0
		30	70.7	6187	8	0.13±0.05	0	0
		60	52.1	9120	15	0.16±0.04	0	0
		90	40.00	13960	27	0.19±0.04	0	0
		120	13.2	23050	48	0.21±0.03	0	0

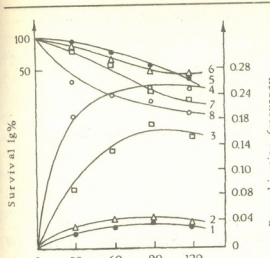

Fig. 1. Yeast cell survival and mitotic recombinations induction frequency dependence upon exposure duration for Zinebi
Recombination frequency dependence upon the doze 1. T1; 2. T2; 3. T51; 4. T423
Survival dependence upon the doze 5. T1; 6. T2; 7. T51; 8. T423

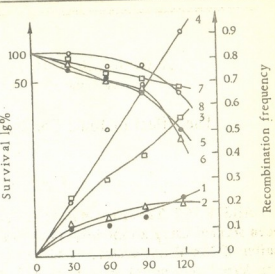

Fig. 2. Yeast cell survival and mitotic recombinations induction frequency dependence upon exposure duration for Acartan
Recombination frequency dependence upon the doze 1. T1; 2. T2; 3. T51; 4. T423
Survival dependence upon the doze 5. T1; 6. T2; 7. T51; 8. T423

While studying the cell survival we also analyzed pesticides-induced mitotic recombinations. The whole and sector adenine-requiring auxotrophic colonies were registered. Increasing exposure duration recombination frequency increased. Preparations revealed different recombinogenic activity.

Zinebi exhibited high recombinogenic activity. Induced recombination frequency was higher in diploid cells of T423 strain than in the other ones. In this line at the doze of 120 sec recombination frequencies were: 0.9% for Zinebi and 0.25% for Acartan. As it appeared Acartan-induced both intragene and intergene mitotic recombinations occured with the far less frequencies then Zinebi-induced.

8 defoliants studied by other researches, exhibited different genetic activity on T1 and T2 strains [5].

Pesticides also induced various genetic changes in Soybean [6].

Tbilisi I.Javakhishvili State University

REFERENCES

1. *R. Lekiavichus.* Khimicheskii mutagenez i zagryazneniye okruzhayushchei sredy, Vilnius,1983, (Russian).
2. *A. Shatirishvili.* The Works of Tbilisi State University. 240, 1983, 147-151.
3. *I. Zakharov, S. Marfin, G. Kosikova.* Genetica, **18**, 1, 1982, 36-41 (Russian).
4. *I. Zakharov, S. Kozhin, I. Fedorova.* Sbornik metodik po genetike drozhzhei sakharomitsetov. L., 1984 (Russian).
5. *I. Zakharov, I. Davronov.* Genetika, v. XXI, 11, 1985, 1854-1868 (Russian).
6. *N. Baratashvili, K. Chiqvinidze, A. Shatirishvili.* Bull. Georg. Acad. Sci, **152**, 1, 1995, 156-159 (Georgian).

საქართველოს მეცნიერებათა აკადემიის მოამბე, 159, №1, 1999
BULLETIN OF THE GEORGIAN ACADEMY OF SCIENCES, 159, №1, 1999

BIOPHYSICS

A. Gvritishvili, N. Butkhuzi, K. Adeishvili, E. B. Boot,
Member of the Academy M. Zaalishvili

The Effect of Ionic Force and Temperature on Troponin I Molecule

Presented February 10, 1998

ABSTRACT. **The effect of ionic force and temperature on troponin I molecule has been studied using an intrinsic fluorescence method. It has been shown that in the buffer of 20mM tris-acetate 0.2M KCl, pH 8.8 a complete renaturation of troponin I molecule does not occur. An increase in KCl molarity from 0.2M to 1M has no considerable effect on the conformational state of troponin I molecule. Within 10^{-6}-10^{-5}M concentration ranges of the protein that corresponds to 0.0025-0.1mg/ml area, fluorescence intensity and spectrum position at λ_{exc}=296nm are strong concentration dependent.**

Key words: an intrinsic fluorescence of protein, troponin I.

Troponin I is an inhibitor of the troponin complex which interacts with the rest two components of this complex: Ca^{2+} - sensitive troponin C and troponin T. The latter is responsible for binding troponin with tropomyosin. The three components form the troponin complex that is involved in the interaction of actin with Ca^{2+} - sensitive myosin in striated muscles. The molecular mass of a troponin I obtained from a skeletal muscle is equal to ~21000 Da.

The most part of the study with intrinsic fluorescence method deals with the interaction of Ca^{2+} -ions with troponin and its components [1-3], mainly with troponin C [4-6].

In the present work, using the protein intrinsic fluorescence method, the effect of temperature rise, dithiothreitol addition as well as the changes of ionic force of the environment on the conformational state of troponin I were studied.

Troponin I was obtained from the troponin complex [7] isolated from the rabbit skeletal muscle with a chromatographic method on DEAE cellulose [8], followed by its purification on CM sephadex A-50 [9].

For the purpose of fluorescence studies the lyophilized troponin was dissolved in a buffer which contained 6M urea, depending on the experimental conditions, either 1mM DTT and 1mM EDTA, or 1mM EGTA. Then it was dialyzed against 20mM trisacetate buffer with pH 8.8, which contained 0.2M KCl as well, whenever necessary. DTT and EDTA of the firm "Serva" and EGTA of "Fluka" were used.

Instrinsic fluorescence parameters were measured on the spectrofluorometer RF-5000 "Shimadzy". According to the intensity of spectrum maximum the fluorescence quantum yield value was determined [10].

The method of proteins intrinsic fluorescence has been commonly employed to study

the conformational state of their molecules. Registration of this state is made by means of fluorescent amino acids, tryptophans and tyrosines, contained in proteins. Replacement of one buffer by another, change in temperature, pH, ionic force, etc. cause response of the protein molecule conformation to these changes, reflected in the changes of intrinsic fluorescence spectrum parameters. Troponin I is known to contain tryptophan in 159 position and two tyrosines [11]. At λ_{exc}=280nm, both tyrosines and tryptophans are excited, while at λ_{exc}=296nm only tryptophans are actually excited [10]. Therefore, analysis of fluorescence spectra at λ_{exc}=296nm enables to judge about the position of a single tryptophan in a troponin I molecule and the conformational state of the protein.

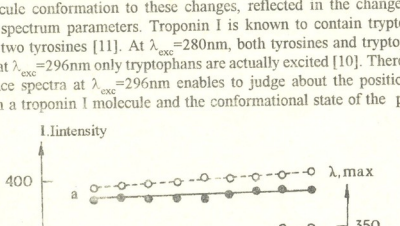

Fig.1 An intrinsic fluorescence intensity (a) and dependence of spectrum position (b) on KCl molarity l_{max}=296nm. Solvent: 20mM tris-acetate, 1mM DTT.

We were interested whether the molecules of troponin I could recover the primary conformation after thermal influence, or renaturation. To this end, after preliminary study of spectrum quantum yield and temperature dependent position of the spectrum, the preparation was stored in the refrigerator for 18th. Thereafter the fluorescence spectrum parameters were again measured. The results of primary heating of troponin I obtained by us, were published elsewhere [12]. The experiments carried out with this method demonstrate that a complete renaturation of troponin I molecule does not occur in the buffer of 20mM tris-acetate, 0,2 M KCl, pH 8.8.

The change of quantum yield at high temperature value (T>>transition temperature) shows that troponin I could not be fully denatured in the experimental temperature range as it was shown for arc repressor dimer, leucine zipper dimer. The question whether general denatured state is "random coil" or partially folded structure would be answered by high resolution NMR analysis [13,14].

Secondary heating, as compared to the primary one, proceeds with low values of quantum yield. The position of fluorescence spectra does not recover either. The transfer sites observed in the temperature dependent quantum yield curves alter slightly.

Troponin I molecule contains residues of three cysteine amino acids in 48, 64, and 133 positions. It is accepted that Cys-48 and Cys-64 are within the molecule and are reaction incapable, while Cys-133 is on the surface of the molecule. Just this positions appears to be essential for the interaction of troponin I with troponin T and Troponin C [15]. For the formation of the troponin I-troponin T complex a complete reduction of SH groups in the troponin I molecule is necessary. Reaction capable Cys-133 can form

intermolecular disulfide bridges, contributing thereby to protein aggregation (dimerisation). To avoid this process, we added to the solvent 1mM DTT, which, in our conditions, was sufficient for the complete restoration of SH-groups in the troponin molecule. As shown by the experiments, the addition of DTT does not alter the pattern of curves expressing temperature dependence of intrinsic fluorescence intensity of the troponin I molecule.

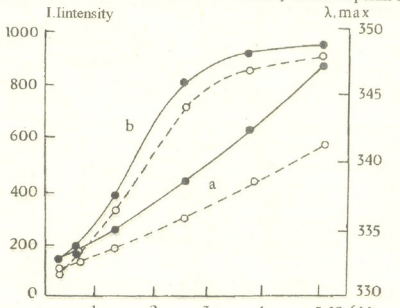

Fig. 2. Concentration dependence of troponin I intrinsic fluorescence intensity (a) and spectrum position (b). ·. without DTT o. in the presence of DTT.

At increasing temperature on the face of decay of fluorescence quantum yield, the temperature shift to the following areas 23^0-26^0C and 50^0-54^0C is noted. In this presence of 1mM DTT at λ_{exc}=296nm secondary heating starts whith λ_{max} which is equal to the respective λ_{max} of fluorescence spectra at the primary heating termination. Taking into account that the position of fluorescence spectra represents absolute variable of the sample [10], after thermal influence one cannot speak about a complete restoration of the troponin I molecule.

We have studied whether KCl molarity in the buffer affects the proteins intrinsic fluorescence spectrum. Figure 1 shows that the value of fluorescence intensity undergoes no change as KCl molarity increases in the environment from 0.2M to 1M.

In order to reduce oxidation effect of DTT by atmospheric oxygen, addition of 1mM EDTA to the protein dialyzing solution resulted in a slight slope of KCl concentration dependent fluorescence intensity curves, while the curves plotting fluorescence spectra position as dependent on KCl molarity remained unaltered. These results testify that an increase in KCl molarity from 0.2M to 1M has no considerable effect on the conformational state of the troponin I molecule.

It appeared that within 10^{-6}-10^{-5}M concentration ranges of the protein that corresponds to 0.0025-0.1mg/ml area, fluorescence intensity and spectrum position at λ_{exc} = 296nm are strongly concentration dependent (Fig.2). Similar dependence is noticed in the solutions containing 1M KCl as well as 1mM EDTA or 1mM EGTA.

At 0.08-0.1mg/ml concentrations troponin I appears to have rather a high λ_{max} which approximates the respective λ_{max} of free tryptophan in water solution. This enables to suggest that tryptophan 159 is in the superficial hydrophilic area of the troponin I molecule [2]. As the protein concentration decreases, apart from the reduction of quantum yield, there is a significant displacement of spectrum position to a short-wave site. This indicates tryptophan transport to rather a deep hydrophobic site.

Georgian Academy of Sciences
Institute of Molecular Biology and Biological Physics

REFERENCES

1. *J.-P. van Eerrd, Y. Kawasaki.* Biochemistry **12**, 24, 1973, 4972-4980.
2. *J. R. Lakowicz, I. Gryzynski et al.* Biochemistry **27**, 26, 1988, 9149-9160.
3. *M. H. Han, E. S. Benson.* Biochem. and Biophys. Res. Commun. **38**, 3, 1970, 378-383.
4. *W. -I. Dong, Ch. Wang et al.* Biophys J. **72**, 2, part 1, 1977, 850-857.
5. *T. Ilo, H. J. Kondo.* Biochem. **92**, 4, 1982, 1141-1143.
6. *B. Nagy, J. J. Gergely.* Biol. chem. **254**, 24, 1979, 12732-12737.
7. *I. Staprans, H. Takahashi et al.* Biochem. **72**, 1972, 723-729.
8. *S. V. Perry, H. A.Cole.* Biochem. J. **141**, 3, 1974, 733-743.
9. *J. D. Potter.* Methods in Ensymology. **85**, 1982, 241-263.
10. *E. A. Cherniski.* Lyuminestsentsiya i structurnaya lab·ilnost belkov v rastvore i kletke. Minsk, 1972 (Russian).
11. *H. Syska, J. M. Wielkinson et al.* S. V. Biochem. J., 149, 1975, 493-496.
12. *A. G. Gvritishvili, N. I. Butkuzi et al.* Proc. of Georg. Acad. Sci., biol. ser. **22**, 1-6, 1996 (Russian).
13. *K. Wüthrich.* NMR of proteins and nucleic acids, N. Y., 1986.
14. *K. Wüthrich, R. Shulman.* Uspekhi fizicheskikh nauk, 707-720, 1971, 105 (Russian).
15. *H. Sh. Parr et al.* Biophys. J. **66,** 1994, 2062-2065.

საქართველოს მეცნიერებათა აკადემიის მოამბე, 159, №1, 1999
BULLETIN OF THE GEORGIAN ACADEMY OF SCIENCES, 159, №1, 1999

BIOCHEMISTRY

A. Belokobilsky, N. Tsibakhashvili, A. Rcheulishvili, L. Mosulishvili

Accumulation of Cd(II) in c-Phycocyanin from *Spirulina platensis*

Presented by Corr. Member of the Academy D. Jokhadze, February 3, 1998.

ABSTRACT. **High-purity c-Phycocyanin preparations have been obtained from the cells of microalga *Spirulina plantensis*. For estimation of the purity degree the spectrophotometric and chromatograpic methods were used. It was established that c-Phycocyanin has the ability to accumulate the toxic element -Cd.**

Key words: c-Phycocyanin, *Spirulina platensis*, Cd(II) impurity, ESIS, HPLC.

c-Phycocyanin (PhC) is discovered in blue-green alga *Spirulina plantensis*. Under certain conditions the cells of alga can accumulate PhC in concentrations that make up 24% of dry biomass [1]. Previously we have shown that the cells of *Spirulina plantensis* accumulate a considerable amount of Cd at the expense of impurity inclusions of this element into reagents of nutrient medium [2-3]. Since PhC is an acidic globular protein containing 4 pyrrol rings with two carboxyl groups bound with central pyrrol rings, one can assume that PhC molecules are able to accumulate both biogenic and toxic metals. For cheking the assumption of possible accumulation of toxic elements by PhC molecules we carried out the present work.

Spirulina platensis was used as a biological object of investigation. Its growth was carried out in nutrient medium Zaraucha [5] in light-driven photobioreactor with mechanical agitation at the temperature of 34-36^{0}C and illumination of 4-6 thousand lux in accumulation regime. The harvest was gathered in 7-9 days of cultivation in logarithmic phase of growth.

The cells were precipitated by centrifugation at 3600g for 30 min, at 4^{0}C. After rinsing in distilled water the cells were again precipitated by centrifugation under the same conditions. The rinsed mass was dried by lyophilization for subsequent isolation of PhC from it. This was done in order to facilitate the extraction of PhC, as it is difficult for the cells of this microalga to be destroyed at homogenization.

PhC from lyophilized biomass was obtained by extraction from biomass in 0.1M $NaHPO_4$-KH_2PO_4 phospate buffer pH 6.0. The extract containing PhC and other proteins dissoluble in water was isolated from undissolved components by centrifugation during 20 min at 12000g. PhC from the extract was deposited by adding 0.7 volumes of saturated solution of $(NH_4)_2SO_4$. All further procedures were carried out in close agreement with F. W. Teal and R. E. Dale methods [4]. All procedures were carried out at 4^{0}C in darkness. As our task was to determine CD bound endogenously with PhC we made all necessary measures, excluding the contamination of PhC by exogeneous Cd contained in reagents, water and chemical vessel. At all stages the solutions were prepared only on the basis of deionized water obtained on Milli Q(USA) equipment, containing 0.2 mM EDTA.

To determine the degree of purity of PhC preparations the spectrophotometric and chromatographic methods were used.

Recording of absorption spectra (in the region of 250-700nm) was carried out on

spectrophotometer Hitachi (Japan).

Gas-liquid chromatography (GC) was carried out using gas chromatography "Tsvet-104" equipped with a flame ionization detector. The detector and evaporator temperatures were 100°C and 200°C, respectively. The temperature of column at the moment of injection of sample was 50°C, then the programmed increase of temperature up to 70°C with the rate of 5°C/min was conducted. The detection was carried out at ratio 1:2 of hydrogen and oxygen. The stainless steel column of 1.5m x 3mm was used. As an immobile phase 15% carbowax 20M (with particle size 0.16-25μm) was selected that was superimposed on inertonsuper. As a gas carrier helium was used. Consumption of helium is 24ml/mm. Analysis was carried out by means of direct injection of 5μl aqeous solution of Phycocyanin.

High performance liquid chromatography (HPLC) was carried out on a microcolumn HPLC "Milichrom-4" (Nauchpribor, Russia). Detection was carried out with an ultraviolet detector (wave length 190-360nm). The effluent was monitored at 230 nm. HPLC was performed by using stainless-steel 62x2mm column, packed with 5μm Lichrospher WP 300 RP-18. The mixture-ethanol: butanol (4:1) and 12 mM HCl was used as a mobile phase. The amount of mobile phase was 500μl, flow rate of mobile phase 50 ml/min.

Absorption spectra of PhC preparations in 0.1M phospate buffer pH 6.0 shown in Fig.1 gives evidence of their high frequency (A_{621}/A_{277} ~3).

In Fig. 2 results of HPLC analysis for purified (a) and partially purified (b) PhC preparations are presented. As it is seen, in one case (a) the PhC was eluted within 24 min in the form of symmetrical peak, but in other case the impurity peaks were also observed.

The degree of purity of PhC samples was also estimated by using GC method. As it is seen from the Fig.3 at low temperatures for the purified PhC only the peak of solvent (water) is observed, but for the partially purified preparation in addition three well resolved light fractions are detected.

Thus, we can state that by us high-purity PhC

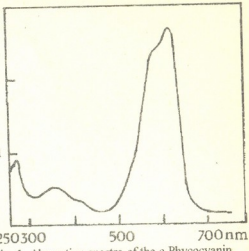

Fig. 1. Absorption spectra of the c-Phycocyanin solution in 0.01M phospate buffer pH6.0. c-Phycocyanin was removed from *Spirulina platensis* by F. Teale and R. Dale method

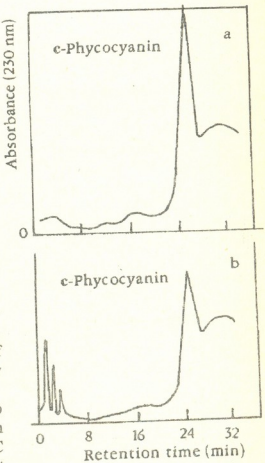

Fig. 2. Chromatograms of the c-Phycocyanin obtained by HPLC. a) purified c-Phycocyanin, b) partially purified c-Phycocyanin.

preparations have been obtained from the cells of microalga *Sp. platensis*. The content of Cd in these samples were determined by modified atomic-absorption method at 228.9 nm wave lenght.

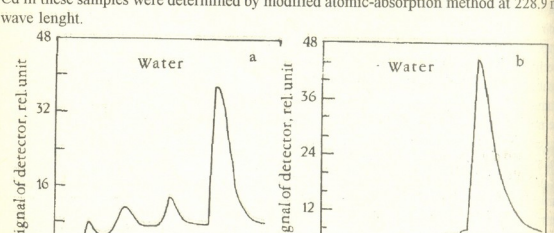

Fig. 3. Chromatograms of the c-Phycocyanin obtained by injection of 5 μl sample into column of gas-liquid chromatography. a) purified c-Phycocyanin, b) partially purified c-Phycocyanin.

By the method of atomic-spectroscopy it was established that in the preparations of "unpurified" PhC with high amount of impurity proteins, the content of Cd was 14-15μg/g in PhC dried by lyopihlization, while pure PhC preparations, the content of Cd is more than 3 times higher and equals to 53μg/g on the average of lyophilized PhC. Obviously, the impurity proteins in unpurified PhC preparations do not contain Cd and hence its concentration is decreased.

Thus, on the basis of the results obtained we can assume that PhC being reserve protein in the of *Spirulina platensis*, can accumulate significant amount of Cd. The obtained results allow to make the assumption that other toxic metals can accumulate in PhC and probably in Phycoerythrin of other alga where it plays a role of storing protein [1]. We hope to carry out these works in near future.

The work was supported by the Grant (N 2.22) of the Georgian Academy of Sciences.

Georgian Academy of Sciences
Institute of Physics

REFERENCES

1. *G. Britton.* The Biochemistry of Natural Pigments. Cambridge University Press, Cambridge, London, New York, Rochelle, Melburne, Sydney, 1983.
2. *A. Belokobilsky, M. Gelashvili et al.* Proc. Georg. Acad. Sci., Biological Series, **22**, 1-6, 1996.
3. *N. Tsibakhashvili, L. Mosulishvili et al.* Zhurnal fizicheskoi khimii, **72**, 5, 1998, 956 (Russian).
4. *F. W. J. Teatle R. E. Dale.* Biochem. J., 2, 1970, 161.

საქართველოს მეცნიერებათა აკადემიის მოამბე, 159, №1, 1999
BULLETIN OF THE GEORGIAN ACADEMY OF SCIENCES, 159, №1, 1999

R.Mdivani, B.Khurcia

Phytopathogenic Bacteria Effect on Tomato Free Amino Acids and Amids Composition

Presented by Member of the Academy T.Chanishvili, November 3, 1998

ABSTRACT. **We observed that during bacterial infections important changes occured in the plant free amino acids and amids composition, which negatively affected physiologic-biochemical condition of plant.**

We examined the phytopathogenic effect on several free amino acids in tomato tissue.

Key words: *Pseudomonas lycopersici, Corynebacterium michiganense, Xanthomonas vesicatoria, Pseudomonas capsici.*

Free amino acids and amids composition is very labile in healthy as well as in diseased plants. In spite of this, during tomato diseases essential differences in free amino acids composition are revealed [1].

During bacterial infection there is established common tendency of free amino acids accumulation in diseased plant tissues [2].

Rise of protein proteolysis activity as well as change of free amino acids primary synthesis and metabolism is one of the characteristic features of nitrogen metabolism breach caused by phytopathogenic bacteria effect in tomatoes.

During tomato bacteriolysis reduction of free amino acids and amids composition and number is conditioned by negative effect of metabolites produced by bacteria on amino acids synthesis and metabolism. These metabolites are represented by pathogens toxic products. Their existence is proved by experimental data and the character of symptoms manifestation. Till the symptoms are revealed, reduction or complete disappearance of particular amino acids is conditioned by their direct usage by phytopathogenic bacteria [3].

When tomatoes are artificially contaminated with phytopathogenic bacteria, there is observed considerable increase of a number of acids and amids. But this process isn't always accompanied with expansion of free amino acids composition. Increase of common number of free amino acids is possible at the expense of proteolysis strenghtening as well as in the result of protein synthesis weakening.

Pathogens causing bacterial diseases in tomatoes studied by us differently affect free amino acids and amids composition in plants [4].

The chromatogram shows changes happened in amino acids composition in tissues of tomatoes contaminated artificially by phytopathogenic bacteria causing "Tomatoes bacterial cancer", "Bacterial black spot", "Pepper spot" and "Top suppurativenses", in comparison with a healthy one (Fig.).

Results are deciphered in Table.

Fig. 1. Phytopathogenic bacteria effect on tomato free amino acids and amids composition:

I-control; II-*Pseudomonas lycopersici*; III-*Corynebacterium michiganence*; IV-*Xanthomonas vesicatoria* (N133); V-*Pseudomonas capsici*; VI-*Xanthomonas vesicatoria* (IV-148).

1. Cystein+cystine; 2. Ornithine+lysine; 3. Histhidine; 4. Arginine; 5. Asparaginic acid+asparagine; 6. Cerine+glycine; 7. Oxyproline+glutamine acid+citrulline; 8. Threonine; 9. Alanine; 10. β-alanine; 11. Tyrosine; 12. Tryptophan; 13. γ-aminobutyric acid-methionine; 14. Valine; 15. Norvaline; 16. β-phenylalanine; 17. Isoleucine; 18. Leucine+norleucine.

As it is clear from data, in tomato tissues inoculated by "Top suppurativeness" pathogens γ-aminobutyric acid, methionine, valine, norvaline and β-phenylalanine have completely disappeared. Number of oxyproline, glutamine acid and citrulline is reduced, as compared with control, concentrations of β-alanine and tyrosine are small.

In tomato tissues contaminated with "Tomatoes bacterial cancer" pathogene - *Coryne-*

Table

Free amino acids and aminds qualitative and quantitative composition in tomato tissues diseased by bacteriosis.

I-Control: II-*Pseudomonas lycopersici*, III-*Corynebacterium michiganense*, IV-*Xanthomonas vesicatoria* (No133); V-*Pseudomonas capsici*, VI-*Xanthomonas vesicatoria* (n-148).

	1	2	3	4	5	6	7	8	9	10	11	12	13	14	15	16	17	18
	Cystein+Cystine	ornithine+Lysine	Histhidine	Orginine	Asparagine Acid+ Asparagine	Cerine+Glycine	Oxyproline+Glutamine Acid+Citruline	Threonine	Alanine	β-Alanine	Tyrosine	Tryptophan	γ-Aminobutyric Acid Methionine	Valine	Norvaline	β-Phenylalanine	Isoleucine	Leucine+Norleucine
I	-	tr	tr	tr	⊕	⊕	⊕	⊕	+	+	+	⊕	tr	tr	⊕	tr	⊕	⊕
II	-	tr	tr	tr	⊕	⊕	tr	⊕	+		⊕	⊕	⊕	-	-	-	⊕	⊕
III	-	tr	tr	tr	⊕	⊕	tr	⊕	+	⊕	+	-	-	-	-	-	tr	tr
IV	tr	tr	tr	tr	⊕	tr	tr	⊕	⊕	-	+	-	-	-	-	-	tr	tr
V	-	⊕	⊕	⊕	+	⊕	+	+	+	+	+	⊕	tr	⊕	⊕	tr	⊕	⊕
VI	⊕	⊕	⊕	⊕	⊕	⊕	+	+	+	⊕	+	tr	tr	tr	tr	-	-	-

"-" isn't found; "TR"-traces only; "⊖"-small number "+"-great number; "+"-surplus number.

bacterium michiganense, there aren't found tryptophan, γ-aminobutyric acid, methionine, valine, norvaline and β-phenylalanine, but there are traces of oxyproline, glutamine acid, citrulline, isoleucine, norleucine and leucine [5].

Various strains of "Bacterial black spot" pathogen-*Xanthomonas vesicatoria* - causes different changes in tomatoes. But development of all the types of diseases is accompanied with amino acid metabolism breach [6].

In tomato tissues inoculated with the strain N133 of *Xanthomonas vesicatoria* there aren't observed β-alanine, tryptophan, γ-aminobutyric acid, methionine, valine, norvaline and β-phenylalanine. There is a scanty number of serine, glycine, oxyproline, glutamine acid, citrulline, isoleucine, leucine and norleucine. But in the case of strain N148 of the same pathogen the increase of free amino acids total number and composition in plant tissues is obvious.

Cystein and cystine aren't found in healthy tomatoe tissues. In tissues of plants inoculated with strain N148 the above-mentioned amino acids appear in a small number. But in case of strain N133 there are only their traces. There is also observed complete disappearance of β-phenylalanine, isoleucine, leucine and norleucine and accumulation of threonine and alanine in surplus concentrations. The total number of the other amino acids is increased in comparison with healthy one.

In comparison with the healthy one in tomato tissues surplus accumulation of oxyproline, glutamine acid, citrulline, threonine and alanine is characteristic for "Pepper spot" pathogen - *Pseudomonas capsici*. During development of the above mentioned disease number of all the amino acids except β-alanine, tyrosine, norvaline, isoleucine, leucine and norleucine (their concentrations don't change) increases [7].

The changes revealed in free amino acids and amids composition of contaminated plants aren't connected only with their direct usage by pathogens. Because at the begin-

ning of disease development or by the time of increase of bacteria number, fluctuation of free amino acids and amids composition may be caused by strengthening the transaminable systems or intensification of protein synthesis.

So, infectious process caused by phytopathogenic bacteria in tomatoes is accompanied by deviations in various circles of metabolism in damaged plant tissues in comparison with a healthy one.

The revealed changes concern interrelations break of separate prosesses of metabolism, that affects physico-chemical condition of plant cell biocolloids [8].

L. Kanchaveli Research Institute of Plant Protection

REFERENCES

1. *N. A. Krasilnikov.* Biokhimiya plodov i ovoshchei, Moscow, 1970 (Russian).
2. *M. S. Matishevskaia.* Vliyanie fitogennykh bakterii na fiziologo-biokhimicheskie svoistva rastenii
3. *V. L. Kretovich.* Osnovy biokhimii rastenii. Moscow, 1961 (Russian).
4. Short determinant of Behri Bacteria. Ed. G. Hoult; G. A. Zavarzin; Moscow, 1980.
5. *MC Carter, S. Jones, R. Gitaitis, P. Smithley.* Phytopatology, 1983.
6. *A.E.Brownschtein.* Biokhimiya aminokislotnogo obmena. 1949 (Russian).
7. *V. I. Bilay.* Microorganizmy-vozbuditeli boleznei rastenii, Kiev, 1988 (Russian).
8. *B.P.Pleshkov.* Biokhimiya selskokhozyaistvennykh rastenii. Moscow, 1965 (Russian).

საქართველოს მეცნიერებათა აკადემიის მოამბე, 159, №1, 1999
BULLETIN OF THE GEORGIAN ACADEMY OF SCIENCES, 159, №1, 1999

ZOOLOGY

M.Gergedava

Tortricids (*Lepidoptera, Tortricidae*) Fauna of *Apotomis* Hbn. and *Hedya* Hbn. genera in Western Georgia

Presented by Member of the Academy I.Eliava, June 1, 1998

ABSTRACT. **The paper reports on two representatives (*Apotomis* Hbn. and *Hedya* Hbn.) from lepidopterous *Tortricidae* family in the fauna of Western Georgia. From *Apotomis* Hbn. family 7 species are revealed and from *Hedya* Gbn. – 5 species.**

Key words: tortricids

Tortricids (*Lepidoptera, Tortricidae*) represent one of the most numerous and significant family of Insecta class. In this family by the diversity of species tribe *Olethreutini* is identified to which *Apotomis* Hbn. and *Hedya* Hbn. genera belong. The goal of the present paper is to establish species composition of the mentioned families, their bioecological and morphological characteristics for Western Georgia. Based on the data obtained in different regions of Georgia it becomes evident that 12 species from the given genera inhabit in Georgia. Species and genera nomenclature and terminology of wings and genital elements are taken from Kuznetsov's works [1,2]. The data on species biology and worms nourishing ties are obtained from [3-9]. Imago morphology is given after characterization of species, then the information on nutrient plants and on species phenology follows. In each known case generation number is marked. We report on the data obtained on the basis of material collected by the author. The collection kept at St.Petersburg Institute of Zoology of the RAS was used. The species revealed in the fauna of Western Georgia are as follows:

Apotomis Lineana Den. Et Schiff. Front wings wide band in costal part is greish-white. Cornutus is thin. By its length it almost equals to aedeagus. Tortricids size with extended wings varies from 17 mm up 20 mm. The worms basically develop in curved leaves of willow. The material was obtained in Tsalenjikha region (v.Nakipu) and in Zugdidi district (v.Tsaishi).

A.Semifasciana Hw. In the aedeagus of this species cornutus are placed and additionally at the base short bristled sclerites are developed. Distal block of aedeagus is smooth. The lower edge of sacculus is round. The moths with extended wings are of 16-19 mm. The worms develop in young curved leaves of willow buds. The material is obtained in Tsalenjikha region (v. Mukhuri).

A.Lutosana Kenn. The exterior boundary at the base of front wings is not contoured which is characteristic to the individuals of different species of this genus. Cornutus is too short and by its length it is not more than one eights of aedeagus. The moths with stretched wings are of 15-17 mm. The worms are feeding between the stuck leaves of willow. Several generations develop. Some specimens were obtained at Zugdidi Botanical Gardens.

A.turbidana Hbn. The front wings of this species tortricids are comparatively wide,

about 4-5 mm. The aedeagus in distal extremity is prominent. Cornutus at the base is round. On long appendage of sacculus 50-60 short bristle sclerites are located. The moths with extended wings are of 14-20 mm. The worms develop in curved leaves of willow.

A.betuletana Hw. The band between the exterior and middle fields of front wings is continuous. It has no black spots in discal part of sineus. Discal part of aedeagus similar to the above mentioned species is prominent here too. The moths with extended wings are of 17-22 mm. The worms twist the leaves of poplar and feed on them.

A.cepriana Hbn. The exterior band of front wings is 1.5-2 mm in width and is of white color. The base of cornutus is comparatively long. The half of sacculus appendage is covered by acicular appendages. The moths length with extended wings is 17-21 mm. The worms develop in willow buds or in curved leaves, sometimes in curved leaves of poplar. Some specimens of this species were obtained in v.Nakipu.

A.sororculana Zett. The worms develop in curved leaves of tree. The tortricids fly from May up to the end of the summer. Some species are obtained in Mukhuri.

Hedya salicella L. These torticids are of comparatively big size. The dorsal half of front wings from the base to pretornal part is of white color with greyish points and colorless spots. Cuccullus is narrowed distally. The moths with extended wings are of about 21-23 mm. The worms feed on willow and poplar young leaves. The moths fly in July. The material was obtained in Martvili region (v.Salkhino).

H.nubiferana Hw. Black points are dislocated in discal part of front wings. Uncus is widened and discally divided in two. It has harpa on sacculus. The moths with extended wings are of 18-21 mm. The worms feed on apple, pear, plum, quince, cherry, brier and other leaves of *Rosaceae* family plants.

H.pruniana Hbn. The tortricids of this species have no black points. Uncus is thin and is not divided at the end. The harpa on sacculus is not developed. The tortricids with extended wings are of 15-20 mm. The worms develop on sweetbriers and roses. Several tens of specimens have been obtained in v.Tsaishi.

H.atropunctana Zett. Black spots are developed between exterior and middle fields of discal part of front wings. Uncus is thin and is not divided at the end. Females have big and wide socia. The moths with extended wings are of 14-18 mm. The worms develop in twisting leaves of birch. The material was obtained in Tsaishi and Mukhuri.

Thus, in Western Georgia 7 species from *Apotomis* genus have been obtained for the first time, whereas from *Hedya* genus 5 species become known mainly the pests.

Teachers Advanced Training Institute, Zugdidi

REFERENCES

1. *V.I.Kuznetsov*. In: Opredelitel nasekomykh evropeiskoi chasti SSSR. 4.1, 1978, 193-686.
2. *Idem*. Nasekomye i kleshchi – vrediteli selskokhozyaistvennykh kultur. St. Petersburg, I, 144, 1994, 154.
3. *F.N.Pierce, J.W.Metcalfe*. The genitalis of the British *Tortricidae-Oundle*. Northants. 1922, 101.
4. *A.S.Danilevski, V.I.Kuznetsov*. Fauna SSSR. M., 1968, 635.
5. *J.Razowski*. Acta zool. Cracow, 22, 5, 1977, 55-205.
6. *I.B.Bradly et al*. British Tortricoid Moths. *Tortricidae: Olethreutinae*. London, 1979.
7. *Yu.O.Kostyuk*. Fauna Ukrainy. Listovertki. Tortritsiny. Kiev, 15, 1, 1980, 421.
8. *G.K.Esartia* Entomologicheskoe obozrenie. L., 67, 1, 1988.
9. *H.I.Hanneman*. Kleinschmetterlinge oder *Microlepidoptera*. I. Jena, 1961, 233.

საქართველოს მეცნიერებათა აკადემიის მოამბე, 159, №1, 1999
BULLETIN OF THE GEORGIAN ACADEMY OF SCIENCES, 159, №1, 1999

EXPERIMENTAL MEDICINE

M. Jebashvili, Member of the Academy N. Kipshidze, N. Kakauridze

Characteristics of Lipid Metabolism in Menopausal Women

Presented July 6, 1998

ABSTRACT. **We have studied lipid metabolism characteristics (total cholesterol, high density lipoprotein cholesterol) in pre- and postmenopausal women. The results of the investigation have shown that dyslipidemia begins in the premenopausal period and becomes deeper during menopause which is a great risk for the development of coronary heart disease. Hence, it is more advisable to begin preventive activities during menopause before the process becomes deeper and irreversible.**

Key words: menopause, lipid metabolism

It is universally known that in women, aged 50-55, coronary heart diseases and mortality caused by them are rare. But in women (as well as in men) over that age, among all the reasons of mortality the first place is taken by coronary heart diseases. Coronary heart diseases in women proceed, upon the average, 7-15 years later than in men. It is considered in modern medicine that the age difference of this kind between men and women is caused by the cardioprotective effect of female sexual hormones [1-4].

Many clinical physicians distinguish 2 critical biological phases in female life: pubertative and climacteric. The climacteric phase is a physiological process which is going on in the reproductive system against the background of age processes with involutionary processes dominating.

It has been shown in many studies that estrogens have the ability to affect the lipid spectrum, blood coagulation and the wall of the blood vessel [5-11]. Besides, estrogens are characterised by antioxidant, calcium antagonistic, α_2-inhibitory properties and can reduce insulinoresistance [10, 12-16].

A number of investigations have shown that the beginning of menopause is accompanied by changes of lipid profile, in particular, the increase of total cholesterol, low density lipoprotein cholesterol, triglicerids, lipoprotein (a) and decrease of high density lipoprotein cholesterol that is mainly caused by the deficiency of estrogens [6-9, 17].

As a result of numerous investigations, it becomes known that cholesterol is an independent risk factor of coronary heart diseases, and high density lipoprotein cholesterol is an antiatherosclerosis factor. Following from this the main goal of our study is the investigation of these two factors in pre- and postmenopausal women.

The investigations were carried out over 44 premenopausal women, aged 40-45 (I group), 47 postmenopausal women, aged 50-60 (II group) and 35 women, aged 40-45, who do not have menopause yet (control group). The blood lipids were studied by the method based on the international standards using the spectrophotometer "LOMO-46" and France BIOLABO reagents. According to the data, obtained as a result of investigations, total cholesterol in group I amounted to 6.71±1.21 Mmol/l. High density lipopro-

tein cholesterol in group I was 2.76±0.72 Mmol/l, in group II - 0.78±0.07 Mmol/l, and in the control group - 1.85±0.87 Mmol/l.

As it is shown by the above data, dyslipidema begins in the premenopausal period and becomes deeper during menopause which is a great risk for the development of coronary heart disease. Hence, it is more advisable to begin preventive activities during menopause before the process becomes deeper and irreversible.

As it is studied in special literature, estrogens have positive effects on the lipid profile, but in spite of this a patient with a history of breast cancer is considered to have an absolute contraindication to estrogen therapy. Because of subtle changes in homeostasis, women with coagulation disorders may not be appropriate candidates for hormone replacement. Although there are not known interactions of estrogen replacement with commonly used medications, this issue has not been specifically addressed. Finally, the role of ethnic and sociologic differences in response to therapy may be significant and requires further evaluation.

Until more concrete data are available, we would recommend long term dietary treatment of premenopausal women with coronary heart disease.

Institute of Therapy, Tbilisi

REFERENCES

1. *R. Bugliosi et al.* Clinica Therapeutical. **146**, 8-9, 1995, 503-18.
2. *E. D. Eaker.* Circulation. **88**, 1993, 1999-2009.
3. *K. Gehenck-Gustaffson.* Eur. Heart J. 17, 1996, 9-14.
4. *H. Kuhl.* Therapeutische Umschau. **51**, 11, 1994, 748-54.
5. *M. G. Conlan.* Thrombosis and Haemostasis. **47**, 1, 1994, 551-6.
6. *A. Curcic et al.* Meditsinski Pregled. **47**, 1, 1995, 226-9.
7. *U. J. Gaspard et al.* Maturitas. **21**, 3, 1995, 171-8.
8. *F. Pansini et al.* Maturistas. **17**, 3, 1993, 181-90.
9. *V. Richter et al.* Zeitschrift für Gerontologie. **26**, 4, 1993, 260-4.
10. *M. N. Sack et al.* Lancet. **343**, 8892, 1994, 269-70.
11. *D. A. Shewmon.* Obstetrics and Gynecology Clinics of North America. **21**, 2, 1994, 337-55.
12. *G. I. Gorodeski.* Exp. Gerotrol. **29**, 1994, 357-375.
13. *H. Moini et al.* Endothelium. **5**, 1997, 11-19.
14. *V. A. Rifici.* Metabolism. **41**, 1992, 1110-1114.
15. *G. M. C. Rosano et al.* Eur. Heart J. 17, 1996, 15-19.
16. *S. A. Samaan et al.* J. Am. Coll. Cardiol. 26, 1995, 1403-1410.
17. *B. M. Posner.* Heart J. 125, 1993, 483-489.

საქართველოს მეცნიერებათა აკადემიის მოამბე, 159, №1, 1999
BULLETIN OF THE GEORGIAN ACADEMY OF SCIENCES, 159, №1, 1999

EXPERIMENTAL MEDICINE

A. Abdusamatov

The Effect of Cobalt Coordinate Compounds on Bile Secretion Function of Liver in Experimental Heliotrin Hepatitis

Presented by Member of the Academy T.Oniani, November 9, 1998

ABSTRACT. **Cobavit, phytat-cobalt, preparation VUC and silibor effect on the bile secretion in animals with experimental hepatitis was studied. Rats were infected with toxic hepatitis by alkaloid heliotrin. It was marked that preparations stimulated bile secretion in rats with hepatitis. Chemical composition of the bile was normalized.**

Key words: toxic hepatitis.

At present one of the important roles in increasing of liver toxic diseases belongs to weeds. The most poisonous is heliotrope fetusfallen which getting into man's food with bread grains causes heavy poisonings. This plant contains heliotrin alkaloid, causing inhibition of hepatocyte ferment system activity and excretory and bile forming liver function depression [1].

The aim of our investigation was to study the effect of new cobalt coordinate compounds: VUC preparation (vitamin U with cobalt), cobavit (vitamin U and glutamine acid with cobalt) and phytat-cobalt (phytine with cobalt) - on bileforming and excretory liver function compared with essentiale and silibor during experimental hepatitis.

The experiments were carried out on white male rats with 160-180 gr. body mass weight, which were infected with chronic hepatitis by intravenously introduced heliotrin [2]. Seven groups with 9-10 rats in each were put under test. Animals of intact (1st) group were given an appropriate volume of water during the investigation. Animals of control (2nd) group were injected with heliotrin. Animals of 3-7 groups to prevent the development of toxic hepatitis together with hepatotoxin were injected with cobavit, phytat cobalt, essentiale, silibor and VUC hypodermically in the doses of 5, 200, 50, 100 and 5 mg/kg during 30 days.

The bile excretory intensity, bilirubin, cholesterin excression and bile acids according to methods in [3] showed functional liver condition. The results were worked up by the method of variation statistics at $P=0.05$ [4].

The data show that long introduction of heliotrin to rats sufficiently decreases bile secretion intensity and as a result it decreases its general quantity, which was gotten for 4 hours of observation on 48.55% against the intact group 1.01 ± 0.045 ml. Bile acid synthesis is distinctly inhibited, cholesterin and bilirubin excretion becomes harder. Their content in the bile composition decreased correspondingly on 71.6, 64.4 and 57.5%, while bile acid level of intact rats composed 12.28 ± 0.44 mg, cholesterin 0.132 ± 0.016 and bilirubin 0.04 ± 0.0017 mg.

საქართველოს მეცნიერებათა აკადემიის მოამბე, 159, №1, 1999
BULLETIN OF THE GEORGIAN ACADEMY OF SCIENCES, 159, №1, 1999

PALAEOBIOLOGY

E. Kharabadze

Trunk Vertebra of the Worm Snake (*Typhlops vermicularis*) from Tsurtavi (South-Eastern Georgia; Holocene)

Presented by Member of the Academy L. Gabunia, February 20, 1998

ABSTRACT. **In the present paper single trunk vertebra of worm snake *Typhlops vermicularis* (Reptilia:Serpentes:Typhlopidae) is described. It has been discovered in Tsurtavi locality (South-Eastern Georgia; Holocene). This is a very first finding of fossil *Typhlops* for the whole territory of the former USSR and particularly for the Caucasus.**

Key words: snake, fossil, *Typhlops*, Tsurtavi, SE Georgia, Holocene.

Tsurtavi locality is situated in South-Eastern part of the Republic of Georgia, Bolnisi region, on the left bank of the river Khrami, village Tsurtavi (former Qolagir, erroneously Arakhlo or Arukhlo [1-3]), 30 km South-Westwards from Tbilisi.

It presents lias type scorched, reddish clays, which are allocated directly under the doleritic lava. Quantity of clayey fraction is less than such of sandy sediment. Here and there we can find calcinated concretions. During the expedition in 1997 in the same layer, a little westwards we found seeds of *Celtis*. The same plant is known also from Dmanisi locality.

As far back as in 1977 here were A. Vekua and V. Chkhikvadze on a short time excursion where the latter found fossil remains of the following amphibians and reptiles: *Bufo viridis, Rana ridibunda, Pelobates siriacus, Daboia lebetina* and *Natrix sp.* [4].

Till now there was no consensus about the age of this layer. A. Vekua reputed it Holocene and considered that all this fauna is brought under the doleritic lava by water flow and presents an aluvial sediment of the river Khrami. During the expedition in November, 1997 (V. Chkhikvadze, E. Kharabadze) it became clear that the red layer under dolerits containing molluscs is Pliocenic (probably, Upper Pliocenic) and it is older than Dmanisi locality. As for vertebrate remains (see below), thay are fell from above, just from sediments accumulated in gaps between single doleritic lava blocks. These sediments evidently must be Holocenic.

During an expedition in 1997 we washed nearly 0.25 m^3 sediments and discovered *Typhlops vermicularis* (Fig.) and *Rodentia indet.*

In this layer we found lots of remains of terrestrial molluscs (at least 3 species). Morphologically they are alike of recent *Xerophila* and *Melanopsis.*

Though only one single trunk vertebra of a worm snake has been discovered, it gives us right to consider that this species does live nowadays in Bolnisi region (South-Eastern Georgia). It must be said that *Typhlops vermicularis* was not known for this region till now [5, 6]. Moreover, for the present day in this part of Eurasia only this one species of

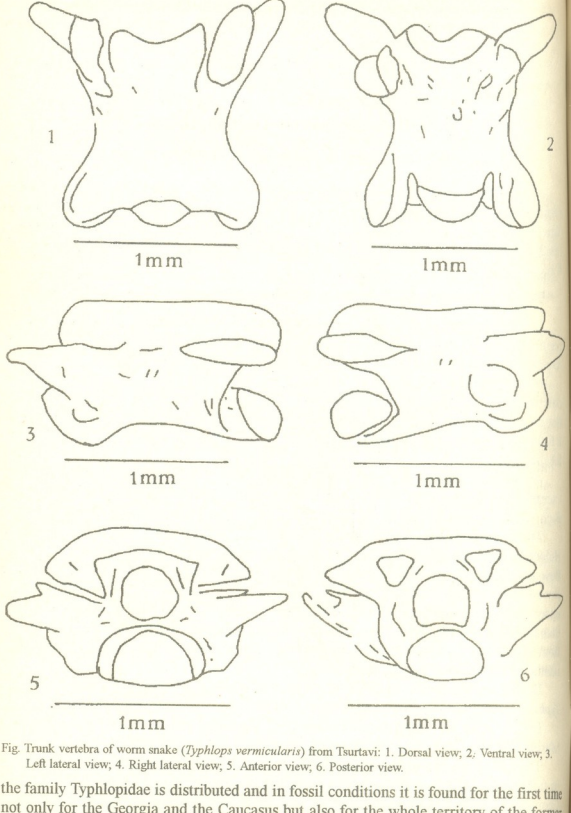

Fig. Trunk vertebra of worm snake (*Typhlops vermicularis*) from Tsurtavi: 1. Dorsal view; 2. Ventral view; 3. Left lateral view; 4. Right lateral view; 5. Anterior view; 6. Posterior view.

the family Typhlopidae is distributed and in fossil conditions it is found for the first time not only for the Georgia and the Caucasus but also for the whole territory of the former Soviet Union. We must underline that a trunk vertebra of worm snake found in Tsurtavi

is very small in size, what is typical for this species. Perhaps, only with this we can clarify the fact that till present there is not a single finding of fossil remains of snakes from the given family for this vast territory [7, 8].

Below follows the description of this material. Anatomical terminology and basic ratios see in [9, 10].

Order **SERPENTES**
Suborder **Scolecophidia**
Family **Typhlopidae**
Worm snake *Typhlops vermicularis*

Description: extremely small sized trunk vertebra. Centrum has a shape of prolongated cilindre narrower in the middle part. In the lateral view the ventral part is clearly concave. Haemal keel absent. Cotyle and condyle oval, flattened from below. Articular surface of condyle is evidently dorsally oriented. From below we can see not only the upper edge of condyle but also a considerable part of the contiguous articular surface. An upper edge of cotyle is deeply notched. Paracotylar foramina situated too close to cotyle. Paradiapophyses are big enough. Among them parapophyses are bigger than diapophyses and neither of them has processes. Long axises of paradiapophyses inclined to the main axis of centrum. Subcentral ridges not well developed but clear enough. Interzigapophyseal ridges discontinious and weakly developed. Subcentral foramina situated unusually close to cotyle, near the postero-lateral edges of diapophyses (ventral view). Lateral foramina are situated approximately in the center of centrum (lateral view). Prezigapophyseal articular surfaces have a shape of very prolongated ovals. Longest axis of each of them is nearly parallel to medial line or makes with them very keen angle. Sum of these angles is approximately $45\text{-}50^0$. Prezygapophyseal processes of middle size and obtuse. From above each of them is prolongated antero-laterally and the line between them obviously overlap lateral edges of zygosphene. From above the width of these processes is narrowly less than the width of prezygapophyseal articular surfaces. Postzygapophyseal articular surfaces have a shape of very prolongated ovals and the longest axis of each of them is nearly parallel to medial line. Epizygapophyseal processes are not presented but the caudal edge of the roof of neural arch on the both sides of axis of symmetry is clearly concave. Caudal part of neural arch is very wide and its hind edge has a form of double waved contour with a very small sized process in the center. Zygosphene is wide enough but maximal width of it (zw) is lesser than centrum width (cw,=naw). Lateral edges of zygosphene from above prolongates anteriorly and central part is shorter and has a form of concave arch. From anterior view dorso-ventral thickness of zygosphene (zt) is far more lesser than the height of a neural canal (nch). Articular facets of zygosphene are oval and they make keen angle with a medial plane. Neural canal round. Its height (nch) is nearly the same as its width (nsw) and has a form of full circle in transverse cutting. A height of neural arch from the bottom of neural canal to the surface of zygosphene's upper edge (nah) is a little lesser than the height of cotyle (cth). Neurapophysis absent. Dorsal edge of zyganthrum is too wide and its fossae have nearly the shape of regular triangles. Slope of zyganthral articular facets conform to slope of zygosphenal articular surfaces (z^0).

The most important ratios are given in the Table.

Table

cl/naw	nlu/nls	naw/po-po	cl/col	nlu/nh	cl/zt	ctw/cth
1.68	-	0.67	4.21	-	14.75	1.33
cl/nlu	zw/naw	nlu/cl	pr-pr/pr-po	zw/cl	cl/zw	pr-pr/naw
-	0.77	-	0.79	0.46	2.18	1.43

By morphological characteristics vertebra of worm snake discovered in Tsurtavi does not differ from the vertebrae of the same species of snake living nowadays in Europe [11].

Thus it has been ascertained that the remains of amphibians and reptiles found in Tsurtavi till present are of Holocene age and not of Pliocene (Late Pliocene) as they consider before. Vertebra of *Typhlops vermicularis* discovered here is a unique finding as despite of its extremely small size, it has been found for the first time not only for the Georgia and the Caucasus but for the vast territory of the former Soviet Union.

Finally, I would like to thank Dr. V. M. Chkhikvadze helping me to collect material and prepare the manuscript.

Georgian Academy of Sciences
L. Davitashvili Institute of Palaeobiology

REFERENCES

1. *E. Kharabadze.* Bull. Georg. Acad. Sci. **153**, 3, 1996, 470-473.
2. *E. Kharabadze.* Bull. Georg. Acad. Sci. **156**, 1, 1997, 151-154.
3. *E. Kharabadze.* The Third World Congress of Herpetology. Abstracts. Prague, 1997, 2-10 August, 110-111.
4. *V. Chkhikvadze.* Proc. Acad. Georg. Sci. **152**, 3, 1995, 663-667 (Russian).
5. *T. Muskhelishvili .* Reptiles of the Eastern Georgia. Thilisi, 1970, 1-242 (Russian).
6. *A. Bannikov, I. Darevski, et al.* Guide for the fauna of amphibians and reptiles of the USSR. Moscow, 1977, 1-414 (Russian).
7. *G. Zerova, V. Chkhikvadze.* Proc. Georg. Acad. Sci., ser. biol. **10**, 5, 1984, 319-326 (Russian).
8. *M. Bakradze, V. Chkhikvadze.* Bull. Georg. Mus., Tbilisi, 34-A, 1987, 176-193 (Russian).
9. *E. Kharabadze.* Bull. Georg. Acad. Sci. **153**, 1, 1996, 150-153.
10. *J.-C. Rage.* Serpentes. Encyclopedia of Paleoherpetology, G. Fischer Verlag, Stuttgart - New York, 11, 1984, 1-80.
11. *R. Hoffstetter, J.-P. Gasc.* Vertebrae and ribs of modern reptiles. Biology of the Reptilia, 1. A. Academic, London, 1969, 201-310.

საქართველოს მეცნიერებათა აკადემიის მოამბე, 159, №1, 1999
BULLETIN OF THE GEORGIAN ACADEMY OF SCIENCES, 159, №1, 1999

Corr. Member of the Academy G.Nakhutsrishvili

To the Study of Biotopes Diversity in Kazbegi Region

Presented November 9, 1998

ABSTRACT. **Some regularities of biotopes diversity have been studied in Kazbegi region.**

Key words: ecotope, biotope, subalpine, alpine.

The study of biotopes is of great significance for integrated knowledge of natural environment [1,2]

Kazbegi region is situated on the boundary of Central and East Caucasus (42°48′N, 44°99′E). It is distinguished by great range of species and biotopological diversity which should be mainly explained by its disposition on the junction of numerous quite different phytolandscapes of the Caucasus, and also by strong ruggedness of relief and rather complicated geological structure. The intensive anthropogenic action (felled forests, heavy grazing, oil pipelines building, etc.) has a negative effect on biological and biotopological diversity of the given region.

Thus, for example, on singles of the Terek River alluvion as a result of building material an endemic and rare species *Cladocheta candidissima* disappeared and on the Jvari pass as a result of oil pipeline the biotope of endemic species *Galanthus platyphyllus* passed into a pit.

The aim of our studies was to reveal the biotopes diversity and their floristic composition on one of the sections of Kazbegi region and to give ecological and phytocenotical characteristics of these biotopes. The study of biotopes was carried out from 1800 to 2500 m ASL in 1998. The description of biotopes was conducted utilizing the methods of Wilmanns and Pedrotti [2,3]. For describing the vegetation the transective method was applied. The area of biotopes description (elevation above sea level; slope exposure; fall; mechanical compositions of the soil; species composition) is mainly 5mx5m. Only phanerogamous plants have been recorded in the floristic list.

We have distinguished the following biotopes in Kazbegi region (with various combinations of plant species - phytocenosis): water, swampy, heavily moistened, mesophytic, mesoxerophytic, arid, cool humid, cool arid, rock and scree biotopes.

There are few water biotopes in Kazbegi region. They are mostly found on the shore of the Terek River (1700-1800 m ASL); their species composition is not marked by diversity: *Hyppuris vulgaris, Batrachyum divaricatum, B.rioni, B.trichophyllum, Veronica anagalis-aquatica* etc. The names of species are given according to Sakhokia and Khutsishvili [3].

Swamp biotopes in the region under study are found almost in all vertical belts. Their floristic composition is not rich within one biotope. More than 30 species are seldom found.

Mesophytic and mesoxerophytic biotopes are the richest in species. Here are found more than 50-60 species (within the whole biotope).

To make an image about the diversity of these biotopes we have studied a small section, by profile extension 2.5 km (from the Georgian Military Highway, 1800 m to Mount Elia, 2050 m ASL)

1.Swampy meadow: *Phragmites australis - Equisetum palustre - Parnassia palustris - Calamagrostis pseudophragmites*; 1800 m ASL, peat soil, plant coverage is 80%, the height of grass stand is 50-60 cm; number of species is 15 (area 5mx6 m).

2.Mesophytic fertile meadow: *Hordeum violaceum - Festuca pratensis - Seseli transcaucasica - Ranunculus elegans*; 1850 m ASL, southern slope exposure, fall – 5-7°, the soil is very skeleton, slightly swardy, grass stand height is 120 cm, plant coverage - 100%, number of species is 25.

3.Mesoxerophytic rough meadow: *Festuca ovina - Bromopsis variegata - Ranunculus oreophilus*, 1870 m ASL, southern slope exposure, fall-5°, swardy, very skeleton soil, plant coverage is 90%, grass stand height is 20 cm, number of species - 26.

4. Mesophytic rough meadow: *Festuca ovina - Agrostis tenuis - Trifolium ambiguum - Ranunculus oreophilus*, 1870 m ASL, flat relief, swardy, very skeleton soil, plant coverage - 90%, the height of grass stand is 40 cm, number of species - 28.

5.Dry rough meadow: *Bromopsis variegata - Festuca ovina - Koeleria caucasica*, 1900 m ASL, the slope of southern exposition, fall 30°, swardy, very skeleton soil, plant coverage 70%, height of grass stand - 50 cm, number of species - 23 (5mx1m).

6.Mesophytic rough meadow: *Bromopsis variegata - Agrostis tenuis - Trifolium ambiguum*, 1900 m, southern slope exposure, fall 5°, swardy, very skeleton soil, plant coverage - 100, the height of grass stand - 70 cm, number of species - 29 (5mx10 m).

7.Mesophytic rough meadow: *Arrenatherum elatius - Festuca ovina - Ranunculus oreophilus - R.caucasicus*, 1900 m ASL, southern slope exposure, fall - 5°, soil is slightly swarding, very skeleton plant coverage - 100%, the height of grass stand - 50 cm, number of species - 27.

8.Rock biotope: *Campanula bellidifolia - Pulsatilla violacea - Saxigraga cartilaginea - Sempervivum pumilum*, 1900 m ASL, south-western slope exposure, fall-70°, plant coverage - 30%, number of species - 20.

9.Dry fertile meadow: *Festuce varia - Helictotriochon asiaticus - Oxytropis albana - Carex meinshauseniana*, 1900 ASL, south-western slope exposure, fall - 30°, the soil is developed on mare slates, shallow, very swardy and skeleton, plant coverage - 90%, grass stand height is 70 cm, number of species - 32.

10.Mesophytic fertile meadow: *Festuca varia - Carex meinshauseniana - Polygonum carneum - Betonica macrantha - Anemone fasciculata*, 1950 m ASL, north-western slope exposure, fall-40°, swardy soil, skeleton plant coverage - 100%, grass stand height - 80 cm, number of species - 28.

11. Dry rough meadow: *Festuca rupicola - Koeleria caucasica - Pulsatilla violacea - Carex buschiorum*, 2050 m ASL, the slope of southern exposure, fall-15°, soil is dense-swarding, skeleton plant coverage - 90%, number of species - 32.

12.Dry stony biotope: *Thymus collinus - Campanula bellidifolia - Silene ruprechtii,*

2050 m ASL, southern slope exposure, fall-20°, soil is medium-swardy, plant coverage - 90%, grass stand height 15 cm, number of species - 11 (1mx1m).

13.Mesophytic rough meadow: *Vicia alpestris - Festuca ovina - Bromopsis variegata*, 2050 m ASL, south-western slope exposure, fall-10°, swardy soil, plant coverage - 100%, number of species - 26.

There is one more example: profile in alpine belt (2420-2500 m ASL), at the Cross pass, profile length is 500 m:

1.Cool-humid rough meadow: *Nardus stricta - Phleum alpinum - Poa alpina - Sibbaldia semiglabra*, the slope of western exposition, fall-15°, very swardy, peat soil, plant coverage 95%, grass stand height is 20 cm, number of species - 21.

2. Cold fertile meadow: *Festuca varia - Carex meinshauseniana - Oxytropis albana*, 2500 m ASL, the slope of southern exposition, fall-35°, swardy skeleton, soil, plant covering - 100%, grass stand height is 70 cm, number of species - 23.

3.Cold mesophytic, rough biotope. Low productivity meadow: *Agrostis tenuis – Poa alpina - Phleum alpinum-Sibbaldia semiglabra*, 2500 m ASL; the slope of northern exposition, fall is 10°. Swardy, peaty, small stony soil. Plant coverage - 100%, grass stand height is 30 cm, number of species is 19.

Thus, quite different biotopes are rather clearly distinguished on comparatively small area of Kazbegi region. Their species composition is rather rich, e.g. in subalpine belt on the area (5x5 m^2) in average 26 species of phanerogamous plants are found.

Biotopes of southern slopes are distinguished by the richest species composition (about 32 species) and swamp biotopes - by the lowest one (15 species). In alpine belt biotopes species composition is a little lower and as it is in subalpine zone, comparatively numerous species (23 species) are found on the southern slope.

Georgian Academy of Sciences
N.Ketskhoveli Institute of Botany

REFERENCES

1. Biotoptypen in Österreich. Umweltbundesamt. Wien, 1989.
2. *F.Pedrotti*. Ecologie, **29**, 1-2, 1998, 105-119.
3. *M.Sakhokia, E.Chutzishvili*. Consepectus florea plantarum vascularium Chewii. Tbilisi, 1975.
4. *O.Wilmanns*. Ökologische Pflanzensociologie. Quelle, Meyer Heidelberg – Wiesebaden, 1993.

საქართველოს მეცნიერებათა აკადემიის მოამბე, 159, №1, 1999
BULLETIN OF THE GEORGIAN ACADEMY OF SCIENCES, 159, №1, 1999

ECOLOGY

M.Gabunia

The Influence of Technogenic Factors on the Content of Plastid Pigments in Woody Plant Leaves

Presented by Member of the Academy G.Gigauri, July 8, 1998

ABSTRACT. **The action of technogenic factors on the leaves of woody plants (*Quercus Hartwissiana* stev., *Fraxinus excelsior* L., *Ulmus minor* Mill, *Robinia pseudoacacia* L.) has been studied. The analysis of anatomic structure of woody plant leaves testify that *Fraxinus excelsior* L. appears to be the most stable.**

Key words: woody plants, chlorophyll, carotene, xanthophyll.

The study of plastid pigments (chlorophyll, carotene, xanthophyll) amount and dynamics has a great practical significance, because determinant process of plants productivity – photosynthesis is in close connection with pigments accumulation in leaf mesophyll. Among plastid pigments, chlorophyll is of special importance, which is not limited only by the participation in photosynthesis. As a dynamic system it is characterized by vividly expressed diversity of biological functions. Chlorophyll affects plant growth and morphogenetic processes [1-2]. In some cases it fulfills the function of substance of temporal storage, and takes part in secondary synthesis of organic substances.

Besides chlorophyll there are yellow pigments in green plastids, i.e. carotenoids among which carotene and xanthophyll are widely spread. Carotenoids represent not only pigments widely spread in nature, but substances fulfilling variety of functions in plant organism. Particularly, carotenoids represent storage carbohydrates and participate in the process of carbon assimilation [1,3], influence growth [4] and reproductive processes [5].

The experimental materials were obtained in the districts of Kutaisi polluted by waste products such as large industrial objects as Kutaisi automobile factory, factory of rubber goods, area of Kutaisi airport. Ecologically pure object was considered to be the territory of the resort house Sairme. The plants in the polluted districts of the town are conditionally called experimental, whereas the same species plants in ecologically pure zone – control.

The experiment was done on four species of woody plants which by their anatomic structure belong to arched vessel species. They are: *Quercus Hartwissiana* stev., *Fraxinus excelsior* L., *Ulmus minor* Mill, *Robinia pseudoacacia* L.

In plants of the same species leaf plastid pigments have been studied on control area which is in 70 km from the zone polluted by industrial waste products.

The content of plastid pigments in mature leaves of both control and experimental variants is studied by D.Sapozhnikov's method. The material for analysis was taken in July 1993-96. The results of the analysis are given in the Table.

Table

Plastid pigments content (mg) in mature leaves of woody plants

Plant		Chlorophyll	Carotene	Xanthopyll
Quercus Hartwissiana Stev.	Control	0.281	0.072	0.093
	Experimental	0.148	0.035	0.045
Ulmus minor Mill.	Control	0.169	0.071	0.089
	Experimental	0.124	0.043	0.052
Fraxinus excelsior L.	Control	0.191	0.033	0.067
	Experimental	0.164	0.023	0.048
Robinia pseudoacacia L.	Control	0.177	0.068	0.072
	experimental	0.111	0.036	0.035

As it is seen from the Table the experimental plants differ from each other by the content of plastid pigments. Chlorophyll dominates in leaves of all studied plants , then comes xanthophyll, but carotene amount is far back chlorophyll and xanthophyll. This regularity is noted both in control and experimental plants. It was established that air pollution by technogenic factors makes negative influence on chlorophyll, carotene and xanthophyll content. That's why the amount of the mentioned pigments in control variant is far more than it is in the leaves of the same plant in experimental variants.

Among the studied plants the oak appeared to be less resistant towards air pollution. Under the action of technogenic factors in the leaves of oak chlorophyll content decreases to 47.3%, carotene to 51.3%, but xanthophyll to 51.0%.

Robinia pseudoacacia in leaves of which the difference between control and experimental variants in chlorophyll content makes 37.0%, in carotene and xanthophyll content correspondingly 47.0% and 51.3% shows less resistance.

According to our data in conditions of western Georgia particularly in Kutaisi region *Fraxinus excelsior* L. in the leaves of which under the action of technogenic factors chlorophyll amount is decreased only by 14%, carotene by 30.3% and xanthophyll by 28.3% reveals more resistance.

Plants of different species respond to the above mentioned factors not in the same way. In our conditions *Fraxinus excelsior* L. seems to be the most stable, *Robinia pseudoacacia* L. and *Ulmus minor* Mill. are less resistant, but the oak (*Quercus Hartwissiana* Stev.) suffers most of all from the action of technogenic factors. Thus the negative influence of waste products on woody trees is revealed in decrease of plastids and especially chloroplasts in leaf mesophyll retarding photosynthesis activity whose intensity conditions the synthesis of organic substances and productivity of ecosystems also confirmed in [7].

Kutaisi A.Tsereteli State University

REFERENCES

1.*S.I.Lebedev.* Fotosintez. Kiev, 1961 (Russian).
2.*E.R.Giubenet.* Rastenie i khlorofil. M., 1951 (Russian).
3.*V.B.Savinov.* Karotin (provitamin A), poluchenie ego preparatov. M.-L., 1948 (Russian).
4.*M.Kh.Chailakhyan.* Doklady AN SSSR. 2, 1952.
5.*E.V.Budnitskaia.* Doklady AN SSSR. 4, 1952.
6.*D.I.Sapozhnikov.* Eksperimentalnaya botanika. IV. 8. M.-L., 1966 (Russian).
7.*M.Gabunia, R.Tutberidze.* Bull. Georg. Acad. Sci. **157**, 1, 1998.

11. "მოამბე", ტ. 159, №1, 1999

ECOLOGY

A. Saralidze, G. Saralidze

Ecologically Safe Technology of Vegetable Growing on the Poor and Inarable Lands

Presented by Member of the Academy P. Naskidashvili, July 13, 1998.

ABSTRACT. **We offer a method of gutter ecotechnology, which guarantees intensive cultivation of vegetables and other cultured plants in all kinds of soils and provides double yield of ecologically pure production without environment pollution.**

Key words: perforated partition, drainage glass fibre, washed sand.

The area of arable lands of Georgia is about 780 thousand hectare including a great deal of poor lands not satisfying the demands of market economy. Therefore, profitable use of these lands and reclamation of about half a million hectare of inarable lands is of great significance.

Out of inarable and poor lands reclamation of 205 thousand hectare of saline soils and salt-marshes is very actual because a great deal of this kind of lands occupy plain, irrigatable zone of high solar irradiation (Gardabani, Marneuli, Sighnaghi), cultivation of which permits to grow vegetable all the year round and satisfy the chief demands of the population of the country on these products. Consequently the released fertile lands can be used for grain growing. Unfortunately, existing methods do not permit complete cultivation of these lands.

It must be noted that traditional methods of vegetable production do not conform to the ecology safety demands. Due to irrigation and rainfalls 5-15% of applied fertilizers passes from the tillage strata of the soil to the open ground polluting the lower horizon of the soil and the ground waters too. Besides, on applying the dry fertilizers 5-24% of nitrogen is sublimated [1]. In the protected ground the fertilizers are washed down more intensively reaching 70% [2].

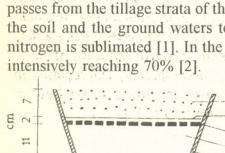

Fig. 1. Ecological gutter drainage (cross section): 1) gutter; 2) perforated partition; 3) drainage and percolator channel; 4) drainage glass fibre; 5) washed sand and metallurgic slag.

In order to "revive" the mentioned lands to receive the high yield of desirable vegetables and other competitive cultures (sugar beet, sunflower, cotton, etc) without polluting the environment we must use ecologically safe gutter technology (ecotechnology). It is based on the method of intensive cultivation of the plant on the reduced area and volume of the soil medium (without changing the air medium). The principle of the ecotechnology lies on the ecological gutter drainage (ecodrainage) (Fig. 1).

Gutter technology is used in the principal zone of plant root extension. The gutter is better to be made of plastics which can be moulded

in the extrusive plant. The gutter is to be installed in ecological vegetation ditch of 82-85 cm width by 60-65 cm depth and 0.5-1.0:100 inclination (Fig. 2).

Before planning, the best part of local ground must be selected for the soil-ground, which should be added by manure, peat, treated refuse, sawdust or any kind of vegetation remaineder to obtain quite a fertile soil-ground.

Vegetation ditches, including idling sprocket tracks, drainage and irrigation system complex are generally called ecologically safe system of plant intensive cultivation (ESSPIC) or the gutter ESSPIC (Fig. 2).

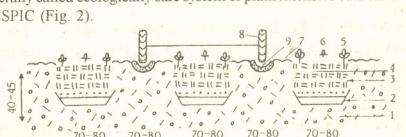

Fig. 2. Gutter FSSPIC (cross section): 1) soil; 2) gutter ecodrainage; 3) channel wall; 4) nutritive soil-ground; 5) plant; 6) watering system; 7) vegetation ecoditch track; 8) tractor wheel; 9) idling sprocket track.

In gutter ESSPIC the irrigation system, nutritive soil-ground and the mineralized water passing from it make one circuit (Fig. 3). It provides optimal regulation of humidity and nutrition regime as well as complete ecological safety. In the process of watering and rainfall the superfluous water containing a great deal of nutritive materials passes to the gutter drainage skimming channel, gets to the watercatchment main and then goes to the reservoir, where it is added by the conditioned water, necessary for the next watering. After that it is delivered to the watering system by means of a pump. The same process is repeated per watering. It ensures the artificial circulation of water and nutritive materials, which provide significant economy of water and fertilizers and also protects the underground and groundwater from pollution. Besides, sublimation of applied fertilizers is reduced to minimum.

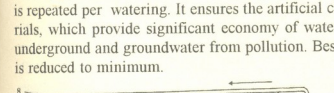

Fig. 3. Scheme of artificial circulation of water and nutritive materials in the gutter ESSPIC (longitudinal section): 1) gutter ecodrainage; 2) partition; 3)drainage and percolator channel; 4) drainage glass fibre; 5)metallurgic slag or washed sand; 6) soil-ground; 7) plants; 8) water deflector; 9)water reservoir; 10) pump; 11) water tap (the point shows the direction of water flow).

The system permits to carry out watering with the increased norm in cloudy periods and to keep the drainage water for the sunny period. It guarantees the reduction of nitrate azote content in production. And when the content of heavy metals in the drainage water is increased the ground must be washed down to reach the permittable norm and the water must be transferred from the reservoir to the cleaning structure.

Main principle of cultivating the salinizated soil by gutter ecotechnology is that the best part of the soil of the territory is to be placed in the channel. After fertilizing it the

channel will be filled up by organic fertilizer. At first the soil is periodically watered by condition water until its desalinization. Its resallinization is excluded.

Gutter ecotechnology was tested in the open as well as in protected ground in Okhurei (Ochamchire region), Akhalsopeli (Khobi region) and in the territory of Krtsanisi greenhouse complex with the best results [3].

The gutter ecotechnology guarantees vegetable continuous production all the year round in the open ground of Gardabani, Marneuli, Lagodekhi, Tskaltubo and Samtredia warm zones.

Out of 2-3 harvest 80-120 t of ecologically pure production can be obtained per hectare that will give the profit of 4500-5500 GEL. Double effect is guaranteed by the use of temporary cover of polymeric film. Gutter ecotechnology construction will cost about 45 thousand GEL per hectare. Exploitation endurance is 50-60 years. To use them in farming is advisable. Besides, it must be tax free.

Realization of mentioned ecotechnology on great area must be carried out according to the project made by designing organization while on small areas practical participation of Agricultural Institute is sufficient.

Georgian Scientific Research
Institute of Agriculture

REFERENCES

1. *O. Zardalishvili, T. Urushadze.* Sasukebis gamoqeneba da garemo, Tbilisi, 1992 (Georgian).
2. *G. G. Vendilo, V. N. Mikanaev,, V. N. Petrichenko, A. A. Skarzhinskii.* Udobrenie ovoshnykh kultur. Moskva, 1986 (Russian).
3. *A. Saralidze.* Proceedings of the Scientific-Research Institute of Agriculture. XXXIX, Tbilisi, 1995 (Georgian).

საქართველოს მეცნიერებათა აკადემიის მოამბე, 159, №1, 1999
BULLETIN OF THE GEORGIAN ACADEMY OF SCIENCES, 159, №1, 1999

LINGUISTICS

M. Rusieshvili

Toward the Binary Oppositional Archetypal Structure of a Proverb

Presented by Corr. Member of the Academy A. Gvakharia, February 24, 1998

ABSTRACT. **The author proposes that the distinctive feature of a proverb differentiating it from other forms is the existence of an archetype in its semantic structure.**

Key words: proverb, archetype, binary opposition, layer, semantics, presupposition, explicit, implicit, level.

We propose that a proverb contains a binary semantic opposition on every layer of its semantics and on the layer of its logical perception, to be more concrete, we propose that a proverb is based on an archetype. This property of a proverb may be considered to be distinctive, differentiating a proverb from other forms of a language containing a trope on the one hand (idioms, phraseological units) and paremiological or literary-folklore small forms (aphorisms, riddles, jokes, etc.) on the other. The existence of an archetypal opposition in the semantic structure of a proverb can be explained by the fact that a proverb is a metaphoric expression of wisdom accumulated by a man in the process of the perception and differentiation of the world and the archetype is a result of general (and not concrete) human differentiation of the world.

We propose also that the semantic structure of a proverb can be presented as hierarchical synthesis of three interdependent and interwoven levels: presuppositional, explicit and implicit levels. In the situation "Don't be angry with him, you know, birds of a feather flock together" the explicit level actualizes a metaphoric proverb with an intensive, easily-remembered image; on the same level implicit and allusive components of meaning are actualized and on the presuppositional level the part of the model of the world connected with the knowledge of the fact that the birds of the same breed tend to flock together is realized [1].

If the speaker uses "an ordinary" utterance instead of a proverb, e.g. "Don't be angry with him, they have much in common and, consequently, they're friends", the rich presuppositional background and the effect connected with the usage of the proverb will be lost.

The implicit level of the semantic structure of the proverb, on its turn, is characterized by a hierarchical structure consisting of two layers: one of them actualizes the second (implied) meaning of the trope (metaphor). The implicit meaning of the Georgian proverb "sxvisi čiri, ɣobes čxiri (other man's trouble, a stick to a fence) means that a man doesn't care about the other man's trouble. Besides this, here we see one more layer of the implication, concretely, the implied meaning of "ɣobes čxiri" or "uninteresting, insignifi-

cant problem".

One more example, e. g. "vardi ueklod aravis moukrepia" (nobody has ever picked a rose without a thorn). In this example, on the explicit layer there is an opposition between a rose and a thorn (emotional-perceptive opposition). On the first layer of implication it can be perceived that kindness can't be achieved without evil and troublesome.

We propose that beyond this layer there's another one. The 2nd layer of the implication, the archetypal layer emerging up from the depth of human perception, is realized as a background and fixing an archetypal opposition: kind/evil: bad/good.

Some proverbs are based on more than one archetypal opposition: e. g. "csixe šignidan ţqdeba" (a castle is broken from inside). Here on the first layer of implication the fact that one is betrayed by one's kin is realized. On the second layer of the implication two archetypal structures are arranged: mine/the other's; betrayal/devotion; The latter opposition can be reduced to good/bad ~ kind/evil.

The objective character of our proposal can be strengthened by the fact that the words "devotion" and "betrayal" have the semes of logic assessment in their semantic structure. In betrayal there's a seme "bad" and in "devotion" - good;

One archetype can be a foundation for more than one many proverbs. The more general is the archetype or, in other words, the deeper it submerges into the depth of the "collective unconscious" [2] the more proverbs may be based on it. This phenomenon can have the opposite side: one proverb containing one explicit opposition may be based on more than one implicit archetypal oppositions (see above).

The aim of a proverb is to state some wisdom and not a fact. The Georgian proverb "rac mogiva davitao, qvela šeni tavitao" (what happens to you, happens because of you) is based on the wisdom equal to karma "you're the author of your own life"; the archetypal structure of this proverb is evident the permanent problem from the Greek tragedy up till today- I/the other; (I ~ my life, the other ~ fate).

Judging from the above mentioned we can propose that on the underlying layer (2nd layer) of the implication of the semantic structure of a proverb universal archetypal structure is realized, and on its surface layer its unique national structure.

The fact of existence of archetypal opposition is the underlying nucleus of a proverb and we think that this fact can become the clue to various classifications of a proverb.

Tbilisi I. Javakhishvili State University

REFERENCES

1. *M. Rusieshvili*. Andazis semantikuri struqturis ierarkiis šesaxeb. B. Jorbenaqis sazogadoebis IV samecniero konperenciis masalebi, Tbilisi, 1997 (Georgian).
2. *C. G. Jung*. Analytical Psychology, Its theory and Practice. London, 1995.

საქართველოს მეცნიერებათა აკადემიის მოამბე, 159, №1, 1999
BULLETIN OF THE GEORGIAN ACADEMY OF SCIENCES, 159, №1, 1999

LINGUISTICS

T. Sikharulidze

The Languages of National Minorities and Diasporas

Presented by Member of the Academy K.Lomtatidze, February 14, 1998

ABSTRACT. **We tried to distinguish the notions of the language of the National Minority and the language of Diaspora and their extralinguistic features.**

Key words: diaspora, minority, languages.

Terms National Minority and Diaspora are used in special literature in relation to nontitled ethnolinguistic groups, being presented on the administrative territories for quite a long time. Due to some subjective factors the distinct difference among the groups is not always carried out. To some extent by the name National Minority the so-called "native" population, living on the territory together with "titled" nation, sometimes even earlier (Udins in Azerbajan, Ugro-Finish living in Russia near the Volga river, etc.) can be named.

To Diaspora we refer compact settlements of immigrants coming to the given territory from outside and saving in some way or another their independence from native population (Russians in the Baltic countries, Assirians in Georgia, etc.)

Naturally we can not draw a line between these two notions, because having lived on the territory for a long time, people of Diaspora can feel themselves as "native" population and not arrivals. This fact sometimes can lead to ethnolinguistic conflict with the "titled" nation. Such is the example of Osetians in Georgia. The situation becomes more sensitive with the disintegration of the State when the question of status of the ethnolinguistic group goes out of the limits of the State, making serious complications.

The difference between Diaspora and national Minority has quite important State's appeals (repercussions): in most States the rights of the Minorities are guaranteed (including language), while we can hardly hear about special difference of the language rights of Diaspora.

The outside factor, that is whether the National Minority (Diaspora) has its own state formation out of the country, is quite significant while solving the problem. Such State usually gives moral and material help to their compatriots abroad (e. g., marches of Russians to help their people in Estonia and Lithuania), in another case, there is no support on the governmental level (Kurds, Assirians etc.).

The most interesting problem is the problem of bilingualism among the representatives of National Minorities and Diasporas. The most natural is the case when people speak their own language (for "inner" use, if having political autonomy; for local self management) and government language (for all the rest spheres), having the ability to get education with the choice of the language.

However such harmony is not always met. In those cases,when National Minority

(Diaspora) is presented by people of the former "imperial" nation, bilingualism, as a rule, is not spread among them and if the "imperial" language loses its official government status, those people are left without the language. Position of Germany in the countries of Central Europe after the disintegration of Austro-Hungarian monarchy, position of Russians in the former Soviet Republics are the examples.

It must be noted however, that if the National Minority (Diaspora) has its government formation outside the country of the inhabitance (historical country), officials of that country usually support their compatriots morally or financially. In this case inner language policy is crossed with the outside one. In the cases when there is no support from outside and, especially, if the language has no written tradition, a real threat to the language appears. Native language can be lost. There is a move from bilingualism to the language of the surrounding even without special compulsion measures from the other side.

I. Javakhishvili Tbilisi State University

საქართველოს მეცნიერებათა აკადემიის მოამბე, 159, №1, 1999
BULLETIN OF THE GEORGIAN ACADEMY OF SCIENCES, 159, №1, 1999

PHILOLOGY

M. Iamanidze

The Role of Accompanying Persons in the Activity of French Travellers

Presented by Corr. Member of the Academy G. Sharadze, December 30, 1998

ABSTRACT. **We report on the role of accompanying persons in estimations of French travellers of XIII-XVIII centuries.**

Key words: French travelling literature.

The letters sent by French King to Philippe le Belley (1268-1314) in 1289 and 1305 are considered to be the beginning of France-East interrelations. According to the historical documents from the archives of National Library of Paris the powerful Moslem Eastern country proposed military alliance to true Christian French King [1].

From the XIII century some French travellers (W. Rubruk, J. Gaillefontaine, etc.) took their orientation to Mongolia which by that time had become the powerful empire in the world. The silk route from Europe to Asia passed through Mongolia. European travellers, missionaries, statesmen, tradesmen used this road to the East. Newly emerged states (Mongolia, Iran, Turkey) provoked the interest of France.

On the way to the East the travellers had to pass Transcaucasia. Since 13th century in different periods Transcaucasia was attacked by Mongolia, Persia and Turkey. That hindered direct contacts with the countries of Western Europe.

The period from the XIII to XVIII centuries is considered to be the most tragic in the history of Georgia. In the 30th of the XIII century Georgia became the victim of the Mongols. At the end of the XIV century devastating invasions of Tamerlane took place.

In 1471 Georgia was attacked by Iran. In the XVI century the East Georgia (Kartli-Kakheti) struggled against Iran and the West Georgia against Osman Turkey. At the beginning of the XVII century (1614) Shah Abbas attacked the country (Kartl-Kakheti). At the same time Osmans attacked from the West. In 1795 disintegrated and distructed Georgia became the object of Agha Mohammed-Khan of Persia invasion who turned the country in ruins [2].

The travellers passing through Georgia at that period of time became the witnesses of ruined and disintegrated into several provinces Christian country surrounded by aggressive Moslem States: Osman Turkey and Persia.

It is historically known that trade promotes development of interrelations between the countries. The French goverment sent the tradesmen, missionaries, researchers, statesmen into oriental countries to develop trade. They used to follow the caravans of merchants. They had their communities and churches in the places of trade [4]. Knowledge of languages, customs and traditions made it easy to contact with people from different countries. An Armenian merchant could work as an agent, translator, clerk, diplomat and for

the local authorities or be a Europians' companion in a foreign country [5].

For unexperienced traveller to travel with merchants' caravan was profitable, and less dangerous. It should be noted that theoretical knowledge and imagination about oriental countries immediately dissapeared when they left Europe. In such a trip the travellers could receive practical knowledge and experience which was not written in books. However it was rather dangerous to cross Transcaucasia that time, but the high sense of duty and aim was stronger than fear.

The study of traveller's notes of the XIII-XIV centuries shows that Georgia occupies special place. Although the final points of French travellers were the Oriental countries (Mongolia, Iran, Osman Turkey, etc.) they had an opportunity to be acquainted with Georgia. The interest and good attitude of French travellers towards Georgia is expressed in their writings, where Georgia is mentioned as a country with heroic past, with beautiful, noble and hospitable people. However, there were travellers who either crossed the country with no interest and paid attention only to other bordering countries or expressed antipathy and indifferently estimatied the exhausted from numerous wars Georgia and its suffering population.

The reports of French travellers of the XIII - XVIII centuries show that there was less written about Georgia than about its neigbour country Armenia which was in the same social and political situation. In numerous writings of French travellers (Jean du Mont, Petis de la Croix, Michel Febre, Raphael du Mans, Baron de Gourminin, Francois Piquet, Loran D'Arvieux, François Bernier, etc.) [6], Georgia was either ignored or little described, but Armenia and Armenians were described in details. Many of the travellers even studied Armenia in order to know more about the country, its culture and literature. It should be also noted that Armenians who accompanied French travellers are mentioned with gratitude (e. g., Arno, Gaspar, Antuan....) as they dilligently served the travelling.

Generally the voyager either he was known or not while travelling in the remote country chose companion who knew the country and the language. Evidently the merchants' caravans and the existence of Armenian communities in different countries helped European and French travellers.

Besides, in the XVII-XVIII centuries there existed a special institute of interpreters, professional accompanying persons which was founded by Jean-Baptiste Colbert (1649-1683), State ministry of France in the reign of King Lui XIV, who greatly appreciated travellers and travelling literature. He sent young people to the East to study languages, customs and traditions. They could work as translators in different oriental countries. A well-known French researcher Henri Cordier [7] stated that the translators who worked in Moslem countries stood between the ambassador and the authorities and they acted independently during negotiations. Before the XVIII century these interpreters were called **truchman** and later **drogman.** "They could be guides, servants, guards. **Drogman** was eastern Christian,as a rule Greek or Armenian, very rearly Hebrew; he seemed to be bifurcated due to his profession: close to Europe by belief and by culture he belonged to Asia." [8].

So the accompanying person of French traveller could be a tradesman, educated interpreter (**truchman** or **drogman**) or simply an interested person. As it is evident from French travelling literature of the XVII-XVIII centuries very often an accompanying

person was Armenian. The work of an accompanying person or translator appeared to be a guiding force between two countries. Very often their activity made bad service to the travellers and their research. In French travelling literature the work of drogman or guide-interpreter in most cases was found to be unsatisfactory [9]. In their memories the travellers express their negative attitude to the translators their moral and intellectual abilities. A well known investigator J. Sear advised the travellers to do without guides and to experience the foreign countries themselves. [10].

If we take into account an exciting socio-political situation of the oriental countries of that time and a traveller who was either wrongly informed by a guide (i. e. accompanying person) or he himself created faulse image out of his own fantasy then it becomes understandable why the information about Georgia was so colourless and subjective in the writings of French travellers of the XV-XVIII centuries.

The writings of the following French travellers in the period of XIII-XVIII centuries have been studied: W. Rubruk, J. de Gaillefontaine, G. Bouvier, (XIII-XV c.c.) J. B. Tournefort, J. B. Tavernier, J. Chardin, B. le Gouz, M. D'Herbelot (XVII c.), Ferrieres-Sauveboeuf, l' Abbé Gaudereau, G. de l'Isle, M. du Hautchamps, Ch. de Peyssonnel (XVIII c.).

Despite some inaccuracy the French travellers of the XIII-XVIII centuries among which are the persons of different origin, profession, and aim supply us with interesting material about our country which as a travelling genre represents the part of the history of French literature.

Georgian Academy of Sciences
Sh. Rustaveli Institute of Georgian Literature

REFERENCES

1. *M. Saba.* Bibliographie de L'Iran, 1936, IX, Biblothéque Natioanale de Paris.
2. Georgian History. Ed. G. Melikishvili. Tbilisi, 1980.
3. *M. Polievktov.* Europian Travellers. Tiflis.
4. *M. Aghassian, K. Kevonian.* Le commerce armenien dans l'Océan Indien au 17^{e} et 18^{e} siecles. Bibliothéque de la Maison des Sciences de l'Homme, Paris, 1975.
5. Ibidem, 18.
6. Bibliothéque Natioanalt, bibliothéque de l'Arsenal. Paris.
7. *H. Cordier.* Un iterprete du général Brune et la fin de l'Ecole de leunes de Langues, Paris, 1911.
8. *M. Sarga.* Eczize le voyage, Paris, 1994, 102.
9. Encyclopédie Diderot - Almbert, vol. XVII, 1765, 447.
10. *J. Ceard.* Voyage et voyageurs à la renaissance, 1988, Paris, 29.

საქართველოს მეცნიერებათა აკადემიის მოამბე, 159, №1, 1999
BULLETIN OF THE GEORGIAN ACADEMY OF SCIENCES, 159, №1, 1999

S.Kasyan

Analysis of Creative Works of Franco-Flemish Composers from the View-point of the Renaissance World Outlook

Presented by Corr.Member of the Academy P.Zakaraia, May 11, 1998

ABSTRACT. **The present paper explores the creative works of the leading composers of the Franco-Flemish school. The analysis is done from the viewpoint of the Renaissance world outlook, which leads to the philosophic category of identity.**

Key words: Franco-Flemish composers.

During XV century the Netherlands brought up the whole generation of unordinary personalities: Dufay, Ockeghem, Obrecht and Jocquin de Pre. Each of them grew on the heritage of predecessors and gave a new beginning, conditioned by bright individuality. As a result the school of Netherlandish polyphony was formed.

The study of creative heritage of Franco-Flemish composers from the viewpoint of the Renaissance outlook represents a new word in musicology. While investigating the basic principles of thinking of the Renaissance period we came to the philosophic category of identity, which determines the peculiarities of epochal and historical stylistic level in many respects and predetermines the peculiarities of seeing "world's picture".

As the logic of variety in the context of culture was based on interchangeability of identical paradigms, that's why when based on something confirmed the set on self expression was realized. All this was organic for the world outlook of the identity type. In our opinion its characteristics are wholeness, stability, norm and typification of high degree domination of giveness principle in a form of support on the sample, stability of expressive means, individuality as of awared type of a man.

Therefore, in the society with a system of values oriented on identical reproduction the art based on regularities of philosophic category of identity was formed .

Comparative analysis of creative works of Dufay, Ockeghem, Obrecht, Jocquin de Pre showed the multiform of identical regularities manifestation and allows to make the following conclusions.

1.Dufay, Ockeghem, Obrecht, Jocquin de Pre developed in their creative works the norms of writing which agree with aesthetic demands of the epoch (XV century - first part of XVI century). Their creations are marked by unrepeatable individuality and at the same time all of them are united by the fact that the leading principle of the world perception was the world outlook of identical type. Therefore, they created such system of writing which reflects the basic set of the world outlook of that time.

2. If the fundamental principle of the composers of the first half of XV century was the principle of "varietas" (Dufay, Benshua, partially Ockeghem), for the composes of the second half of XV and the beginning of XVI centuries (Ockeghem, Obrecht, Jocquin de

Pre) it was ostinato-immitational principle of writing [1].

3.Domination of "varietas" principle was conditioned by the following reasons:

a) ripening of prerequisites for the shift of accents in the pair ostinato-variant on the second paradigm of this pair already in the depths of the Middle Ages; b)leading significanee of Mass genre which in the whole represents a chain of unfolding relative images, each part of which is built according to monodramaturgic feature. This led to the variant principle of developing the images inside the cycle and domination of varietas principle both in music dramaturgy and in principles of musical development and polyphonic facture; c) predomination of melodic conception of polyphony; d) tendency of polyphony development to complete thematic homogeneity of voices.

4. From the second half of XV century polymelodic conception took a turn to ostinato-imitational polyphony of "strict style". New tendencies in development of phylosophic-aesthetic thought of epoch, the openining of linear perspective, fascinated by numeric proportions, adding of typical intonational material promote this.

5. On the basis of realization of varietas principle the following technical means have been formed:colouring, reduction, simultaneous variation. Principle of "varietas" was also spread on *cantus prius factus*. The means of its realization have been worked out which connect more closely the voices stimulating their inner unity [2].

6. From the second half of XV century the highest priority was given to the following techniques of writing based on the regularities of identity: immitation, cannon, simple cannonic sequention, ostinato. For Dufay's texture motive immitations are more characteristic, and he first starts to use them in the function of the material exposition.

Ockeghem's novelty is connected with successive use of transparent immitational development on the material of motif of typical character. In the creations of Obrecht and Josquin various kinds of complicated contrapunct formed and the technique of initial connections with following derivative variants were worked out and established. More and more frequently they repeat big initial connections based on the material characteristic to the given composition.

7.The realization of the unity of cyclic form was the sphere of particular interest for the representatives of Franco-Flemish school. Various means revealing identic relations among the elements of musical texture have been employed for that, and one of them is *motto*. Dufay was the first composer who used this means. *Motto* in his cylcle is not big and is exactly conducted at the beginning of each part.

As to Ockeghem here *motto* is crossed with dominated artistic principle of time "varietas". Therefore initial composition is developed in polyphonic fabric of each part of his Masses. At the same time Ockeghem enriches it by certain logic of development: if at the beginning of the cycle he shows the fabric of motto, and in middle parts he developes its separate voices, then in the final part of the cycle he repeats it again. Thus the contoures of framed symmetric form are created which also add to the unity, constructive wholeness of the cyclic form.

In Obrecht's works intersection of *motto* with initial melodic phrase *cantus firmus* is marked. This leads to the approximation of two identical in its factoral functions. It seems as if the composer brings nearer two traditionally isolated factural layers. This serves as means of achieving intonational unity both on the level of parts and the entire polyphonic texture.

In earlier Masses Josquin de Pre preserves traditional initial *motto*. Further he uses common for all parts "theme" built on the material of the first chorale phrase as means of achieving the wholeness.

8.The identic relations also embrace the sphere of all voices interactions. In creative works of each composer its own system of achieving the unity of intonational and melodic material of polyphonic facture was formed.

New approach to the development of *cantus prius factus* material in free voices is connected with Dufay. In accordance with coloring technique he uses the means of free voices coming out of *cantus prius factus* which results in achieving of high pitch productivity of upper voices melody.

In Ockeghem's works the examples of "thematization" of polyphony, for the first time appeared and a complex of means was formed which developed was by Obrecht and Jocsquin. It is the means of anticipation and migration of *cantus firmus* in free voices, which leads to the facture-tembre variant innovation. The sphere of compositional and constructive work on *cantus prius factus* is strengthened in Obrecht's compositions. Combination with the given initial material overcomes the variant productivity. Therefore along with the technique of tenor Masses (enriched by polyphonic means of development) he also develops ostinato-segment technique. Specific weight of ostinato-imitational technique is increased more in Jocquin de Pre's creations. *Cantus prius factus* penetrates into all voices of polyphony which leads to functional and factural equality of voices.

Thus in creations of Franco-Flemish composers a style based on regularities of identity was developed; form creation means and compositional structures corresponding to it were formed. As a result, a system was created which incarnates in music the united spiritual state in music, develops certain emotional imaginary, representing a type of monodramaturgy. Therefore in many respects the specificity of this stage of development of European professional music can be explained by the knowledge of the phenomena of identity which reflects the basic principles of the Renaissance.

Tbilisi V.Sarajishvili State Conservatory

REFERENCES

1. *V.Konanov*. Niderlandskie kompozitory XV-XVI v. L., 1996 (Russian).
2. *Yu.Evdokimova*. Muzyka epokhi vozrozhdeniy a; XV v., M., 1989 (Russian).

საქართველოს მეცნიერებათა აკადემიის მოამბე, 159, №1, 1999
BULLETIN OF THE GEORGIAN ACADEMY OF SCIENCES, 159, №1, 1999

N. Iamanidze

Importance of Landscape and Architectural Background in the Altar Screen Reliefs of the 11th Century

Presented by Member of the Academy V. Beridze, October 26, 1998

ABSTRACT. **Landscape and architectural background in the medieval altar screen reliefs is described on the example of Sapara, Urtkhva, and Shiomghvime churches (eleventh century, the Renaissance of Georgian plastics).**

Key words: medieval art, altar screen, stone carving.

The eleventh century is a peak of Georgian Medieval Art development. Up to that period Georgian local traditional plastic art passed its independent way of development and achieved success in reproduction of figures and theme compositions in sculptural and voluminous forms.In the altar screen reliefs of the 11th century the background was devoted to vivid comprehension of the composition, therefore special importance was given to the problem of interrelation between the figures and the background. At that time when the images had been relatively freely disposed on the relief surface it was necessary to find special background for the figure, to make the background concrete. That's why the growing interest towards representation of architectural and landscape background connected with the scene content was noticed.

The eleventh century has left for us splendid examples of altar screens decorated with figure reliefs. Importance of background is especially noticed on Sapara, Urtkhva and Shiomghvime altar screen reliefs, where landscape and architectural elements are mainly used to show the scene of action. At the same time they play a great role in the whole compositional solution of the scene. However, the figures themselves with their poses and gestures showing a kind of moving relations are very important in creating the scenes.

Landscape elements showing the scene action often have symbolic significance. In Urtkhva altar screen composition, "Mission of the Apostles", the presence of two trees is first of all conditioned by the content of the scene, following the creative reading of the Gospel. These trees show that the action takes place on the Illion Mountain. At the same time the leafy upward branches of the trees point to the Ascension immediately following the episode "Mission of the Apostles". Traditionally these compositions are represented together and the trees from the scene of Ascension have passed to the composition "Mission of Apostles".

The role of these trees is also interesting from the compositional view point: their symmetrical disposition closes and completes the whole scene and their conditional representation with their linear harmonic structure adds decorativeness to the whole compo-

sition.

The two trees represented in "The Holy Trinity" scene of the Shiomghvime altar screen also play a decorative and compositional role. Landscape importance is especially great in the scene, which is not limited with canonical iconographic scheme. Representing an episode from the life of one of the "Sirian Fathers" St. Shio (his meeting with Chief Evagre) the master tries to show the real place where it happens. He depicts St. Shio's figure in a small cave and a church on the hill, a big leafy tree instead of the forest and a pigeon with bread in its beak on the tree. Despite rather decorative solution the master tries to connect the figures with the landscape in the way of scale evaluation.

Thus, in the art of that period together with the growing interest to the historic themes an interest to represent the background appears. Georgian masters try to use background to create the environment for the figures.

But due to plastic character of Georgian art in which the laws of perspective were absent the interrelations of figures, landscape and architectural background remained rather conditional.

Expressing architectural elements in the altar screen reliefs of the 11th century the masters used well-known elements of the medieval art. Two scenes on the Sapara church altar screen: Presentation and Annunciation are of special interest. The use of architecture as the background for figures was conditioned by iconographic necessity, i. e., when architectural background denotes the place of action. At the same time it serves to logical accentuation of figures. It defines figures and by its construction it harmonically goes with them. High Priest Simon and Virgin Maria observed in a group in the centre of "Presentation" composition appear against the background of three bay arcade. The shape of arch rythmically reproduces the form of halo. It doesn't contain any specific sign of special functional application. Side figures isolated from the basic group are presented against the background of individual architectural elements. Thus the architecture plays a compositional role.

The same can be said about the architectural background of Annunciation scene: a big figure of the Virgin in the centre of composition goes in size with a building represented in low relief which defines the place of action.

It should be noted that Sapara reliefs are constructed in opposition of two basic planes, i. e., the figures treated plastically and the architectural background represented in low relief which contributes to the change of perspective.

The master of Shiomghvime altar screen aims to represent architectural background in dynamics. In the scene of one of the episodes of St. Simon's life there is a column erected on the hill in the centre of the composition, the wall built behind it and monastery buildings indicating the place. The master of Shiomghvime uses the architectural background to create decorative impression. He depicts the column ornament, its head decoratively shaped, geometric ornament of the wall, etc. He tries to render numerous details as if he wants to add decorativeness to architectural background.

Thus, in altar screen reliefs of the 11th century saved up to now the landscape and architectural background play significant role and it carries various compositional and contextual load. At the same time each master has individual interpretation. Georgian plastic art which further failed to develop, landscape and architectural elements also stopped further development and remained within the limits of decorative background due to the general character of Georgian plastics which also stopped to develop.

Georgian Academy of Sciences
G. Chubinashvili Institute of the History
of Georgian Art

REFERENCES

1. *R. Shmerling.* Small forms in the architecture of middle Aged Georgia. Tbilisi, 1962.
2. *A. Volskaya.* Ars Georgia 8, A, Tbilisi, 1979 (Russian).
3. *D.Talbot.* Rice. The Church of Haghia Sophia at Trabizond. Edinburgh. 1968.
4. *O. Devus.* Byzantine art and the West. New-York. 1970.

Subscription Information

Bulletin of the Georgian Academy of Sciences
is published bimonthly

Correspondence regarding subscriptions, back issues should be sent to:

Georgian Academy of Sciences,
52, Rustaveli Avenue, Tbilisi, 380008, Georgia
Phone : + 995-32 99-75-93;
Fax/Phone : + 995-32 99-88-23
E-mail : BULLETIN@PRESID.ACNET.GE

Annual subscription rate including postage for 1999 is US $ 400

To Support our Journal Subscribe to it Now

Copy this form to mail or fax your order number today

Title	Volume	ISSN	Issues	Rate in US Dollars	Your order
BULLETIN of the Georgian Academy of Sciences	159 & 160	76181	6	400	$_____

1. Name_____

Institution_____

_____

Address_____

_____

City_____

State_____

Zip/Postal Code_____

Country_____

Telephone (_____)_____

Fax (_____)_____

E-mail _____

2. My payment for $_____ is enclosed

Or

Bill me. My library's purchase order number is_____

3.Send this order and payment to:

Mrs. Ludmila Gverdtsiteli,
Editorial Manager

52, Rustaveli avenue, 380008,
Tbilisi, Georgia
Tel.: (+995-32) 99-75-93
Fax: (+995-32) 99-88-23
E-mail: Bulletin@presid.acnet.ge

The Journal will be published in 1999

გადაეცა წარმოებას 20.01.1999. ხელმოწერილია დასაბეჭდად 15.04.1999.
ფორმატი 70×108 1/16. ოფსეტური ბეჭდვა.
პირობითი ნაბ. თ. 11. საღრიცხვო-საგამომცემლო თაბახი 11.
ტირაჟი 250. შეკვ. № 84 ფასი სახელშეკრულებო.

რედაქციის მისამართი: 380008, თბილისი-8, რუსთაველის პრ. 52, ტელ. 99-75-93.
საქართველოს მეცნიერებათა აკადემიის საწარმოო-საგამომცემლო გაერთიანება „მეცნიერება",
380060, თბილისი, ლ. გამრეკელის ქ. 19, ტელ. 37-22-97.